JAERI-M
84-229

A MAIN STEAM LINE BREAK EXPERIMENT AT ROSA III-RUN 952 (STANDARD RUN WITH FULL ECCS)

December 1984

Masahiro KAWAJI, Hideo NAKAMURA,
Mitsuhiro SUZUKI, Kanji TASAKA,
Yoshinari ANODA, Hiroshige KUMAMARU,
Taisuke YONOMOTO, Hideo MURATA,
and Masayoshi SHIBA

日 本 原 子 力 研 究 所
Japan Atomic Energy Research Institute

JAERI-Mレポートは，日本原子力研究所が不定期に公刊している研究報告書です。
入手の問合わせは，日本原子力研究所技術情報部情報資料課（〒319－11茨城県那珂郡東海村）あて，お申しこしください。なお，このほかに財団法人原子力弘済会資料センター（〒319-11茨城県那珂郡東海村日本原子力研究所内）で複写による実費頒布をおこなっております。

JAERI-M reports are issued irregularly.
Inquiries about availability of the reports should be addressed to Information Division, Department of Technical Information, Japan Atomic Energy Research Institute, Tokai-mura, Naka-gun, Ibaraki-ken 319-11, Japan.

編集兼発行　日本原子力研究所
印　　刷　日立高速印刷株式会社

A MAIN STEAM LINE BREAK EXPERIMENT AT ROSA III - RUN 952
(Standard Run with Full ECCS)

Masahiro KAWAJI, Hideo NAKAMURA, Mitsuhiro SUZUKI,
Kanji TASAKA, Yoshinari ANODA, Hiroshige KUMAMARU,
Taisuke YONOMOTO, Hideo MURATA and Masayoshi SHIBA

Department of Nuclear Safety Research,
Tokai Research Establishment, JAERI

(Received November 29, 1984)

This report presents the experimental data for RUN 952, a 100% Main Steam Line (MSL) break experiment performed at the ROSA-III test facility. The ROSA-III facility is a volumetrically scaled (1/424) system of a BWR/6 used for integral BWR LOCA simulation experiments. RUN 952 is a reference MSL break test performed with a 100% break upstream of the main steam isolation valve (MSIV) and full ECCS actuation logic. The MSL break is characterized by a relatively slower depressurization of the system due to a break flow of high mass quality, in comparison with a recirculation line break test, RUN 901. Continuous flashing of the fluid in the pressure vessel was observed and a slow decrease in the downcomer water level eventually led to actuation of HPCS but not LPCS and LPCI. About 2/3 of the core was uncovered, however, the coolant level recovered quickly following the HPCS injection. The peak cladding temperature reached was 752 K, which is 28 K lower than that obtained in RUN 901.

Keywords : BWR, LOCA, ECCS, Integral Test, ROSA-III Program,
100% Main Steam Line Break, PCT, Downcomer Water Level,
Flashing, Reactor Safety

ROSA－Ⅲ主蒸気ライン破断実験－RUN952
（全ECCS作動標準実験）

日本原子力研究所東海研究所安全工学部
川路　正裕・中村　秀夫・鈴木　光弘・田坂　完二
安濃田良成・熊丸　博滋・与能本泰介・村田　秀男
斯波　正誼

（1984年11月29日受理）

本報はROSA－Ⅲ実験装置を用いて行った主蒸気管ライン100％破断実験，RUN952，の実験結果について述べたものである。この実験は主蒸気管ライン破断実験シリーズ（RUN951～954）の標準ケースとして全ECCS作動可の条件で行ったものである。主蒸気管ライン破断では高クオリティの破断流が生じるため，圧力降下が再循環ライン破断　RUN901）に比べて緩かである。また減圧沸騰が長く続き上部ダウンカマーでの水位が余り低下せずHPCSは作動したがLPCSとLPCIは作動しなかった。炉心は約2／3が露出した後，HPCS作動により水位が急速に回復したためPCTは752Kであった。これは再循環ライン破断実験RUN901のPCTより，28K低いものである。

CONTENTS

目　　次

LIST OF TABLES

LIST OF FIGURES

ABBREVIATIONS

ADS	Automatic Depressurization System
AT	Air Tank
AV	Air Actuation Valve
(2)B	(2) inches pipe of Schedule 80
BN	Boron Nitride
BWR	Boiling Water Reactor
CA	Chromel-Alumel
CCFL	Counter Current Flow Limiting
CHV	Check Valve
CP	Conductivity Prove
CV	Control Valve
CWT	Cooling Water Tank
D	Differential Pressure
d	Diameter
DF	Density of Fluid
DL(+100)	Elevation (+100 mm) from the bottom of PV
ECCS	Emergency Core Cooling System
ESF	Engineered Safety Features
EX	Heat Exchanger
F	Flow Rate
Fig.	Figure
FS	Full Scale
FW	Feedwater
FWLF	Feedwater Line Flashing
FWP	Feedwater Pump
FWT	Feedwater Tank
HPCS	High Pressure Core Spray
HPCSP	High Pressure Core Spray Pump
HPCST	High Pressure Core Spary Tank

HPWP	High Pressure Water Pump
ID	Inner diameter
INC 600	Inconel 600
JP	Jet Pump
K	Kelvin
kg	Kilogram
kPa	Kilopascal
kW	Kilowatt
L	Liter
LB	Liquid Level in Channel Box
LBWR	Large Boiling Water Reactor
LL	Liquid Level
LOCA	Loss-of-Coolant Accident
LOCE	Loss-of-Coolant Experiment
LP	Lower Plenum
LPCI	Low Pressure Coolant Injection
LPCIP	Low Pressure Coolant Injection Pump
LPCIT	Low Pressure Coolant Injection Tank
LPCS	Low Pressure Core Spray
LPCSP	Low Pressure Core Spary Pump
LPCST	Low Pressure Core Spary Tank
LPF	Lower Plenum Flashing
LTP	Lower Tie Plate
M	Momentum Flux
m	Meter
mm	Milimeter
MLHR	Maximum Linear Heat Rate
MPa	Megapascal
MRP	Main Recirculation Pump
MSIV	Main Steam Isolation Valve
MSL	Main Steam Line

MW	Megawatt
N	Rotation Speed
OR	Orifice
P	Pressure
	Power
PCT	Peak Cladding Temperature
PV	Pressure Vessel
PWT	Pure Water Tank
QOBV	Quick Opening Blowdown Valve
QSV	Quick Shut-off Valve
RCN	Rapid Condencer
ROSA	Rig of Safety Assessment
rpm	Revolution per Minute
S	Signal
s	Second
Sch	Schedule
SUS	Stainless Steel
T	Temperature
T/C	Thermocouple
TC	Temperature of Fluid
TF	Temperature of Fuel
TS	Temperature of Structure Material
UTP	Upper Tie Plate
V	Valve
VF	Void Fraction
W	Watt
WL	Water Level
WSP	Water Supply Pump

1. Introduction

The Rig of Safety Assessment (ROSA)-III program was initiated in 1976 to study the thermal-hydraulic behavior of a Boiling Water Reactor (BWR) during a postulated Loss of Coolant Accident (LOCA) with the Emergency Core Cooling System (ECCS) actuation and to provide the data base necessary for evaluation of computer codes developed for reactor safety analysis. The ROSA-III test facility, which was completed in 1978, consists of a volumetrically scaled (1/424) primary system of a 3800 MW BWR/6-251 with an electrically heated core, a break simulator and a scaled ECCS(1).

Special emphasis has been placed on the following objectives in the ROSA-III program :

(1) To provide the system data required for improvement and evaluation of analytical methods currently used to predict the LOCA response of large BWRs. In particular, the performance of Engineered Safety Features (ESFs), with an emphasis on ECCSs, and the quantitative margins of safety inherent in performance of the ESFs are of primary interest.

(2) To identify and investigate any unexpected event(s) or threshold(s) in the response of either the plant or the ESFs and to develop analytical techniques that adequately describe and account for such unexpected behavior.

The information acquired from Loss of Coolant Experiments (LOCEs) is thus used for evaluation and development of LOCA analytical methods and assessment of the ESFs in response to a LOCA.

RUN 952 was conducted on July 14, 1982 to simulate a 100% Main Steam Line (MSL) break LOCA with full ECCS actuation logic.

The specific objectives of this test were as follows :

(1) To acquire test data on a 100% MSL break LOCA with full ECCS actuation logic, and

(2) To determine the characteristics of the system response for a MSL break LOCA and compare them to those obtained in the recirculation line break tests.

In this report, all of the data obtained in RUN 952 are presented and discussed, including the processed data such as mass inventory in the pressure vessel. The data from this test are then compared with the results of a 200% recirculation line break test, RUN 901, in which a double-ended break was assumed at the main recirculation pump suction line[6]. Some important parameters describing the system response from both experiments are compared to determine the major differences between the MSL and recirculation line break LOCA.

2. ROSA-III Test Facility

The ROSA-III test facility is a volumetrically scaled (1/424) BWR system with an electrically heated core designed to study the response of the primary system, the core and the ECCS during a postulated LOCA. The test facility is instrumented to measure and record various thermal-hydraulic parameters during the test. Details of the instrumentation are described in section 3.

The test facility consists of four subsystems. These subsystems are : (a) pressure vessel, (b) steam line and feedwater line, (c) recirculation loops and (d) ECCS. Figures 2.1 through 2.3 illustrate the configuration of the test facility including the pressure vessel internals and piping schematics. Table 2.1 compares the major dimensions of the ROSA-III test facility with the corresponding dimensions of the reference BWR.

The ROSA-III pressure vessel includes various components simulating the internal structures of the reactor vessel in the BWR system as shown in Fig. 2.4. The interior of the vessel is divided into the core, lower plenum, upper plenum, downcomer annulus, steam separator, steam dome and steam dryer. The core consists of four model fuel assemblies of half length and a control rod simulator. Each fuel assembly contains 62 heater rods (Fig. 2.5) and 2 water rods spaced in a 8 x 8 square array and supported by spacers and upper and lower tie plates. The heater rod is heated electrically with chopped cosine power distribution along the axis as shown in Fig. 2.6. The effective heated length is 1880 mm, one half of the active length of a BWR fuel rod. The electric power supplied to the model fuel assembly A is 1.4 times larger than the power supplied to each of the other assemblies, B, C and D. The heater rods in each assembly are divided into three groups in terms of heat generation rate as shown in Fig. 2.7.

The relative power generation rate of a heater rod in each group is 1.1, 1.0, and 0.875 respectively. The orifice plates are inserted at the core inlet to control the core inlet flow(1).

The steam line and the feedwater line simulate those of a BWR. The steam line of the ROSA III system has three branches as shown in Fig. 4.3. The first branch is initially closed by a valve AV-165 and used for the simulation of steam line break by opening the valve AV-165. The steam discharge flow after break is limited by the break orifice OR-5 with 31.0 mm I.D. shown in Fig. 4.1 located in the first branch and is led to the outdoor pool through the break unit B where a gamma densitometer and a drag disk are installed to measure the break flow. The break unit A was not used in RUN 952 and the quick shutoff valve between the break units was also closed. The inner diameter of the orifice in the break unit B was 49.5 mm.

The second branch is the Automatic Depressurization Line which was not used in RUN 952. The third branch is used for controlling the steady state system pressure and the steam is used partially for heating-up the feedwater. Immediately after the break initiation, the third branch is shut off by closing the main steam isolation valve (MSIV), AV-168, so that the steam is discharged only through the first branch simulating the break. A control valve is installed in the steam line to control the steam dome pressure at steady state before the initiation of tests. The steam line has a branch in which the Automatic Depressurization System (ADS) is installed. The operation of valves in the steam line is described in sec. 4. The feedwater is supplied from the feedwater tank (FWT) through the feedwater line and the sparger below the steam separator.

Figure 2.8 shows the recirculation line consisting of two loops. Each loop is furnished with a pump and two jet pumps. The jet pumps are installed outside the pressure vessel to simulate the relative volume and height with respect to the core. The ROSA-III test facility is furnished with all types of ECCS which are available in the BWR system, i.e., High Pressure Core Spray (HPCS), Low Pressure Core Spray (LPCS), Low Pressure Coolant Injection (LPCI), and Automatic Depressurization System (ADS). The HPCS and LPCS provide the cooling water from the top of the core. The LPCI injects the cooling water into the core bypass. Each ECCS consists of a pump, a tank, piping, and a control and measurement system. Reference (1) provides more detailed information on the ROSA-III facility.

3. Instrumentation

The instrumentation for the ROSA-III facility has been designed to provide thermal-hydraulic data for a simulated BWR LOCA. The data obtained from the experiments are used for the assessment of analytical computer codes. Table 3.1 summarizes the instrumentation used in RUN 952.

Tables 3.2 and 3.3 show the measurement list and the core instrumentation list, respectively. Instrument locations are shown in Fig. 3.1 through Fig. 3.6.

Typical parameters measured in the ROSA-III facility are pressure, differential pressure, flow rate, electric power, pump speed, fluid and metal temperatures, collapsed liquid level, two-phase mixture level, coolant density, on-off type signals and so on.

Pressure and differential pressure transducers are two-wire, direct-current type which convert diaphragm displacement to electric capacitance. The pressure lead lines are either the standard single, cylindrical pipes used in conjunction with condensate pots, or dual concentric cylinders capable of circulating the cooling water to prevent flashing of the fluid.

The flow rate is measured either by an orifice or a venturi type flow meter depending on the fluid condition and measurement location.

The temperatures of the fluid, structural materials and the cladding of fuel rods are measured with sheathed chromel-alumel (C/A) thermocouples of 1.6mm or 0.5 mm diameter.

Liquid level is measured by either differential pressure transducers described above or needle type electrical conduction probes (CP) developed specially for the ROSA-III program. These probes are distributed in the pressure vessel to detect the presence of water or vapor at different heights.

The electric power supplied to the simulated fuel rods is controlled to follow the predetermined decay curve and measured by a fast response electric power meter.

Pump speed is measured by a pulse generator integral to the pump. On-off signals indicating the valve positions selected, core power decay and pump coastdown initiation and so on are also detected and recorded.

Fluid density in the pipe is measured by means of multi-beam gamma densitometers. Preliminary studies indicated that a three-beam densitometer should be used to determine the flow regime. Figures 3.7 and 3.8 show the beam directions of the three-beam and two-beam gamma densitometers, respectively. The gamma-ray source is ^{137}Cs and the detector is a water cooled NaI(Tl) scintillation counter.

Momentum flux is measured by a drag disk shown in Fig. 3.9. The combination of signals from a drag disk and a gamma densitometer is used to determine the two-phase flow rate as shown in Fig. 3.10.

The data acquisition system (DATAC 2000B, Iwasaki Tsushinki Co.) scans all of the 700 instrument channels at a rate of up to 30 Hz. The data recorded on magnetic tapes are processed by the FACOM M380/200 computer system after the experiment. More detailed information on the instrumentation and the data processing procedure is available in reference (2).

4. Test Conditions and Procedure

RUN 952 is a 100% Main Steam Line break test with a break located at the main steam line. The break area is adjusted by inserting an orifice shown in Fig. 4.1 in the main steam line. Blowdown is initiated by opening the QOBV and closing the valve AOV-168 in the steady steam flow line. The initial conditions of the test were specified as follows: the steam dome pressure of 7.35 MPa, the lower plenum temperature of 552 K giving the subcooling of 10.7 K, the core inlet flow rate of 16.6 kg/s, and the core heat generating rate of 3.962 MW. The quality in the upper plenum was estimated to be 12.5%. The actual conditions are summarized in Table 4.1.

To prepare for the test, makeup water (pure water) was pumped into the primary system of the test facility and electric power was supplied to the core to heat the water in the system and to achieve saturation conditions in the upper region of the pressure vessel. The core power was maintained at 3.962 MW before the break initiation, which is 44% of the steady state power of 8.96 MW necessary to achieve the same power-to-volume ratio as in the reference BWR. The core power was decreased during the transient following the break as shown in Fig. 4.2. Here, the power is kept constant for the first 9.0 seconds and reduced along the decay curve that simulates the total heat transfer rate in the core of the reference BWR (the delayed neutron fission power, the decay power of fission products and actinides and the stored heat in the nuclear fuel) neglecting the stored heat of ROSA-III heater rods(3). The maximum linear heat rate of the peak power rod before the break initiation is 16.6 kW/m.

The schematics of the main steam line and the feedwater line are shown in Figs. 4.3 and 4.4 respectively. The main steam line of the ROSA-III has three branches: (1) steady flow branch, (2) ADS branch and (3) transient branch. Before the break initiation, CV-130 in the steady flow branch controls the steam flow rate to maintain the steam dome pressure constant and CV-1 and CV-2 are opened to provide steam to the heat exchanger to heat the feedwater. At the break initiation, the steam flow is switched to the transient branch by opening AV-165 and closing AV-168, CV-1 and CV-2. The break flow during the MSL break test was limited by an orifice OR-5 of 31.0 mm ID (inner diameter) shown in Fig. 4.1 installed upstream of AV-165 as shown in Fig. 4.3. The ADS was not actuated in the present MSL break test and Tables 4.2 and 4.3 respectively show the characteristics and control sequence of steam discharge line valves in the present test.

The details of the feedwater line is shown in Fig. 4.5. The feedwater flow is terminated at 1.3 s after break by closing the valve AV-112 in the feedwater line. However, some feedwater remained in the piping between AV-112 and the feedwater sparger below the steam separator in the pressure vessel.

The coolant recirculation pumps are tripped to start coasting down at the time of break initiation.

The liquid level signal in the downcomer is used to actuate the ECCS in the ROSA-III MSL break tests. The downcomer water level during a steady state operation is set at the scram level L3 (5.00 meters above the bottom of the pressure vessel). When the liquid level in the downcomer falls to the L2 level (4.76m), HPCS is actuated with a time delay of 27 s. If the liquid level further falls to the L1 level (4.25m), both LPCS and LPCI are actuated with a time delay of 40 s in the present test. The delay times given above are used in a safety analysis of the reference BWR(4). Injection of emergency coolant by LPCS and LPCI in the reference BWR, however, occurs when the primary system pressure falls below 2.16 MPa and 1.57 MPa respectively, because of early actuation of the high containment pressure signal which activates the LPCS and LPCI pumps. This occurs despite a delay in the lowering of the downcomer water level. Thus, the actuation of LPCS and LPCI by the L1 level signal in the present test corresponds to the failure of the containment pressure signal in the case of main steam line break of the reference BWR. The system pressures selected for actuation of LPCS and LPCI were calculated from the pump characteristics used in the safety analysis of the reference BWR[(5)]. The test was terminated after the entire core was quenched and the top of the pressure vessel was nearly filled with water.

5. Data Processing

In the present test, data acquisition with DATAC 2000B was started 120 s before the break initiation and terminated at 1183 s after break. The data sampling rate was 10 Hz throughout the test. The test data were processed and a set of 1000 data points was selected for plotting. The time span and frequency of the reduced data for plotting were 460 s and 2.2 Hz, respectively.

Measured Data

The test data from RUN 952 are shown in Fig. 5.1 through 5.157. In these figures, each measurement is identified by the channel number shown in Table 3.2. The major test sequences and events observed are summarized in Table 5.1.

Figures 5.1 through 5.5 show the pressure data obtained in the pressure vessel and in the recirculation line. Figures 5.6 through 5.33 show differential pressures measured between various locations in the pressure vessel, break unit and recirculation line. Figures 5.34 and 5.35 show the liquid levels in the pressure vessel and ECCS tanks. Figures 5.36 through 5.41 show the flow rates in MSL, ECC injection, feedwater and recirculation lines. Differential pressures measured across the orifice and venturi flow meters located in the MSL and recirculation lines are useful for checking out the flow rate instrumentation. They are shown in Figs. 5.42 through 5.52. Figure 5.53 shows the power supplied to the core from two power supplies with maximum capacities of 2100 kW and 3150 kW. The revolution speeds of the recirculation pumps are shown in Fig. 5.54. On-off signals indicating the break initiation, the status of ECCS, pump and valve operations are shown in Figs. 5.55, 5.56 and 5.57. Figures 5.58 through 5.65

show the fluid densities measured by the gamma densitometers. Figures 5.66 through 5.68 show momentum fluxes measured at jet pump outlets and break unit using drag disks. Figures 5.69 through 5.81 show the fluid temperatures at various locations in the loop. The fuel rod cladding temperatures and the surface temperatures of the water rods and the channel boxes measured at positions 1 through 7 are given in Figs. 5.82 through 5.101. Figures 5.102 through 5.126 compare the cladding temperatures of different fuel rods at the same elevation. Figures 5.127 through 5.143 show the fluid temperatures at the inlet and outlet of the channel box. The surface temperatures of the channel box and the fluid temperature in the lower plenum are shown in Figs. 5.144 and 5.145 respectively. The liquid level signals in the core, upper and lower plena, guide tube and downcomer are shown in Figs. 5.146 through 5.157. The Peak Cladding Temperature (PCT) distribution in the core is given in Table 5.2

Derived Data

Quantities calculated from the measured data are shown in Figs. 5.158 through 5.180.

Figure 5.158 shows the estimated mixture level in the pressure vessel obtained from the conductivity probe signals shown in Figs. 5.146 through 5.157. Figures 5.159 and 5.160 show the location of the dryout front and the quench front obtained from the fuel rod cladding temperature data.

Figures 5.161 through 5.163 show the average fluid densities at the jet pump outlet and break unit, which are claculated from the three-beam and two-beam gamma densitometer data shown in Figs. 5.58 through 5.65. The beam configurations of the gamma densitometers installed in the ROSA-III facility are shown in Figs. 3.7 and 3.8. The average density is calculated as an arithmetic mean of the chordal-average densities using the chord length as the weighting factors.

For the three beam densitometer at the jet pump outlet spool piece, the average fluid density is calculated using the following equation.

$$\rho_{av} = 0.3221\rho_A + 0.43\rho_B + 0.2479\rho_C \quad (5.1)$$

where,

ρ_{av} = average density obtained from the three-beam gamma densitometer,

ρ_A = density measured by beam A (bottom),

ρ_B = density measured by beam B (middle),

ρ_C = density measured by beam C (top).

For the two-beam densitometer at the break spool piece,

$$\rho_{av} = 0.5863\rho_A + 0.4137\rho_B \quad (5.2)$$

where,

ρ_{av} = average density obtained from the two-beam gamma densitometer,

ρ_A = density measured by beam A (bottom),

ρ_B = density measured by beam B (top).

Figure 5.164 shows the flow rate at the break computed from the drag disk and gamma densitometer data using the following equation.

$$G = C_D \cdot A \cdot \sqrt{\rho_{av} \cdot \rho v^2} \quad (5.3)$$

where,

G = mass flow rate,

C_D = drag coefficient (= 1.13),

A = flow area (= 1.923×10^{-3} m^2),

ρ_{av}= average density from gamma densitometer,

ρv^2= momentum flux from drag disk.

Figures 5.165 through 5.175 show the fluid flow rates at the main steam line, channel inlet orifices, bypass hole and jet pump outlets. These flow rates are calculated from the pressure drop measured across the orifice or venturi flow meters and the vapor or liquid density obtained from the temperature and pressure measurements. The equation used for this calculation is as follows :

$$G = C_D \cdot A \cdot \sqrt{2g \cdot \rho_l \cdot \Delta P} \tag{5.5}$$

where,

G = flow rate,

ΔP = pressure drop across the orifice,

C_D = discharge coefficient,

= 0.6552 (orifice to measure the steam discharge flow rate)

= 0.4761 (channel inlet orifice)

= 0.8032 (bypass hole)

= 0.7383 (orifice to measure the jet pump outlet flow rate)

= 1.1260 (venturi tube to measure the jet pump outlet flow rate)

A = flow area (m^2)

= 2.875×10^{-3} (orifice to measure the steam discharge flow rate)

= 1.521×10^{-3} (channel inlet orifice)

= 1.758×10^{-4} (bypass hole)

$= 1.133 \times 10^{-3}$ (orifice to measure the jet pump outlet flow rate)

$= 9.095 \times 10^{-4}$ (venturi tube to measure the jet pump outlet flow rate)

g = gravitational acceleration (= 9.807 m/s^2),

ρ_l = density of the single-phase liquid (kg/m^3),

Although the above calculation method is not applicable to two-phase flow conditions after the initiation of flashing in the lower plenum, the values calculated are useful in determining a trend in two-phase flow rates. Total channel inlet flow rate represents the sum of four separate channel inlet flow rates.

Figures 5.176 and 5.177 show the collapsed water levels outside and inside the core shroud, respectively. The collapsed water level is obtained from the differential pressure measurement in the pressure vessel. The differential pressure may include the friction and acceleration effects, however, these effects are considered to become negligible after completion of the recirculation pump coastdown.

Finally, Figures 5.178 through 5.180 show the fluid mass inventories in the downcomer, core shroud and pressure vessel. The fluid mass inventory is determined from the density and the volume of liquid outside and inside the core shroud as follows.

$$M = \rho_l \cdot Q \tag{5.6}$$

where,

M = fluid inventory,

ρ_l = liquid density estimated from the saturation temperature and/or pressure,

Q = liquid volume calculated from the liquid level.

The volume Q (m^3) outside the core shroud is given below as a function of height.

$$
\begin{aligned}
&Q = 0.0 && (\qquad L \leqq 0.494) \\
&Q = 0.0225L - 0.0111 && (0.494 < L \leqq 1.384) \\
&Q = 0.0697L - 0.0769 && (1.384 < L \leqq 1.519) \\
&Q = 0.0225L - 0.0048 && (1.519 < L \leqq 3.355) \\
&Q = 0.0801L - 0.1980 && (3.355 < L \leqq 4.250) \\
&Q = 0.2443L - 0.8959 && (4.250 < L \leqq 4.413) \\
&Q = 0.2611L - 0.9700 && (4.413 < L \leqq 4.578) \\
&Q = 0.2504L - 0.9211 && (4.578 < L \leqq 4.654) \\
&Q = 0.2375L - 0.8610 && (4.654 < L \leqq 4.815) \\
&Q = 0.2866L - 1.0974 && (4.815 < L \leqq 4.915) \\
&Q = 0.3396L - 1.3580 && (4.915 < L \leqq 5.143) \\
&Q = 0.3607L - 1.4665 && (5.143 < L \leqq 5.365) \\
&Q = 0.3848L - 1.5960 && (5.365 < L \leqq 5.955) \\
&Q = 0.7111 && (5.955 < L \qquad)
\end{aligned}
\tag{5.7}
$$

The volume Q (m^3) inside the core shroud is similarly given below as a function of height.

$$
\begin{aligned}
&Q = 0.0 && (\qquad L \leqq 0.0) \\
&Q = 0.2350L && (0.0 < L \leqq 0.497) \\
&Q = 0.1245L + 0.0549 && (0.497 < L \leqq 1.354) \\
&Q = 0.0698L + 0.1290 && (1.354 < L \leqq 3.589) \\
&Q = 0.1648L - 0.2120 && (3.589 < L \leqq 3.744) \\
&Q = 0.1963L - 0.3299 && (3.744 < L \leqq 4.243) \\
&Q = 0.0196L + 0.4199 && (4.243 < L \leqq 4.578)
\end{aligned}
\tag{5.8}
$$

$$Q = 0.0186L + 0.4244 \qquad (4.578 < L \leqq 4.654)$$

$$Q = 0.0410L + 0.3201 \qquad (4.654 < L \leqq 5.099)$$

$$Q = 0.0196L + 0.4292 \qquad (5.099 < L \leqq 5.365)$$

$$Q = 0.5344 \qquad (5.365 < L)$$

The total fluid mass inventory in the pressure vessel is given by the sum of the mass inventories inside and outside of the core shroud. The initial mass inventory before the break initiation is estimated to be at 640 kg.

6. Discussion of Test Results

Experimental data for RUN 952 are discussed in this section.

6.1 Pressure Response and Sequence of Events

The pressure response in various parts of the pressure vessel, recirculation line and break unit are shown in Figs. 5.1 through 5.5. The pressure response shows monotonous depressurization throughout the test, which is reasonable in a steam line break or a continuous steam discharge transient with a large amount of vapor generation in the whole system.

Initiation of vapor generation or flashing at each location of the ROSA-III system can be determined from the liquid level, differential pressure and fluid temperature data. The liquid in the middle downcomer began to evaporate at 4.2 s after break as shown in the differential pressure data (see Fig. 5.8). At the same time, flashing started to occur in the lower plenum, resulting in a decrease in the depressurization rate. The fluid in the top part of jet pumps began to evaporate also at 4.2 s (see Fig. 5.16). The fluid in the feedwater line with an initial temperature of 491 K began to flash at 95 sec after break (see Fig. 5.38).

The HPCS was actuated at the system pressure of 2.23 MPa at 94 s after break. The water level in the upper downcomer did not drop to the L1 level, because of the vapor generation in the lower downcomer, lower plenum and recirculation line (see Fig. 5.35) and mass recovery due to HPCS injection. Early in the transient, temporary exposure of fuel rods occurred in the upper region of the core and small peaks in fuel rod temperatures are observed at about 10 s after break. More significant core uncovery started to occur from the top of the core at 40 s after break. The lower part of the core below position 6 was not uncovered and exposed to the steam environment, because HPCS was actuated at 94 sec after break delivering a sufficient amount of emergency coolant to the core. The reflooding of the core followed the HPCS actuation and the entire core was quenched at 231 s after break (137 s after HPCS actuation) except at some peak power locations as described in section 6.10.

6.2 Differential Pressure

Differential pressure and collapsed water level in the pressure vessel are discussed in this section. The collapsed water level is estimated from the corresponding differential pressure data neglecting the effects of friction and acceleration terms.

Figures 5.6 through 5.9 show differential pressure data between the lower and upper plena (D1), between the upper plenum and steam dome (D2), between the bottom and middle regions of the downcomer (D4), and between the lower plenum and steam dome (D5) respectively. Flow stagnation due to coasting down of the recirculation pumps occurred shortly after the break, resulting in a rapid decrease in the differential pressure (D1).

The differential pressure, D1, shows large fluctuations after HPCS actuation at 94 s after break. D1 increased gradually after HPCS actuation indicating an increase in mass inventory.

The differential pressure, D2, between the upper plenum and steam dome shows a rapid increase due to the fluid acceleration in the steam line immediately after the break. The effect of lower plenum flashing is observed after 4.2 s. D2 decreased gradually even after HPCS actuation.

The differential pressure, D4, in the lower downcomer shows a rapid decrease after 4.2 s indicating coolant flashing in the downcomer. The void fraction in the downcomer was estimated from the data to be approximately

55% at 100 s, 56% at 250 s and 55% at 350 s.The differential pressure, D4, began to increase gradually at about 350 s, indicating a decrease in void fraction in the downcomer. The maximum void fraction was estimated to be 56.5% at 150 s. It is noted from the D4 data that a large amount of vapor existed in the downcomer for a long time even after HPCS actuation.

The differential pressure, D5, between the top and bottom of the pressure vessel is the same as the sum of D1 and D2. A sudden increase and a rapid drop in D5 just after break reflects a similar behavior in the D2 data. After 8.5 s, D5 decreased less rapidly but nevertheless indicating a decrease in the pressure vessel mass inventory. D5 began to increase gradually after about 170 s due to HPCS actuation at 94 s. The rate of increase for D5 was 22.8 Pa/s, which is calculated to be less than the rate expected from the HPCS injection, at a rate of 8.3×10^{-4} m^3/s (see Fig. 5.37). This means that a part of HPCS injection flow went into the downcomer and leaked out through the main steam line break for a long time even after most of the fuel rods had been quenched. The collapsed water levels inside and outside the core shroud estimated from the differential pressure data are shown in Figs. 5.176 and 5.177 and will be discussed shortly.

Figures 5.10 through 5.52 show differential pressure data in the pressure vessel and recirculation line, which represent primarily the changes in the flow rate and mass inventory. Rapid decreases in differential pressure shown in these figures immediately after break indicate flow stagnation caused by the recirculation pump coast down. The coolant in the recirculation line began to flash at 4.2 s after break and the transient differential pressure data, D16 (Fig. 5.15), D17 (Fig. 5.16), and D21 (Fig. 5.18) show decreases in the mass inventory. After HPCS actuation at 94 s, D21 began to decrease indicating gradual accumulation of coolant at the jet pump discharge piping. On the other hand, D16 and D17 decreased to very small values indicating that a small quantity of coolant remained in the recirculation line.

Figures 5.29 through 5.33 show the differential pressures measured across the core inlet orifices of the four channel boxes and the bypass hole simulating a leakage path from the lower plenum to the guide tube in BWR/6. At steady state before the break, the differential pressure across the core inlet orifice of the peak power channel A is slightly lower than those of the average power channels due to larger vapor generation rate in channel A. The differential pressures dropped to small values immediately after break due to flow stagnation. At the time of lower plenum flashing (4.2 s), the differential pressure increased temporarily. The differential pressure across the bypass hole show negative values indicating a downward flow through the bypass hole. The negative values after 105 s indicate a downward flow caused by the HPCS water accumulating in the core bypass.

The collapsed water levels in the upper and the lower regions of the downcomer are estimated from the corresponding differential pressure data and shown in Figure 5.35. The collapsed water level in the upper downcomer (between 3.90m EL and 6.04m EL) stayed above the L1 level (4.25m EL) throughout the transient, while the water level in the downcomer (between 0.938m EL and 3.90m EL) decreased after 4.2 s indicating generation of a large amount of steam due to flashing. The steam generated due to flashing of the coolant in the lower downcomer contributed to the water hold up in the upper downcomer. Continuous flashing and high water level in the downcomer are uniquely observed in the MSL break test. The collapsed water level in the upper downcomer decreased to the L2 level at 71 s after break and continued to further decrease slowly. But the rate of decrease was slowed down due to the actuation of HPCS at 94 s, and the water level started to recover at about 370 s. The lowest level reached in the upper downcomer was 4.28m EL, which is still above the L1 level (4.25m EL). As a result, LPCS and LPCI were not actuated in RUN 952.

Figures 5.176 and 5.177 show the collapsed water level in the pressure vessel. The collapsed water level inside the core shroud was estimated from the differential pressure data shown in Fig. 5.9 assuming no friction and acceleration terms. The total water head in the downcomer was obtained by adding the collapsed water levels in the upper and lower regions of the downcomer. It is evident from these figures, that the collapsed water level in the upper downcomer was higher than the water level inside the core shroud, however, the total downcomer head approached the water level inside the core shroud after HPCS actuation. HPCS injection increased the mass inventory inside the core shroud and decreased the difference in the water level inside and outside the core shroud.

6.3 Coolant Flow Rate

The steam flow rate in the MSL, as well as HPCS and feedwater flow rates were measured in RUN 952. Figure 5.36 shows the steam mass flow rates measured by the high range and high-high range orifice flow meters. The steam flow rate was initially at 2.06 kg/s, but increased instantaneously to 4.92 kg/s at the initiation of break and subsequently decreased following the system pressure transient shown in Fig. 5.1. These steam flow rates are slightly lower than the break flow rate measured with the drag disk and gamma densitometer in the break unit (see Fig. 5.164). Figure 5.37 shows the HPCS flow rate. HPCS was actuated at 94 s after break at the system pressure of 2.23 MPa. HPCS was triggered by the L2 level signal in the upper downcomer with a time delay of 27 s. The HPCS flow rate was steady at 0.83×10^{-3} m^3/s (0.83 kg/s). The actuation time of 94 s is slightly earlier than the time estimated from the collapsed water level reaching the L2 level and a time delay of 27 s (see Fig. 5.35). This discrepancy may be attributed to fluctuations in the water level data.

Figure 5.38 shows the feedwater flow rate. The average steady flow rate was equal to 2.44×10^{-3} m^3/s (2.04kg/s). The feedwater flow started to decrease at 1.3 s after break and was terminated completely at 4.2 s. A large spike appeared in the flow rate at about 95 s indicating the flashing of the feedwater remaining in the feedwater line at a system pressure of 2.22 MPa.

The volumetric flow rates through the jet pumps and the main recirculation pumps are shown in Figures 5.39 through 5.41. The flow rates dropped to near zero immediately after break following the pump coast down and remained near zero thereafter.

Figures 5.42 through 5.52 show the differential pressures measured across the orifice or venturi flow meters in the MSL, jet pumps and recirculation pumps. These pressure drop data were used to calculate the flow rates in the respective locations shown previously.

6.4 Process Control

There are two electric power supply systems used to heat up the core, namely A system (2.1 MW max.) for the peak power channel A, and the B system (3.15MW max.) for the other three average power channels, B, C, and D. The power transients of A and B systems are shown in Fig. 5.53. Initial power was 1.262 MW for the system A and 3.70 MW for system B. The corresponding maximum linear heat rates of heater rods are shown in Table 4.1. The radial and axial power distributions in the core are shown in Figs. 2.6 and 2.7. The steady state power was maintained for the first 9.0 s after break and then reduced along the decay curve shown in Fig. 4.2.

The coast down characteristics of the main recirculation pumps are shown in Fig. 5.54. The coast down was initiated at the time of break and completed in about 10 s for both pumps.

The on-off signals indicating the operation of valves, ECCS and the main recirculation pumps are shown in Fig. 5.55 through 5.57. Only the HPCS is seen to be actuated at 94 s.

6.5 Density and Momentum Flux

Fluid density was measured by using two-beam and three-beam gamma densitometers.

Figures 5.58 through 5.63 show the fluid density data of beams A, B, and C at a location downstream of jet pumps 1,2 and jet pumps 3,4, respectively. These data indicate that the fluid density decreased due to steam generation after the initiation of flashing at 4.2 s until 130 s and increased thereafter due to the arrival of HPCS water. Flow separation is also indicated in these figures.

Figures 5.64 and 5.65 show the fluid density data of beams A and B at the break. The densities before break were nearly 1000 kg/m^3, because the steam that leaked out through AV165 was condensed and accumulated at the cooler measurement location far downstream of the MSL. Immediately after the break, steam began to pass through the measurement location. Pressure and fluid temperature at the break unit were 7.28 MPa and 501 K prior to the break initiation, 1.04 MPa and 447 K at 100 s after break and 0.37 MPa and 433 K at 300 s after break.

Figures 5.66 through 5.68 show the momentum fluxes measured at the jet pump outlet and the break. The break flow is seen to gradually decrease with time.

6.6 Coolant Temperature

The coolant temperatures measured at various parts of the pressure vessel and recirculation loops except at the core inlet and outlet are shown in Figs. 5.69 through 5.81. The data show a gradual decrease that corresponds to the rate of system depressurization.

The fluid temperatures at the core inlet and outlet, and at lower plenum are shown in Figs. 5.127 through 5.145. The temperature of the fluid entering the core decreases gradually following the saturation temperature corresponding to the system pressure. The fluid exiting the core, however, shows superheating during the period of core dryout.

6.7 Fuel Rod Surface Temperature

Fuel rod surface temperatures were measured by CA thermocouples of 1.0 mm O.D. imbedded in the fuel rod sheath made of Inconel 600. Figures 5.82 through 5.89 show the fuel rod surface temperatures of the rods A11, A12, A13, A22, A33, A77, A87 and A88 in the peak power channel A. Each fuel rod has seven thermocouples along the axial direction.

Figures 5.90 through 5.98 show the surface temperatures of the fuel rods B11, B22, B77, C11, C13, C22, C33, C77 and D22 in the average power channels. The surface temperatures of water rod simulators, A45 and C45, and the outer surface temperatures of the channel box A are shown in Figs. 5.99 through 5.101. The upper part of the water rod simulators experienced a temperature increase due to heat transfer during the fuel rod dryout. On the other hand, the channel box temperature was not affected by the dryout of fuel rods. The temperatures of different fuel rods at the same elevation are compared in Figs. 5.103 through 5.128. The peak cladding temperature (PCT) in RUN 952 was 752 K (479 C) observed at 108 s after break at position 4 of the A31 rod.

Following observations have been obtained from the fuel rod surface temperature data. (1) Temporary dryout occurred at the upper part (pos.

1-3) of channel A between 10 and 20 s after break due to the higher power in channel A than the other channels. This temporary dryout was not observed in the average power channels B, C and D. The surfaces of the fuel rods in channel A were shortly rewetted due to cooling effected by the lower plenum flashing which started to occur at 4.2 s after break. Total head in downcomer was lower than that in the core shroud during the lower plenum flashing. The pressure in the downcomer was higher than that in the core shroud resulting in a flow from the downcomer to the core. (2) The dryout of core due to the fall in water level was initiated at approximately 26 s after break in channels B, C, D and 40 s after break in the peak power channel A. Temperature rise was observed at position 5 and above. After HPCS injection at 94 s, the core was soon quenched from the bottom. The upper part of the core (ie. pos. 1-3) was cooled by the fall back of water supplied by HPCS and accumulating in the upper plenum. The fuel rods were not uncovered and exposed to the steam environment at positions 6 and 7. (3) The core was quenched at 231 s after break with the water supplied by HPCS except for pos. 4 of the rods A31, A68, A71, A82, and A88 (see sec. 6.10). The dryout and quench fronts of these fuel rods will be shown and discussed in the next section.

6.8 Liquid Level

Liquid levels in the pressure vessel were detected by the conduction probes (CP). Figures 5.146 through 5.148 show conduction probe signals obtained at the inner surfaces of channel boxes A, B, and C. Seven conduction probes are attached axially on the channel box wall. Liquid level fall and its recovery in each channel are clearly shown in these figures. The signals show that at positions 6 and 7, the fuel rods did not dryout. This result is consistent with the fuel rod surface temperature data described in sec. 6.7.

Figures 5.150 through 5.153 show the conduction probe signals near the outlet of channels A and C. Figures 5.154 and 5.155 show the signals obtained at the inlet of the same channels. It is shown in these figures that a clear liquid level was not formed in the core inlet, but two-phase mixture with high void fraction existed in the upper part of the core. Figure 5.156 shows the CP signals at the north side of the lower plenum. Figures 5.157 and 5.158 show the signals in the guide tube and the downcomer, respectively. These data indicate that the lower plenum, guide tube and the lower part of the downcomer (0.525m - 3.325 m EL) were not exposed to the steam environment throughout the whole test. It is also shown from these signals that the steam generation was vigorous in the downcomer compared to that in the lower plenum and the guide tube.

The liquid level transients estimated from the liquid level signals shown in Figs. 5.146 through 5.157 are presented in Fig. 5.158 for the upper plenum and core. Following can be observed from this figure. (1) The core uncovery started at 25 s in the average channel C and at 41 s in the peak power channel A. However, the uncovery times of channels A and C between pos. 3 and 5 are nearly the same. (2) After HPCS actuation, the liquid level in the peak power channel A rose immediately and reached pos. 1 at 120 s. On the other hand, the liquid level in the average power channel C rose slowly and arrived at pos. 1 at 187 s.

Figures 5.159 and 5.160 show the dryout and quench front movement in channels A and C, respectively, which are estimated from the heater rod surface temperature transients shown earlier. The liquid level data shown in Fig. 5.158 are also duplicated for comparison. It is clear from these figures that the propagation of the dryout front corresponds to the fall in the core liquid level.

6.9 Density, Momentum Flux and Break Flow

Figures 5.161 through 5.163 show the average fluid densities downstream of the jet pumps and at the break. The average densities were obtained by weighted averaging of the chordal density data shown in Figs. 5.58 through 5.65. The flow rate at the break, namely the discharge flow through the MSL, is calculated from the average density and the momentum flux measured with the high range drag disk as shown in Fig. 5.164.

The steam discharge flow through the MSL was also measured at a location upstream of the orifice, OR-5, by orifice flow meters as shown in Fig. 5.165. The flow rates measured by the orifice and drag disk show similar trends through the transient, however, the orifice flow meter data are not reliable, because a single-phase vapor flow was assumed throughout the test during conversion to the mass flow rate.

Mass flow rates in the core and recirculation loops are calculated from the orifice flow meter data and are shown in Figs. 5.166 through 5.175. The coolant flow through the core inlet decreased rapidly after break and stagnated throughout the test, however, large oscillations are observed after about 200 s as shown in Fig. 5.171. The flow through the recirculation loops also dropped rapidly after break due to the pump coast down. The values shown are, however, not quantitatively accurate during the two-phase flow conditions which prevailed following the initiation of lower plenum flashing.

The collapsed liquid levels in the downcomer and the core shroud are shown in Figs. 5.176 and 5.177. From these figures, the coolant inventory in the downcomer and inside the core shroud as well as the total coolant inventory are calculated and shown in Figs. 5.178 through 5.180. The coolant inventory in the pressure vessel decreased steadily after break until the liquid level in the downcomer dropped to the L2 level and the

HPCS was actuated at 94 s. Thereafter, the coolant inventory started to increase inside the core shroud leading to quenching of the whole core at 231 s after break.

It should be noted that due to the effectiveness of HPCS in reflooding the core, the liquid level in the downcomer did not fall below the L1 level and LPCI and LPCS were not actuated. Although this result demonstrates the effectiveness of HPCS in recovering the partially uncovered core with the coolant and limiting the peak cladding temperature to 752 K, which is well below the regulatory PCT limit of 1473 K, long term cooling of the core was not entirely satisfactory as discussed in the next section.

6.10 Re-Dryout at the Mid-plane of Core

The whole core was quenched at 231 s after break in RUN 952, except for certain locations in channel A. Figure 5.181 shows the fuel rod surface temperatures at pos. 4 of the rods A31, A68, A71, A82 and A88, and those of the rods A11 and A77 are also shown for comparison. Surface temperatures of A31, A68, A71, A82 and A88 decreased following the HPCS actuation at 94 s after break, but began to rise again. Thereafter, the surface temperatures at these locations remained above the saturation temperature until manual activation of LPCI was made at 1017 s after break. This local re-dryout behavior after quench has not been observed in the previous ROSA-III tests.

It is noted that these five rods are located in the peripheral region of the peak power channel A having a local peaking factor of 1.1 and that pos. 4 corresponds to the peak of the axial power distribution. By comparing the surface temperatures of the A87 and A88 rods at pos. 4 (see Figs. 5.88 and 5.89), the phenomenon is seen to be localized to the peak power locations. Locally high void fraction, relatively lower fluid velocity compared with that in the center of bundle and high linear heat rate are considered to be the cause of re-dryout.

Although the increases in fuel rod temperature during the period of re-dryout were not severe enough to be of great concern, this phenomenon points out a slight deficiency in long term cooling of the core with only the HPCS actuation. As described in section 4, a pressure increase in the drywell can actuate the ECCS in an actual BWR. Unless a failure occurs in the drywell pressure logic, LPCS and LPCI would supply the emergency coolant when the system pressure drops below the respective set points and are expected to provide sufficiently effective core cooling over the long term. However, if this logic fails during a MSL break LOCA, LPCS and LPCI may not be actuated due to the high water level in the downcomer, leading to the local re-dryout of the core just as in this test. The consequences of such a local re-dryout phenomenon can not be precisely determined for a BWR.

7. Comparison of MSL and Recirculation Line Break Tests

The system behavior for a MSL break test, RUN 952, has been described in the previous section through examination of the experimental data. Gradual system depressurization, continuous flashing in the pressure vessel, and high water level in the downcomer have been observed to characterize the MSL break LOCA.

In this section, the present results are compared with those of a 200% double-ended break test, RUN 901, to determine the differences in system behavior between the MSL and recirculation line break tests.[6]

The initial conditions and sequence of major events from these two tests are compared in Table 7.1. RUN 901 was selected for comparison because the total break area is similar to that used in RUN 952. The break area for RUN 952 is calculated to be 754.8 mm^2. For RUN 901, because of the flow area restriction at the jet pump upstream of the break orifice, the total break area is calculated to be 650.0 mm^2.

The lower plenum pressure histories are compared in Fig. 7.1. A gradual decay in pressure is observed in both tests, however, the rate of decrease is somewhat different. For RUN 901, it is slower in the early period, but faster afterwards than in RUN 952. A small peak due to repressurization is observed in RUN 901 following the MSIV closure, but not in RUN 952.

The differential pressure between the top and bottom of the core is shown in Fig. 7.2. This comparison shows a similar decrease in the pressure vessel mass inventory in the early period, but after the LPCS and LPCI are actuated in RUN 901, the mass inventory increases rapidly in comparison with RUN 952.

The steam flow rate in the main steam line is totally different between the two tests as shown in Fig. 7.3. This is expected due to the difference in the break locations. The feedwater flow rate, shown in Fig. 7.4, indicates more frequent flashing of the fluid in the feedwater line in RUN 901.

The major difference between the two tests is seen in the collapsed water level behavior and the mass inventory in the downcomer and core as shown in Figs. 7.5 through 7.8. The collapsed water levels in both the upper and lower downcomer show a rapid decrease soon after break in RUN 901. On the other hand, the decrease is more gradual and the water level remains at a much higher level in RUN 952. This difference is also reflected in the mass inventory in the downcomer as shown in Fig. 7.6, and led to the differences in the ECCS actuation and subsequent system behavior in the two tests.

The water level inside the core shroud decreased much faster but also recovered much earlier in RUN 901 than in RUN 952, due to the actuation of LPCS and LPCI. The core mass inventory in RUN 952 could not recover to the original level with only the HPCS injection, and this probably led to the re-dryout phenomenon as described in the previous section. The ECCS flow rates are compared in Fig. 7.10.

The flow inside the core is seen in Fig. 7.9 to be stagnated in both tests. Finally, the surface temperatures of the fuel rod, A31 in RUN 952 and A11 in RUN 901, that recorded the PCT respectively are compared in Fig. 7.11. In RUN 901, the PCT of 780 K occurred shortly after break, following the core dryout during the blowdown phase. In RUN 952, the PCT of 752 K was reached soon after the HPCS injection and its magnitude was less than that recorded in RUN 901.

8. Conclusions

RUN 952 is a 100% Main Steam Line (MSL) break test with full ECCS actuation logic conducted as a reference MSL break test in the ROSA-III program. Most of the instrumentation performed satisfactorily. The following is a summary of the major findings obtained through the examination of the present test results.

(1) The system pressure decreased monotonously after the break initiation. The rate of depressurization also decreased gradually with time. The steam discharge rate through the main steam line break decreased with time in response to the transient decay in the system pressure. Continuous depressurization led to fairly high void fraction in the downcomer which sustained the upper downcomer water level rather high. The void fraction in the lower downcomer increased up to 40-60% during the time period between 20 s and 820 s. The collapsed water level in the upper downcomer decreased to the L2 level at 71 s and HPCS was actuated at 94 s after break. The water level never dropped below the L1 level, therefore, LPCS and LPCI were not actuated in RUN 952 in spite of the decrease in the system pressure below the LPCS/LPCI injection pressure set points. The lowest point that the collapsed water level reached in the downcomer was 4.28 m, however, the level inside the core shroud dropped further below during the blowdown phase. The difference in water levels between the upper downcomer and the core decreased after HPCS injection as the water level gradually rose inside the core.

(2) The core uncovery started from the top of the core at 26 s after break in the average power channels and at 40 s in the peak power channel due to a decrease in the core mass inventory. The part of the core below position 6 was not uncovered due to the effectiveness of HPCS in

refilling the core. The whole core was quenched at 231 s after break and within 137 s after the HPCS actuation. In the peak power channel, however, the fuel surface temperatures at position 4 of the fuel rods in the peak power channel remained above the saturation temperature even after the entire core was once quenched. This phenomenon is considered to be due to the local void distribution and peaking of the heater power at these locations. The peak cladding temperature (PCT) of 752 K occurred at position 4 of the A31 fuel rod at 108 s after break.

In comparison with the recirculation line break test, RUN 901, the present MSL break test results showed several different characteristics in the system response. Although the difference in the total break area was not too large between the two tests, the coolant was lost at a significantly slower rate during the blowdown phase in the MSL break test. Consequently, the system pressure decreased gradually except for the early blowdown phase and continuous flashing of the coolant occurred in the pressure vessel and in the recirculation line throughout the test. This resulted in a larger liquid hold up and high collapsed water level in the downcomer. This in turn caused a delay in the actuation of HPCS and prevented the actuation of LPCS and LPCI and led to a smaller mass inventory in the core even after the whole core was quenched.

Acknowledgment

The authors are grateful to H. Murata of the Ship Research Institute, Ministry of Transport, for the support work done on the data analysis. We are also grateful to M. Okazaki of the Institute of Nuclear Safety, Japan, Y. Koizumi of JAERI, and M. Iriko of Computer Services Co. for their contributions to the present test program. Finally, we wish to thank H. Asahi, T. Odaira, T. Takayasu, S. Sekiguchi, Y. Kitano and T. Numata of Nuclear Engineering Corporation for their assistance in conducting the experiment and H. Gotoh of Information System Laboratory Corporation for preparing the data plots.

References

(1) ANODA, Y., et al., "ROSA-III System Descripiton for Fuel Assembly No. 4", JAERI-M 9363 (1981).

(2) SOBAJIMA, M., et al., "Instrumentation and Data Processing for ROSA-III Test" (in Japanese), JAERI-M 8499 (1979).

(3) ABE, N., et al., "Electric Power Transient Curve for ROSA-III Tests", JAERI-M 8728 (1980).

(4) "General Electric Standard Safety Analysis Report, BWR/6", DOCKET-STN-50531-22, General Electric Company.

(5) "BWR Blowdown Emergency Core Cooling Program, Preliminary Facility Description Report for the BT/ECCIA Test Phase", GEAP-23592, NRC-2 (1977).

(6) NAKAMURA, H., et al., "ROSA-III 200% Double-Ended Break Integral Test RUN 901 (Full ECCS Actuation)", JAERI-M 84-007 (1984).

Acknowledgment

The authors are grateful to H. Murata of the Ship Research Institute, Ministry of Transport, for the support work done on the data analysis. We are also grateful to M. Okazaki of the Institute of Nuclear Safety, Japan, Y. Koizumi of JAERI, and M. Iriko of Computer Services Co. for their contributions to the present test program. Finally, we wish to thank H. Asahi, T. Odaira, T. Takayasu, S. Sekiguchi, Y. Kitano and T. Numata of Nuclear Engineering Corporation for their assistance in conducting the experiment and H. Gotoh of Information System Laboratory Corporation for preparing the data plots.

References

(1) ANODA, Y., et al., "ROSA-III System Descripiton for Fuel Assembly No. 4", JAERI-M 9363 (1981).

(2) SOBAJIMA, M., et al., "Instrumentation and Data Processing for ROSA-III Test" (in Japanese), JAERI-M 8499 (1979).

(3) ABE, N., et al., "Electric Power Transient Curve for ROSA-III Tests", JAERI-M 8728 (1980).

(4) "General Electric Standard Safety Analysis Report, BWR/6", DOCKET-STN-50531-22, General Electric Company.

(5) "BWR Blowdown Emergency Core Cooling Program, Preliminary Facility Description Report for the BT/ECCIA Test Phase", GEAP-23592, NRC-2 (1977).

(6) NAKAMURA, H., et al., "ROSA-III 200% Double-Ended Break Integral Test RUN 901 (Full ECCS Actuation)", JAERI-M 84-007 (1984).

Table 2.1 Primary Charecteristics of ROSA-III and BWR/6

	BWR*	ROSA-III	BWR/ROSA-III
Number of Recirc. Loops	2	2	1
Number of Jet Pumps	24	4	6
Number of Separators	251	1	251
Number of Fuel Assemblies	848	4	212
Active Fuel Length (m)	3.76	1.88	2
Total Volume (m^3)	621	1.42	437
Power (MW)	3,800	4.40	864
Pressure (MPa)	7.23	7.23	1
Core Flow (kg/s)	1.54×10^4	36.4	424
Recirculation Flow (l/s)	2,970	7.01	424
Feedwater Flow (kg/s)	2,060	4.86	424
Feedwater Temp. (K)	489	489	1

* BWR/6-251

Table 3.1 ROSA-III Instrumentation Summary List

ITEM	SENSOR	NUMBER	NOTE
Pressure	Pressure Transducer	20	
Differential Pressure	DP Cell	60	PV and Loop 44 Level Measurement 5 Flow Meter 11
Fluid Temperature	CA Thermocouple	85	Primary Loop 23 DTT 4 Tie Rod 28 Upper Plenum 10 Lower Plenum 10 Tie Plate 40 Bypass 14
Fuel Rod Temperature	CA Thermocouple	133	
Slab Surface Temperature	CA Thermocouple	7	Core Barrel 24 Pressure Vessel 3 Channel Box 35 Shroud Support 8
Slab Inner Temperature	CA Thermocouple	0	JP Diffuser 4 PV Wall 5
Volumetric Flow Rate	Turbine Flow Meter Venturi Flow Meter Orifice Flow Meter	3 4 6	ECCS Loop 3 Primary Loop 10
Mass Flow Rate	Turbine Flow Meter Orifice Flow Meter	4 3	Recirculation Loop 4 Main Steam Line 3
Liquid Level	Conductivity Probe Capacitance Probe	56 0	
Density	Gamma Densitometer	10	2 Beam GD 2 3 Beam GD 2
Momentum Flux	Drag Disk	7	JP Spool Piece 2 Break Spool Piece 4 Break Orifice 1
Signal	ON/OFF Switch	14	
Pump Speed	Revolution Counter	2	
Electric Core Power	VA Meter	2	
TOTAL		416	

Table 3.2 Measurement List for RUN 952

1Ch.- 50Ch.

Ch.	Item	Symbol	ID.		Location	Fig.No.	Range			Unit	Accuracy
1	Press.	P- 1	PA	1	Lower Plenum	Fig.5. 1	0.100	-	10.0	MPa	1.08%FS
2	Press.	P- 2	PA	2	Upper Plenum	Fig.5. 1	0.100	-	10.0	MPa	1.08%FS
3	Press.	P- 3	PA	3	Steam Dome	Fig.5. 1,5. 4	0.100	-	10.0	MPa	1.08%FS
4	Press.	P- 4	PA	4	Downcomer Bottom	Fig.5. 1	0.100	-	10.0	MPa	1.08%FS
5	Press.	P- 5	PA	5	JP-3 Drive	Fig.5. 2	0.100	-	10.0	MPa	1.08%FS
6	Press.	P- 6	PA	6	JP-4 Drive	Fig.5. 2	0.100	-	10.0	MPa	1.08%FS
7	Press.	P- 7	PA	7	JP-3 Suction	Fig.5. 2	0.100	-	10.0	MPa	1.08%FS
8	Press.	P- 8	PA	8	JP-4 Suction	Fig.5. 2	0.100	-	10.0	MPa	1.08%FS
9	Press.	P- 9	PA	9	MRP-1 Suction	Fig.5. 3	0.100	-	10.0	MPa	1.08%FS
10	Press.	P-10	PA	10	MRP-2 Suction	Fig.5. 3	0.100	-	10.0	MPa	1.08%FS
11	Press.	P-11	PA	11	MRP-2 Delivery	Fig.5. 3	0.100	-	10.0	MPa	1.08%FS
12	Press.	P-12	PA	12	Break Steam Line	Not Measured	0.100	-	10.0	MPa	1.08%FS
13	Press.	P-13	PA	13	Break A Downstream	Not Used	0.100	-	10.0	MPa	1.08%FS
14	Press.	P-14	PA	14	Break B Downstream	Fig.5. 4	0.100	-	10.0	MPa	1.08%FS
15	Press.	P-15	PA	15	Break B Downstream	Fig.5. 4	0.100	-	10.0	MPa	1.08%FS
16	Press.	P-16	PA	16	Steam Line	Failure	0.100	-	10.0	MPa	1.08%FS
17	Press.	P-17	PA	17	JP-1,2 Outlet Spool	Fig.5. 5	0.100	-	10.0	MPa	1.08%FS
18	Press.	P-18	PA	18	JP-3,4 Outlet Spool	Fig.5. 5	0.100	-	10.0	MPa	1.08%FS
19	Press.	P-19	PA	19	Break A Spool Piece	Not Used	0.100	-	10.0	MPa	1.08%FS
20	Press.	P-30	PA	20	Break B Spool Piece	Fig.5. 4	0.100	-	10.0	MPa	1.08%FS
21	Diff.P.	D- 1	PD	21	Lower Pl.-Upper Pl.	Fig.5. 6	-50.0	-	350.	kPa	0.63%FS
22	Diff.P.	D- 2	PD	22	Upper Pl.-Steam Dome	Fig.5. 7	-10.0	-	90.0	kPa	0.63%FS
23	Diff.P.	D- 3	PD	23	Lower Plenum Head	Not Measured					
24	Diff.P.	D- 4	PD	24	Downcomer Head	Fig.5. 8	0.0	-	100.	kPa	0.63%FS
25	Diff.P.	D- 5	PD	25	PV Bottom-Top	Fig.5. 9	-100.	-	900.	kPa	0.63%FS
26	Diff.P.	D- 6	PD	26	JP-1 Disch.-Suction	Fig.5.10	-100.	-	300.	kPa	0.63%FS
27	Diff.P.	D- 7	PD	27	JP-1 Drive -Suction	Fig.5.11	0.0	-	2.50	MPa	0.63%FS
28	Diff.P.	D- 8	PD	28	JP-2 Disch.-Suction	Fig.5.10	-100.	-	300.	kPa	0.63%FS
29	Diff.P.	D- 9	PD	29	JP-2 Drive -Suction	Fig.5.11	0.0	-	2.50	MPa	0.63%FS
30	Diff.P.	D-10	PD	30	JP-3 Disch.-Suction	Fig.5.12	-100.	-	300.	kPa	0.63%FS
31	Diff.P.	D-11	PD	31	JP-3 Drive -Suction	Fig.5.13	-4.00	-	2.00	MPa	0.63%FS
32	Diff.P.	D-12	PD	32	JP-4 Disch.-Suction	Fig.5.12	-100.	-	300.	kPa	0.63%FS
33	Diff.P.	D-13	PD	33	JP-4 Drive -Suction	Fig.5.13	-4.00	-	2.00	MPa	0.63%FS
34	Diff.P.	D-14	PD	34	MRP-1 Deliv.-Suction	Fig.5.14	-0.100	-	2.50	MPa	0.63%FS
35	Diff.P.	D-15	PD	35	MRP-2 Deliv.-Suction	Fig.5.14	-0.100	-	2.50	MPa	0.63%FS
36	Diff.P.	D-16	PD	36	DC Bottom- MRP-1 Suc.	Fig.5.15	-50.0	-	50.0	kPa	0.63%FS
37	Diff.P.	D-17	PD	37	MRP1 Deliv.-JP1 Drive	Fig.5.16	0.0	-	250.	kPa	0.63%FS
38	Diff.P.	D-18	PD	38	MRP1 Deliv.-JP2 Drive	Fig.5.16	0.0	-	250.	kPa	0.63%FS
39	Diff.P.	D-19	PD	39	DC Middle-JP1 Suction	Fig.5.17	0.0	-	250.	kPa	0.63%FS
40	Diff.P.	D-20	PD	40	DC Middle-JP2 Suction	Fig.5.17	0.0	-	250.	kPa	0.63%FS
41	Diff.P.	D-21	PD	41	JP1 Disch.-Lower Pl.	Fig.5.18	-100.	-	100.	kPa	0.63%FS
42	Diff.P.	D-22	PD	42	JP2 Disch.-Lower Pl.	Fig.5.18	-100.	-	100.	kPa	0.63%FS
43	Diff.P.	D-23	PD	43	DC Bottom- Break B	Fig.5.19	0.0	-	7.00	MPa	0.63%FS
44	Diff.P.	D-24	PD	44	Break B- Break A	Not Used	0.0	-	100.	kPa	0.63%FS
45	Diff.P.	D-25	PD	45	Break A- MRP2 Suction	Not Measured	-500.	-	100.	kPa	0.63%FS
46	Diff.P.	D-26	PD	46	MRP2 Deliv.-JP3 Drive	Fig.5.20	-500.	-	500.	kPa	0.63%FS
47	Diff.P.	D-27	PD	47	MRP2 Deliv.-JP4 Drive	Fig.5.20	-500.	-	500.	kPa	0.63%FS
48	Diff.P.	D-28	PD	48	DC Middle-JP3 Suction	Fig.5.21	-250.	-	250.	kPa	0.63%FS
49	Diff.P.	D-29	PD	49	DC Middle-JP4 Suction	Fig.5.21	-250.	-	250.	kPa	0.63%FS
50	Diff.P.	D-30	PD	50	JP3 Disch.-Confluence	Fig.5.22	-100.	-	100.	kPa	0.63%FS

Table 3.2 Measurement List for RUN 952 (Continued)

51Ch.- 100Ch.

Ch.	Item	Symbol	ID.		Location	Fig.No.	Range	Unit	Accuracy
51	Diff.P.	D-31	PD	51	JP4 Disch.-Confluence	Fig.5.22	-100. - 100.	kPa	0.63%FS
52	Diff.P.	D-32	PD	52	Confluence -Lower Pl.	Fig.5.23	-50.0 - 50.0	kPa	0.63%FS
53	Diff.P.	D-33	PD	53	Lower Pl.-DC Middle	Fig.5.24	-250. - 250.	kPa	0.63%FS
54	Diff.P.	D-34	PD	54	Lower Pl.-DC Bottom	Fig.5.25	-250. - 250.	kPa	0.63%FS
55	Diff.P.	D-35	PD	55	DC Bottom-DC Middle	Fig.5.26	-50.0 - 50.0	kPa	0.63%FS
56	Diff.P.	D-36	PD	56	DC Middle-Steam Dome	Fig.5.27	-50.0 - 50.0	kPa	0.63%FS
57	Diff.P.	D-37	PD	57	Lower Pl.Mid-Upper PL	Not Measured			
58	Diff.P.	D-38	PD	58	Lower Pl.Bottom-middle	Fig.5.28	0.0 - 50.0	kPa	0.63%FS
59	Diff.P.	D-39	PD	59	Upper Pl. Head	Not Used	-20.0 - 100.	kPa	0.63%FS
60	Diff.P.	D-40	PD	60	Channel Orifice A	Fig.5.29	-50.0 - 50.0	kPa	0.63%FS
61	Diff.P.	D-41	PD	61	Channel Orifice B	Fig.5.30	-50.0 - 50.0	kPa	0.63%FS
62	Diff.P.	D-42	PD	62	Channel Orifice C	Fig.5.31	-25.0 - 75.0	kPa	0.63%FS
63	Diff.P.	D-43	PD	63	Channel Orifice D	Fig.5.32	-50.0 - 50.0	kPa	0.63%FS
64	Diff.P.	D-44	PD	64	Bypass Hole	Fig.5.33	-100. - 100.	kPa	0.63%FS
65	Level	WL- 1	LM	65	HPCS Tank	Fig.5.34	0.0 - 2.30	m	1.00%FS
66	Level	WL- 2	LM	66	LPCS Tank	Fig.5.34	0.0 - 2.30	m	1.00%FS
67	Level	WL- 3	LM	67	LPCI Tank	Fig.5.34	0.0 - 4.25	m	1.00%FS
68	Level	WL- 4	LM	68	Pressure Vessel	Fig.5.35	3.90 - 6.04	m	1.00%FS
69	Level	WL- 5	LM	69	Downcomer	Fig.5.35	0.938 - 3.90	m	1.00%FS
70	Mass.F.	F- 1	FM	70	Steam Line (Low Range)	Not Measured	0.0 - 1.13	kg/s	0.92%FS
71	Mass.F.	F- 2	FM	71	Steam Line(High Range)	Fig.5.36	0.0 - 3.00	kg/s	0.92%FS
72	Mass.F.	F- 3	FM	72	Steam Line (High-High)	Fig.5.36	0.0 - 14.3	kg/s	1.40%FS
73	Vol.F.	F- 7	FV	73	HPCS (Upper Plenum)	Fig.5.37	0.0 - 0.250E-02	m3/s	0.79%FS
74	Vol.F.	F- 9	FV	74	LPCS (Upper Plenum)	Fig.5.37	0.0 - 0.250E-02	m3/s	0.79%FS
75	Vol.F.	F-11	FV	75	LPCI (Core Bypass)	Fig.5.37	0.0 - 0.830E-02	m3/s	0.79%FS
76	Vol.F.	F-15	FV	76	Feedwater	Fig.5.38	0.0 - 0.100E-01	m3/s	0.79%FS
77	Vol.F.	F-16	FV	77	HPWP Suction	Not Measured	0.0 - 0.420E-02	m3/s	0.79%FS
78	Vol.F.	F-17	FV	78	JP1 Discharge	Fig.5.39	0.0 - 0.170E-01	m3/s	0.88%FS
79	Vol.F.	F-18	FV	79	JP2 Discharge	Fig.5.39	0.0 - 0.170E-01	m3/s	0.88%FS
80	Vol.F.	F-19	FV	80	JP3 Disch. Positive	Fig.5.40	0.0 - 0.170E-01	m3/s	0.92%FS
81	Vol.F.	F-20	FV	81	JP3 Disch. Negative	Not Measured	0.0 - 0.500E-02	m3/s	0.92%FS
82	Vol.F.	F-21	FV	82	JP4 Disch. Positive	Fig.5.40	0.0 - 0.170E-01	m3/s	0.92%FS
83	Vol.F.	F-22	FV	83	JP4 Disch. Negative	Not Measured	0.0 - 0.500E-02	m3/s	0.92%FS
84	Mass.F.	F-23	FM	84	JP1,2 Outlet Spool	Not Measured	0.0 - 30.0	kg/s	1.40%FS
85	Mass.F.	F-24	FM	85	JP3,4 Outlet Spool	Not Measured	0.0 - 30.0	kg/s	1.40%FS
86	Mass.F.	F-25	FM	86	Break A Spool Piece	Not Measured	0.0 - 30.0	kg/s	1.40%FS
87	Mass.F.	F-26	FM	87	Break B Spool Piece	Not Measured	0.0 - 30.0	kg/s	1.40%FS
88	Vol.F.	F-27	FV	88	MRP-1	Fig.5.41	0.0 - 0.120E-01	m3/s	0.88%FS
89	Vol.F.	F-28	FV	89	MRP-2	Fig.5.41	0.0 - 0.120E-01	m3/s	0.63%FS
90	Diff.P.	D-F1	PD	90	F1 Orifice	Fig.5.42	0.0 - 4.90	kPa	0.63%FS
91	Diff.P.	D-F2	PD	91	F2 Orifice	Fig.5.43	0.0 - 34.9	kPa	0.63%FS
92	Diff.P.	D-F3	PD	92	F3 Orifice	Fig.5.44	0.0 - 800.	kPa	0.63%FS
93	Diff.P.	D-F17	PD	93	F17 Venturi	Fig.5.45	0.0 - 98.1	kPa	0.63%FS
94	Diff.P.	D-F18	PD	94	F18 Venturi	Fig.5.46	0.0 - 98.1	kPa	0.63%FS
95	Diff.P.	D-F19	PD	95	F19 Orifice	Fig.5.47	0.0 - 147.	kPa	0.63%FS
96	Diff.P.	D-F20	PD	96	F20 Orifice	Fig.5.48	0.0 - 13.2	kPa	0.63%FS
97	Diff.P.	D-F21	PD	97	F21 Orifice	Fig.5.49	0.0 - 147.	kPa	0.63%FS
98	Diff.P.	D-F22	PD	98	F22 Orifice	Fig.5.50	0.0 - 13.2	kPa	0.63%FS
99	Diff.P.	D-F27	PD	99	F27 Venturi	Fig.5.51	0.0 - 200.	kPa	0.63%FS
100	Diff.P.	D-F28	PD	100	F28 Venturi	Fig.5.52	0.0 - 200.	kPa	0.63%FS

Table 3.2 Measurement List for RUN 952 (Continued)

101Ch.- 150Ch.

Ch.	Item	Symbol	ID.		Location	Fig.No.	Range			Unit	Accuracy
101	Power	W- 1	WE	101	2100 KW Power Supply	Fig.5.53	0.0	-	0.210E+04	KW	1.00%FS
102	Power	W- 2	WE	102	3150 KW Power Supply	Fig.5.53	0.0	-	0.315E+04	KW	1.00%FS
103						Not Used					
104	Rev.	N- 1	SR	104	MRP-1 Revolution	Fig.5.54	0.0	-	0.500E+04	RPM	1.08%FS
105	Rev.	N- 2	SR	105	MRP-2 Revolution	Fig.5.54	0.0	-	0.500E+04	RPM	1.08%FS
106	Signal	S- 1	EV	106	Break Signal A	Fig.5.55					
107	Signal	S- 2	EV	107	Break Signal B	Fig.5.55					
108	Signal	S- 3	EV	108	QSV Signal	Fig.5.55					
109	Signal	S- 6	EV	109	HPCS Valve	Fig.5.56					
110	Signal	S- 7	EV	110	LPCS Valve	Fig.5.56					
111	Signal	S- 8	EV	111	LPCI Valve	Fig.5.56					
112	Signal	S- 9	EV	112	Feedwater Control	Fig.5.55					
113	Signal	S-10	EV	113	MSIV Signal	Fig.5.55					
114	Signal	S-11	EV	114	Steam Line Valve	Fig.5.55					
115	Signal	S-12	EV	115	ADS Valve	Fig.5.56					
116	Signal	S-13	EV	116	MRP-1 Power OFF	Fig.5.57					
117	Signal	S-14	EV	117	MRP-2 Power OFF	Fig.5.57					
118	Signal	RD- 1	EV	118	MRP-1 Rev. Direction	Fig.5.57					
119	Signal	RD- 2	EV	119	MRP-2 Rev. Direction	Fig.5.57					
120	Density	DF- 1	DE	120	JP1,2 Outlet Beam A	Fig.5.58	0.0	-	0.100E+04	kg/m3	1.00%FS
121	Density	DF- 2	DE	121	JP1,2 Outlet Beam B	Fig.5.59	0.0	-	0.100E+04	kg/m3	1.00%FS
122	Density	DF- 3	DE	122	JP1,2 Outlet Beam C	Fig.5.60	0.0	-	0.100E+04	kg/m3	1.00%FS
123	Density	DF- 4	DE	123	JP3,4 Outlet Beam A	Fig.5.61	0.0	-	0.100E+04	kg/m3	1.00%FS
124	Density	DF- 5	DE	124	JP3,4 Outlet Beam B	Fig.5.62	0.0	-	0.100E+04	kg/m3	1.00%FS
125	Density	DF- 6	DE	125	JP3,4 Outlet Beam C	Fig.5.63	0.0	-	0.100E+04	kg/m3	1.00%FS
126	Density	DF- 7	DE	126	Break A Beam A	Not Measured	0.0	-	0.100E+04	kg/m3	1.00%FS
127	Density	DF- 8	DE	127	Break A Beam B	Not Measured	0.0	-	0.100E+04	kg/m3	1.00%FS
128	Density	DF- 9	DE	128	Break B Beam A	Fig.5.64	0.0	-	0.100E+04	kg/m3	1.00%FS
129	Density	DF-10	DE	129	Break B Beam B	Fig.5.65	0.0	-	0.100E+04	kg/m3	1.00%FS
130	Mo.Flux	M- 1	MF	130	JP1,2 Outlet Spool	Fig.5.66	0.0	-	0.220E+05	kg/ms2	1.00%FS
131	Mo.Flux	M- 2	MF	131	JP3,4 Outlet Spool	Fig.5.67	0.0	-	0.220E+05	kg/ms2	1.00%FS
132	Mo.Flux	M- 3	MF	132	Break A (Low Range)	Not Used	0.0	-	0.220E+05	kg/ms2	1.00%FS
133	Mo.Flux	M- 4	MF	133	Break B (Low Range)	Not Measured	0.0	-	0.220E+05	kg/ms2	1.00%FS
134	Mo.Flux	M- 5	MF	134	Break A (High Range)	Not Used	0.0	-	0.220E+06	kg/ms2	1.00%FS
135	Mo.Flux	M- 6	MF	135	Break B (High Range)	Fig.5.68	0.0	-	0.220E+06	kg/ms2	1.00%FS
136	Mo.Flux	M- 7	MF	136	Break Orifice	Not Measured	0.0	-	0.220E+05	kg/ms2	1.00%FS
137						Not Used					
138	Fluid T.	T- 1	TE	138	Lower Plenum	Fig.5.69	273.	-	673.	K	0.64%FS
139	Fluid T.	T- 2	TE	139	Upper Plenum	Fig.5.69	273.	-	673.	K	0.64%FS
140	Fluid T.	T- 3	TE	140	Steam Dome	Fig.5.70	273.	-	673.	K	0.64%FS
141	Fluid T.	T- 4	TE	141	Upper Downcomer	Fig.5.71	273.	-	673.	K	0.64%FS
142	Fluid T.	T- 5	TE	142	Lower Downcomer	Fig.5.71	273.	-	673.	K	0.64%FS
143	Fluid T.	T- 6	TE	143	JP-1 Drive	Fig.5.72	273.	-	673.	K	0.64%FS
144	Fluid T.	T- 7	TE	144	JP-2 Drive	Fig.5.72	273.	-	673.	K	0.64%FS
145	Fluid T.	T- 8	TE	145	JP-3 Drive	Fig.5.73	273.	-	673.	K	0.64%FS
146	Fluid T.	T- 9	TE	146	JP-4 Drive	Fig.5.73	273.	-	673.	K	0.64%FS
147	Fluid T.	T-10	TE	147	JP-1 Discharge	Fig.5.74	273.	-	673.	K	0.64%FS
148	Fluid T.	T-11	TE	148	JP-2 Discharge	Fig.5.74	273.	-	673.	K	0.64%FS
149	Fluid T.	T-12	TE	149	JP-3 Discharge	Fig.5.75	273.	-	673.	K	0.64%FS
150	Fluid T.	T-13	TE	150	JP-4 Discharge	Fig.5.75	273.	-	673.	K	0.64%FS

Table 3.2 Measurement List for RUN 952 (Continued)

151Ch.- 200Ch.

Ch.	Item	Symbol	ID.		Location	Fig.No.	Range			Unit	Accuracy
151	Fluid T.	T-14	TE	151	MRP-1 Suction	Fig.5.72	273.	-	673.	K	0.64%FS
152	Fluid T.	T-15	TE	152	MRP-1 Delivery	Fig.5.72	273.	-	673.	K	0.64%FS
153	Fluid T.	T-16	TE	153	MRP-2 Suction	Fig.5.73	273.	-	673.	K	0.64%FS
154	Fluid T.	T-17	TE	154	MRP-2 Delivery	Fig.5.73	273.	-	673.	K	0.64%FS
155	Fluid T.	T-18	TE	155	Break A Upstream	Not Used	273.	-	673.	K	0.64%FS
156	Fluid T.	T-19	TE	156	Break B Upstream	Fig.5.76	273.	-	673.	K	0.64%FS
157	Fluid T.	T-20	TE	157	RCN A Condensed Water	Not Used	273.	-	698.	K	0.64%FS
158	Fluid T.	T-21	TE	158	RCN B Condensed Water	Not Used	273.	-	698.	K	0.64%FS
159	Fluid T.	T-22	TE	159	Discharged Steam	Fig.5.70	273.	-	673.	K	0.64%FS
160	Fluid T.	T-24	TE	160	JP-1,2 Outlet Spool	Not Measured	273.	-	763.	K	0.64%FS
161	Fluid T.	T-25	TE	161	JP-3,4 Outlet Spool	Not Measured	273.	-	763.	K	0.64%FS
162	Fluid T.	T-26	TE	162	Break A Spool Piece	Not Used	273.	-	763.	K	0.64%FS
163	Fluid T.	T-27	TE	163	Break B Spool Piece	Not measured	273.	-	763.	K	0.64%FS
164	Fluid T.	T-28	TE	164	Feedwater	Fig.5.77	273.	-	673.	K	0.64%FS
165	Fluid T.	T-29	TE	165	Break Orifice Top	Fig.5.78	273.	-	673.	K	0.64%FS
166	Fluid T.	T-30	TE	166	Break Orifice Bottom	Fig.5.78	273.	-	673.	K	0.64%FS
167	Fluid T.	T-31	TE	167	Break A Downst. Drag	Not Measured	273.	-	673.	K	0.64%FS
168	Fluid T.	T-32	TE	168	Break B Downst. Drag	Not Measured	273.	-	673.	K	0.64%FS
169	Fluid T.	T-33	TE	169	Break A Upst. of Drag	Not Measured	273.	-	673.	K	0.64%FS
170	Fluid T.	T-34	TE	170	Break B Upst. of Drag	Not Measured	273.	-	673.	K	0.64%FS
171	Slab T.	TS- 1	TE	171	JP-1 Diffuser Wall	Fig.5.79	273.	-	673.	K	0.64%FS
172	Slab T.	TS- 2	TE	172	JP-2 Diffuser Wall	Fig.5.79	273.	-	673.	K	0.64%FS
173	Slab T.	TS- 3	TE	173	JP-3 Diffuser Wall	Fig.5.79	273.	-	673.	K	0.64%FS
174	Slab T.	TS- 4	TE	174	JP-4 Diffuser Wall	Fig.5.79	273.	-	673.	K	0.64%FS
175	Fluid T.	T-35	TE	175	Feedwater 2	Fig.5.80	273.	-	673.	K	0.64%FS
176	Fluid T.	T-36	TE	176	Discharged Steam	Fig.5.81	273.	-	673.	K	0.64%FS
177	Slab T.	TS-13	TE	177	Filler Block C Pos.1	Not Measured	273.	-	673.	K	0.64%FS
178	Slab T.	TS-14	TE	178	Filler Block C Pos.2	Not Measured	273.	-	673.	K	0.64%FS
179	Slab T.	TS-15	TE	179	Filler Block C Pos.3	Not Measured	273.	-	673.	K	0.64%FS
180	Slab T.	TS-16	TE	180	Filler Block C Pos.4	Not Measured	273.	-	673.	K	0.64%FS
181	Slab T.	TS-17	TE	181	Filler Block C Pos.5	Not Measured	273.	-	673.	K	0.64%FS
182	Slab T.	TS-18	TE	182	Filler Block C Pos.6	Not Measured	273.	-	673.	K	0.64%FS
183	Slab T.	TS-19	TE	183	Filler Block A Pos.1	Not Measured	273.	-	673.	K	0.64%FS
184	Slab T.	TS-20	TE	184	Filler Block A Pos.2	Not Measured	273.	-	673.	K	0.64%FS
185	Slab T.	TS-21	TE	185	Filler Block A Pos.3	Not Measured	273.	-	673.	K	0.64%FS
186	Slab T.	TS-22	TE	186	Filler Block A Pos.4	Not Measured	273.	-	673.	K	0.64%FS
187	Slab T.	TS-23	TE	187	Filler Block A Pos.5	Not Measured	273.	-	673.	K	0.64%FS
188	Slab T.	TS-24	TE	188	Filler Block A Pos.6	Not Measured	273.	-	673.	K	0.64%FS
189	Slab T.	TS-25	TE	189	JP-1 Diffuser Wall	Not Measured	273.	-	673.	K	0.64%FS
190	Slab T.	TS-26	TE	190	JP-2 Diffuser Wall	Not Measured	273.	-	673.	K	0.64%FS
191	Slab T.	TS-27	TE	191	JP-3 Diffuser Wall	Not Measured	273.	-	673.	K	0.64%FS
192	Slab T.	TS-28	TE	192	JP-4 Diffuser Wall	Not Measured	273.	-	673.	K	0.64%FS
193	Slab T.	TS-29	TE	193	PV Wall Inside 1-1	Not Measured	273.	-	673.	K	0.64%FS
194	Slab T.	TS-30	TE	194	PV Inner Surface 1-2	Not Measured	273.	-	673.	K	0.64%FS
195	Slab T.	TS-31	TE	195	PV Inner Surface 1-3	Not Measured	273.	-	673.	K	0.64%FS
196	Slab T.	TS-32	TE	196	PV Wall Inside 2	Not Measured	273.	-	673.	K	0.64%FS
197	Slab T.	TS-33	TE	197	PV Wall Inside 3	Not Measured	273.	-	673.	K	0.64%FS
198	Slab T.	TS-34	TE	198	PV Wall Inside 4	Not Measured	273.	-	673.	K	0.64%FS
199	Slab T.	TS-35	TE	199	L.P. Inner Surface	Not Measured	273.	-	673.	K	0.64%FS
200	Slab T.	TS-36	TE	200	L.P. Wall Inside	Not Measured	273.	-	673.	K	0.64%FS

Table 3.2 Measurement List for RUN 952 (Continued)

201Ch.- 250Ch.

Ch.	Item	Symbol	ID.	Location	Fig.No.	Range	Unit	Accuracy
201	Temp.	TF- 1	TE 201	A11 Fuel Rod Pos.1	Fig.5.82, 106	273. - 0.147E+04	K	0.64%FS
202	Temp.	TF- 2	TE 202	A11 Fuel Rod Pos.2	Fig.5.82, 107	273. - 0.147E+04	K	0.64%FS
203	Temp.	TF- 3	TE 203	A11 Fuel Rod Pos.3	Fig.5.82, 108	273. - 0.147E+04	K	0.64%FS
204	Temp.	TF- 4	TE 204	A11 Fuel Rod Pos.4	Fig.5.82, 109	273. - 0.147E+04	K	0.64%FS
205	Temp.	TF- 5	TE 205	A11 Fuel Rod Pos.5	Fig.5.82, 110	273. - 0.147E+04	K	0.64%FS
206	Temp.	TF- 6	TE 206	A11 Fuel Rod Pos.6	Fig.5.82, 111	273. - 0.147E+04	K	0.64%FS
207	Temp.	TF- 7	TE 207	A11 Fuel Rod Pos.7	Fig.5.82, 112	273. - 0.147E+04	K	0.64%FS
208	Temp.	TF- 8	TE 208	A12 Fuel Rod Pos.1	Fig.5.83, 106	273. - 0.147E+04	K	0.64%FS
209	Temp.	TF- 9	TE 209	A12 Fuel Rod Pos.2	Fig.5.83, 107	273. - 0.147E+04	K	0.64%FS
210	Temp.	TF- 10	TE 210	A12 Fuel Rod Pos.3	Fig.5.83, 108	273. - 0.147E+04	K	0.64%FS
211	Temp.	TF- 11	TE 211	A12 Fuel Rod Pos.4	Fig.5.83, 109	273. - 0.147E+04	K	0.64%FS
212	Temp.	TF- 12	TE 212	A12 Fuel Rod Pos.5	Fig.5.83, 110	273. - 0.147E+04	K	0.64%FS
213	Temp.	TF- 13	TE 213	A12 Fuel Rod Pos.6	Fig.5.83, 111	273. - 0.147E+04	K	0.64%FS
214	Temp.	TF- 14	TE 214	A12 Fuel Rod Pos.7	Fig.5.83, 112	273. - 0.147E+04	K	0.64%FS
215	Temp.	TF- 15	TE 215	A13 Fuel Rod Pos.1	Fig.5.84, 106	273. - 0.147E+04	K	0.64%FS
216	Temp.	TF- 16	TE 216	A13 Fuel Rod Pos.2	Fig.5.84, 107	273. - 0.147E+04	K	0.64%FS
217	Temp.	TF- 17	TE 217	A13 Fuel Rod Pos.3	Fig.5.84, 108	273. - 0.147E+04	K	0.64%FS
218	Temp.	TF- 18	TE 218	A13 Fuel Rod Pos.4	Fig.5.84, 109	273. - 0.147E+04	K	0.64%FS
219	Temp.	TF- 19	TE 219	A13 Fuel Rod Pos.5	Fig.5.84, 110	273. - 0.147E+04	K	0.64%FS
220	Temp.	TF- 20	TE 220	A13 Fuel Rod Pos.6	Fig.5.84, 111	273. - 0.147E+04	K	0.64%FS
221	Temp.	TF- 21	TE 221	A13 Fuel Rod Pos.7	Fig.5.84, 112	273. - 0.147E+04	K	0.64%FS
222	Temp.	TF- 22	TE 222	A14 Fuel Rod Pos.1	Not Measured	273. - 0.147E+04	K	0.64%FS
223	Temp.	TF- 23	TE 223	A14 Fuel Rod Pos.2	Not Measured	273. - 0.147E+04	K	0.64%FS
224	Temp.	TF- 24	TE 224	A14 Fuel Rod Pos.3	Not Measured	273. - 0.147E+04	K	0.64%FS
225	Temp.	TF- 25	TE 225	A14 Fuel Rod Pos.4	Not Measured	273. - 0.147E+04	K	0.64%FS
226	Temp.	TF- 26	TE 226	A14 Fuel Rod Pos.5	Not Measured	273. - 0.147E+04	K	0.64%FS
227	Temp.	TF- 27	TE 227	A14 Fuel Rod Pos.6	Not Measured	273. - 0.147E+04	K	0.64%FS
228	Temp.	TF- 28	TE 228	A14 Fuel Rod Pos.7	Not Measured	273. - 0.147E+04	K	0.64%FS
229	Temp.	TF- 29	TE 229	A15 Fuel Rod Pos.1	Not Measured	273. - 0.147E+04	K	0.64%FS
230	Temp.	TF- 30	TE 230	A15 Fuel Rod Pos.4	Not Measured	273. - 0.147E+04	K	0.64%FS
231	Temp.	TF- 31	TE 231	A17 Fuel Rod Pos.1	Not Measured	273. - 0.147E+04	K	0.64%FS
232	Temp.	TF- 32	TE 232	A17 Fuel Rod Pos.4	Fig.5.102	273. - 0.147E+04	K	0.64%FS
233	Temp.	TF- 33	TE 233	A22 Fuel Rod Pos.1	Fig.5.85, 113	273. - 0.147E+04	K	0.64%FS
234	Temp.	TF- 34	TE 234	A22 Fuel Rod Pos.2	Fig.5.85, 114	273. - 0.147E+04	K	0.64%FS
235	Temp.	TF- 35	TE 235	A22 Fuel Rod Pos.3	Fig.5.85, 115	273. - 0.147E+04	K	0.64%FS
236	Temp.	TF- 36	TE 236	A22 Fuel Rod Pos.4	Fig.5.85, 116	273. - 0.125E+04	K	0.64%FS
237	Temp.	TF- 37	TE 237	A22 Fuel Rod Pos.5	Fig.5.85, 117	273. - 0.125E+04	K	0.64%FS
238	Temp.	TF- 38	TE 238	A22 Fuel Rod Pos.6	Fig.5.85, 118	273. - 0.125E+04	K	0.64%FS
239	Temp.	TF- 39	TE 239	A22 Fuel Rod Pos.7	Fig.5.85, 119	273. - 0.125E+04	K	0.64%FS
240	Temp.	TF- 40	TE 240	A24 Fuel Rod Pos.1	Failure	273. - 0.125E+04	K	0.64%FS
241	Temp.	TF- 41	TE 241	A24 Fuel Rod Pos.2	Not Measured	273. - 0.125E+04	K	0.64%FS
242	Temp.	TF- 42	TE 242	A24 Fuel Rod Pos.3	Not Measured	273. - 0.125E+04	K	0.64%FS
243	Temp.	TF- 43	TE 243	A24 Fuel Rod Pos.4	Not Measured	273. - 0.125E+04	K	0.64%FS
244	Temp.	TF- 44	TE 244	A24 Fuel Rod Pos.5	Not Measured	273. - 0.125E+04	K	0.64%FS
245	Temp.	TF- 45	TE 245	A24 Fuel Rod Pos.6	Not Measured	273. - 0.125E+04	K	0.64%FS
246	Temp.	TF- 46	TE 246	A24 Fuel Rod Pos.7	Not Measured	273. - 0.125E+04	K	0.64%FS
247	Temp.	TF- 47	TE 247	A26 Fuel Rod Pos.1	Not Measured	273. - 0.125E+04	K	0.64%FS
248	Temp.	TF- 48	TE 248	A26 Fuel Rod Pos.2	Not Measured	273. - 0.125E+04	K	0.64%FS
249	Temp.	TF- 49	TE 249	A28 Fuel Rod Pos.1	Failure	273. - 0.125E+04	K	0.64%FS
250	Temp.	TF- 50	TE 250	A28 Fuel Rod Pos.4	Fig.5.102	273. - 0.125E+04	K	0.64%FS

Table 3.2 Measurement List for RUN 952 (Continued)

251Ch.- 300Ch.

Ch.	Item	Symbol	ID.	Location	Fig.No.	Range	Unit	Accuracy
251	Temp.	TF- 51	TE 251	A31 Fuel Rod Pos.1	Failure	273. - 0.125E+04	K	0.64%FS
252	Temp.	TF- 52	TE 252	A31 Fuel Rod Pos.4	Fig.5.102	273. - 0.125E+04	K	0.64%FS
253	Temp.	TF- 53	TE 253	A33 Fuel Rod Pos.1	Fig.5.86	273. - 0.125E+04	K	0.64%FS
254	Temp.	TF- 54	TE 254	A33 Fuel Rod Pos.2	Fig.5.86	273. - 0.125E+04	K	0.64%FS
255	Temp.	TF- 55	TE 255	A33 Fuel Rod Pos.3	Fig.5.86	273. - 0.125E+04	K	0.64%FS
256	Temp.	TF- 56	TE 256	A33 Fuel Rod Pos.4	Fig.5.86	273. - 0.125E+04	K	0.64%FS
257	Temp.	TF- 57	TE 257	A33 Fuel Rod Pos.5	Fig.5.86	273. - 0.125E+04	K	0.64%FS
258	Temp.	TF- 58	TE 258	A33 Fuel Rod Pos.6	Fig.5.86	273. - 0.125E+04	K	0.64%FS
259	Temp.	TF- 59	TE 259	A33 Fuel Rod Pos.7	Fig.5.86	273. - 0.125E+04	K	0.64%FS
260	Temp.	TF- 60	TE 260	A34 Fuel Rod Pos.1	Not Measured	273. - 0.125E+04	K	0.64%FS
261	Temp.	TF- 61	TE 261	A34 Fuel Rod Pos.2	Failure	273. - 0.125E+04	K	0.64%FS
262	Temp.	TF- 62	TE 262	A34 Fuel Rod Pos.3	Not Measured	273. - 0.125E+04	K	0.64%FS
263	Temp.	TF- 63	TE 263	A34 Fuel Rod Pos.4	Not Measured	273. - 0.125E+04	K	0.64%FS
264	Temp.	TF- 64	TE 264	A34 Fuel Rod Pos.5	Not Measured	273. - 0.125E+04	K	0.64%FS
265	Temp.	TF- 65	TE 265	A34 Fuel Rod Pos.6	Not Measured	273. - 0.125E+04	K	0.64%FS
266	Temp.	TF- 66	TE 266	A34 Fuel Rod Pos.7	Not Measured	273. - 0.125E+04	K	0.64%FS
267	Temp.	TF- 67	TE 267	A37 Fuel Rod Pos.1	Not Measured	273. - 0.125E+04	K	0.64%FS
268	Temp.	TF- 68	TE 268	A37 Fuel Rod Pos.4	Not Measured	273. - 0.125E+04	K	0.64%FS
269	Temp.	TF- 69	TE 269	A42 Fuel Rod Pos.1	Not Measured	273. - 0.125E+04	K	0.64%FS
270	Temp.	TF- 70	TE 270	A42 Fuel Rod Pos.4	Failure	273. - 0.125E+04	K	0.64%FS
271	Temp.	TF- 71	TE 271	A44 Fuel Rod Pos.1	Not Measured	273. - 0.125E+04	K	0.64%FS
272	Temp.	TF- 72	TE 272	A44 Fuel Rod Pos.2	Not Measured	273. - 0.125E+04	K	0.64%FS
273	Temp.	TF- 73	TE 273	A44 Fuel Rod Pos.3	Not Measured	273. - 0.125E+04	K	0.64%FS
274	Temp.	TF- 74	TE 274	A44 Fuel Rod Pos.4	Not Measured	273. - 0.125E+04	K	0.64%FS
275	Temp.	TF- 75	TE 275	A44 Fuel Rod Pos.5	Not Measured	273. - 0.125E+04	K	0.64%FS
276	Temp.	TF- 76	TE 276	A44 Fuel Rod Pos.6	Not Measured	273. - 0.125E+04	K	0.64%FS
277	Temp.	TF- 77	TE 277	A44 Fuel Rod Pos.7	Not Measured	273. - 0.125E+04	K	0.64%FS
278	Temp.	TF- 78	TE 278	A48 Fuel Rod Pos.1	Not Measured	273. - 0.125E+04	K	0.64%FS
279	Temp.	TF- 79	TE 279	A48 Fuel Rod Pos.4	Not Measured	273. - 0.125E+04	K	0.64%FS
280	Temp.	TF- 80	TE 280	A51 Fuel Rod Pos.1	Not Measured	273. - 0.125E+04	K	0.64%FS
281	Temp.	TF- 81	TE 281	A51 Fuel Rod Pos.4	Not Measured	273. - 0.125E+04	K	0.64%FS
282	Temp.	TF- 82	TE 282	A53 Fuel Rod Pos.1	Not Measured	273. - 0.125E+04	K	0.64%FS
283	Temp.	TF- 83	TE 283	A53 Fuel Rod Pos.4	Not Measured	273. - 0.125E+04	K	0.64%FS
284	Temp.	TF- 84	TE 284	A57 Fuel Rod Pos.1	Not Measured	273. - 0.125E+04	K	0.64%FS
285	Temp.	TF- 85	TE 285	A57 Fuel Rod Pos.4	Fig.5.102	273. - 0.125E+04	K	0.64%FS
286	Temp.	TF- 86	TE 286	A62 Fuel Rod Pos.1	Not Measured	273. - 0.125E+04	K	0.64%FS
287	Temp.	TF- 87	TE 287	A62 Fuel Rod Pos.4	Not Measured	273. - 0.125E+04	K	0.64%FS
288	Temp.	TF- 88	TE 288	A66 Fuel Rod Pos.1	Not Measured	273. - 0.125E+04	K	0.64%FS
289	Temp.	TF- 89	TE 289	A66 Fuel Rod Pos.4	Failure	273. - 0.125E+04	K	0.64%FS
290	Temp.	TF- 90	TE 290	A68 Fuel Rod Pos.1	Not Measured	273. - 0.125E+04	K	0.64%FS
291	Temp.	TF- 91	TE 291	A68 Fuel Rod Pos.4	Fig.5.103	273. - 0.125E+04	K	0.64%FS
292	Temp.	TF- 92	TE 292	A71 Fuel Rod Pos.1	Not Measured	273. - 0.125E+04	K	0.64%FS
293	Temp.	TF- 93	TE 293	A71 Fuel Rod Pos.4	Fig.5.103	273. - 0.125E+04	K	0.64%FS
294	Temp.	TF- 94	TE 294	A73 Fuel Rod Pos.1	Not Measured	273. - 0.125E+04	K	0.64%FS
295	Temp.	TF- 95	TE 295	A73 Fuel Rod Pos.4	Fig.5.103	273. - 0.125E+04	K	0.64%FS
296	Temp.	TF- 96	TE 296	A75 Fuel Rod Pos.1	Not Measured	273. - 0.125E+04	K	0.64%FS
297	Temp.	TF- 97	TE 297	A75 Fuel Rod Pos.4	Not Measured	273. - 0.125E+04	K	0.64%FS
298	Temp.	TF- 98	TE 298	A77 Fuel Rod Pos.1	Fig.5.87, 120	273. - 0.125E+04	K	0.64%FS
299	Temp.	TF- 99	TE 299	A77 Fuel Rod Pos.2	Fig.5.87, 121	273. - 0.125E+04	K	0.64%FS
300	Temp.	TF-100	TE 300	A77 Fuel Rod Pos.3	Fig.5.87, 122	273. - 0.125E+04	K	0.64%FS

Table 3.2 Measurement List for RUN 952 (Continued)

301Ch.- 350Ch.

Ch.	Item	Symbol	ID.	Location	Fig.No.	Range	Unit	Accuracy
301	Temp.	TF-101	TE 301	A77 Fuel Rod Pos.4	Fig.5.87, 123	273. - 0.125E+04	K	0.64%FS
302	Temp.	TF-102	TE 302	A77 Fuel Rod Pos.5	Fig.5.87, 124	273. - 0.125E+04	K	0.64%FS
303	Temp.	TF-103	TE 303	A77 Fuel Rod Pos.6	Fig.5.87, 125	273. - 0.125E+04	K	0.64%FS
304	Temp.	TF-104	TE 304	A77 Fuel Rod Pos.7	Failure	273. - 0.125E+04	K	0.64%FS
305	Temp.	TF-105	TE 305	A82 Fuel Rod Pos.1	Not Measured	273. - 0.125E+04	K	0.64%FS
306	Temp.	TF-106	TE 306	A82 Fuel Rod Pos.4	Failure	273. - 0.125E+04	K	0.64%FS
307	Temp.	TF-107	TE 307	A84 Fuel Rod Pos.1	Fig.5.104	273. - 0.125E+04	K	0.64%FS
308	Temp.	TF-108	TE 308	A84 Fuel Rod Pos.4	Fig.5.104	273. - 0.125E+04	K	0.64%FS
309	Temp.	TF-109	TE 309	A85 Fuel Rod Pos.1	Not Measured	273. - 0.125E+04	K	0.64%FS
310	Temp.	TF-110	TE 310	A85 Fuel Rod Pos.2	Failure	273. - 0.125E+04	K	0.64%FS
311	Temp.	TF-111	TE 311	A85 Fuel Rod Pos.3	Failure	273. - 0.125E+04	K	0.64%FS
312	Temp.	TF-112	TE 312	A85 Fuel Rod Pos.4	Not Measured	273. - 0.125E+04	K	0.64%FS
313	Temp.	TF-113	TE 313	A85 Fuel Rod Pos.5	Not Measured	273. - 0.125E+04	K	0.64%FS
314	Temp.	TF-114	TE 314	A85 Fuel Rod Pos.6	Not Measured	273. - 0.125E+04	K	0.64%FS
315	Temp.	TF-115	TE 315	A85 Fuel Rod Pos.7	Not Measured	273. - 0.125E+04	K	0.64%FS
316	Temp.	TF-116	TE 316	A87 Fuel Rod Pos.1	Fig.5.88, 106	273. - 0.125E+04	K	0.64%FS
317	Temp.	TF-117	TE 317	A87 Fuel Rod Pos.2	Fig.5.88, 107	273. - 0.125E+04	K	0.64%FS
318	Temp.	TF-118	TE 318	A87 Fuel Rod Pos.3	Fig.5.88, 108	273. - 0.125E+04	K	0.64%FS
319	Temp.	TF-119	TE 319	A87 Fuel Rod Pos.4	Fig.5.88, 109	273. - 0,125E+04	K	0.64%FS
320	Temp.	TF-120	TE 320	A87 Fuel Rod Pos.5	Fig.5.88, 110	273. - 0.125E+04	K	0.64%FS
321	Temp.	TF-121	TE 321	A87 Fuel Rod Pos.6	Fig.5.88, 111	273. - 0.125E+04	K	0.64%FS
322	Temp.	TF-122	TE 322	A87 Fuel Rod Pos.7	Fig.5.88, 112	273. - 0.125E+04	K	0.64%FS
323	Temp.	TF-123	TE 323	A88 Fuel Rod Pos.1	Fig.5.89, 106	273. - 0.125E+04	K	0.64%FS
324	Temp.	TF-124	TE 324	A88 Fuel Rod Pos.2	Fig.5.89, 107	273. - 0.125E+04	K	0.64%FS
325	Temp.	TF-125	TE 325	A88 Fuel Rod Pos.3	Fig.5.89, 108	273. - 0.125E+04	K	0.64%FS
326	Temp.	TF-126	TE 326	A88 Fuel Rod Pos.4	Fig.5.89, 109	273. - 0.125E+04	K	0.64%FS
327	Temp.	TF-127	TE 327	A88 Fuel Rod Pos.5	Fig.5.89, 110	273. - 0.125E+04	K	0.64%FS
328	Temp.	TF-128	TE 328	A88 Fuel Rod Pos.6	Fig.5.89, 111	273. - 0.125E+04	K	0.64%FS
329	Temp.	TF-129	TE 329	A88 Fuel Rod Pos.7	Fig.5.89, 112	273. - 0.125E+04	K	0.64%FS
330	Temp.	TF-130	TE 330	B11 Fuel Rod Pos.1	Fig.5.90	273. - 0.125E+04	K	0.64%FS
331	Temp.	TF-131	TE 331	B11 Fuel Rod Pos.2	Fig.5.90	273. - 0.125E+04	K	0.64%FS
332	Temp.	TF-132	TE 332	B11 Fuel Rod Pos.3	Fig.5.90	273. - 0.125E+04	K	0.64%FS
333	Temp.	TF-133	TE 333	B11 Fuel Rod Pos.4	Fig.5.90	273. - 0.125E+04	K	0.64%FS
334	Temp.	TF-134	TE 334	B11 Fuel Rod Pos.5	Fig.5.90	273. - 0.125E+04	K	0.64%FS
335	Temp.	TF-135	TE 335	B11 Fuel Rod Pos.6	Fig.5.90	273. - 0.125E+04	K	0.64%FS
336	Temp.	TF-136	TE 336	B11 Fuel Rod Pos.7	Failure	273. - 0.125E+04	K	0.64%FS
337	Temp.	TF-137	TE 337	B13 Fuel Rod Pos.4	Fig.5.103	273. - 0.125E+04	K	0.64%FS
338	Temp.	TF-138	TE 338	B22 Fuel Rod Pos.1	Fig.5.91, 113	273. - 0.125E+04	K	0.64%FS
339	Temp.	TF-139	TE 339	B22 Fuel Rod Pos.2	Fig.5.91, 114	273. - 0.125E+04	K	0.64%FS
340	Temp.	TF-140	TE 340	B22 Fuel Rod Pos.3	Fig.5.91, 115	273. - 0.125E+04	K	0.64%FS
341	Temp.	TF-141	TE 341	B22 Fuel Rod Pos.4	Fig.5.91, 116	273. - 0.125E+04	K	0.64%FS
342	Temp.	TF-142	TE 342	B22 Fuel Rod Pos.5	Fig.5.91, 117	273. - 0.125E+04	K	0.64%FS
343	Temp.	TF-143	TE 343	B22 Fuel Rod Pos.6	Fig.5.91, 118	273. - 0.125E+04	K	0.64%FS
344	Temp.	TF-144	TE 344	B22 Fuel Rod Pos.7	Fig.5.91, 119	273. - 0.125E+04	K	0.64%FS
345	Temp.	TF-145	TE 345	B31 Fuel Rod Pos.4	Not Measured	273. - 0.125E+04	K	0.64%FS
346	Temp.	TF-146	TE 346	B33 Fuel Rod Pos.4	Not Measured	273. - 0.125E+04	K	0.64%FS
347	Temp.	TF-147	TE 347	B51 Fuel Rod Pos.4	Not Measured	273. - 0.125E+04	K	0.64%FS
348	Temp.	TF-148	TE 348	B53 Fuel Rod Pos.4	Not Measured	273. - 0.125E+04	K	0.64%FS
349	Temp.	TF-149	TE 349	B66 Fuel Rod Pos.4	Not Measured	273. - 0.125E+04	K	0.64%FS
350	Temp.	TF-150	TE 350	B77 Fuel Rod Pos.1	Fig.5.92, 120	273. - 0.125E+04	K	0.64%FS

Table 3.2 Measurement List for RUN 952 (Continued)

351Ch.- 400Ch.

Ch.	Item	Symbol	ID.	Location	Fig.No.	Range	Unit	Accuracy
351	Temp.	TF-151	TE 351	B77 Fuel Rod Pos.2	Fig.5.92, 121	273. - 0.125E+04	K	0.64%FS
352	Temp.	TF-152	TE 352	B77 Fuel Rod Pos.3	Fig.5.92, 122	273. - 0.125E+04	K	0.64%FS
353	Temp.	TF-153	TE 353	B77 Fuel Rod Pos.4	Fig.5.92, 123	273. - 0.125E+04	K	0.64%FS
354	Temp.	TF-154	TE 354	B77 Fuel Rod Pos.5	Failure	273. - 0.125E+04	K	0.64%FS
355	Temp.	TF-155	TE 355	B77 Fuel Rod Pos.6	Fig.5.92, 125	273. - 0.125E+04	K	0.64%FS
356	Temp.	TF-156	TE 356	B77 Fuel Rod Pos.7	Fig.5.92, 126	273. - 0.125E+04	K	0.64%FS
357	Temp.	TF-157	TE 357	B86 Fuel Rod Pos.4	Failure	273. - 0.125E+04	K	0.64%FS
358	Temp.	TF-158	TE 358	C11 Fuel Rod Pos.1	Fig.5.93	273. - 0.125E+04	K	0.64%FS
359	Temp.	TF-159	TE 359	C11 Fuel Rod Pos.2	Fig.5.93	273. - 0.125E+04	K	0.64%FS
360	Temp.	TF-160	TE 360	C11 Fuel Rod Pos.3	Fig.5.93	273. - 0.125E+04	K	0.64%FS
361	Temp.	TF-161	TE 361	C11 Fuel Rod Pos.4	Fig.5.93	273. - 0.125E+04	K	0.64%FS
362	Temp.	TF-162	TE 362	C11 Fuel Rod Pos.5	Fig.5.93	273. - 0.125E+04	K	0.64%FS
363	Temp.	TF-163	TE 363	C11 Fuel Rod Pos.6	Fig.5.93	273. - 0.125E+04	K	0.64%FS
364	Temp.	TF-164	TE 364	C11 Fuel Rod Pos.7	Fig.5.93	273. - 0.125E+04	K	0.64%FS
365	Temp.	TF-165	TE 365	C13 Fuel Rod Pos.1	Fig.5.94	273. - 0.125E+04	K	0.64%FS
366	Temp.	TF-166	TE 366	C13 Fuel Rod Pos.2	Fig.5.94	273. - 0.125E+04	K	0.64%FS
367	Temp.	TF-167	TE 367	C13 Fuel Rod Pos.3	Fig.5.94	273. - 0.125E+04	K	0.64%FS
368	Temp.	TF-168	TE 368	C13 Fuel Rod Pos.4	Fig.5.94	273. - 0.125E+04	K	0.64%FS
369	Temp.	TF-169	TE 369	C13 Fuel Rod Pos.5	Fig.5.94	273. - 0.125E+04	K	0.64%FS
370	Temp.	TF-170	TE 370	C13 Fuel Rod Pos.6	Fig.5.94	273. - 0.125E+04	K	0.64%FS
371	Temp.	TF-171	TE 371	C13 Fuel Rod Pos.7	Fig.5.94	273. - 0.125E+04	K	0.64%FS
372	Temp.	TF-172	TE 372	C15 Fuel Rod Pos.4	Not Measured	273. - 0.125E+04	K	0.64%FS
373	Temp.	TF-173	TE 373	C22 Fuel Rod Pos.1	Fig.5.95, 113	273. - 0.125E+04	K	0.64%FS
374	Temp.	TF-174	TE 374	C22 Fuel Rod Pos.2	Fig.5.95, 114	273. - 0.125E+04	K	0.64%FS
375	Temp.	TF-175	TE 375	C22 Fuel Rod Pos.3	Fig.5.95, 115	273. - 0.125E+04	K	0.64%FS
376	Temp.	TF-176	TE 376	C22 Fuel Rod Pos.4	Fig.5.95, 116	273. - 0.125E+04	K	0.64%FS
377	Temp.	TF-177	TE 377	C22 Fuel Rod Pos.5	Fig.5.95, 117	273. - 0.125E+04	K	0.64%FS
378	Temp.	TF-178	TE 378	C22 Fuel Rod Pos.6	Fig.5.95, 118	273. - 0.125E+04	K	0.64%FS
379	Temp.	TF-179	TE 379	C22 Fuel Rod Pos.7	Fig.5.95, 119	273. - 0.125E+04	K	0.64%FS
380	Temp.	TF-180	TE 380	C31 Fuel Rod Pos.4	Not Measured	273. - 0.125E+04	K	0.64%FS
381	Temp.	TF-181	TE 381	C33 Fuel Rod Pos.1	Fig.5.96	273. - 0.125E+04	K	0.64%FS
382	Temp.	TF-182	TE 382	C33 Fuel Rod Pos.2	Fig.5.96	273. - 0.125E+04	K	0.64%FS
383	Temp.	TF-183	TE 383	C33 Fuel Rod Pos.3	Fig.5.96	273. - 0.125E+04	K	0.64%FS
384	Temp.	TF-184	TE 384	C33 Fuel Rod Pos.4	Fig.5.96	273. - 0.125E+04	K	0.64%FS
385	Temp.	TF-185	TE 385	C33 Fuel Rod Pos.5	Fig.5.96	273. - 0.125E+04	K	0.64%FS
386	Temp.	TF-186	TE 386	C33 Fuel Rod Pos.6	Fig.5.96	273. - 0.125E+04	K	0.64%FS
387	Temp.	TF-187	TE 387	C33 Fuel Rod Pos.7	Fig.5.96	273. - 0.125E+04	K	0.64%FS
388	Temp.	TF-188	TE 388	C35 Fuel Rod Pos.4	Not Measured	273. - 0.125E+04	K	0.64%FS
389	Temp.	TF-189	TE 389	C66 Fuel Rod Pos.4	Not Measured	273. - 0.125E+04	K	0.64%FS
390	Temp.	TF-190	TE 390	C68 Fuel Rod Pos.4	Not Measured	273. - 0.125E+04	K	0.64%FS
391	Temp.	TF-191	TE 391	C77 Fuel Rod Pos.1	Fig.5.97, 120	273. - 0.125E+04	K	0.64%FS
392	Temp.	TF-192	TE 392	C77 Fuel Rod Pos.2	Fig.5.97, 121	273. - 0.125E+04	K	0.64%FS
393	Temp.	TF-193	TE 393	C77 Fuel Rod Pos.3	Fig.5.97, 122	273. - 0.125E+04	K	0.64%FS
394	Temp.	TF-194	TE 394	C77 Fuel Rod Pos.4	Fig.5.97, 123	273. - 0.125E+04	K	0.64%FS
395	Temp.	TF-195	TE 395	C77 Fuel Rod Pos.5	Fig.5.97, 124	273. - 0.125E+04	K	0.64%FS
396	Temp.	TF-196	TE 396	C77 Fuel Rod Pos.6	Fig.5.97, 125	273. - 0.125E+04	K	0.64%FS
397	Temp.	TF-197	TE 397	C77 Fuel Rod Pos.7	Fig.5.97, 126	273. - 0.125E+04	K	0.64%FS
398	Temp.	TF-198	TE 398	D11 Fuel Rod Pos.4	Fig.5.105	273. - 0.125E+04	K	0.64%FS
399	Temp.	TF-199	TE 399	D13 Fuel Rod Pos.4	Fig.5.105	273. - 0.125E+04	K	0.64%FS
400	Temp.	TF-200	TE 400	D22 Fuel Rod Pos.1	Fig.5.98, 113	273. - 0.125E+04	K	0.64%FS

Table 3.2 Measurement List for RUN 952 (Continued) 401Ch.- 450Ch.

Ch.	Item	Symbol	ID.	Location	Fig.No.	Range	Unit	Accuracy
401	Temp.	TF-201	TE 401	D22 Fuel Rod Pos.2	Fig.5.98, 114	273. - 0.125E+04	K	0.64%FS
402	Temp.	TF-202	TE 402	D22 Fuel Rod Pos.3	Fig.5.98, 115	273. - 0.125E+04	K	0.64%FS
403	Temp.	TF-203	TE 403	D22 Fuel Rod Pos.4	Fig.5.98, 116	273. - 0.125E+04	K	0.64%FS
404	Temp.	TF-204	TE 404	D22 Fuel Rod Pos.5	Fig.5.98, 117	273. - 0.125E+04	K	0.64%FS
405	Temp.	TF-205	TE 405	D22 Fuel Rod Pos.6	Fig.5.98, 118	273. - 0.125E+04	K	0.64%FS
406	Temp.	TF-206	TE 406	D22 Fuel Rod Pos.7	Fig.5.98, 119	273. - 0.125E+04	K	0.64%FS
407	Temp.	TF-207	TE 407	D31 Fuel Rod Pos.4	Not Measured	273. - 0.125E+04	K	0.64%FS
408	Temp.	TF-208	TE 408	D33 Fuel Rod Pos.4	Not Measured	273. - 0.125E+04	K	0.64%FS
409	Temp.	TF-209	TE 409	D51 Fuel Rod Pos.4	Not Measured	273. - 0.125E+04	K	0.64%FS
410	Temp.	TF-210	TE 410	D53 Fuel Rod Pos.4	Not Measured	273. - 0.125E+04	K	0.64%FS
411	Temp.	TF-211	TE 411	D66 Fuel Rod Pos.4	Not Measured	273. - 0.125E+04	K	0.64%FS
412	Temp.	TF-212	TE 412	D77 Fuel Rod Pos.4	Fig.5.105	273. - 0.125E+04	K	0.64%FS
413	Temp.	TF-213	TE 413	D86 Fuel Rod Pos.4	Fig.5.105	273. - 0.125E+04	K	0.64%FS
414	Fluid T.	TW- 1	TE 414	A45 Tie Rod Pos.1	Fig.5.99	273. - 0.125E+04	K	0.64%FS
415	Fluid T.	TW- 2	TE 415	A45 Tie Rod Pos.2	Fig.5.99	273. - 0.125E+04	K	0.64%FS
416	Fluid T.	TW- 3	TE 416	A45 Tie Rod Pos.3	Fig.5.99	273. - 0.125E+04	K	0.64%FS
417	Fluid T.	TW- 4	TE 417	A45 Tie Rod Pos.4	Fig.5.99	273. - 0.125E+04	K	0.64%FS
418	Fluid T.	TW- 5	TE 418	A45 Tie Rod Pos.5	Fig.5.99	273. - 0.125E+04	K	0.64%FS
419	Fluid T.	TW- 6	TE 419	A45 Tie Rod Pos.6	Fig.5.99	273. - 0.125E+04	K	0.64%FS
420	Fluid T.	TW- 7	TE 420	A45 Tie Rod Pos.7	Fig.5.99	273. - 0.125E+04	K	0.64%FS
421	Fluid T.	TW- 8	TE 421	B45 Tie Rod Pos.1	Not Measured	273. - 0.125E+04	K	0.64%FS
422	Fluid T.	TW- 9	TE 422	B45 Tie Rod Pos.2	Not Measured	273. - 0.125E+04	K	0.64%FS
423	Fluid T.	TW-10	TE 423	B45 Tie Rod Pos.3	Not Measured	273. - 0.125E+04	K	0.64%FS
424	Fluid T.	TW-11	TE 424	B45 Tie Rod Pos.4	Not Measured	273. - 0.125E+04	K	0.64%FS
425	Fluid T.	TW-12	TE 425	B45 Tie Rod Pos.5	Not Measured	273. - 0.125E+04	K	0.64%FS
426	Fluid T.	TW-13	TE 426	B45 Tie Rod Pos.6	Not Measured	273. - 0.125E+04	K	0.64%FS
427	Fluid T.	TW-14	TE 427	B45 Tie Rod Pos.7	Not Measured	273. - 0.125E+04	K	0.64%FS
428	Fluid T.	TW-15	TE 428	C45 Tie Rod Pos.1	Fig.5.100	273. - 0.125E+04	K	0.64%FS
429	Fluid T.	TW-16	TE 429	C45 Tie Rod Pos.2	Fig.5.100	273. - 0.125E+04	K	0.64%FS
430	Fluid T.	TW-17	TE 430	C45 Tie Rod Pos.3	Fig.5.100	273. - 0.125E+04	K	0.64%FS
431	Fluid T.	TW-18	TE 431	C45 Tie Rod Pos.4	Fig.5.100	273. - 0.125E+04	K	0.64%FS
432	Fluid T.	TW-19	TE 432	C45 Tie Rod Pos.5	Fig.5.100	273. - 0.125E+04	K	0.64%FS
433	Fluid T.	TW-20	TE 433	C45 Tie Rod Pos.6	Fig.5.100	273. - 0.125E+04	K	0.64%FS
434	Fluid T.	TW-21	TE 434	C45 Tie Rod Pos.7	Fig.5.100	273. - 0.125E+04	K	0.64%FS
435	Fluid T.	TW-22	TE 435	D45 Tie Rod Pos.1	Not Measured	273. - 0.125E+04	K	0.64%FS
436	Fluid T.	TW-23	TE 436	D45 Tie Rod Pos.2	Not Measured	273. - 0.125E+04	K	0.64%FS
437	Fluid T.	TW-24	TE 437	D45 Tie Rod Pos.3	Not Measured	273. - 0.125E+04	K	0.64%FS
438	Fluid T.	TW-25	TE 438	D45 Tie Rod Pos.4	Not Measured	273. - 0.125E+04	K	0.64%FS
439	Fluid T.	TW-26	TE 439	D45 Tie Rod Pos.5	Not Measured	273. - 0.125E+04	K	0.64%FS
440	Fluid T.	TW-27	TE 440	D45 Tie Rod Pos.6	Not Measured	273. - 0.125E+04	K	0.64%FS
441	Fluid T.	TW-28	TE 441	D45 Tie Rod Pos.7	Not Measured	273. - 0.125E+04	K	0.64%FS
442	Fluid T.	TC- 1	TE 442	Channel Box A Inlet	Fig.5.127	273. - 0.125E+04	K	0.64%FS
443	Fluid T.	TC- 2	TE 443	Channel Box B Inlet	Fig.5.127	273. - 0.125E+04	K	0.64%FS
444	Fluid T.	TC- 3	TE 444	Channel Box C Inlet	Fig.5.127	273. - 0.125E+04	K	0.64%FS
445	Fluid T.	TC- 4	TE 445	Channel Box D Inlet	Fig.5.127	273. - 0.125E+04	K	0.64%FS
446	Fluid T.	TC- 5	TE 446	Channel Box Outlet A-1	Fig.5.128	273. - 0.125E+04	K	0.64%FS
447	Fluid T.	TC- 6	TE 447	Channel Box Outlet A-2	Fig.5.128	273. - 0.125E+04	K	0.64%FS
448	Fluid T.	TC- 7	TE 448	Channel Box Outlet A-3	Fig.5.128	273. - 0.125E+04	K	0.64%FS
449	Fluid T.	TC- 8	TE 449	Channel Box Outlet A-4	Fig.5.128	273. - 0.125E+04	K	0.64%FS
450	Fluid T.	TC- 9	TE 450	Channel Box Outlet A-6	Fig.5.128	273. - 0.125E+04	K	0.64%FS

Table 3.2 Measurement List for RUN 952 (Continued)

451Ch.- 500Ch.

Ch.	Item	Symbol	ID.	Location	Fig.No.	Range	Unit	Accuracy
451	Fluid T.	TC-10	TE 451	Channel Box Outlet C-1	Fig.5.129	273. - 0.125E+04	K	0.64%FS
452	Fluid T.	TC-11	TE 452	Channel Box Outlet C-2	Fig.5.129	273. - 0.125E+04	K	0.64%FS
453	Fluid T.	TC-12	TE 453	Channel Box Outlet C-3	Fig.5.129	273. - 0.125E+04	K	0.64%FS
454	Fluid T.	TC-13	TE 454	Channel Box Outlet C-4	Fig.5.129	273. - 0.125E+04	K	0.64%FS
455	Fluid T.	TC-14	TE 455	Channel Box Outlet C-6	Fig.5.129	273. - 0.125E+04	K	0.64%FS
456	Fluid T.	TG- 1	TE 456	Upper Tieplate A Up.1	Fig.5.130,134	273. - 0.125E+04	K	0.64%FS
457	Fluid T.	TG- 2	TE 457	Upper Tieplate A Up.2	Not Measured	273. - 0.125E+04	K	0.64%FS
458	Fluid T.	TG- 3	TE 458	Upper Tieplate A Up.3	Not Measured	273. - 0.125E+04	K	0.64%FS
459	Fluid T.	TG- 4	TE 459	Upper Tieplate A Up.4	Fig.5.130,135	273. - 0.125E+04	K	0.64%FS
460	Fluid T.	TG- 5	TE 460	Upper Tieplate A Up.5	Not Measured	273. - 0.125E+04	K	0.64%FS
461	Fluid T.	TG- 6	TE 461	Upper Tieplate A Up.6	Not Measured	273. - 0.125E+04	K	0.64%FS
462	Fluid T.	TG- 7	TE 462	Upper Tieplate A Up.7	Not Measured	273. - 0.125E+04	K	0.64%FS
463	Fluid T.	TG- 8	TE 463	Upper Tieplate A Up.8	Not Measured	273. - 0.125E+04	K	0.64%FS
464	Fluid T.	TG- 9	TE 464	Upper Tieplate A Up.9	Not Measured	273. - 0.125E+04	K	0.64%FS
465	Fluid T.	TG-10	TE 465	Upper Tieplate A Up.10	Fig.5.131,136	273. - 0.125E+04	K	0.64%FS
466	Fluid T.	TG-11	TE 466	Upper Tieplate A Lo.1	Fig.5.132,134	273. - 0.125E+04	K	0.64%FS
467	Fluid T.	TG-12	TE 467	Upper Tieplate A Lo.2	Not Measured	273. - 0.125E+04	K	0.64%FS
468	Fluid T.	TG-13	TE 468	Upper Tieplate A Lo.3	Not Measured	273. - 0.125E+04	K	0.64%FS
469	Fluid T.	TG-14	TE 469	Upper Tieplate A Lo.4	Fig.5.132,135	273. - 0.125E+04	K	0.64%FS
470	Fluid T.	TG-15	TE 470	Upper Tieplate A Lo.5	Not Measured	273. - 0.125E+04	K	0.64%FS
471	Fluid T.	TG-16	TE 471	Upper Tieplate A Lo.6	Not Measured	273. - 0.125E+04	K	0.64%FS
472	Fluid T.	TG-17	TE 472	Upper Tieplate A Lo.7	Not Measured	273. - 0.125E+04	K	0.64%FS
473	Fluid T.	TG-18	TE 473	Upper Tieplate A Lo.8	Not Measured	273. - 0.125E+04	K	0.64%FS
474	Fluid T.	TG-19	TE 474	Upper Tieplate A Lo.9	Not Measured	273. - 0.125E+04	K	0.64%FS
475	Fluid T.	TG-20	TE 475	Upper Tieplate A Lo.10	Fig.5.133,136	273. - 0.125E+04	K	0.64%FS
476	Fluid T.	TG-21	TE 476	Upper Tieplate C Up.1	Fig.5.137,141	273. - 0.125E+04	K	0.64%FS
477	Fluid T.	TG-22	TE 477	Upper Tieplate C Up.2	Not Measured	273. - 0.125E+04	K	0.64%FS
478	Fluid T.	TG-23	TE 478	Upper Tieplate C Up.3	Not Measured	273. - 0.125E+04	K	0.64%FS
479	Fluid T.	TG-24	TE 479	Upper Tieplate C Up.4	Fig.5.137,142	273. - 0.125E+04	K	0.64%FS
480	Fluid T.	TG-25	TE 480	Upper Tieplate C Up.5	Not Measured	273. - 0.125E+04	K	0.64%FS
481	Fluid T.	TG-26	TE 481	Upper Tieplate C Up.6	Not Measured	273. - 0.125E+04	K	0.64%FS
482	Fluid T.	TG-27	TE 482	Upper Tieplate C Up.7	Not Measured	273. - 0.125E+04	K	0.64%FS
483	Fluid T.	TG-28	TE 483	Upper Tieplate C Up.8	Not Measured	273. - 0.125E+04	K	0.64%FS
484	Fluid T.	TG-29	TE 484	Upper Tieplate C Up.9	Not Measured	273. - 0.125E+04	K	0.64%FS
485	Fluid T.	TG-30	TE 485	Upper Tieplate C Up.10	Fig.5.138,143	273. - 0.125E+04	K	0.64%FS
486	Fluid T.	TG-31	TE 486	Upper Tieplate C Lo.1	Fig.5.139,141	273. - 0.125E+04	K	0.64%FS
487	Fluid T.	TG-32	TE 487	Upper Tieplate C Lo.2	Not Measured	273. - 0.125E+04	K	0.64%FS
488	Fluid T.	TG-33	TE 488	Upper Tieplate C Lo.3	Not Measured	273. - 0.125E+04	K	0.64%FS
489	Fluid T.	TG-34	TE 489	Upper Tieplate C Lo.4	Fig.5.139,142	273. - 0.125E+04	K	0.64%FS
490	Fluid T.	TG-35	TE 490	Upper Tieplate C Lo.5	Not Measured	273. - 0.125E+04	K	0.64%FS
491	Fluid T.	TG-36	TE 491	Upper Tieplate C Lo.6	Not Measured	273. - 0.125E+04	K	0.64%FS
492	Fluid T.	TG-37	TE 492	Upper Tieplate C Lo.7	Not Measured	273. - 0.125E+04	K	0.64%FS
493	Fluid T.	TG-38	TE 493	Upper Tieplate C Lo.8	Not Measured	273. - 0.125E+04	K	0.64%FS
494	Fluid T.	TG-39	TE 494	Upper Tieplate C Lo.9	Not Measured	273. - 0.125E+04	K	0.64%FS
495	Fluid T.	TG-40	TE 495	Upper Tieplate C Lo.10	Fig.5.140,143	273. - 0.125E+04	K	0.64%FS
496	Slab T.	TB- 1	TE 496	C.B. A1 Inner ,Pos.1	Not Measured	273. - 0.125E+04	K	0.64%FS
497	Slab T.	TB- 2	TE 497	C.B. A1 Inner ,Pos.2	Not Measured	273. - 0.125E+04	K	0.64%FS
498	Slab T.	TB- 3	TE 498	C.B. A1 Inner ,Pos.3	Not Measured	273. - 0.125E+04	K	0.64%FS
499	Slab T.	TB- 4	TE 499	C.B. A1 Inner ,Pos.4	Not Measured	273. - 0.125E+04	K	0.64%FS
500	Slab T.	TB- 5	TE 500	C.B. A1 Inner ,Pos.5	Not Measured	273. - 0.125E+04	K	0.64%FS

Table 3.2 Measurement List for RUN 952 (Continued)

501Ch.- 550Ch.

Ch.	Item	Symbol	ID.	Location	Fig.No.	Range	Unit	Accuracy
501	Slab T.	TB- 6	TE 501	C.B. A1 Inner ,Pos.6	Not Measured	273. - 0.125E+04	K	0.64%FS
502	Slab T.	TB- 7	TE 502	C.B. A1 Inner ,Pos.7	Not Measured	273. - 0.125E+04	K	0.64%FS
503	Slab T.	TB- 8	TE 503	C.B. A2 Inner ,Pos.1	Not Measured	273. - 0.125E+04	K	0.64%FS
504	Slab T.	TB- 9	TE 504	C.B. A2 Inner ,Pos.2	Not Measured	273. - 0.125E+04	K	0.64%FS
505	Slab T.	TB-10	TE 505	C.B. A2 Inner ,Pos.3	Not Measured	273. - 0.125E+04	K	0.64%FS
506	Slab T.	TB-11	TE 506	C.B. A2 Inner ,Pos.4	Not Measured	273. - 0.125E+04	K	0.64%FS
507	Slab T.	TB-12	TE 507	C.B. A2 Inner ,Pos.5	Not Measured	273. - 0.125E+04	K	0.64%FS
508	Slab T.	TB-13	TE 508	C.B. A2 Inner ,Pos.6	Not Measured	273. - 0.125E+04	K	0.64%FS
509	Slab T.	TB-14	TE 509	C.B. A2 Inner ,Pos.7	Not Measured	273. - 0.125E+04	K	0.64%FS
510	Slab T.	TB-15	TE 510	C.B. B Inner ,Pos.1	Not Measured	273. - 0.125E+04	K	0.64%FS
511	Slab T.	TB-16	TE 511	C.B. B Inner ,Pos.2	Not Measured	273. - 0.125E+04	K	0.64%FS
512	Slab T.	TB-17	TE 512	C.B. B Inner ,Pos.3	Not Measured	273. - 0.125E+04	K	0.64%FS
513	Slab T.	TB-18	TE 513	C.B. B Inner ,Pos.4	Not Measured	273. - 0.125E+04	K	0.64%FS
514	Slab T.	TB-19	TE 514	C.B. B Inner ,Pos.5	Not Measured	273. - 0.125E+04	K	0.64%FS
515	Slab T.	TB-20	TE 515	C.B. B Inner ,Pos.6	Not Measured	273. - 0.125E+04	K	0.64%FS
516	Slab T.	TB-21	TE 516	C.B. B Inner ,Pos.7	Not Measured	273. - 0.125E+04	K	0.64%FS
517	Slab T.	TB-22	TE 517	C.B. C Inner ,Pos.1	Not Measured	273. - 0.125E+04	K	0.64%FS
518	Slab T.	TB-23	TE 518	C.B. C Inner ,Pos.2	Not Measured	273. - 0.125E+04	K	0.64%FS
519	Slab T.	TB-24	TE 519	C.B. C Inner ,Pos.3	Not Measured	273. - 0.125E+04	K	0.64%FS
520	Slab T.	TB-25	TE 520	C.B. C Inner ,Pos.4	Not Measured	273. - 0.125E+04	K	0.64%FS
521	Slab T.	TB-26	TE 521	C.B. C Inner ,Pos.5	Not Measured	273. - 0.125E+04	K	0.64%FS
522	Slab T.	TB-27	TE 522	C.B. C Inner ,Pos.6	Not Measured	273. - 0.125E+04	K	0.64%FS
523	Slab T.	TB-28	TE 523	C.B. C Inner ,Pos.7	Not Measured	273. - 0.125E+04	K	0.64%FS
524	Slab T.	TB-29	TE 524	C.B. D Inner ,Pos.1	Not Measured	273. - 0.125E+04	K	0.64%FS
525	Slab T.	TB-30	TE 525	C.B. D Inner ,Pos.2	Not Measured	273. - 0.125E+04	K	0.64%FS
526	Slab T.	TB-31	TE 526	C.B. D Inner ,Pos.3	Not Measured	273. - 0.125E+04	K	0.64%FS
527	Slab T.	TB-32	TE 527	C.B. D Inner ,Pos.4	Not Measured	273. - 0.125E+04	K	0.64%FS
528	Slab T.	TB-33	TE 528	C.B. D Inner ,Pos.5	Not Measured	273. - 0.125E+04	K	0.64%FS
529	Slab T.	TB-34	TE 529	C.B. D Inner ,Pos.6	Not Measured	273. - 0.125E+04	K	0.64%FS
530	Slab T.	TB-35	TE 530	C.B. D Inner ,Pos.7	Not Measured	273. - 0.125E+04	K	0.64%FS
531	Slab T.	TB-36	TE 531	C.B. A Outer ,Pos.1	Fig.5.101,144	273. - 0.125E+04	K	0.64%FS
532	Slab T.	TB-37	TE 532	C.B. A Outer ,Pos.2	Fig.5.101,144	273. - 0.125E+04	K	0.64%FS
533	Slab T.	TB-38	TE 533	C.B. A Outer ,Pos.3	Fig.5.101,144	273. - 0.125E+04	K	0.64%FS
534	Slab T.	TB-39	TE 534	C.B. A Outer ,Pos.4	Fig.5.101,144	273. - 0.125E+04	K	0.64%FS
535	Slab T.	TB-40	TE 535	C.B. A Outer ,Pos.5	Fig.5.101,144	273. - 0.125E+04	K	0.64%FS
536	Slab T.	TB-41	TE 536	C.B. A Outer ,Pos.6	Fig.5.101,144	273. - 0.125E+04	K	0.64%FS
537	Slab T.	TB-42	TE 537	C.B. A Outer ,Pos.7	Fig.5.101,144	273. - 0.125E+04	K	0.64%FS
538	Slab T.	TB-43	TE 538	C.B. C Outer ,Pos.1	Not Measured	273. - 0.125E+04	K	0.64%FS
539	Slab T.	TB-44	TE 539	C.B. C Outer ,Pos.2	Not Measured	273. - 0.125E+04	K	0.64%FS
540	Slab T.	TB-45	TE 540	C.B. C Outer ,Pos.3	Not Measured	273. - 0.125E+04	K	0.64%FS
541	Slab T.	TB-46	TE 541	C.B. C Outer ,Pos.4	Not Measured	273. - 0.125E+04	K	0.64%FS
542	Slab T.	TB-47	TE 542	C.B. C Outer ,Pos.5	Not Measured	273. - 0.125E+04	K	0.64%FS
543	Slab T.	TB-48	TE 543	C.B. C Outer ,Pos.6	Not Measured	273. - 0.125E+04	K	0.64%FS
544	Slab T.	TB-49	TE 544	C.B. C Outer ,Pos.7	Not Measured	273. - 0.125E+04	K	0.64%FS
545	Fluid T.	TP- 1	TE 545	Lower Pl. Center 1	Not Measured	273. - 0.125E+04	K	0.64%FS
546	Fluid T.	TP- 2	TE 546	Lower Pl. Center 2	Not Measured	273. - 0.125E+04	K	0.64%FS
547	Fluid T.	TP- 3	TE 547	Lower Pl. Center 3	Not Measured	273. - 0.125E+04	K	0.64%FS
548	Fluid T.	TP- 4	TE 548	Lower Pl. Center 4	Not Measured	273. - 0.125E+04	K	0.64%FS
549	Fluid T.	TP- 5	TE 549	Lower Pl. Center 5	Not Measured	273. - 0.125E+04	K	0.64%FS
550	Fluid T.	TP- 6	TE 550	Lower Pl. Center 7	Fig.5.145	273. - 0.125E+04	K	0.64%FS

Table 3.2 Measurement List for RUN 952 (Continued)

551Ch.- 600Ch.

Ch.	Item	Symbol	ID.		Location	Fig.No.	Range			Unit	Accuracy
551	Slab T.	TP- 7	TE	551	Lower Pl. North 1	Not Measured	273.	-	0.125E+04	K	0.64%FS
552	Slab T.	TP- 8	TE	552	Lower Pl. North 2	Not Measured	273.	-	673.	K	0.64%FS
553	Slab T.	TP- 9	TE	553	Lower Pl. North 4	Not Measured	273.	-	673.	K	0.64%FS
554	Slab T.	TP-10	TE	554	Lower Pl. North 6	Not Measured	273.	-	673.	K	0.64%FS
555	Slab T.	TP-11	TE	555	Lower Pl. South 1	Not Measured	273.	-	673.	K	0.64%FS
556	Slab T.	TP-12	TE	556	Lower Pl. South 2	Not Measured	273.	-	673.	K	0.64%FS
557	Slab T.	TP-13	TE	557	Lower Pl. South 4	Not Measured	273.	-	673.	K	0.64%FS
558	Slab T.	TP-14	TE	558	Lower Pl. South 6	Not Measured	273.	-	673.	K	0.64%FS
559	Level	LB- 1	LM	559	C.B.Liquid Level A1-1	Not Measured					
560	Level	LB- 2	LM	560	C.B.Liquid Level A1-2	Not Measured					
561	Level	LB- 3	LM	561	C.B.Liquid Level A1-3	Not Measured					
562	Level	LB- 4	LM	562	C.B.Liquid Level A1-4	Failure					
563	Level	LB- 5	LM	563	C.B.Liquid Level A1-5	Not Measured					
564	Level	LB- 6	LM	564	C.B.Liquid Level A1-6	Not Measured					
565	Level	LB- 7	LM	565	C.B.Liquid Level A1-7	Not Measured					
566	Level	LB- 8	LM	566	C.B.Liquid Level A2-1	Fig.5.146					
567	Level	LB- 9	LM	567	C.B.Liquid Level A2-2	Fig.5.146					
568	Level	LB-10	LM	568	C.B.Liquid Level A2-3	Fig.5.146					
569	Level	LB-11	LM	569	C.B.Liquid Level A2-4	Fig.5.146					
570	Level	LB-12	LM	570	C.B.Liquid Level A2-5	Failure					
571	Level	LB-13	LM	571	C.B.Liquid Level A2-6	Fig.5.146					
572	Level	LB-14	LM	572	C.B.Liquid Level A2-7	Fig.5.146					
573	Level	LB-15	LM	573	C.B.Liquid Level B-1	Fig.5.147					
574	Level	LB-16	LM	574	C.B.Liquid Level B-2	Fig.5.147					
575	Level	LB-17	LM	575	C.B.Liquid Level B-3	Fig.5.147					
576	Level	LB-18	LM	576	C.B.Liquid Level B-4	Fig.5.147					
577	Level	LB-19	LM	577	C.B.Liquid Level B-5	Fig.5.147					
578	Level	LB-20	LM	578	C.B.Liquid Level B-6	Fig.5.147					
579	Level	LB-21	LM	579	C.B.Liquid Level B-7	Fig.5.147					
580	Level	LB-22	LM	580	C.B.Liquid Level C-1	Fig.5.148					
581	Level	LB-23	LM	581	C.B.Liquid Level C-2	Fig.5.148					
582	Level	LB-24	LM	582	C.B.Liquid Level C-3	Fig.5.148					
583	Level	LB-25	LM	583	C.B.Liquid Level C-4	Fig.5.148					
584	Level	LB-26	LM	584	C.B.Liquid Level C-5	Fig.5.148					
585	Level	LB-27	LM	585	C.B.Liquid Level C-6	Fig.5.148					
586	Level	LB-28	LM	586	C.B.Liquid Level C-7	Fig.5.148					
587	Level	LB-29	LM	587	C.B.Liquid Level D-1	Not Measured					
588	Level	LB-30	LM	588	C.B.Liquid Level D-2	Not Measured					
589	Level	LB-31	LM	589	C.B.Liquid Level D-3	Not Measured					
590	Level	LB-32	LM	590	C.B.Liquid Level D-4	Not Measured					
591	Level	LB-33	LM	591	C.B.Liquid Level D-5	Failure					
592	Level	LB-34	LM	592	C.B.Liquid Level D-6	Not Measured					
593	Level	LB-35	LM	593	C.B.Liquid Level D-7	Not Measured					
594	Level	LL- 1	LM	594	Ch.Box Outlet A1-5	Failure					
595	Level	LL- 2	LM	595	Ch.Box Outlet A1-6	Failure					
596	Level	LL- 3	LM	596	Ch.Box Outlet A1-7	Fig.5.177					
597	Level	LL- 4	LM	597	Ch.Box Outlet A2-5	Fig.5.149					
598	Level	LL- 5	LM	598	Ch.Box Outlet A2-6	Fig.5.149					
599	Level	LL- 6	LM	599	Ch.Box Outlet A2-7	Fig.5.149					
600	Level	LL- 7	LM	600	Ch.Box Outlet A-1	Failure					

Table 3.2 Measurement List for RUN 952 (Continued)

601Ch.- 650Ch.

Ch.	Item	Symbol	ID.	Location	Fig.No.	Range	Unit	Accuracy
601	Level	LL- 8	LM 601	Ch.Box Outlet A-2	Failure			
602	Level	LL- 9	LM 602	Ch.Box Outlet A-3	Fig.5.150			
603	Level	LL-10	LM 603	Ch.Box Outlet A-4	Fig.5.150			
604	Level	LL-11	LM 604	Ch.Box Outlet A-6	Fig.5.150			
605	Level	LL-12	LM 605	Ch.Box Outlet C1-5	Fig.5.151			
606	Level	LL-13	LM 606	Ch.Box Outlet C1-6	Fig.5.151			
607	Level	LL-14	LM 607	Ch.Box Outlet C1-7	Fig.5.151			
608	Level	LL-15	LM 608	Ch.Box Outlet C2-5	Not Measured			
609	Level	LL-16	LM 609	Ch.Box Outlet C2-6	Not Measured			
610	Level	LL-17	LM 610	Ch.Box Outlet C2-7	Not Measured			
611	Level	LL-18	LM 611	Ch.Box Outlet C-1	Fig.5.152			
612	Level	LL-19	LM 612	Ch.Box Outlet C-2	Fig.5.152			
613	Level	LL-20	LM 613	Ch.Box Outlet C-3	Fig.5.152			
614	Level	LL-21	LM 614	Ch.Box Outlet C-4	Fig.5.152			
615	Level	LL-22	LM 615	Ch.Box Outlet C-6	Fig.5.152			
616	Level	LL-23	LM 616	Ch.Box Inlet A-1	Fig.5.153			
617	Level	LL-24	LM 617	Ch.Box Inlet A-2	Fig.5.153			
618	Level	LL-25	LM 618	Ch.Box Inlet B-1	Not Measured			
619	Level	LL-26	LM 619	Ch.Box Inlet B-2	Not Measured			
620	Level	LL-27	LM 620	Ch.Box Inlet C-1	Fig.5.154			
621	Level	LL-28	LM 621	Ch.Box Inlet C-2	Fig.5.154			
622	Level	LL-29	LM 622	Ch.Box Inlet D-1	Not Measured			
623	Level	LL-30	LM 623	Ch.Box Inlet D-2	Not Measured			
624	Level	LL-31	LM 624	Lower Pl. North 1	Fig.5.155			
625	Level	LL-32	LM 625	Lower Pl. North 2	Fig.5.155			
626	Level	LL-33	LM 626	Lower Pl. North 3	Fig.5.155			
627	Level	LL-34	LM 627	Lower Pl. North 4	Fig.5.155			
628	Level	LL-35	LM 628	Lower Pl. North 5	Fig.5.155			
629	Level	LL-36	LM 629	Lower Pl. North 6	Fig.5.155			
630	Level	LL-37	LM 630	Lower Pl. South 1	Not Measured			
631	Level	LL-38	LM 631	Lower Pl. South 2	Not Measured			
632	Level	LL-39	LM 632	Lower Pl. South 3	Not Measured			
633	Level	LL-40	LM 633	Lower Pl. South 4	Not Measured			
634	Level	LL-41	LM 634	Lower Pl. South 5	Not Measured			
635	Level	LL-42	LM 635	Lower Pl. South 6	Not Measured			
636	Level	LL-43	LM 636	Guide Tube North 0	Fig.5.156			
637	Level	LL-44	LM 637	Guide Tube North 1	Fig.5.156			
638	Level	LL-45	LM 638	Guide Tube North 3	Fig.5.156			
639	Level	LL-46	LM 639	Guide Tube North 6	Fig.5.156			
640	Level	LL-47	LM 640	Guide Tube South 0	Not Measured			
641	Level	LL-48	LM 641	Guide Tube South 1	Not Measured			
642	Level	LL-49	LM 642	Guide Tube South 3	Not Measured			
643	Level	LL-50	LM 643	Guide Tube South 6	Not Measured			
644	Level	L- 1	LM 644	Downcomer D-Side 1	Fig.5.157			
645	Level	L- 2	LM 645	Downcomer D-Side 2	Fig.5.157			
646	Level	L- 3	LM 646	Downcomer D-Side 3	Fig.5.157			
647	Level	L- 4	LM 647	Downcomer D-Side 4	Fig.5.157			
648	Level	L- 5	LM 648	Downcomer D-Side 5	Fig.5.157			
649	Level	L- 6	LM 649	Downcomer B-Side 1	Not Measured			
650	Level	L- 7	LM 650	Downcomer B-Side 2	Not Measured			

Table 3.2 Measurement List for RUN 952 (Continued)

651Ch.- 700Ch.

Ch.	Item	Symbol	ID.	Location	Fig.No.	Range	Unit	Accuracy
651	Level	L- 8	LM 651	Downcomer B-Side 3	Not Measured			
652	Level	L- 9	LM 652	Downcomer B-Side 4	Not Measured			
653	Level	L-10	LM 653	Downcomer B-Side 5	Not Measured			
654	Void	VF- 1	VD 654	A54 Tie Rod Pos.1	Not Measured	0.0 - 1.00		
655	Void	VF- 2	VD 655	A54 Tie Rod Pos.2	Not Measured	0.0 - 1.00		
656	Void	VF- 3	VD 656	A54 Tie Rod Pos.3	Not Measured	0.0 - 1.00		
657	Void	VF- 4	VD 657	A54 Tie Rod Pos.4	Not Measured	0.0 - 1.00		
658	Void	VF- 5	VD 658	A54 Tie Rod Pos.5	Not Measured	0.0 - 1.00		
659	Void	VF- 6	VD 659	A54 Tie Rod Pos.6	Not Measured	0.0 - 1.00		
660	Void	VF- 7	VD 660	A54 Tie Rod Pos.7	Not Measured	0.0 - 1.00		
661	Void	VF- 8	VD 661	B54 Tie Rod Pos.1	Not Measured	0.0 - 1.00		
662	Void	VF- 9	VD 662	B54 Tie Rod Pos.2	Not Measured	0.0 - 1.00		
663	Void	VF-10	VD 663	B54 Tie Rod Pos.3	Not Measured	0.0 - 1.00		
664	Void	VF-11	VD 664	B54 Tie Rod Pos.4	Not Measured	0.0 - 1.00		
665	Void	VF-12	VD 665	B54 Tie Rod Pos.5	Not Measured	0.0 - 1.00		
666	Void	VF-13	VD 666	B54 Tie Rod Pos.6	Not Measured	0.0 - 1.00		
667	Void	VF-14	VD 667	B54 Tie Rod Pos.7	Not Measured	0.0 - 1.00		
668	Void	VF-15	VD 668	C54 Tie Rod Pos.1	Not Measured	0.0 - 1.00		
669	Void	VF-16	VD 669	C54 Tie Rod Pos.2	Not Measured	0.0 - 1.00		
670	Void	VF-17	VD 670	C54 Tie Rod Pos.3	Not Measured	0.0 - 1.00		
671	Void	VF-18	VD 671	C54 Tie Rod Pos.4	Not Measured	0.0 - 1.00		
672	Void	VF-19	VD 672	C54 Tie Rod Pos.5	Not Measured	0.0 - 1.00		
673	Void	VF-20	VD 673	C54 Tie Rod Pos.6	Not Measured	0.0 - 1.00		
674	Void	VF-21	VD 674	C54 Tie Rod Pos.7	Not Measured	0.0 - 1.00		
675	Void	VF-22	VD 675	D54 Tie Rod Pos.7	Not Measured	0.0 - 1.00		
676	Void	VF-23	VD 676	D54 Tie Rod Pos.7	Not Measured	0.0 - 1.00		
677	Void	VF-24	VD 677	D54 Tie Rod Pos.7	Not Measured	0.0 - 1.00		
678	Void	VF-25	VD 678	D54 Tie Rod Pos.7	Not Measured	0.0 - 1.00		
679	Void	VF-26	VD 679	D54 Tie Rod Pos.7	Not Measured	0.0 - 1.00		
680	Void	VF-27	VD 680	D54 Tie Rod Pos.7	Not Measured	0.0 - 1.00		
681	Void	VF-28	VD 681	D54 Tie Rod Pos.7	Not Measured	0.0 - 1.00		
682	Void	VE- 1	VD 682	Channel A Outlet 1	Not Measured	0.0 - 1.00		
683	Void	VE- 2	VD 683	Channel A Outlet 2	Not Measured	0.0 - 1.00		
684	Void	VE- 3	VD 684	Channel A Outlet 3	Not Measured	0.0 - 1.00		
685	Void	VE- 4	VD 685	Channel B Outlet 1	Not Measured	0.0 - 1.00		
686	Void	VE- 5	VD 686	Channel B Outlet 2	Not Measured	0.0 - 1.00		
687	Void	VE- 6	VD 687	Channel B Outlet 3	Not Measured	0.0 - 1.00		
688	Void	VE- 7	VD 688	Channel C Outlet 1	Not Measured	0.0 - 1.00		
689	Void	VE- 8	VD 689	Channel C Outlet 2	Not Measured	0.0 - 1.00		
690	Void	VE- 9	VD 690	Channel C Outlet 3	Not Measured	0.0 - 1.00		
691	Void	VE-10	VD 691	Channel D Outlet 1	Not Measured	0.0 - 1.00		
692	Void	VE-11	VD 692	Channel D Outlet 2	Not Measured	0.0 - 1.00		
693	Void	VE-12	VD 693	Channel D Outlet 3	Not Measured	0.0 - 1.00		
694	Void	VE-13	VD 694	Lower Plenum Bottom 1	Not Measured	0.0 - 1.00		
695	Void	VE-14	VD 695	Lower Plenum Bottom 2	Not Measured	0.0 - 1.00		
696	Void	VE-15	VD 696	Lower Plenum Bottom 3	Not Measured	0.0 - 1.00		
697	Void	VP- 1	VD 697	Lower Plenum Inlet	Not Measured	0.0 - 1.00		
698	Void	VP- 2	VD 698	Lower Plenum Inlet	Not Measured	0.0 - 1.00		

Table 3.3 Core Instrumentation Map

Item	Pos. / DL / Rod NO.	Core Outlet	Pos.1	Pos.2	Pos.3	Pos.4	Pos.5	Pos.6	Pos.7	Core Inlet
		3660	3417	3114.5	2879.5	2527	2174.5	1939.5	1637	1454
Surface Temp.	A11		TF 1	TF 2	TF 3	TF 4	TF 5	TF 6	TF 7	
	A12		TF 8	TF 9	TF 10	TF 11	TF 12	TF 13	TF 14	
	A13		TF 15	TF 16	TF 17	TF 18	TF 19	TF 20	TF 21	
	A14		TF 22	TF 23	TF 24	TF 25	TF 26	TF 27	TF 28	
	A15		TF 29			TF 30				
	A17		TF 31			TF 32				
	A22		TF 33	TF 34	TF 35	TF 36	TF 37	TF 38	TF 39	
	A23		TF 40	TF 41	TF 42	TF 43	TF 44	TF 45	TF 46	
	A24		TF 47	TF 48	TF 49	TF 50	TF.51	TF 52	TF 53	
	A26		TF 54			TF 55				
	A28		TF 56			TF 57				
	A31		TF 58			TF 59				
	A33		TF 60	TF 61	TF 62	TF 63	TF 64	TF 65	TF 66	
	A34		TF 67	TF 68	TF 69	TF 70	TF 71	TF 72	TF 73	
	A35		TF 74			TF 75				
	A37		TF 76			TF 77				
	A42		TF 78			TF 79				
Fluid Temp.	A44	TC 1	TF180	TF181	TF182	TF183	TF184	TF185	TF186	TC 2
Surface Temp.	A45		TF 80			TF 81				
	A46		TF 82			TF 83				
	A48		TF 84			TF 85				
	A51		TF 86			TF 87				
	A53		TF 88			TF 89				
	A54		TF 90							
	A57		TF 91			TF 92				
	A62		TF 93			TF 94				
	A64		TF 95			TF 96				
	A66		TF 97			TF 98				
	A68		TF 99			TF100				
	A71		TF101			TF102				
	A73		TF103			TF104				
	A75		TF105			TF106				
	A77		TF107			TF108				

Table 3.3 Core Instrumentation Map (Continued)

Item	Rod NO. \ Pos. / DL	Core Outlet	Pos.1	Pos.2	Pos.3	Pos.4	Pos.5	Pos.6	Pos.7	Core Inlet
		3660	3417	3114.5	2879.5	2527	2174.5	1939.5	1637	1454
Surface Temp.	A82		TF109			TF110				
	A84		TF111			TF112				
	A86		TF113			TF114				
	A88		TF115			TF116				
	B11					TF117				
	B13					TF118				
	B15		TF119	TF120	TF121	TF122	TF123	TF124	TF125	
	B31					TF126				
	B33					TF127				
	B35					TF128				
Fluid Temp.	B44	TC 3	TF187	TF188	TF189	TF190	TF191	TF192	TF193	TC 4
Surface Temp.	B51					TF129				
	B53					TF130				
	B85		TF131	TF132	TF133	TF134	TF135	TF136	TF137	
	C11					TF138				
	C13					TF139				
	C15					TF140				
	C31					TF141				
	C33		TF142	TF143	TF144	TF145	TF146	TF147	TF148	
	C35					TF149				
Fluid Temp.	C44	TC 5	TF194	TF195	TF196	TF197	TF198	TF199	TF200	TC 6
Surface Temp.	C51					TF150				
	C53					TF151				
	C77		TF152	TF153	TF154	TF155	TF156	TF157	TF158	
	D11					TF159				
	D13					TF160				
	D27		TF161	TF162	TF163	TF164	TF165	TF166	TF167	
	D31					TF168				
	D33					TF169				
	D35					TF170				
Fluid Temp.	D44	TC 7	TF201	TF202	TF203	TF204	TF205	TF206	TF207	TC 8
Surface Temp.	D51					TF171				
	D53					TF172				
	D88		TF173	TF174	TF175	TF176	TF177	TF178	TF179	

Table 3.3 Core Instrumentation Map (Continued)

Item	Rod NO. \ Pos. / DL	Core Outlet	Pos. 1	Pos. 2	Pos. 3	Pos. 4	Pos. 5	Pos. 6	Pos. 7	Core Inlet
		3660	3417	3114.5	2879.5	2527	2174.5	1939.5	1673	1454
Void	A55		VF 1	VF 2	VF 3	VF 4	VF 5	VF 6	VF 7	
	B55		VF 8	VF 9	VF 10	VF 11	VF 12	VF 13	VF 14	
	C55		VF 15	VF 16	VF 17	VF 18	VF 19	VF 20	VF 21	
	D55		VF 22	VF 23	VF 24	VF 25	VF 26	VF 27	VF 28	
Channel Box Surface Temp.	A1*		TB 1	TB 2	TB 3	TB 4	TB 5	TB 6	TB 7	
	A2*		TB 8	TB 9	TB 10	TB 11	TB 12	TB 13	TB 14	
	B*		TB 15	TB 16	TB 17	TB 18	TB 19	TB 20	TB 21	
	C*		TB 22	TB 23	TB 24	TB 25	TB 26	TB 27	TB 28	
	D*		TB 29	TB 30	TB 31	TB 32	TB 33	TB 34	TB 35	
Liquid Level in the Channel Box	A1*		LB 1	LB 2	LB 3	LB 4	LB 5	LB 6	LB 7	
	A2*		LB 8	LB 9	LB 10	LB 11	LB 12	LB 13	LB 14	
	B*		LB 15	LB 16	LB 17	LB 18	LB 19	LB 20	LB 21	
	C*		LB 22	LB 23	LB 24	LB 25	LB 26	LB 27	LB 28	
	D*		LB 29	LB 30	LB 31	LB 32	LB 33	LB 34	LB 35	

Table 4.1 Test conditions of the ROSA-III test Run 952

Item	Specified Value	Measured Value
Break Conditions		
Location	Main Steam Line	Main Steam Line
Type	Single-ended	Single-ended
Break Orifice Diameter (mm)	31.0	31.0
Break Area Ratio (%)	100	100
Break Initiation Logic	Full open of AV-165	Full open of AV-165
Initial Conditions		
Steam Dome Pressure (MPa)	7.35	7.35
Lower Plenum Temperature (K)	552.7 (279.5°C)	552.4 (279.3°C)
Lower plenum Subcooling (K)	10.5	10.7
Core Inlet FLow Rate (*1) (kg/s)	16.0	16.6
Core Outlet Quality (*2) (%)	13.2	12.5
Power Generation (kW)	3960 (1260 + 2700)	3962 (1262 + 2700)
Max. Linear Heat Rate (kW/m)		
Channel A P.F. = 1.1	16.65	16.58
P.F. = 1.0	15.13	15.15
P.F. = 0.875	13.24	13.26
Channel B,C,D P.F. = 1.1	11.89	11.89
P.F. = 1.0	10.81	10.81
P.F. = 0.875	9.46	9.46
Power Simulation (*3)	dh + dn + sh (Fig. 4.2)	dh + dn + sh (Fig. 5.53)
Fuel Assembly Number	4	4
Water Level in PV (m)	5.0	5.07
Feed water Conditions		
Temperature (K)	489 (216°C)	491 (218°C)
Steady State Flow Rate (kg/s)	2.08	2.04
Valve Closure Time (s)	2	Fig.5.55

(*1) Flow rate include core bypass flow, i.e., 10 % of total flow.

(*2) Average quality in the upper plenum.

(*3) decay heat + delayed fission power + stored heat release

Table 4.1 (Continued)

Items	Specified Value	Measured Value
Steam Line Conditions		
Steady Steady Flow Rate (kg/s)	2.08	2.06
Transient Flow Rate (kg/s)	——	Figs.5.36 and 5.165
MSIV closure	——	——
Safety Relief Valve Set Point(MPa)	8.13	not reached
ECCS Conditions		
HPCS		
Injection Location	Upper Plenum	Upper Plenum
Initiation Time t(s)	L2(*4) + 27 ≦ t	94
Initiation Pressure P(MPa)	P ≦ 8.00	2.23
Coolant Temperature (K)	313(40°C)	313(40°C)
Injection Flow Rate (m^3/s)	6.17×10^{-4}	Fig.5.37
LPCS		
Injection Location	Upper Plenum	Upper Plenum
Initiation Time t(s)	L1(*4) + 40 ≦ t	not actuated
Initiation Pressure P(MPa)	P ≦ 2.16	——
Coolant Temperature (K)	313(40°C)	——
Injection Flow Rate (m^3/s)	1.13×10^{-3}	——
LPCI		
Injection Location	Top of Core Bypass	Top of Core Bypass
Initiation Time t(s)	L1 + 40 ≦ t	not actuated
Initiation Pressure P(MPa)	P ≦ 1.57	——
Coolant Temperature (K)	313(40°C)	——
Injection Flow Rate (m^3/s)	3.50×10^{-3}	——
ADS Conditions	not used	not used

(*4) L1: Water level in the downcomer, 4.25 m from PV bottom.
L2: Water level in the downcomer, 4.76 m from PV bottom.

Table 4.2 Characteristics of Steam Discharge Line Valves

Valve	Close to Open (sec)	Open to Close (sec)
AV165	0.1	-
AV168	-	0.1
AV169	not used	not used

Orifice	Diameter (mm)	Area (mm^2)
OR3	18.0	254.5
OR4	not used	not used
OR5	31.0	754.8

Table 4.3 Control Sequence for Steam Discharge Line Valves

Time	t < 0 s	t = 0 s (Break)
CV-1	Open	Close (Manual)
CV-2 (see Fig.2.3)	Open	Close (Manual)
CV-130	Control to maintain steady state pressure	Close (Manual)
AV-168 (MSIV)	Open	Close
AV-165 (Transient Line)	Closed	Open

Table 5.1 Sequence of events in RUN 952

Time (s)	Procedures and Events
-122	- Initiation of data recording with DATAC 2000B system
- 10	- Initiation of data plotting in the figures
0.0	- Initiation of break in the Main Steam Line (AV-165 was opened and AV-168 was closed) - MRP1 coastdown - MRP2 coastdown - system pressure began to decrease
1.3	- Initiation of feedwater line closure (completed at 3.2 s)
4.2	- Initiation of Lower Plenum flashing
9.0	- Initiation of core power decrease
71	- Liquid level in the upper downcomer decreased to L2 level
94	- HPCS actuation (at system pressure of 2.23 MPa)
95	- Initiation of feedwater flashing
100	- PCT at position 4 of A31 rod (752 K)
170	- Initiation of mass recovery in the core shroud
376	- Initiation of liquid level recovery in the upper downcomer (at 4.28m from PV bottom)
450	- Termination of data plotting (except for Fig. 5.181)
1017	- LPCI manual injection
1183	- Termination of data recording

Table 5.2 Maximum Cladding Temperature Distribution in the Core

	Pos.1	Pos.2	Pos.3	Pos.4	Pos.5	Pos.6	Pos.7
A-11 rod	TE 201	TE 202	TE 203	TE 204	TE 205	TE 206	TE 207
PCT (K)	649.9	735.1	737.5	687.1	580.3	568.5	570.3
Time (s)	172.9	160.3	138.6	114.1	104.3	0.0	0.0
A-12 rod	TE 208	TE 209	TE 210	TE 211	TE 212	TE 213	TE 214
PCT (K)	658.3	713.5	726.7	677.5	569.6	568.3	565.9
Time (s)	161.0	144.2	132.3	111.3	0.0	0.0	0.0
A-13 rod	TE 215	TE 216	TE 217	TE 218	TE 219	TE 220	TE 221
PCT (K)	654.7	708.7	730.3	676.3	575.5	568.1	568.2
Time (s)	161.0	160.3	130.9	109.2	104.3	0.0	0.0
A-14 rod	TE 222	TE 223	TE 224	TE 225	TE 226	TE 227	TE 228
PCT (K)	------	------	------	------	------	------	------
Time (s)	------	------	------	------	------	------	------
A-15 rod	TE 229			TE 230			
PCT (K)	------			------			
Time (s)	------			------			
A-17 rod	TE 231			TE 232			
PCT (K)	------			672.7			
Time (s)	------			107.8			
A-22 rod	TE 233	TE 234	TE 235	TE 236	TE 237	TE 238	TE 239
PCT (K)	670.3	715.9	721.9	662.9	571.0	570.4	567.2
Time (s)	165.2	135.8	135.8	107.8	0.0	0.0	0.0
A-24 rod	TE 240	TE 241	TE 242	TE 243	TE 244	TE 245	TE 246
PCT (K)	------	------	------	------	------	------	------
Time (s)	------	------	------	------	------	------	------
A-26 rod	TE 247			TE 248			
PCT (K)	------			------			
Time (s)	------			------			
A-28 rod	TE 249			TE 250			
PCT (K)	------			674.7			
Time (s)	------			110.6			
A-31 rod	TE 251			TE 252			
PCT (K)	------			752.4			
Time (s)	------			107.8			
A-33 rod	TE 253	TE 254	TE 255	TE 256	TE 257	TE 258	TE 259
PCT (K)	573.0	608.5	612.3	573.9	564.3	567.2	562.4
Time (s)	158.2	140.0	130.2	110.6	0.0	0.0	0.0
A-34 rod	TE 260	TE 261	TE 262	TE 263	TE 264	TE 265	TE 266
PCT (K)	------	------	------	------	------	------	------
Time (s)	------	------	------	------	------	------	------
A-37 rod	TE 267			TE 268			
PCT (K)	------			------			
Time (s)	------			------			
A-42 rod	TE 269			TE 270			
PCT (K)	------			------			
Time (s)	------			------			
A-44 rod	TE 271	TE 272	TE 273	TE 274	TE 275	TE 276	TE 277
PCT (K)	------	------	------	------	------	------	------
Time (s)	------	------	------	------	------	------	------

Table 5.2 Maximum Cladding Temperature Distribution in the Core (Continued)

	Pos.1	Pos.2	Pos.3	Pos.4	Pos.5	Pos.6	Pos.7
A-48 rod	TE 278			TE 279			
PCT (K)	------			------			
Time (s)	------			------			
A-51 rod	TE 280			TE 281			
PCT (K)	------			------			
Time (s)	------			------			
A-53 rod	TE 282			TE 283			
PCT (K)	------			------			
Time (s)	------			------			
A-57 rod	TE 284			TE 285			
PCT (K)	------			661.9			
Time (s)	------			109.9			
A-62 rod	TE 286			TE 287			
PCT (K)	------			------			
Time (s)	------			------			
A-66 rod	TE 288			TE 289			
PCT (K)	------			------			
Time (s)	------			------			
A-68 rod	TE 290			TE 291			
PCT (K)	358.3			674.2			
Time (s)	193.2			109.9			
A-71 rod	TE 292			TE 293			
PCT (K)	421.7			690.3			
Time (s)	194.6			110.6			
A-73 rod	TE 294			TE 295			
PCT (K)	416.8			669.5			
Time (s)	202.3			109.9			
A-75 rod	TE 296			TE 297			
PCT (K)	404.0			------			
Time (s)	226.8			------			
A-77 rod	TE 298	TE 299	TE 300	TE 301	TE 302	TE 303	TE 304
PCT (K)	649.5	700.7	708.2	649.5	566.4	567.1	525.8
Time (s)	159.6	140.0	133.7	107.8	0.0	0.0	0.0
A-82 rod	TE 305			TE 306			
PCT (K)	376.7			689.3			
Time (s)	324.8			108.5			
A-84 rod	TE 307			TE 308			
PCT (K)	689.3			674.2			
Time (s)	108.5			109.9			
A-85 rod	TE 309	TE 310	TE 311	TE 312	TE 313	TE 314	TE 315
PCT (K)	415.8	------	------	------	------	------	------
Time (s)	192.5	------	------	------	------	------	------
A-87 rod	TE 316	TE 317	TE 318	TE 319	TE 320	TE 321	TE 322
PCT (K)	612.3	709.2	720.5	674.2	567.5	567.2	564.5
Time (s)	172.9	147.7	133.7	110.6	0.0	0.0	0.0
A-88 rod	TE 323	TE 324	TE 325	TE 326	TE 327	TE 328	TE 329
PCT (K)	617.1	709.2	719.5	678.0	574.9	566.4	565.1
Time (s)	172.2	143.5	138.6	110.6	103.6	0.0	0.0

Table 5.2 Maximum Cladding Temperature Distribution in the Core (Continued)

	Pos.1	Pos.2	Pos.3	Pos.4	Pos.5	Pos.6	Pos.7
B-11 rod	TE 330	TE 331	TE 332	TE 333	TE 334	TE 335	TE 336
PCT (K)	584.5	711.1	719.5	664.7	565.1	566.3	396.1
Time (s)	65.8	137.9	151.2	114.8	0.0	0.0	275.8
B-13 rod				TE 337			
PCT (K)				662.8			
Time (s)				112.0			
B-22 rod	TE 338	TE 339	TE 340	TE 341	TE 342	TE 343	TE 344
PCT (K)	652.4	695.0	713.9	647.6	566.9	564.3	561.3
Time (s)	161.0	142.1	157.5	110.6	0.0	0.0	0.0
B-31 rod				TE 345			
PCT (K)				399.1			
Time (s)				228.9			
B-33 rod				TE 346			
PCT (K)				------			
Time (s)				------			
B-51 rod				TE 347			
PCT (K)				------			
Time (s)				------			
B-53 rod				TE 348			
PCT (K)				------			
Time (s)				------			
B-66 rod				TE 349			
PCT (K)				------			
Time (s)				------			
B-77 rod	TE 350	TE 351	TE 352	TE 353	TE 354	TE 355	TE 356
PCT (K)	646.7	704.5	716.7	650.5	565.1	565.3	563.7
Time (s)	128.8	133.0	147.7	112.0	0.0	0.0	0.0
B-86 rod				TE 357			
PCT (K)				404.0			
Time (s)				270.2			
C-11 rod	TE 358	TE 359	TE 360	TE 361	TE 362	TE 363	TE 364
PCT (K)	571.0	706.4	717.7	669.5	560.3	566.0	559.6
Time (s)	65.8	182.0	157.5	125.3	0.0	0.0	0.0
C-13 rod	TE 365	TE 366	TE 367	TE 368	TE 369	TE 370	TE 371
PCT (K)	589.3	676.1	710.1	664.7	568.0	566.3	563.4
Time (s)	65.8	182.7	159.6	122.5	0.0	0.0	0.0
C-15 rod				TE 372			
PCT (K)				415.8			
Time (s)				184.8			
C-22 rod	TE 373	TE 374	TE 375	TE 376	TE 377	TE 378	TE 379
PCT (K)	660.0	707.3	711.1	653.3	568.9	568.5	562.5
Time (s)	181.3	182.0	157.5	119.7	0.0	0.0	0.0
C-31 rod				TE 380			
PCT (K)				408.9			
Time (s)				188.3			
C-33 rod	TE 381	TE 382	TE 383	TE 384	TE 385	TE 386	TE 387
PCT (K)	641.0	670.4	668.5	624.8	566.3	565.2	561.5
Time (s)	184.1	182.0	157.5	116.2	0.0	0.0	0.0

Table 5.2 Maximum Cladding Temperature Distribution in the Core (Continued)

	Pos.1	Pos.2	Pos.3	Pos.4	Pos.5	Pos.6	Pos.7
C-35 rod				TE 388			
PCT (K)				420.7			
Time (s)				220.5			
C-66 rod				TE 389			
PCT (K)				------			
Time (s)				------			
C-68 rod				TE 390			
PCT (K)				------			
Time (s)				------			
C-77 rod	TE 391	TE 392	TE 393	TE 394	TE 395	TE 396	TE 397
PCT (K)	666.6	713.9	710.1	655.2	567.4	565.4	563.3
Time (s)	186.2	184.1	157.5	119.0	0.0	0.0	0.0
D-11 rod				TE 398			
PCT (K)				678.9			
Time (s)				122.5			
D-13 rod				TE 399			
PCT (K)				654.3			
Time (s)				122.5			
D-22 rod	TE 400	TE 401	TE 402	TE 403	TE 404	TE 405	TE 406
PCT (K)	677.1	725.2	729.9	620.9	566.0	567.1	564.6
Time (s)	185.5	171.5	168.0	118.3	0.0	0.0	0.0
D-31 rod				TE 407			
PCT (K)				427.7			
Time (s)				124.6			
D-33 rod				TE 408			
PCT (K)				------			
Time (s)				------			
D-51 rod				TE 409			
PCT (K)				------			
Time (s)				------			
D-53 rod				TE 410			
PCT (K)				------			
Time (s)				------			
D-66 rod				TE 411			
PCT (K)				------			
Time (s)				------			
D-77 rod				TE 412			
PCT (K)				653.3			
Time (s)				117.6			
D-86 rod				TE 413			
PCT (K)				665.7			
Time (s)				118.3			

Table 5.2 Maximum Cladding Temperature Distribution in the Core (Continued)

** Order of PCT **

No. 1	A-31 rod	Pos. 4	PCT = 752.4 (K)	Time = 107.8 (s)
No. 2	A-11 rod	Pos. 3	PCT = 737.5 (K)	Time = 138.6 (s)
No. 3	A-11 rod	Pos. 2	PCT = 735.1 (K)	Time = 160.3 (s)
No. 4	A-13 rod	Pos. 3	PCT = 730.3 (K)	Time = 130.9 (s)
No. 5	D-22 rod	Pos. 3	PCT = 729.9 (K)	Time = 168.0 (s)
No. 6	A-12 rod	Pos. 3	PCT = 726.7 (K)	Time = 132.3 (s)
No. 7	D-22 rod	Pos. 2	PCT = 725.2 (K)	Time = 171.5 (s)
No. 8	A-22 rod	Pos. 3	PCT = 721.9 (K)	Time = 135.8 (s)
No. 9	A-87 rod	Pos. 3	PCT = 720.5 (K)	Time = 133.7 (s)
No.10	A-88 rod	Pos. 3	PCT = 719.5 (K)	Time = 138.6 (s)

Table 7.1 Test Conditions and Major Events in RUN 952 and RUN 901

(a) Test Conditions

Items	RUN 952	RUN 901
Break Location	Main Steam Line	Recirculation Line
Break Diameter (mm)	31.0 (orifice)	26.2 (nozzle)
Total Break Area (mm)	754.8	650.0
Initial Pressure (MPa)	7.35	7.29
Core Inlet Subcooling (K)	10.7	10.5
HPCS	Actuation	Actuation
LPCS	No-Actuation	Actuation
LPCI	No-Actuation	Actuation
ADS	Failure	Actuation

(b) Time of Events (s)

Items	RUN 952	RUN 901
Break Initiation	0.0	0.0
Power-Decay start	9.0	7.0
Lower Plenum Flashing	4.2	17.0
L2 Level Signal	71.0	3.2
HPCS Actuation	95.0	31.5
L1 Level Signal	-	7.4
LPCS Actuation	-	65.6
LPCI Actuation	-	90.9
Final Core Quench	230.0	127.3

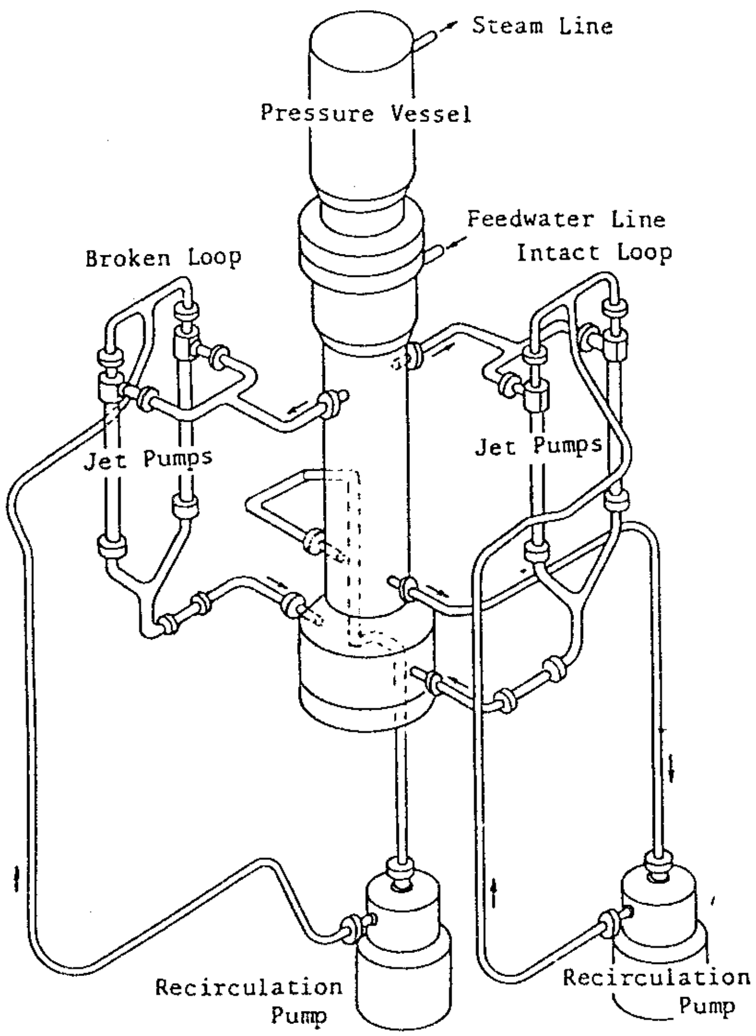

Fig. 2.1 Schematic Diagram of ROSA-III Test Facility

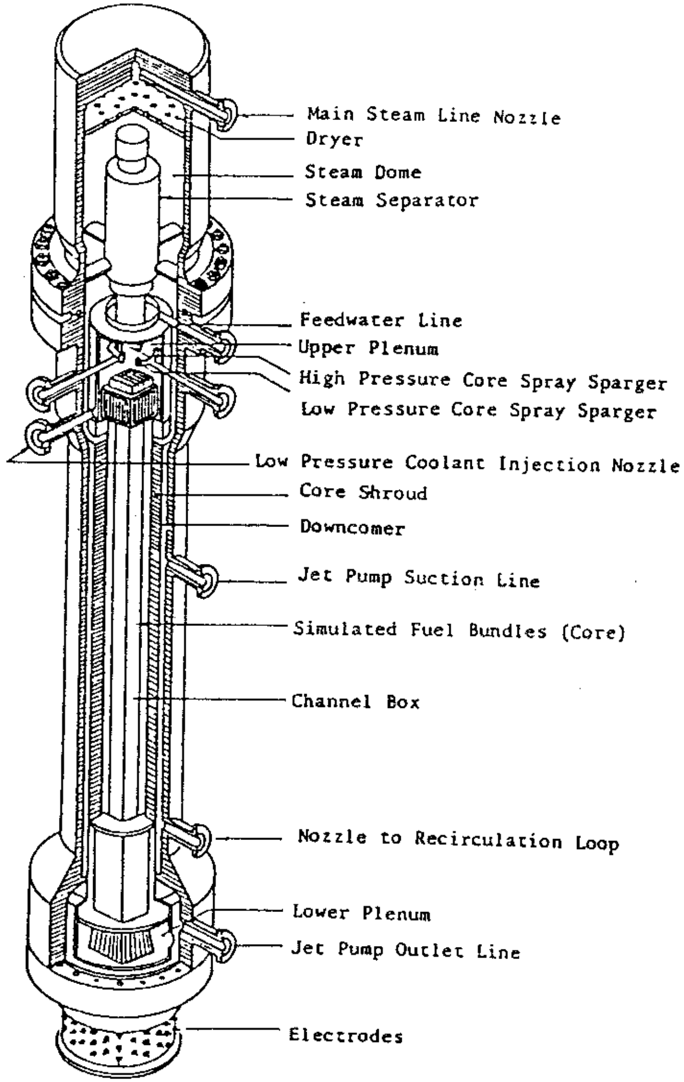

Fig. 2.2 Internal Structure of Pressure Vessel of ROSA-III

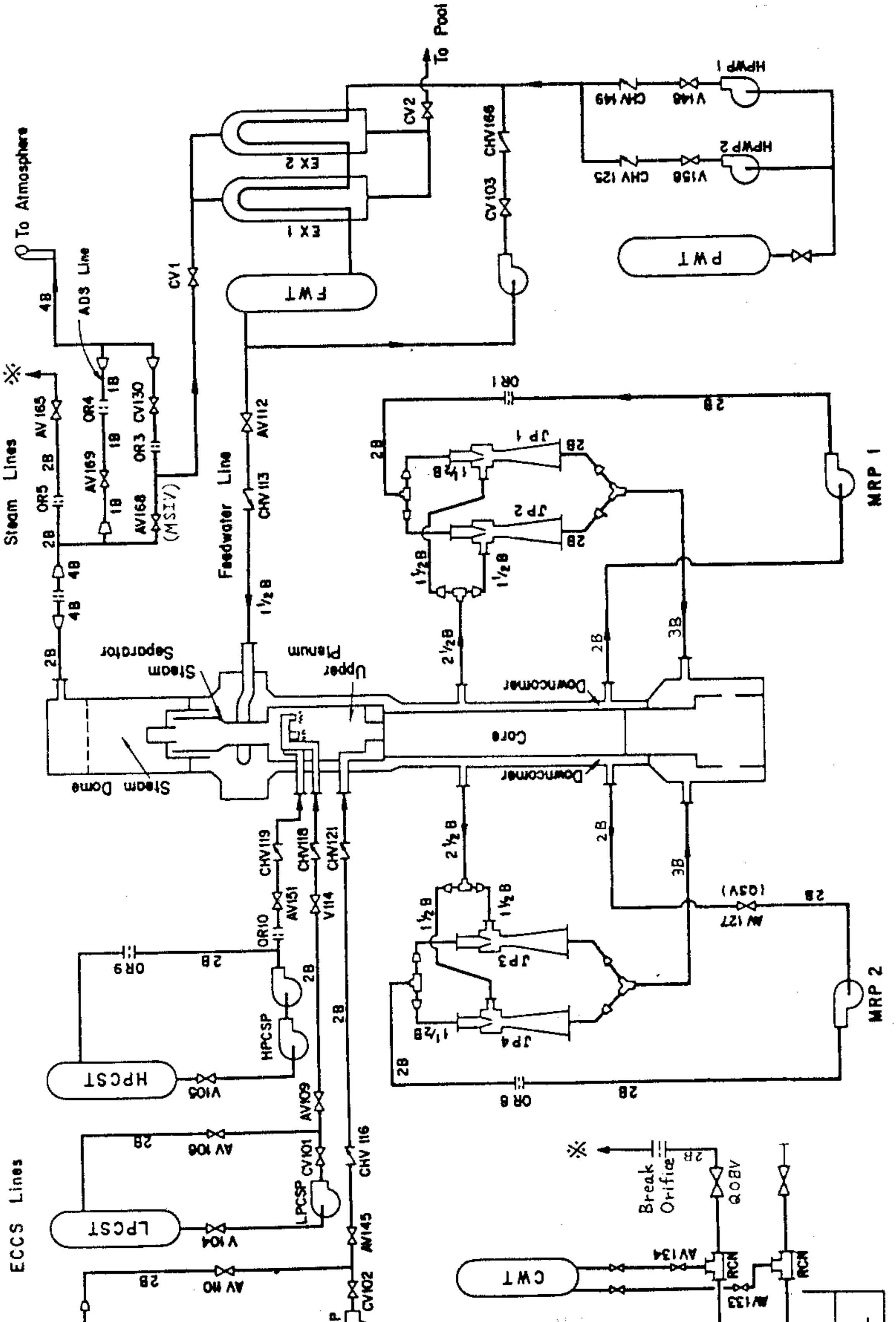

Fig. 2.3 ROSA-III Piping Schematic

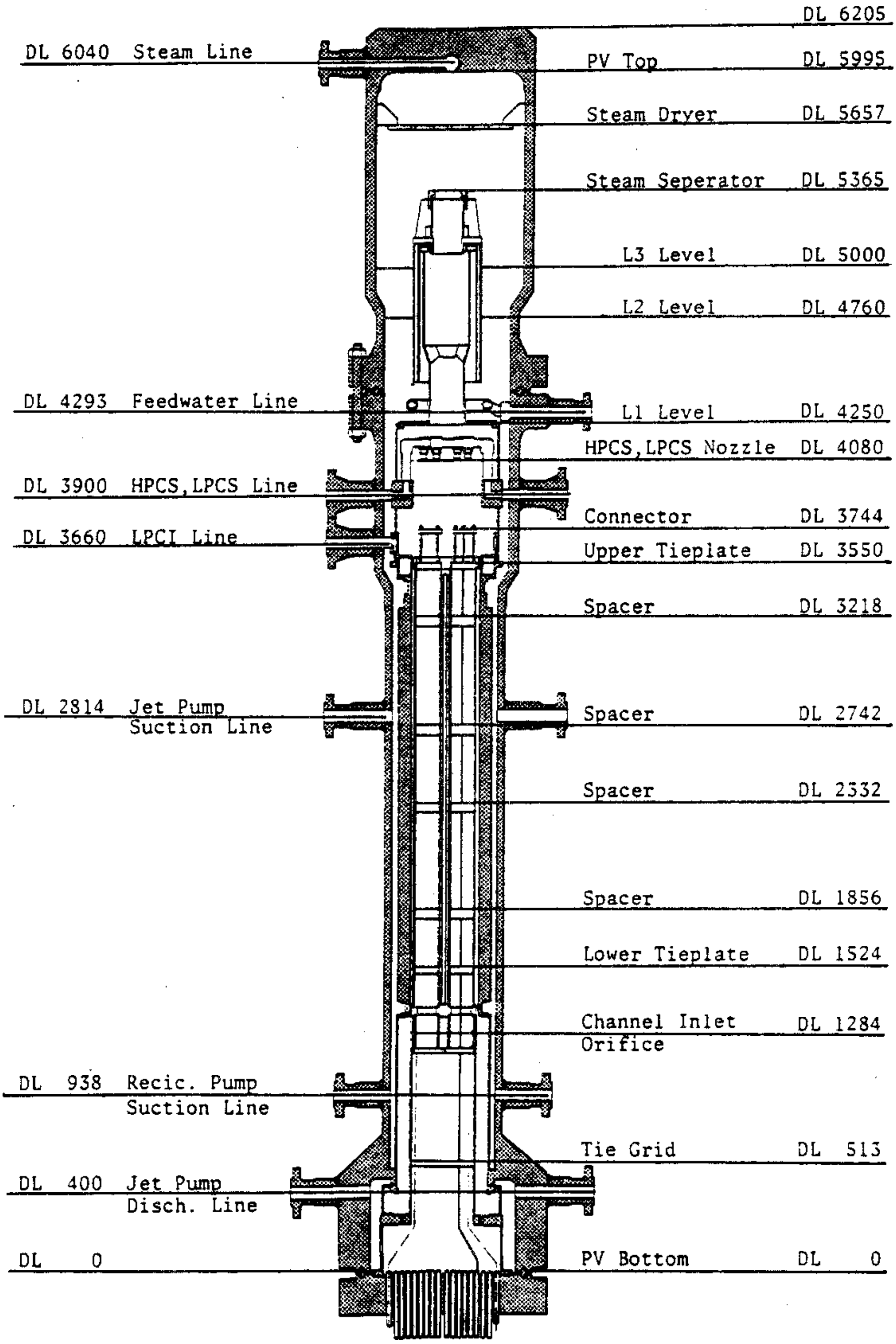

Fig. 2.4 Pressure Vessel Internals Arrangement

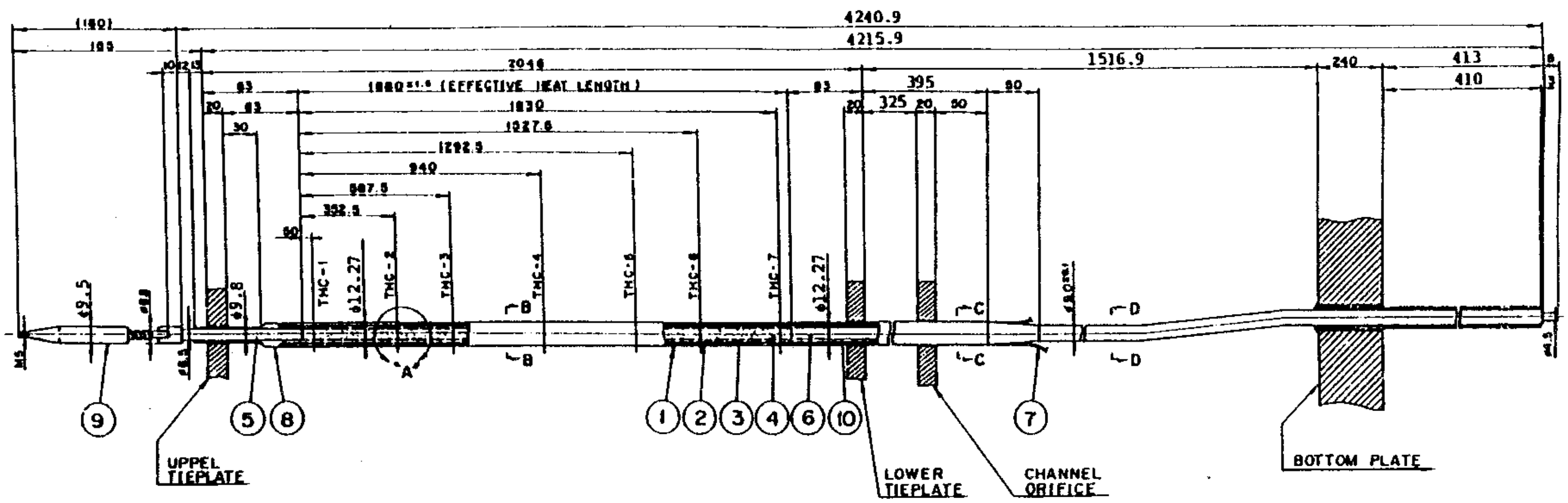

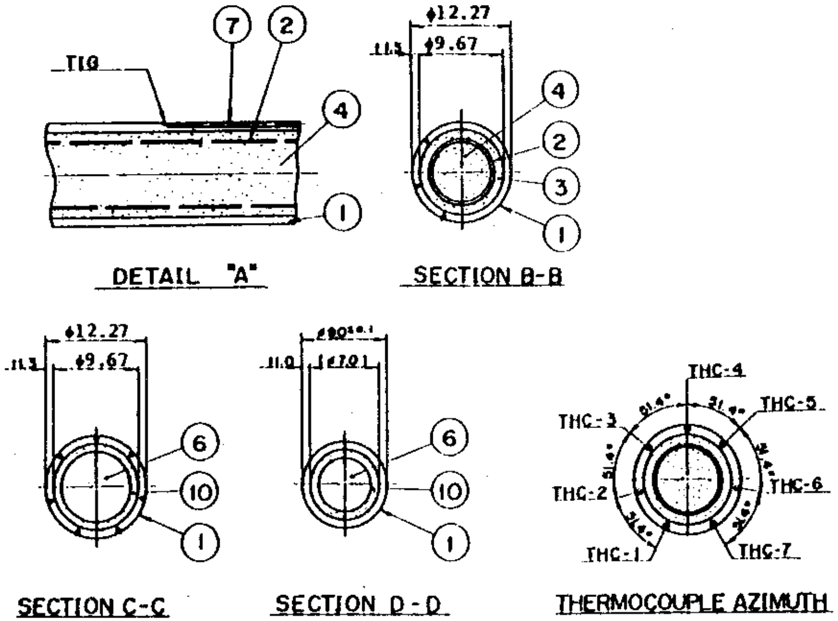

NO	PARTS	MATERITAL
1	SHEATH	INCONEL 600
2	HEATER	NICHROME
3	INSULATOR	BN
4	INSULATOR	BN
5	CONDUCTOR	Ni
6	CONDUCTOR	Cu - Ni
7	THERMOCOUPLE	CA/INC,600
8	SHEATH	SUS 316
9	TERMINAL	Cu - Ni
10	INSULATOR	MgO

Fig. 2.5 Simulated Fuel Rod of ROSA-III

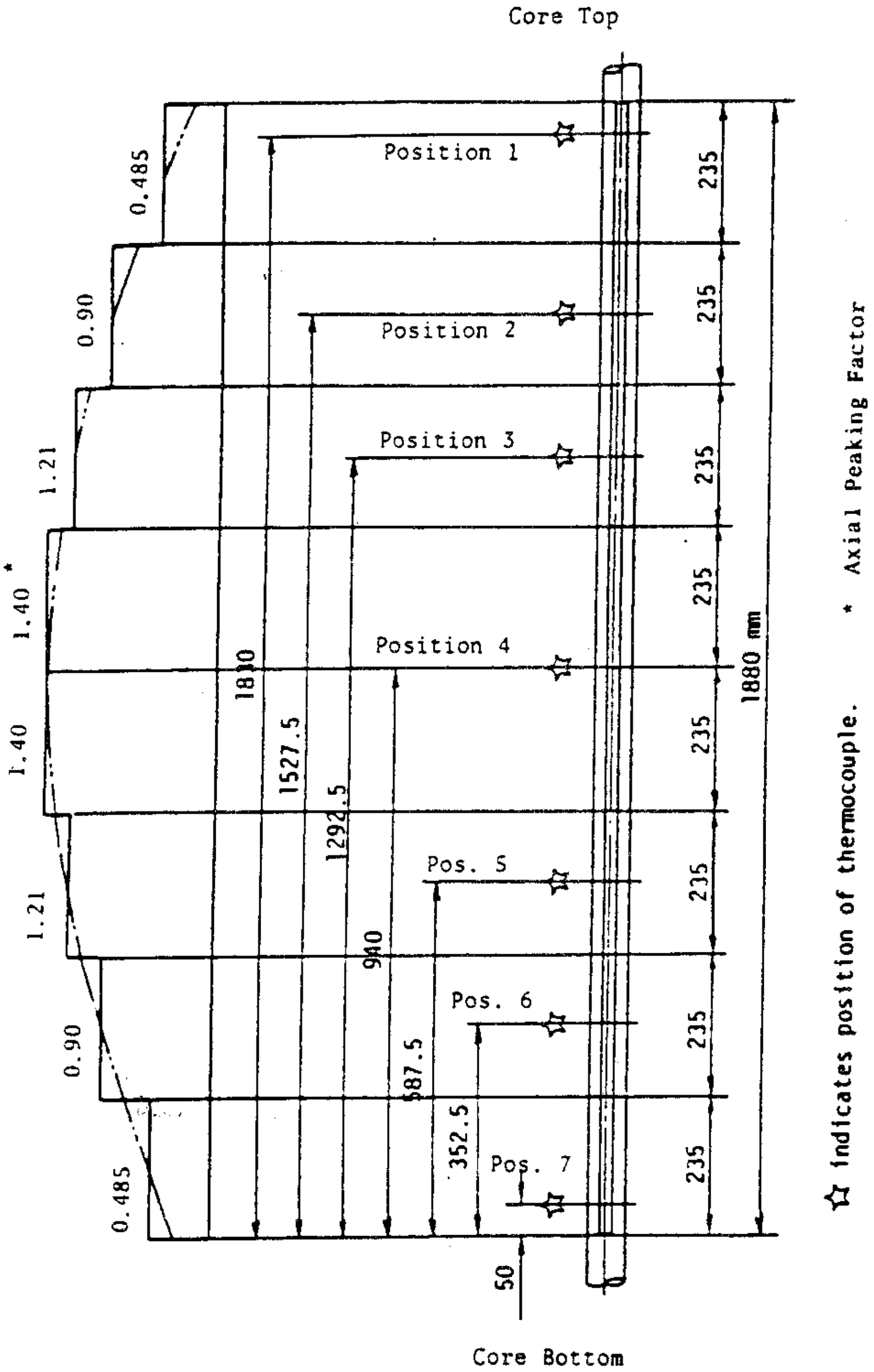

Fig.2.6 Axial Power Distribution of Heater Rod

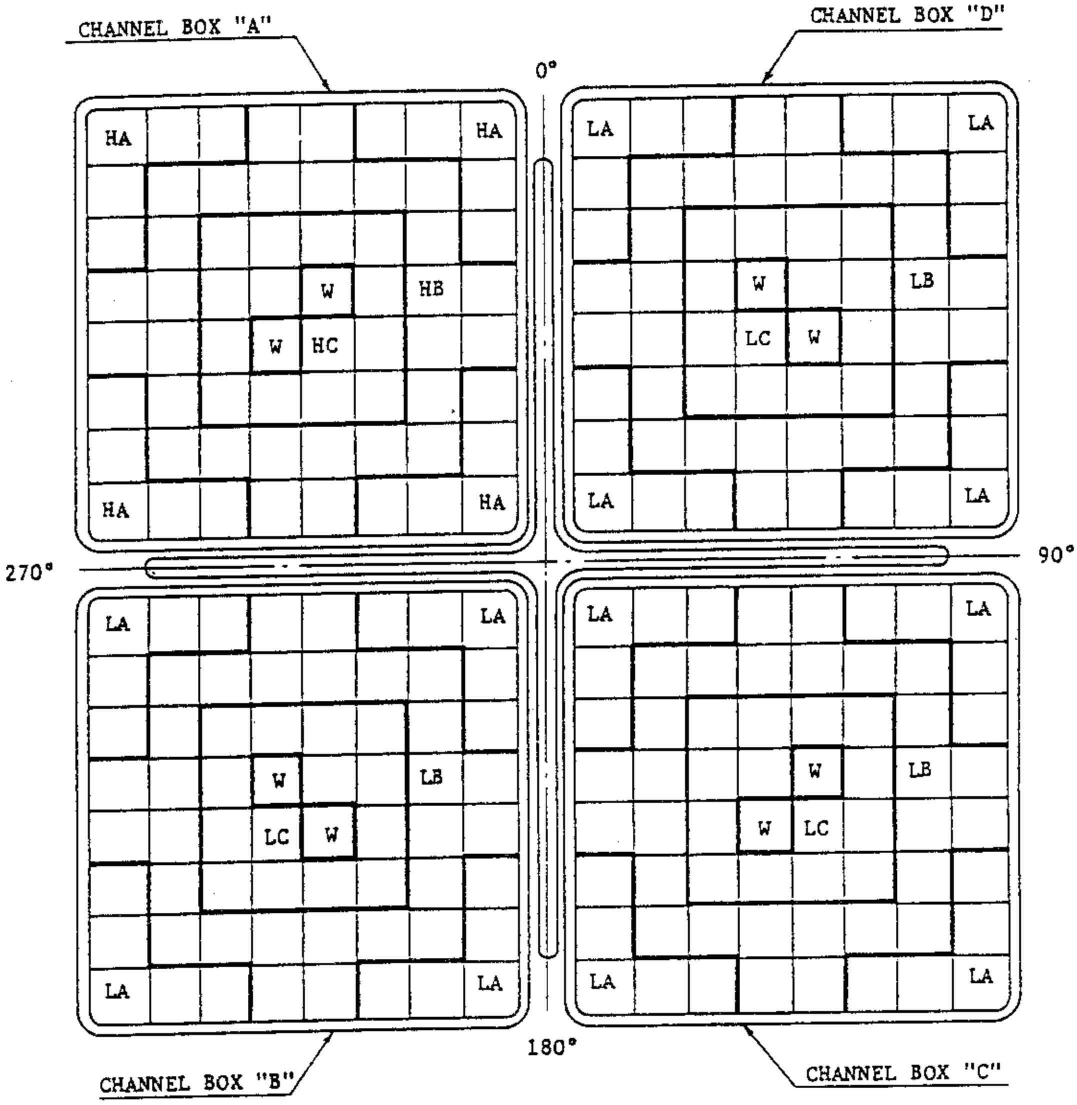

Region	HA	HB	HC	LA	LB	LC	W
Linear Heat Rate (kW/m)	18.5	16.81	14.41	13.21	12.01	10.29	0.0
Local peaking factor	1.1	1.0	0.875	1.1	1.0	0.875	0.0
No. of Rods	20	28	14	60	84	42	8

* note : Radial peaking factor is 1.4

Fig. 2.7 Radial Power Distribution of Core

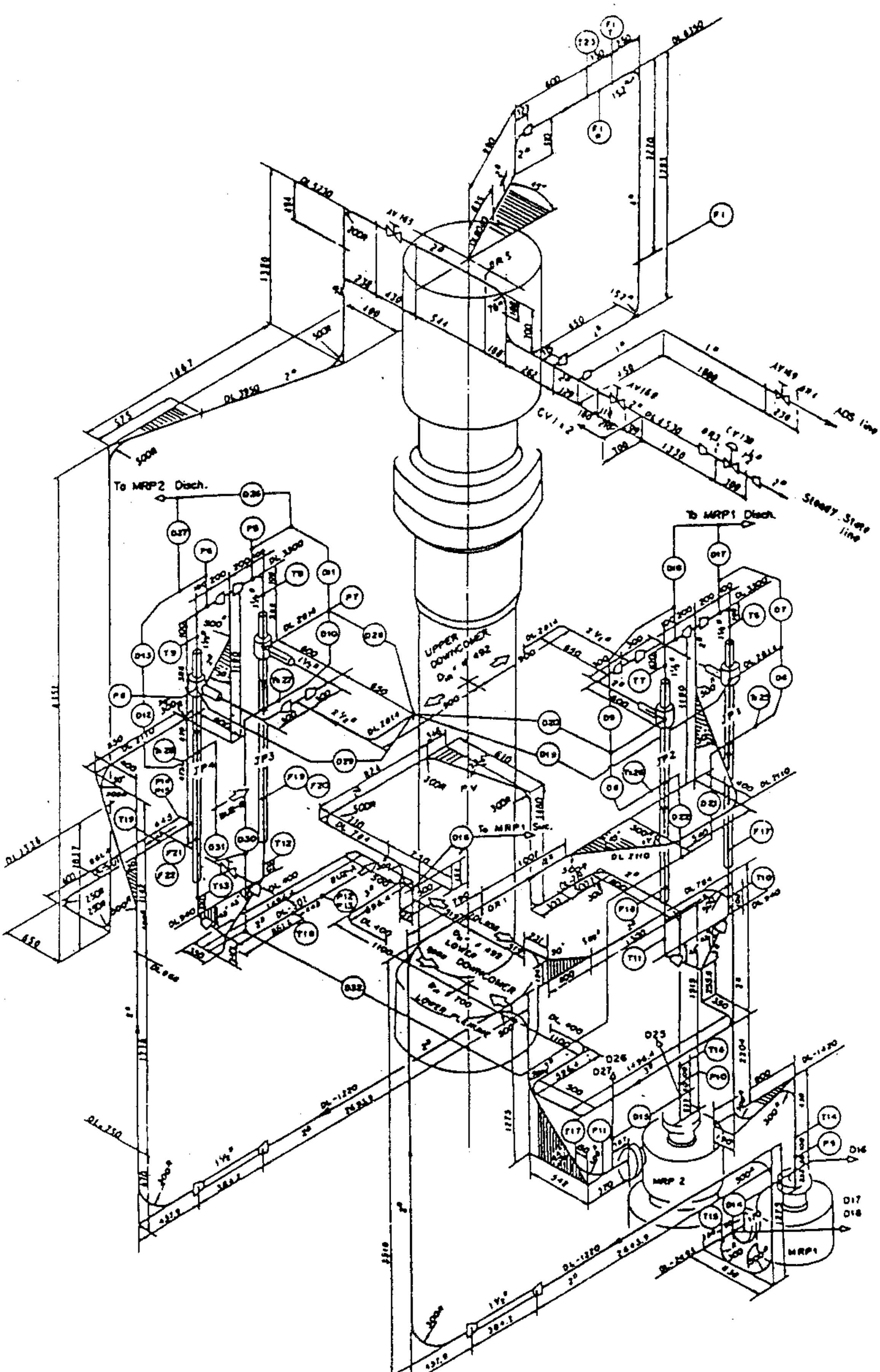

Fig.2.8 Piping Layout of Recirculation Loops and Jet Pumps

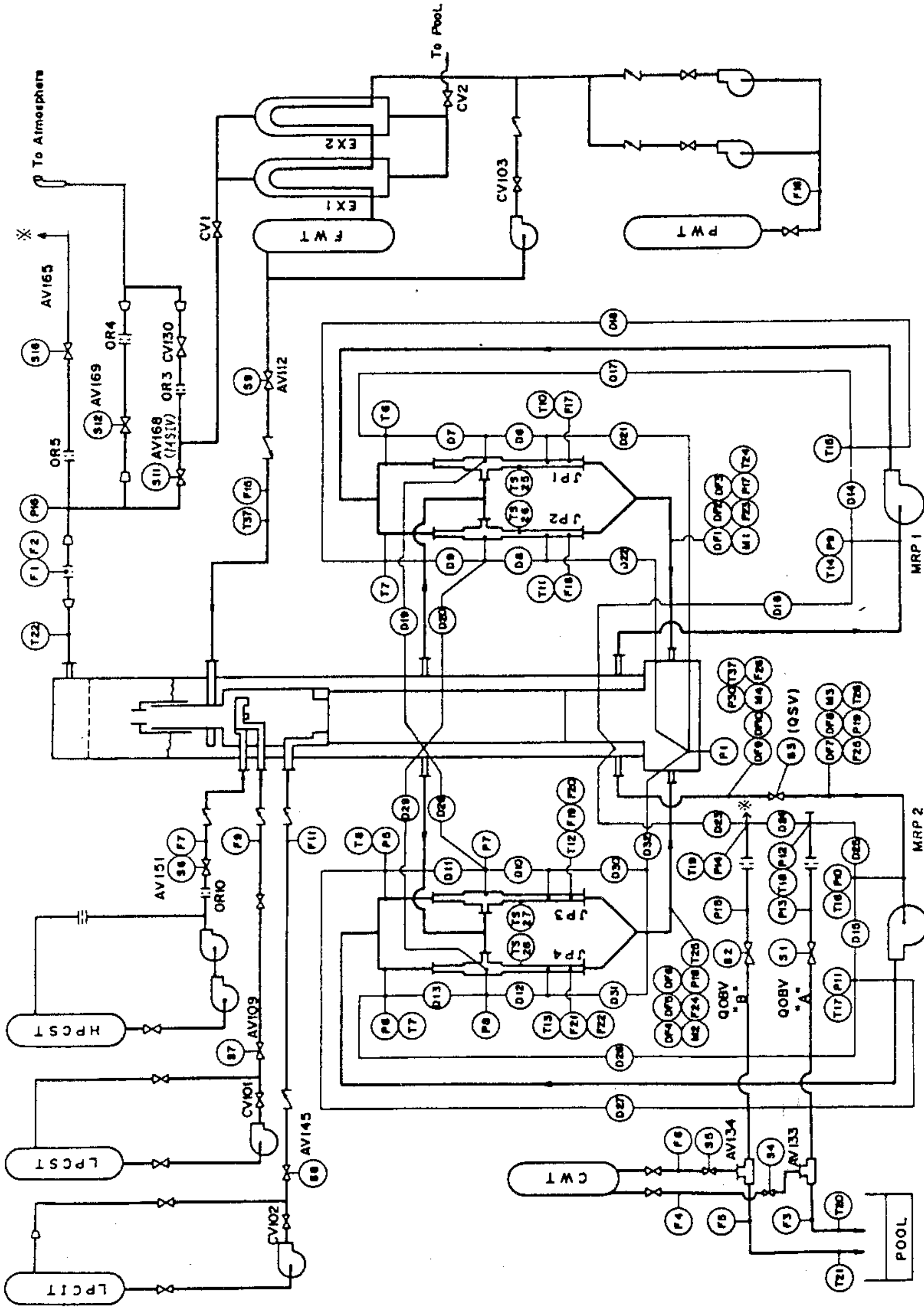

Fig. 3.1 Instrumentation Location of ROSA-III Test Facility

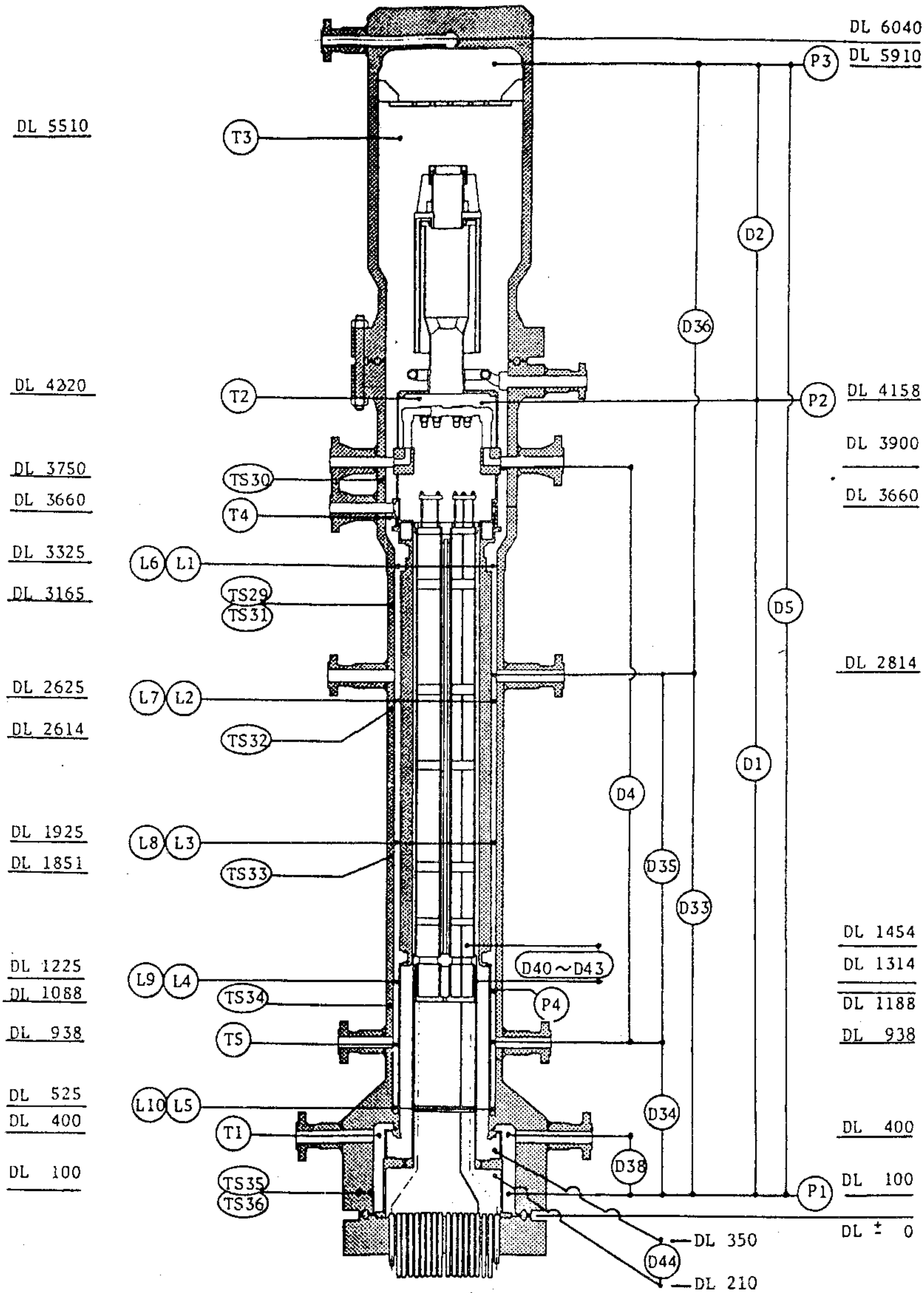

Fig. 3.2 Instrumentation Location in Pressure Vessel

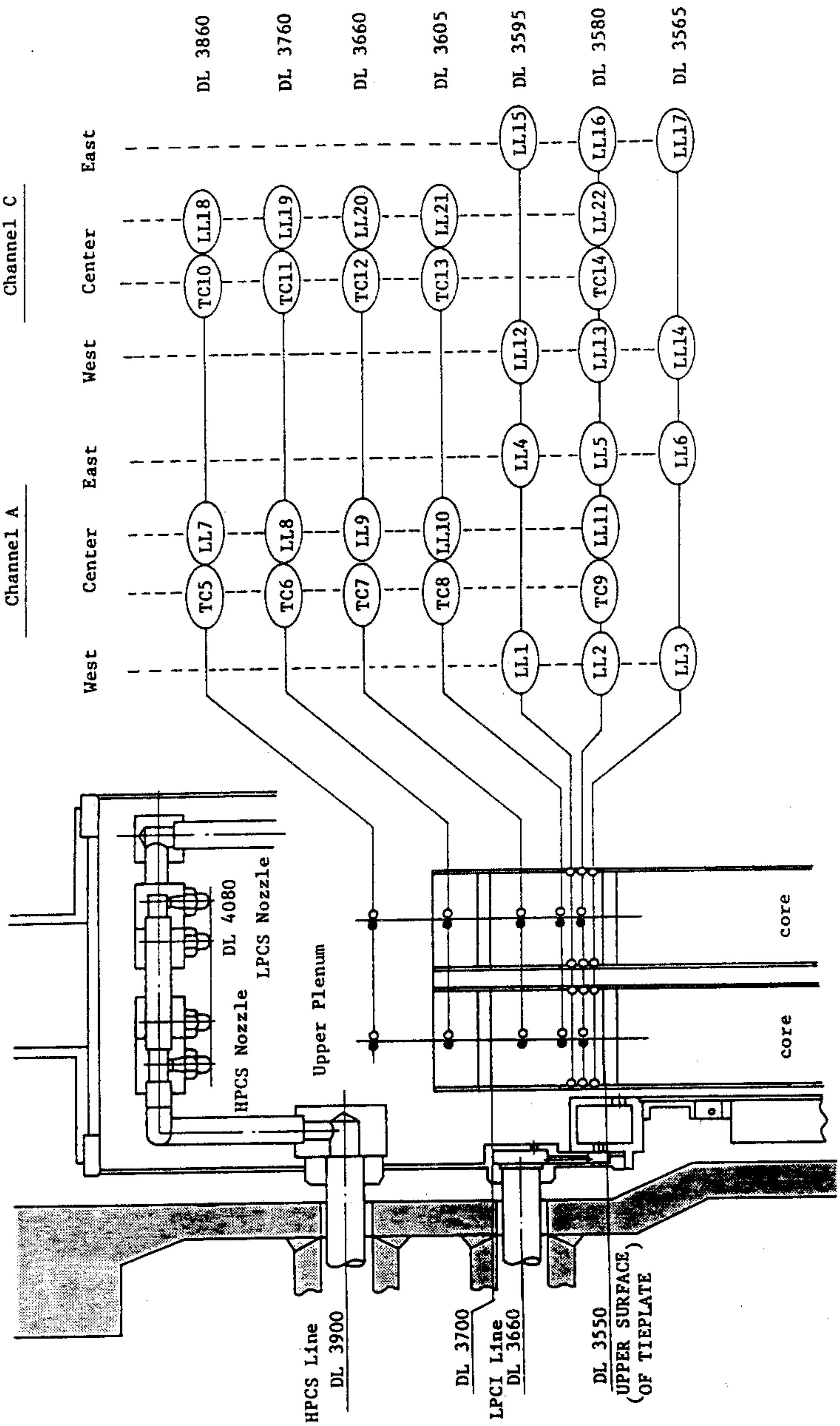

Fig. 3.3 Upper Plenum Instrumentation

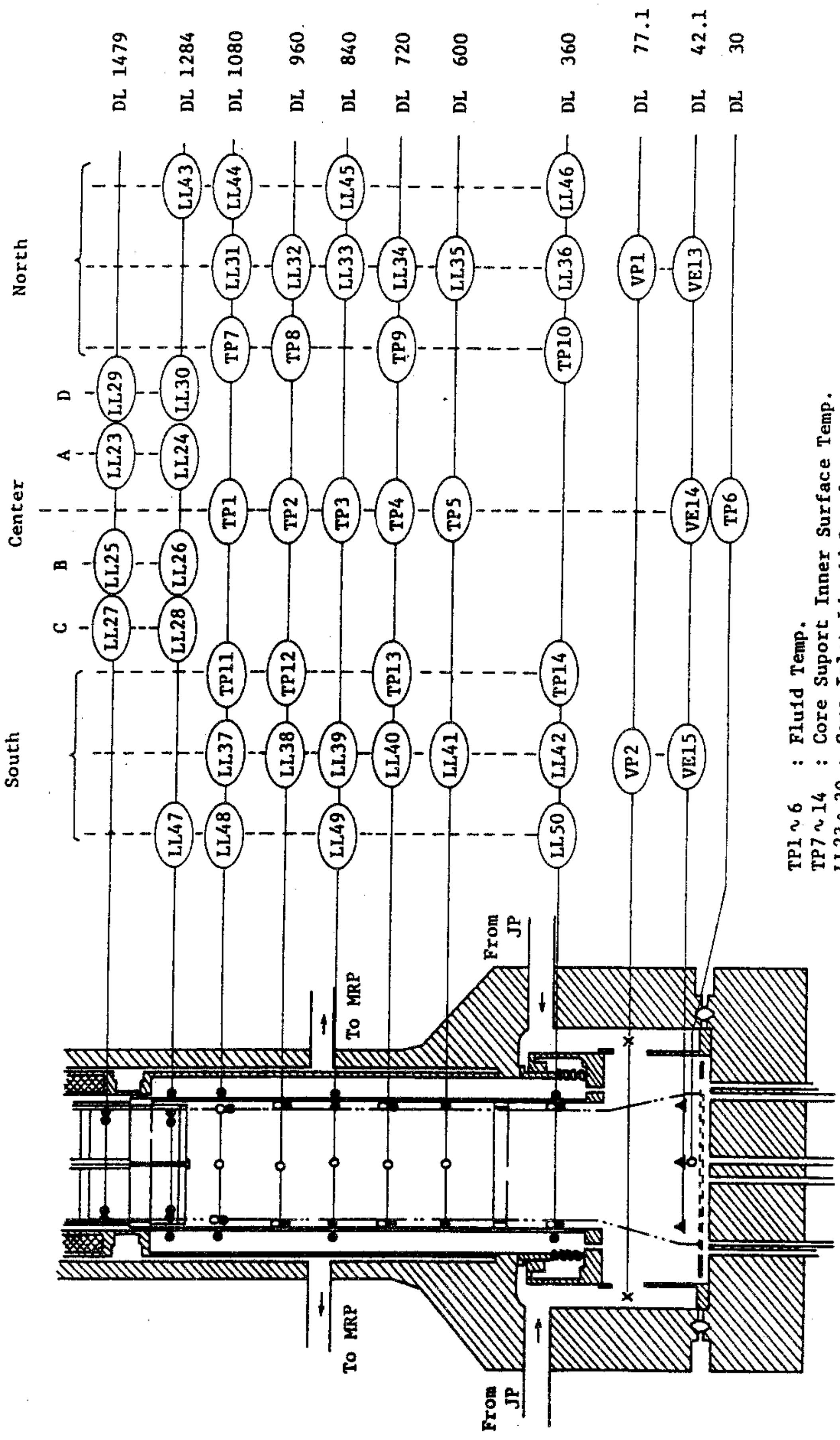

TP1 ~ 6 : Fluid Temp.
TP7 ~ 14 : Core Suport Inner Surface Temp.
LL23 ~ 30 : Core Inlet Liquid Level
LL31 ~ 42 : Lower Plenum Liquid Level
LL43 ~ 50 : Guide Tube Liquid Level

Fig. 3.4 Lower Plenum Instrumentation

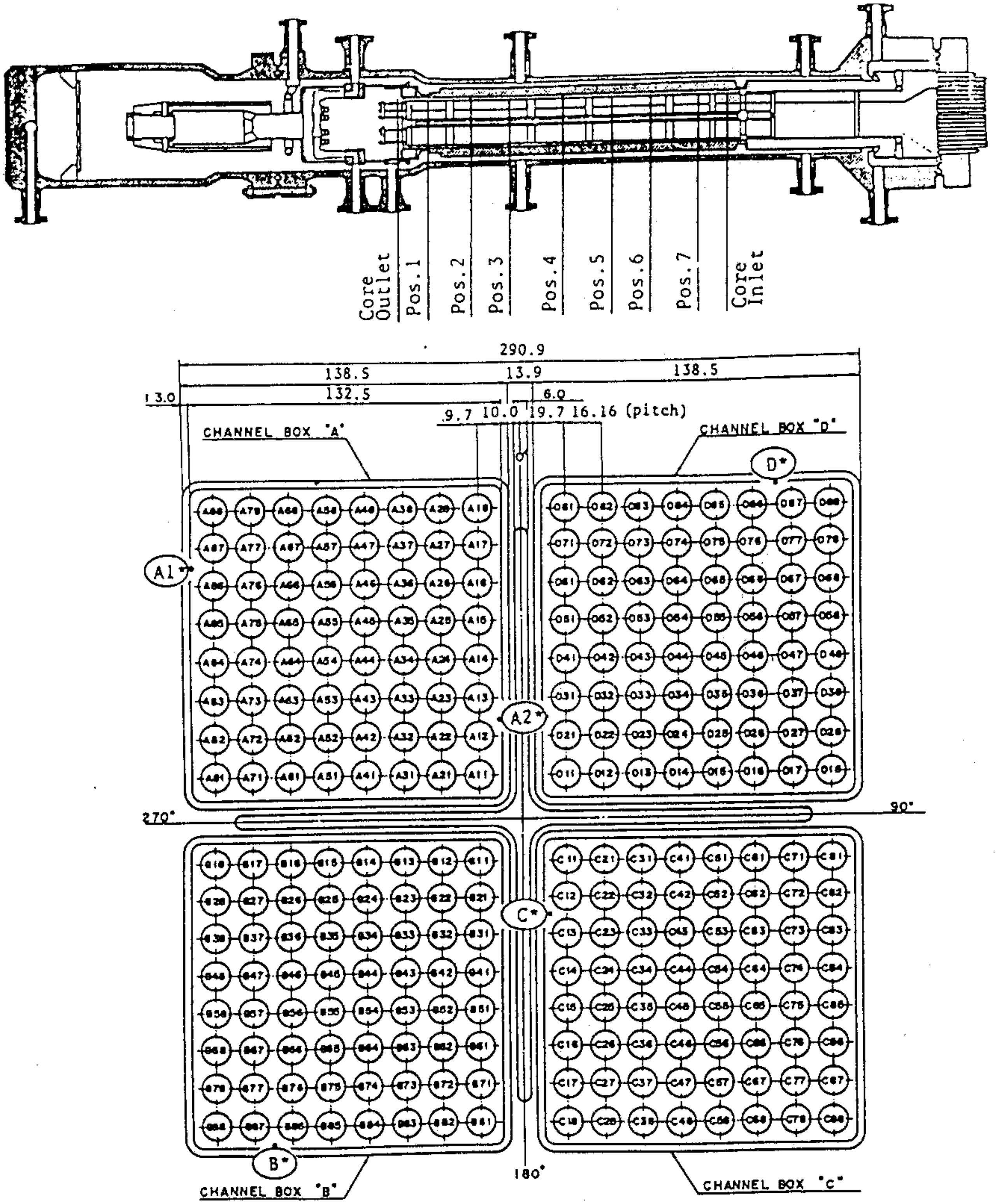

Heater rod O.D. is 12.27mm

A54,B54,C54 and D54 are water rod simulators with void probes, O.D.= 15.01mm

A45,B45,C45 and D45 are water rod simulators with thermocouples, O.D.= 15.01mm

Fig. 3.5 Core Instrumentation (cf. Table 3.3)

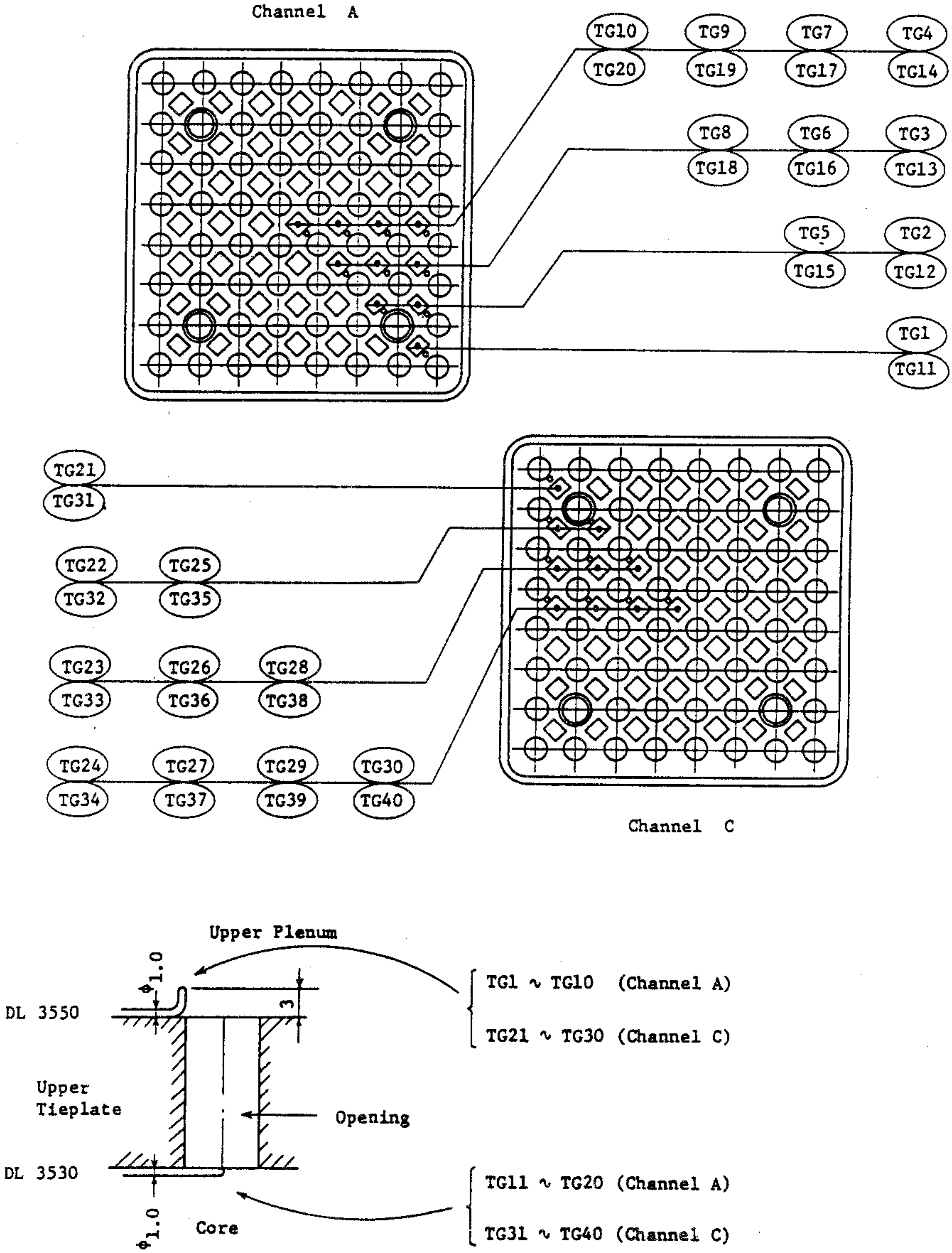

Fig. 3.6 Upper Tieplate Instrumentation

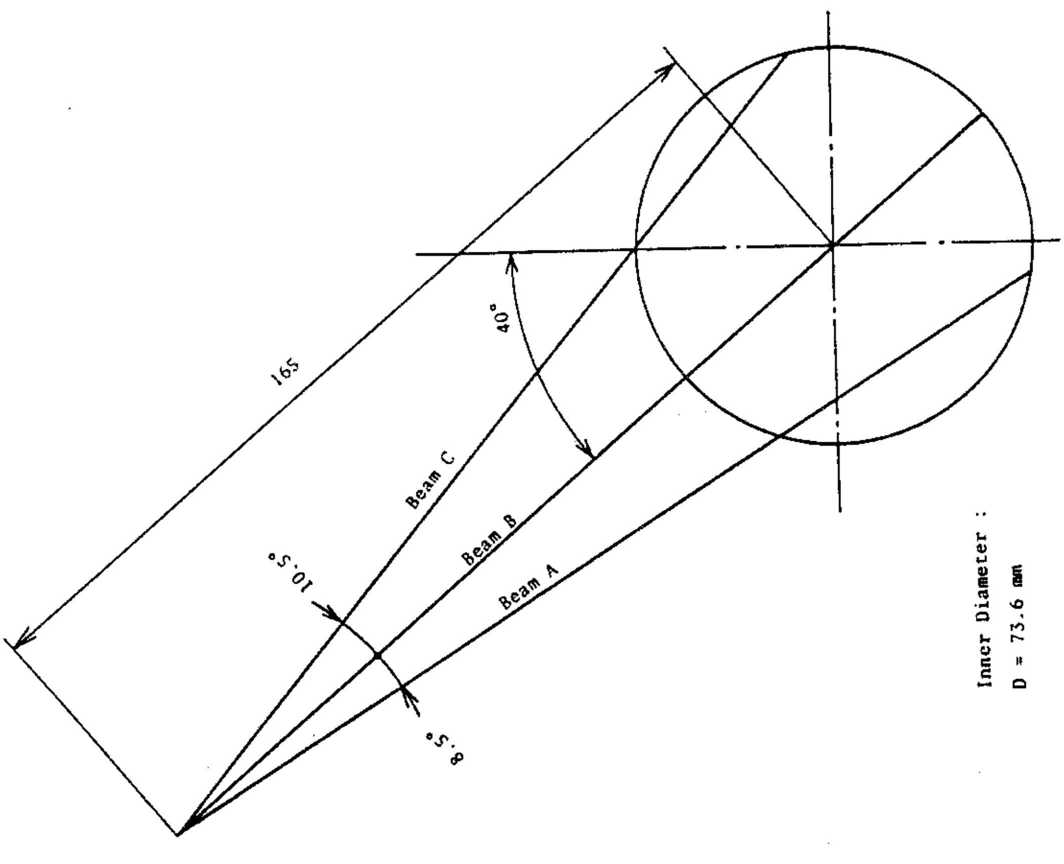

Fig. 3.7 Beam Directions of Three-Beam Gamma Densitometer

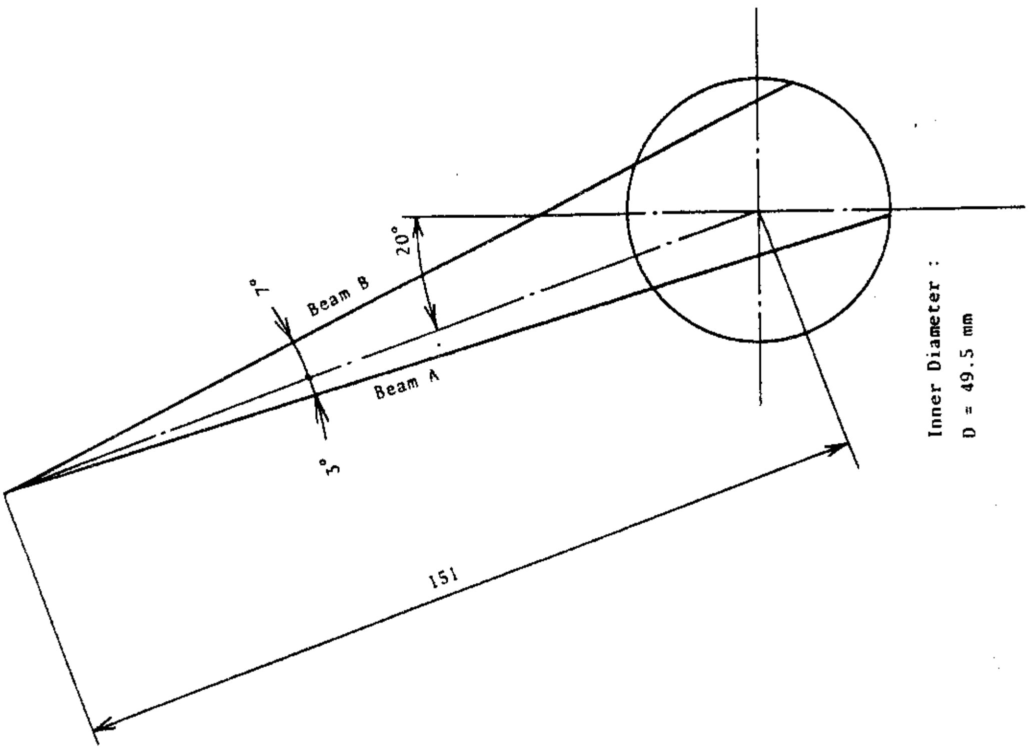

Fig. 3.8 Beam Directions of Two-Beam Gamma Densitometer

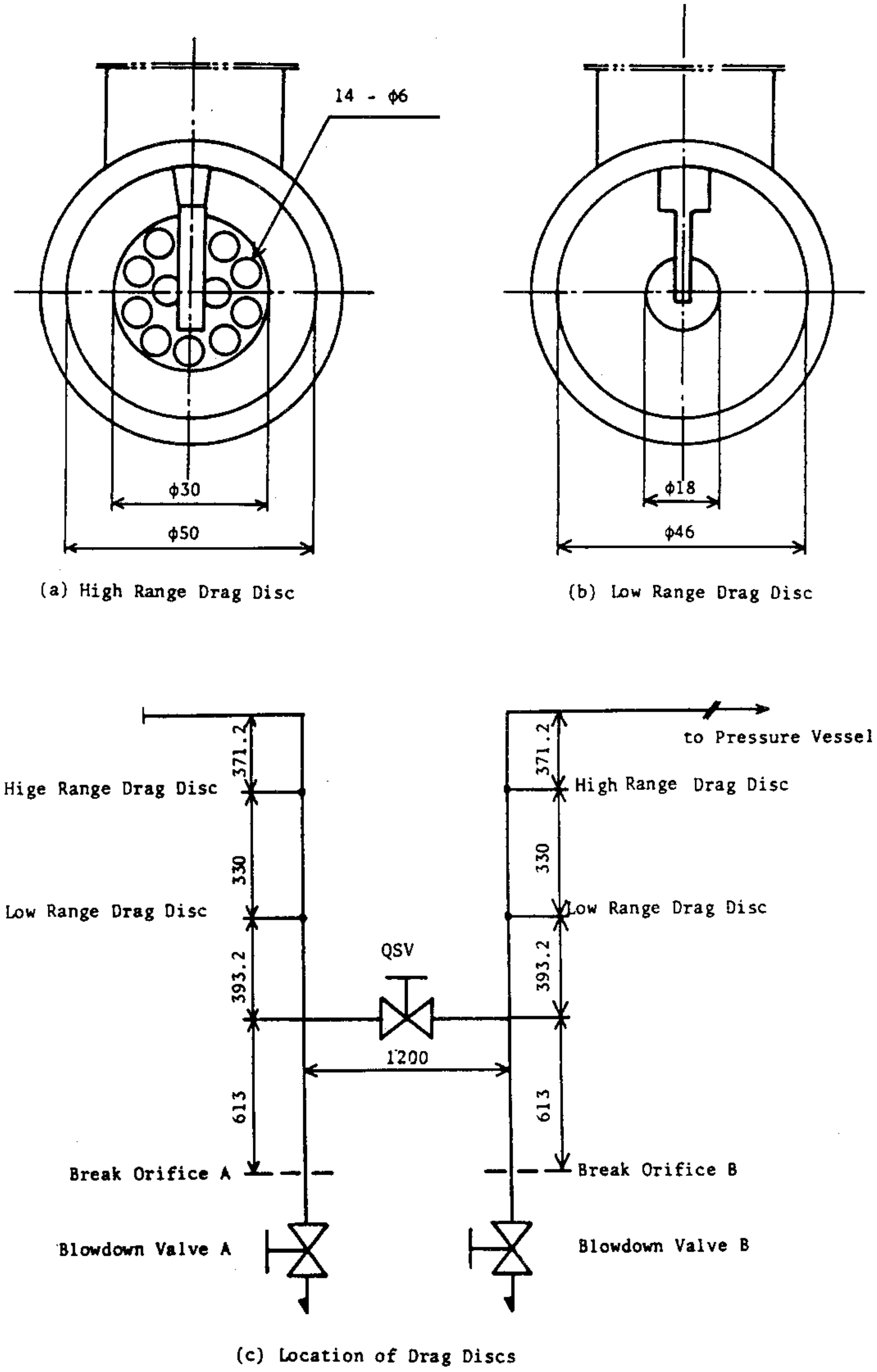

Fig. 3.9 Arrangement and Location of Drag Disks

This Figure shows suction line break and break unit for discharge line break is removed between the recirculation pump and jet pumps in the broken loop. However, four two-phase instrumentation spool pieces are located similarly downstream of the jet pumps and near the break units.

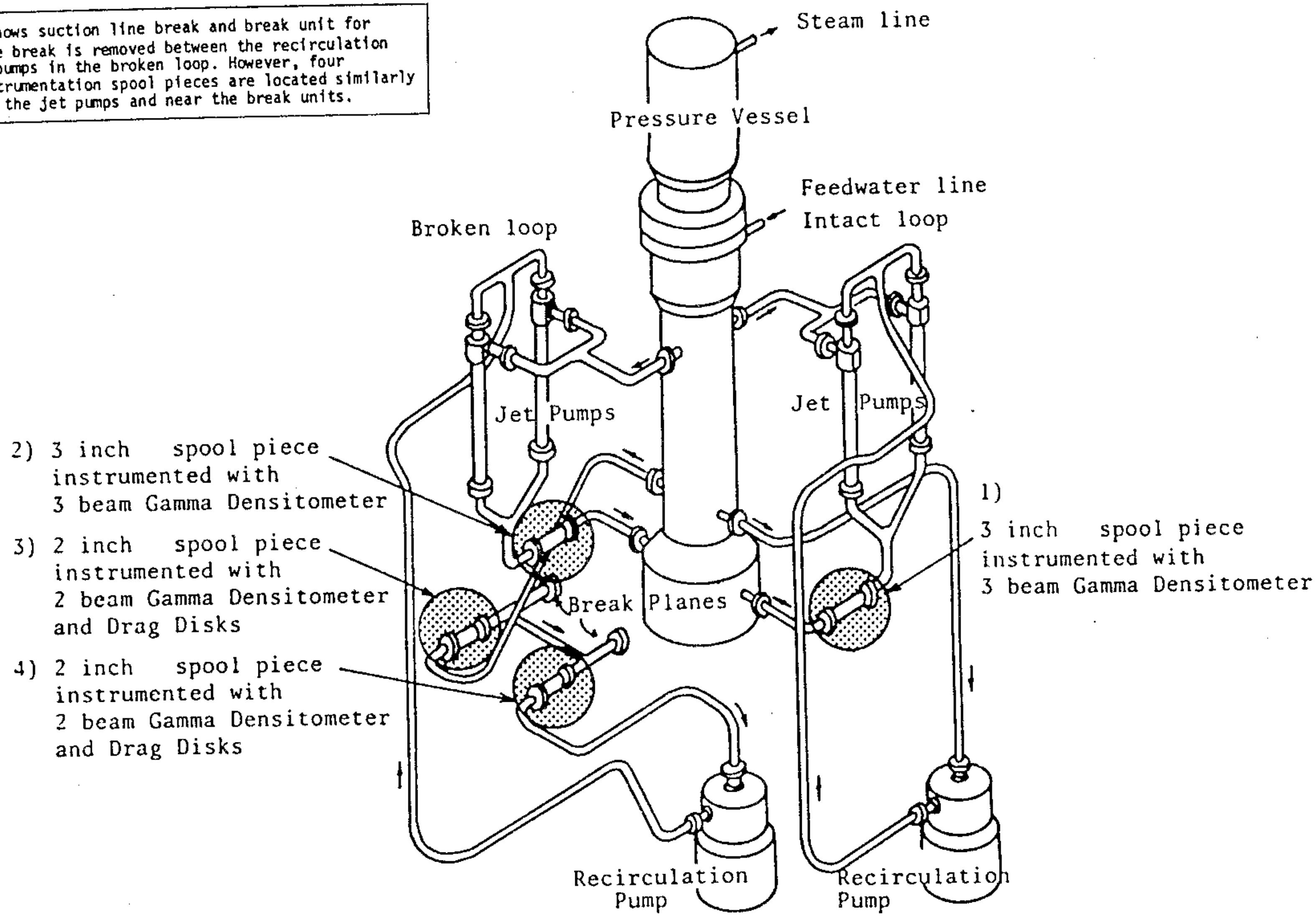

Fig. 3.10 Location of Two-Phase Flow Measurement Spool Pieces

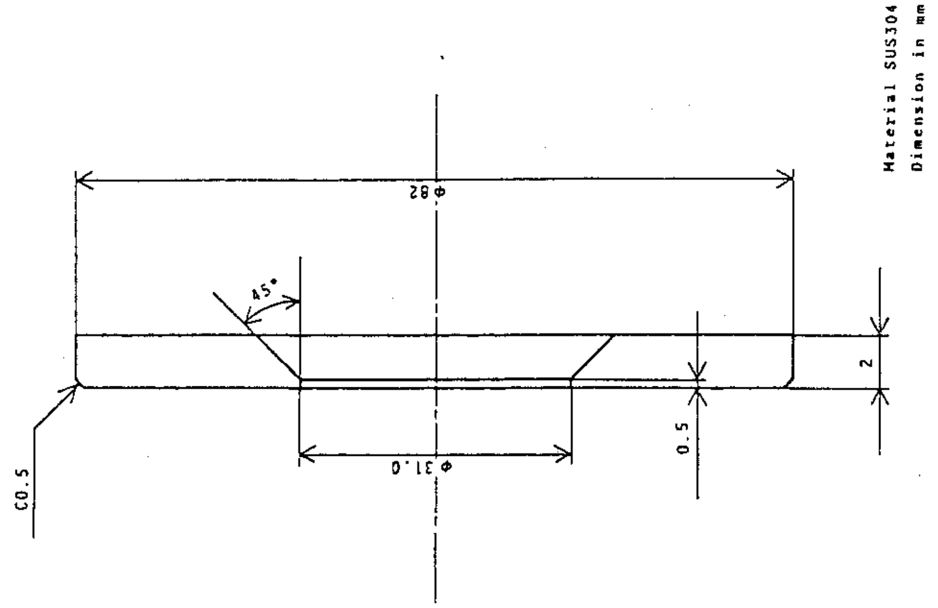

Fig. 4.1 Break Orifice Details

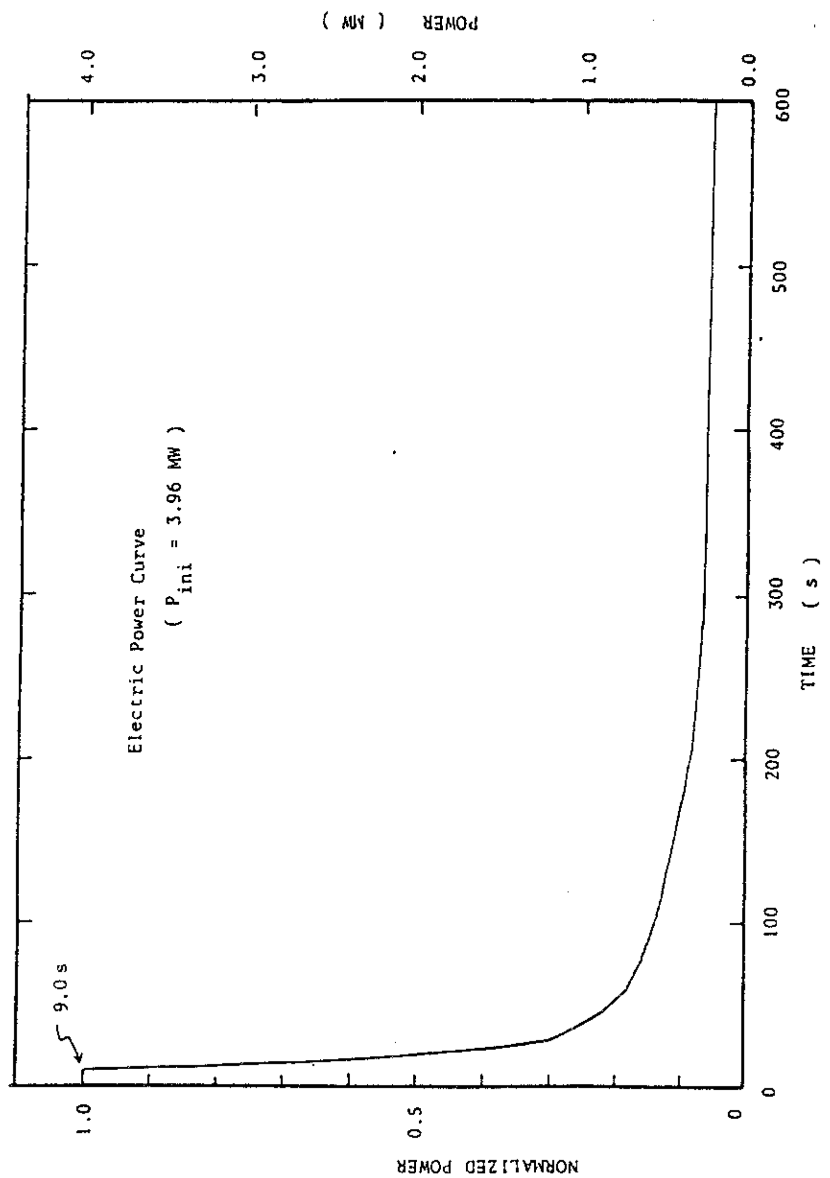

Fig. 4.2 Normalized Poewr Transient for ROSA-III Test

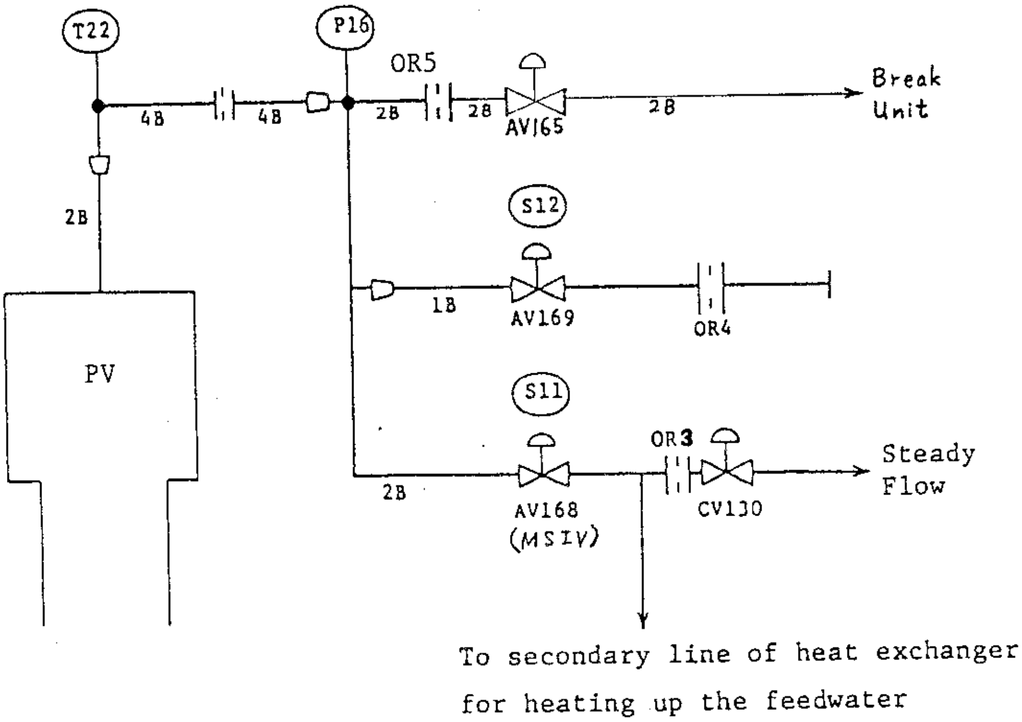

Fig. 4.3 Main Steam Line Schematic

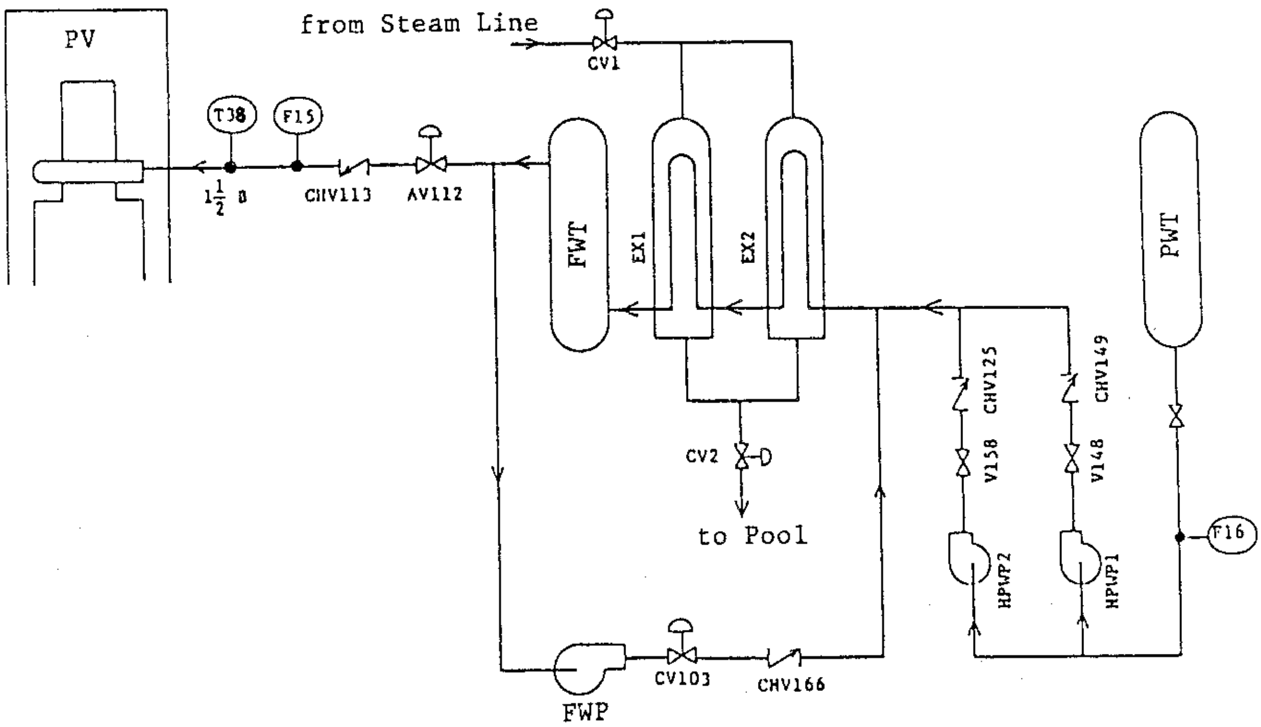

Fig. 4.4 Feedwater Line Schematic

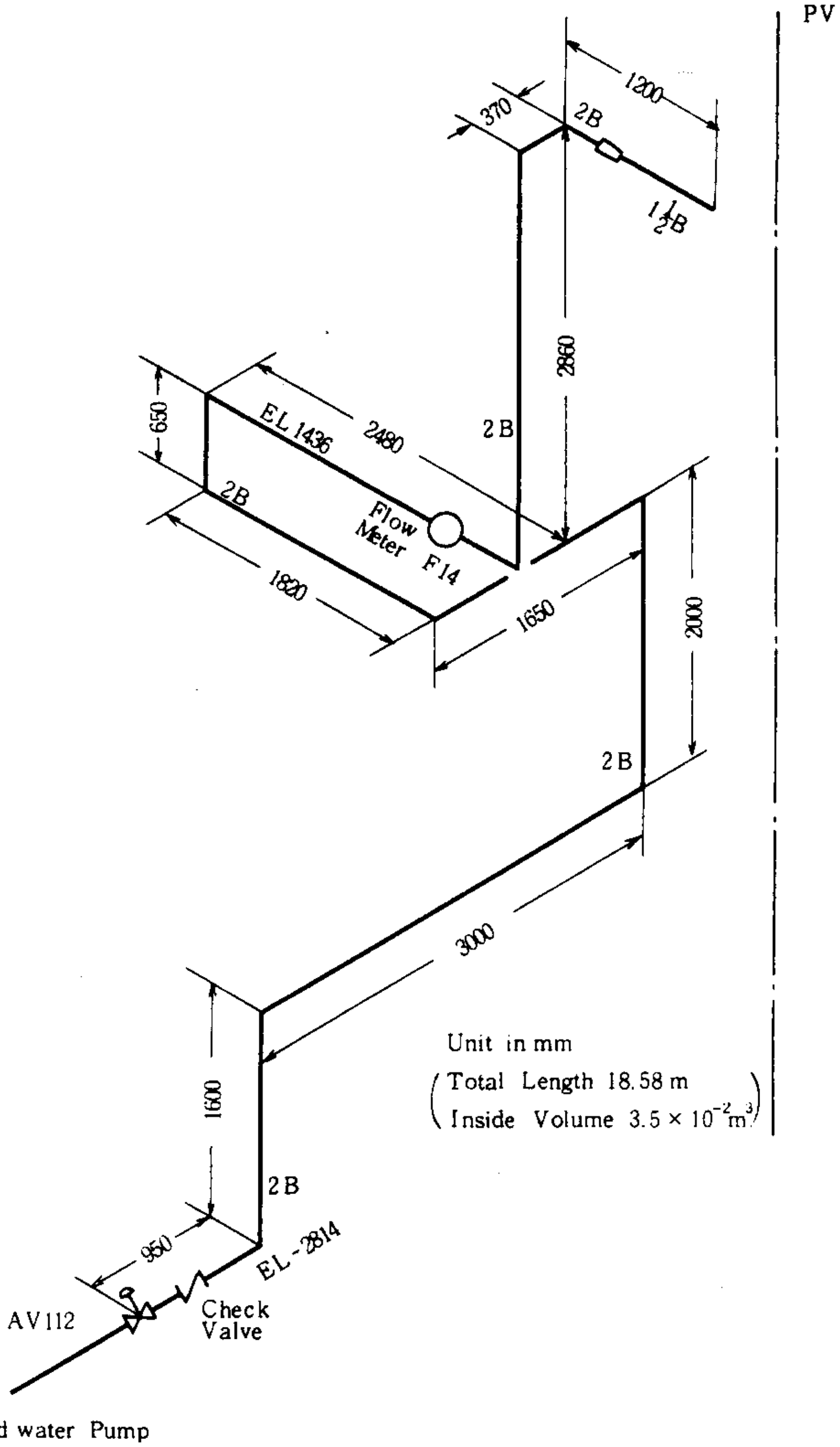

Fig. 4.5 Feedwater Line between Valve AV-112 and Pressure Vessel

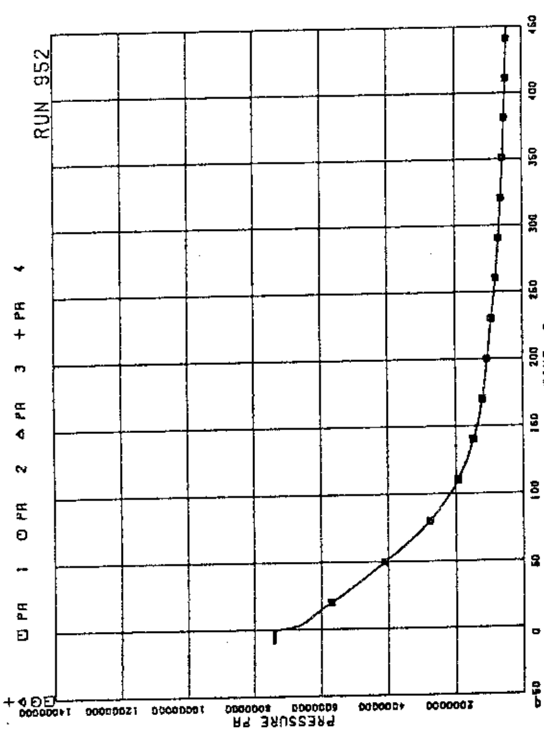

FIG.5. 1 PRESSURE IN PV (PRESSURE VESSEL)

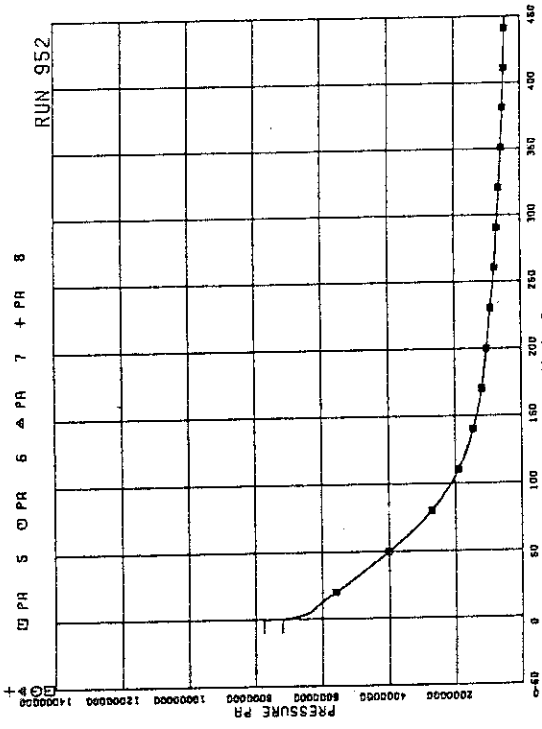

FIG.5. 2 PRESSURE IN RECIRC. LINE (JET PUMP)

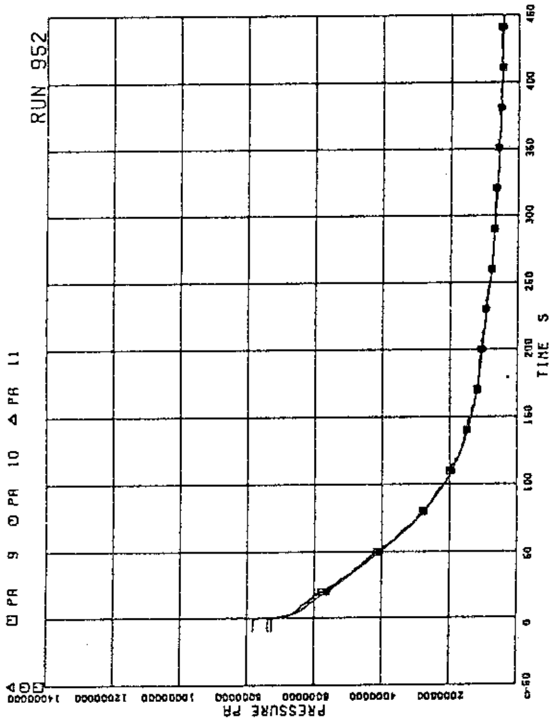

FIG.5. 3 PRESSURE NEAR MRP-1 AND MRP-2 (MAIN RECIRCULATION PUMP)

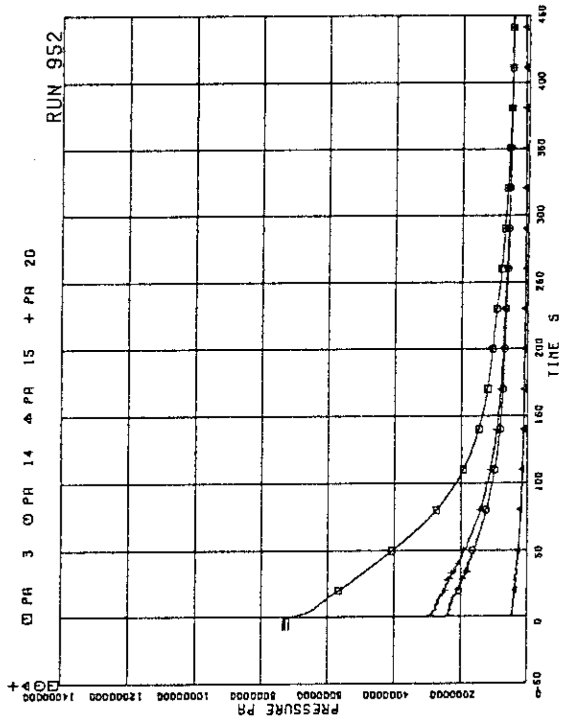

FIG.5. 4 PRESSURE AT BREAK

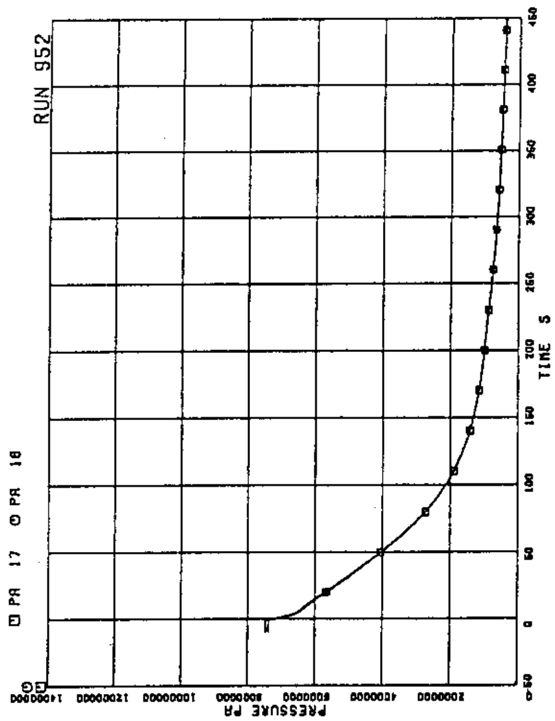

FIG.5. 5 PRESSURE IN JP OUTLET SPOOL

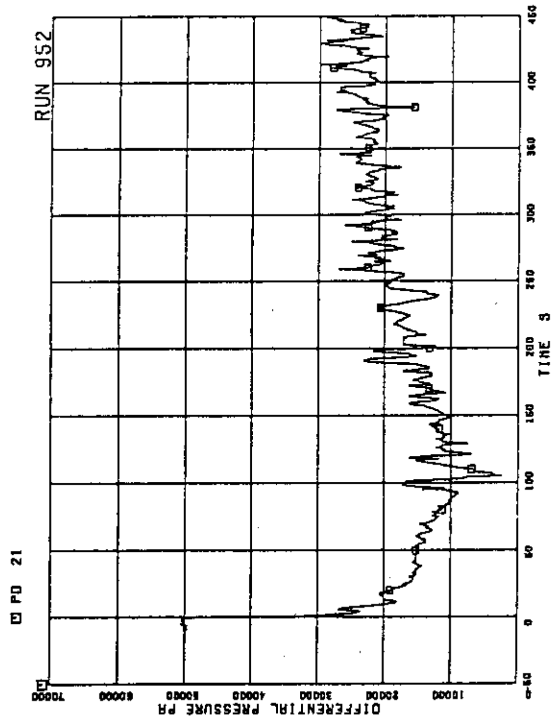

FIG.5. 6 DIFFERENTIAL PRESSURE BETWEEN LOWER PLENUM AND UPPER PLENUM

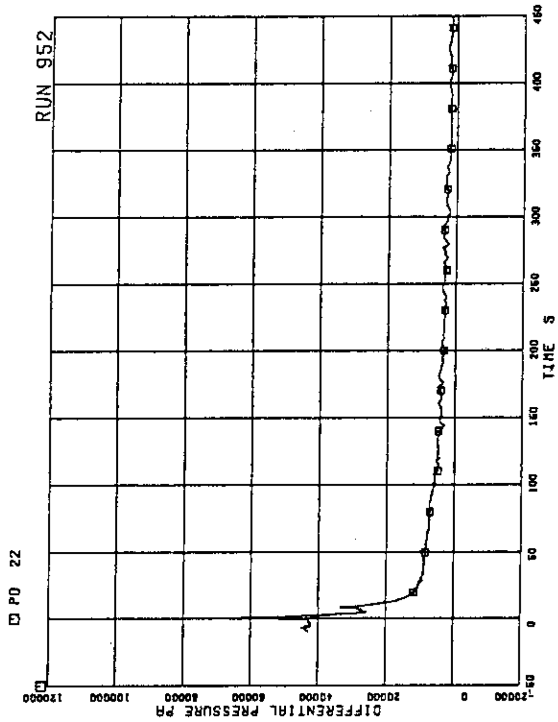

FIG.5. 7 DIFFERENTIAL PRESSURE BETWEEN UPPER PLENUM AND STEAM DOME

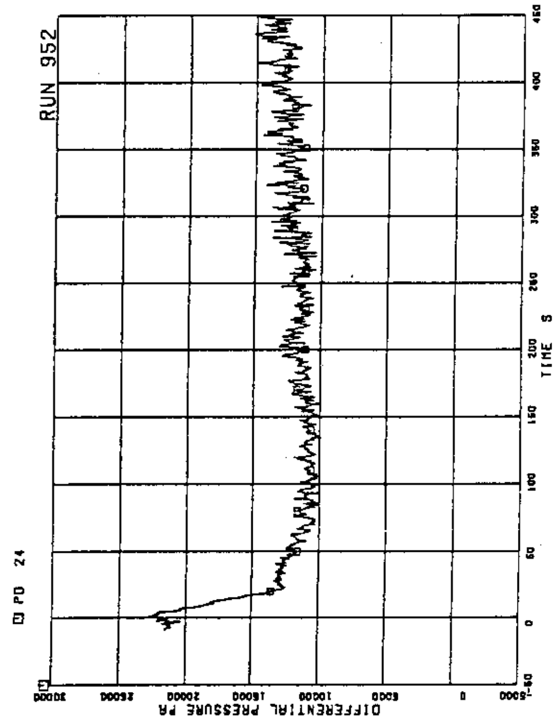

FIG.5. 8 DC (DOWNCOMER) HEAD

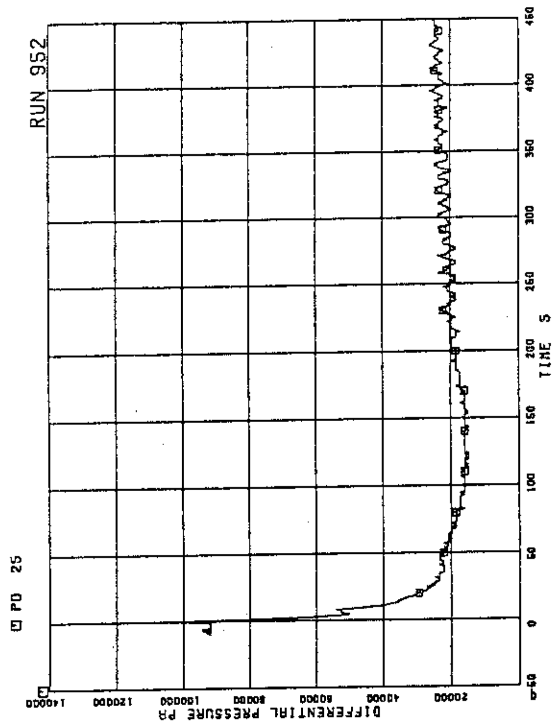

FIG.5. 9 DIFFERENTIAL PRESSURE BETWEEN PV BOTTOM AND TOP

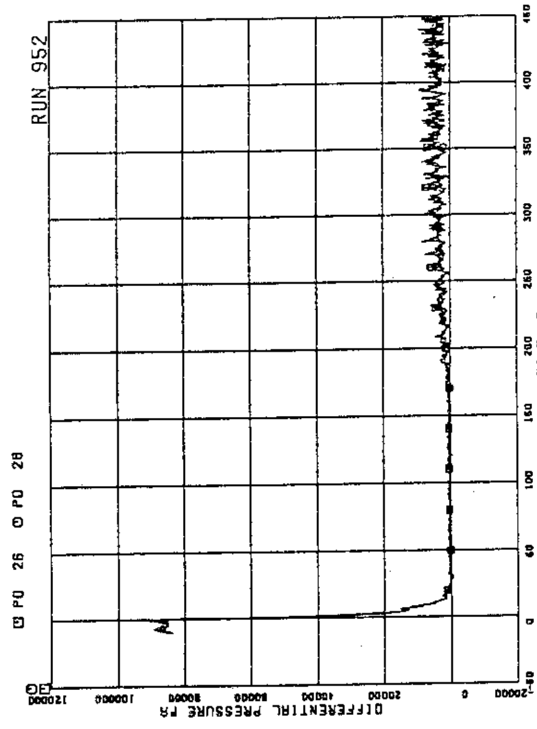

FIG.5. 10 DIFFERENTIAL PRESSURE BETWEEN JP-1.2 DISCHARGE AND SUCTION

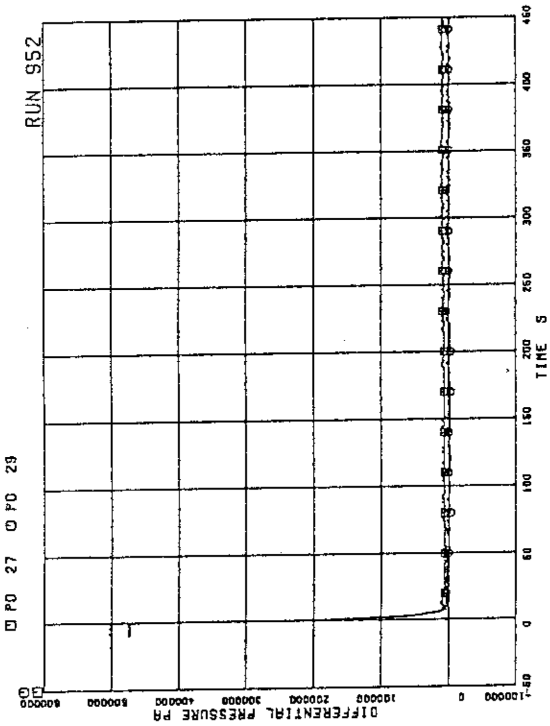

FIG.5. 11 DIFFERENTIAL PRESSURE BETWEEN JP-1,2 DRIVE AND SUCTION

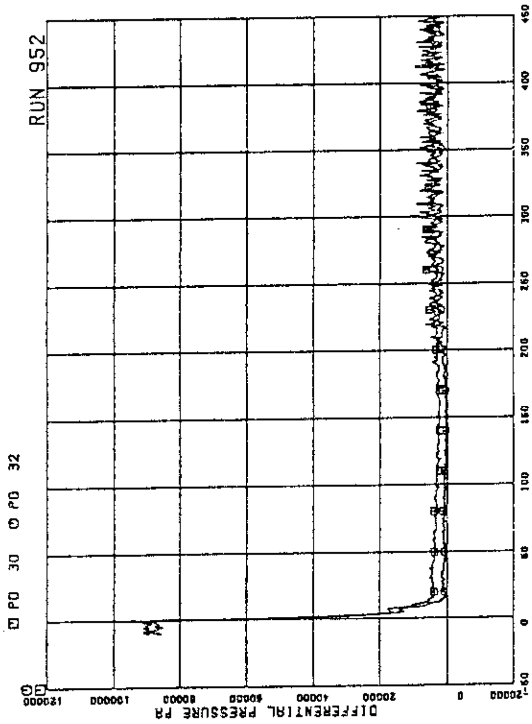

FIG.5. 12 DIFFERENTIAL PRESSURE BETWEEN JP-3.4 DISCHARGE AND SUCTION

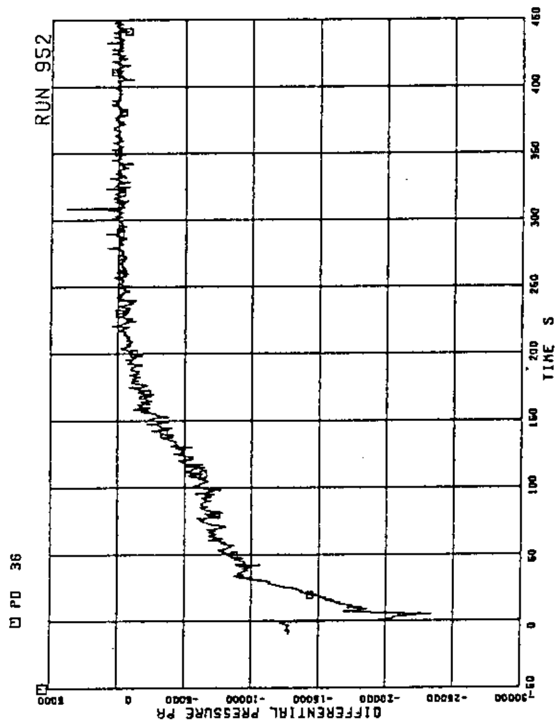

FIG.5. 15 DIFFERENTIAL PRESSURE BETWEEN DOWNCOMER BOTTOM AND MRP1 SUCTION

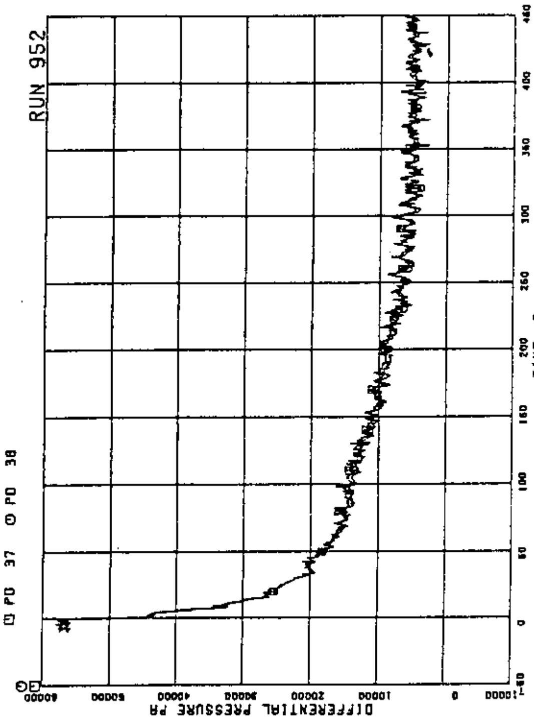

FIG.5. 16 DIFFERENTIAL PRESSURE BETWEEN MRP DELIVERY AND JP-1.2 DRIVE

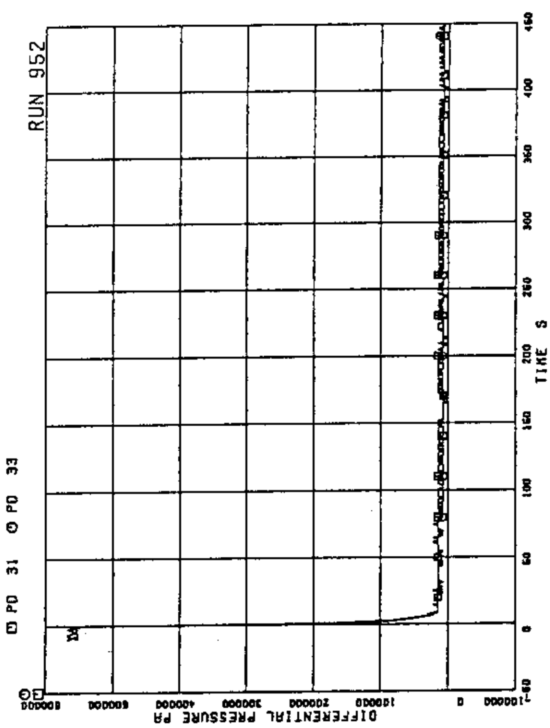

FIG.5. 13 DIFFERENTIAL PRESSURE BETWEEN JP-3.4 DRIVE AND SUCTION

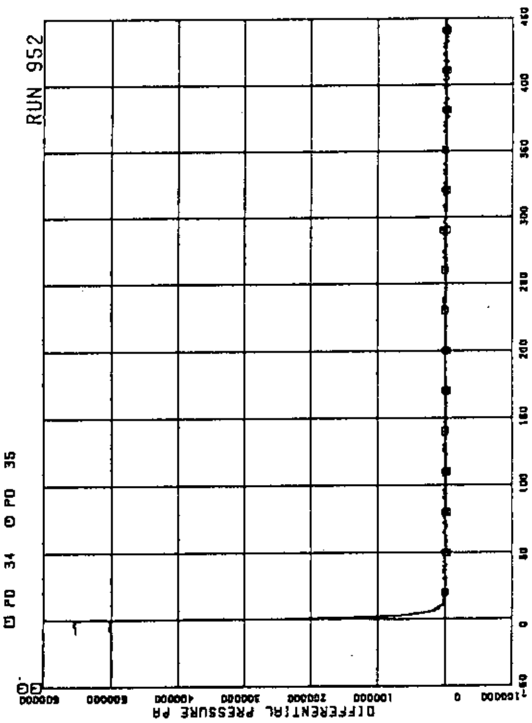

FIG.5. 14 DIFFERENTIAL PRESSURE BETWEEN MRP DELIVERY AND SUCTION

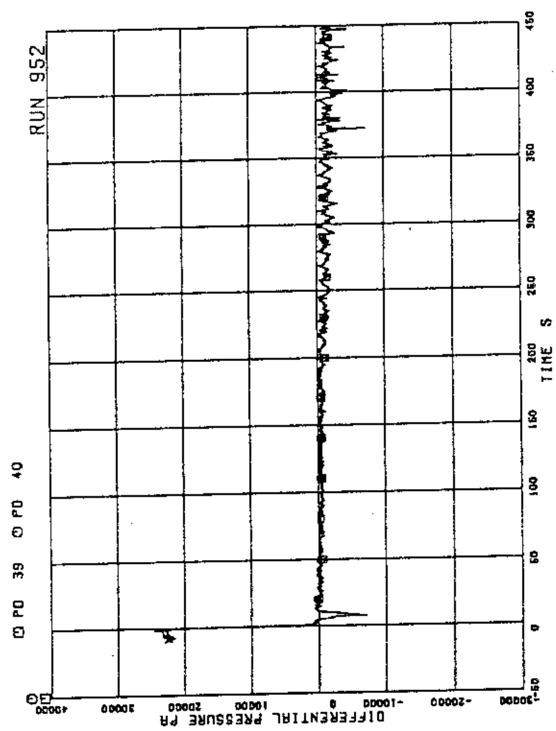

FIG.5. 17 DIFFERENTIAL PRESSURE BETWEEN DOWNCOMER MIDDLE AND JP-1,2 SUCTION

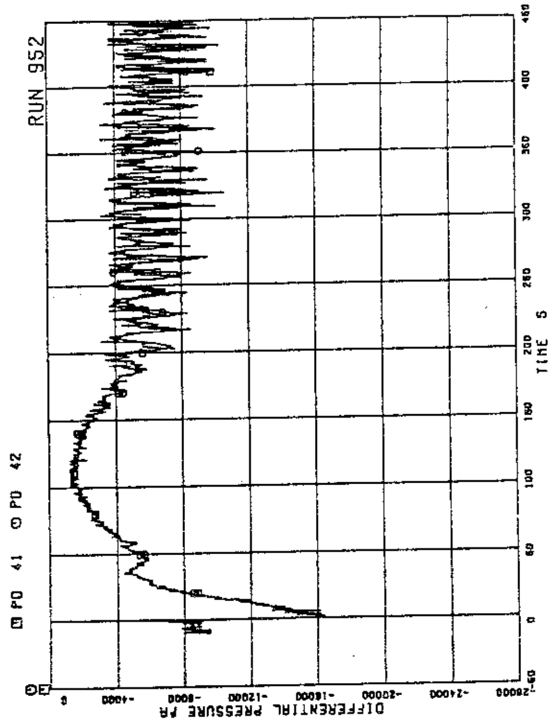

FIG.5. 18 DIFFERENTIAL PRESSURE BETWEEN JP-1,2 DISCHARGE AND LOWER PLENUM

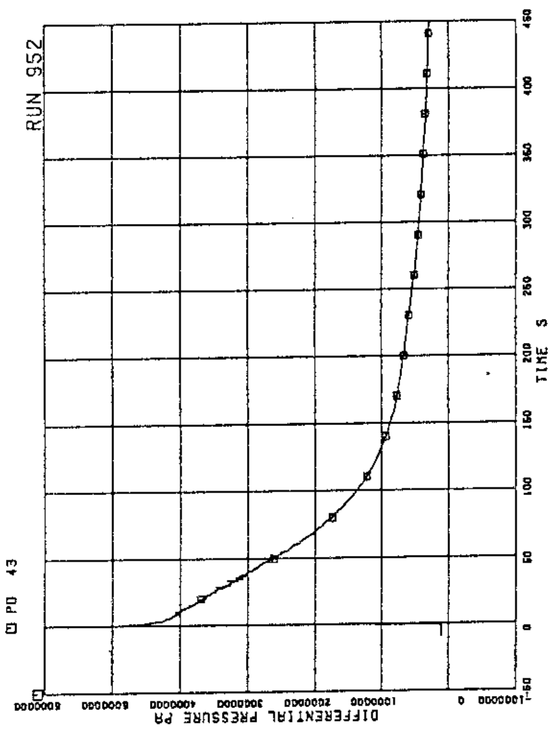

FIG.5. 19 DIFFERENTIAL PRESSURE BETWEEN DOWNCOMER BOTTOM AND BREAK

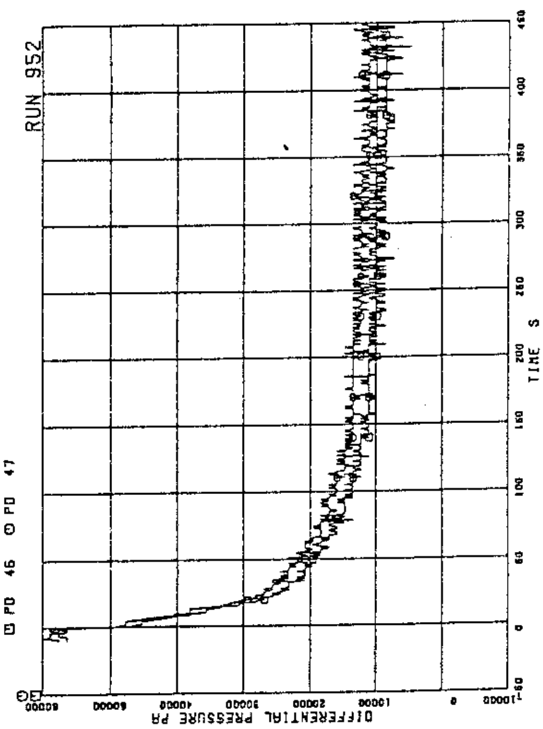

FIG.5. 20 DIFFERENTIAL PRESSURE BETWEEN MRP DELIVERY AND JP-3,4 DRIVE

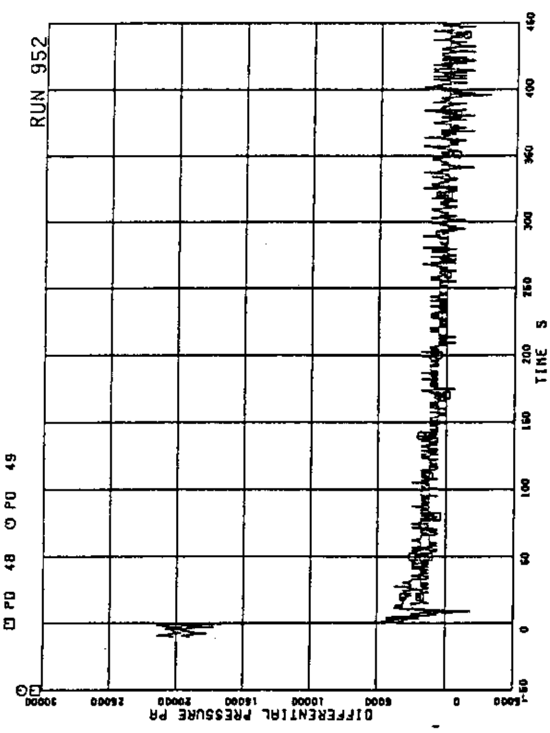

FIG.5. 21 DIFFERENTIAL PRESSURE BETWEEN DOWNCOMER MIDDLE AND JP-3.4 SUCTION

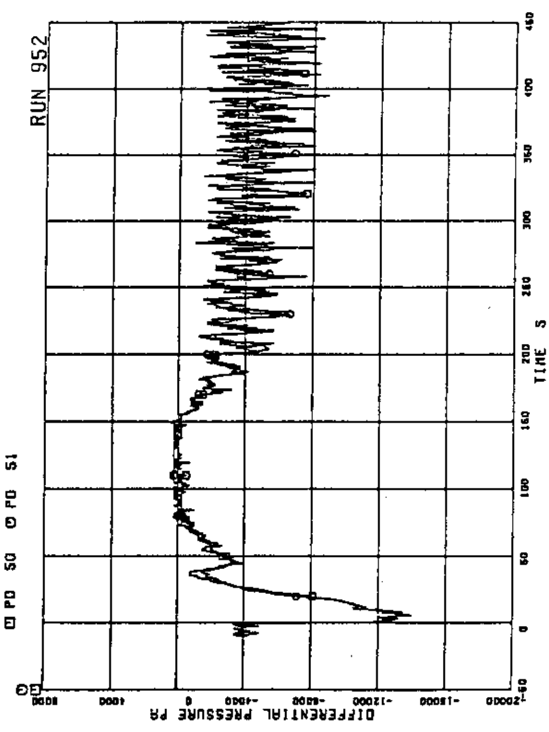

FIG.5. 22 DIFFERENTIAL PRESSURE BETWEEN JP-3.4 DISCHARGE AND CONFLUENCE

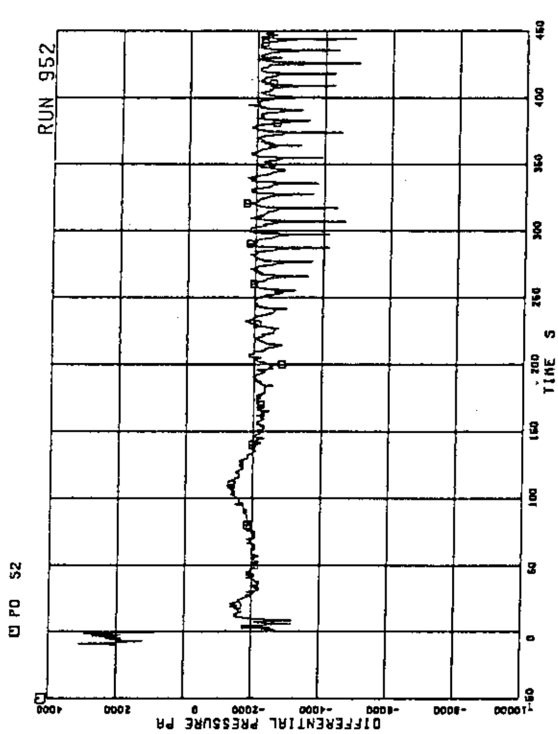

FIG.5. 23 DIFFERENTIAL PRESSURE BETWEEN JP-3.4 CONFLUENCE AND LP

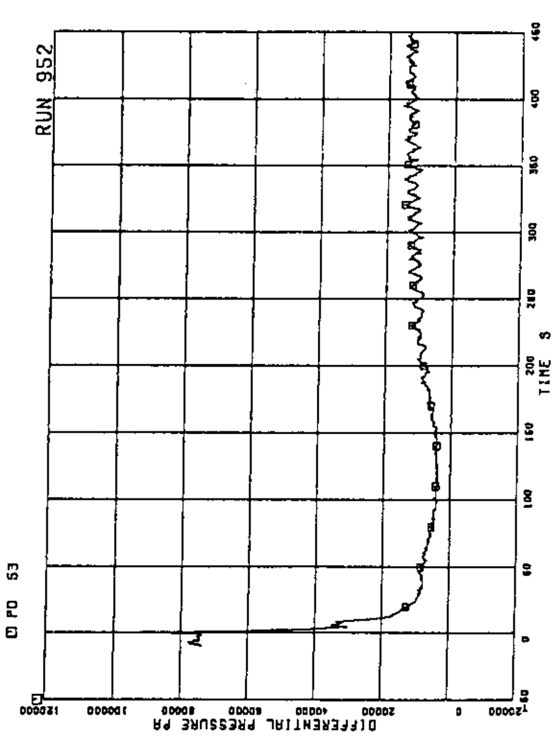

FIG.5. 24 DIFFERENTIAL PRESSURE BETWEEN LOWER PLENUM AND DOWNCOMER MIDDLE

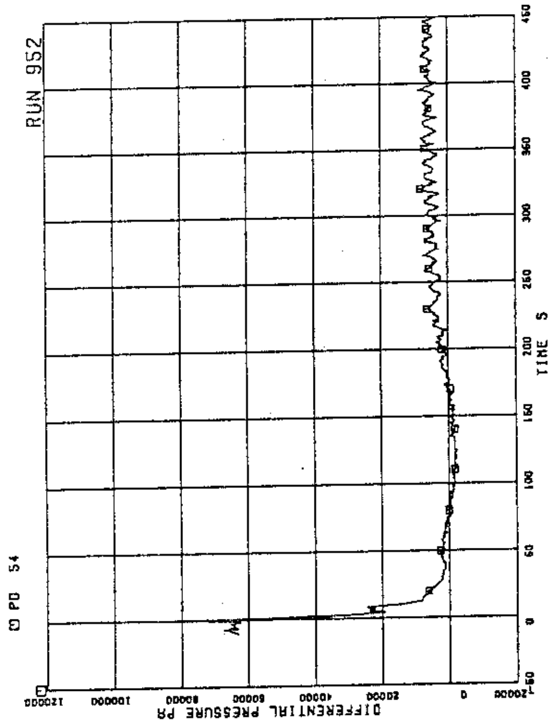

FIG.5. 25 DIFFERENTIAL PRESSURE BETWEEN LOWER PLENUM AND DOWNCOMER (BOTTOM)

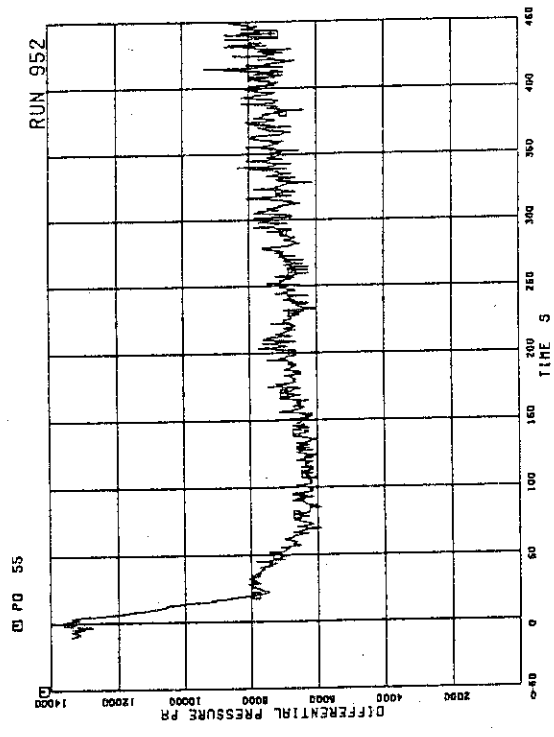

FIG.5. 26 DIFFERENTIAL PRESSURE BETWEEN DOWNCOMER BOTTOM AND DOWNCOMER MIDDLE

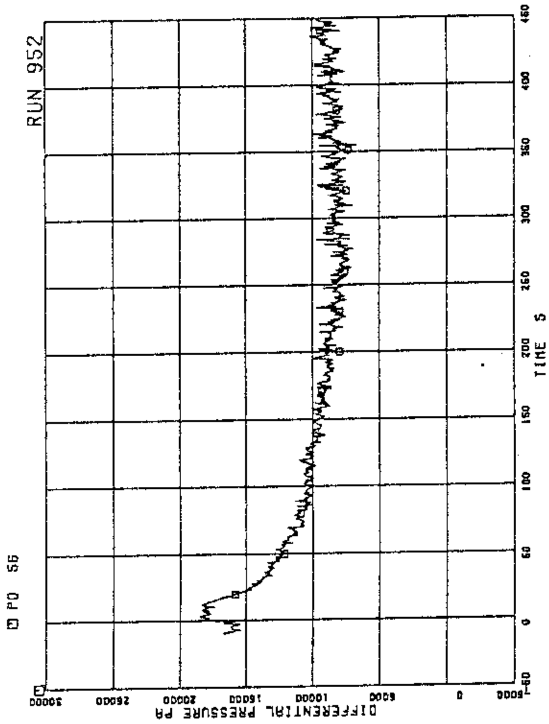

FIG.5. 27 DIFFERENTIAL PRESSURE BETWEEN DOWNCOMER MIDDLE AND STEAM DOME

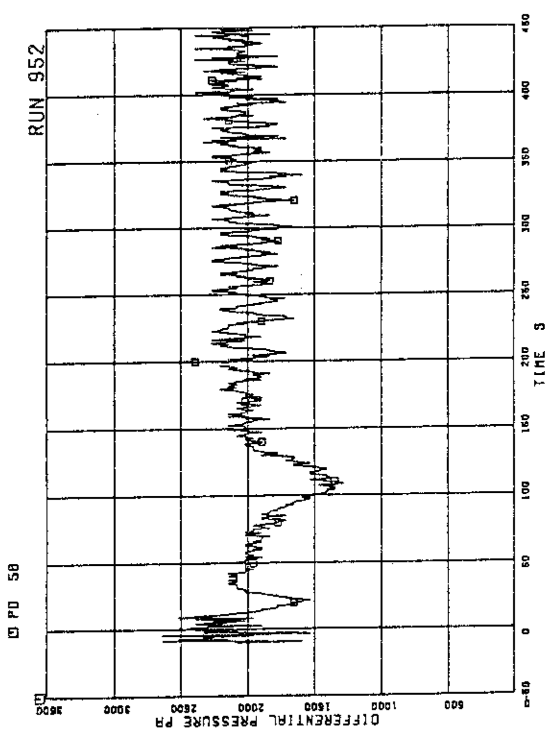

FIG.5. 28 DIFFERENTIAL PRESSURE BETWEEN LP BOTTOM AND LP MIDDLE

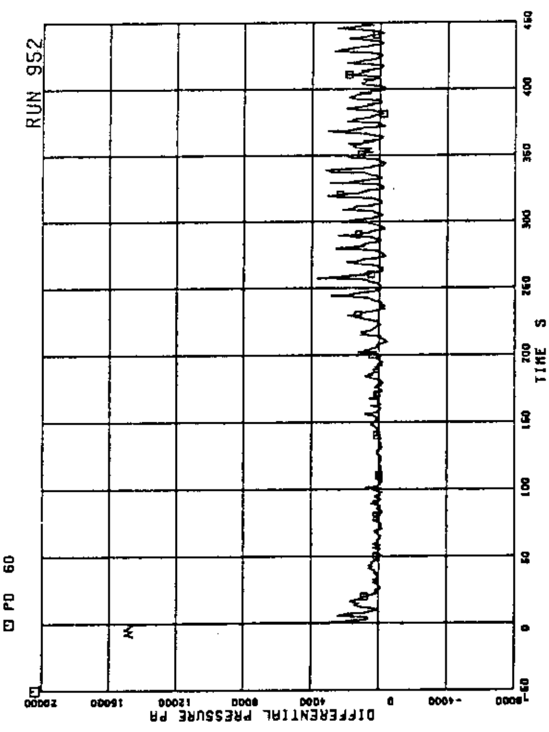

FIG.5. 29 DIFFERENTIAL PRESSURE ACROSS CHANNEL INLET ORIFICE A

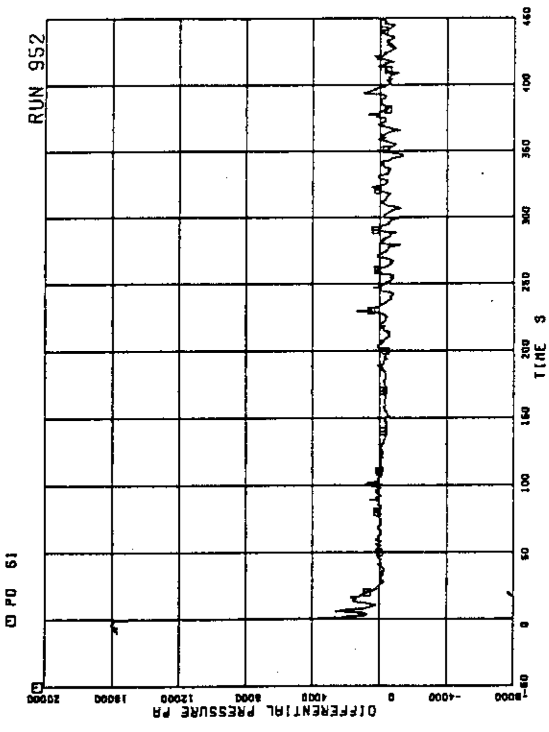

FIG.5. 30 DIFFERENTIAL PRESSURE ACROSS CHANNEL INLET ORIFICE B

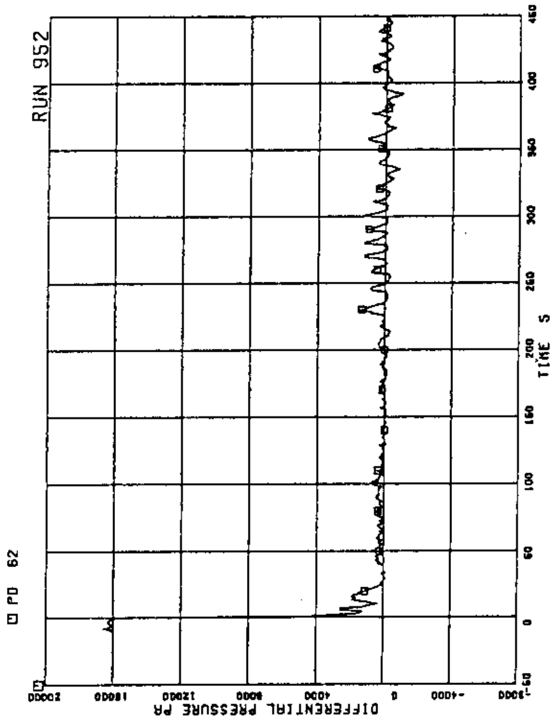

FIG.5. 31 DIFFERENTIAL PRESSURE ACROSS CHANNEL INLET ORIFICE C

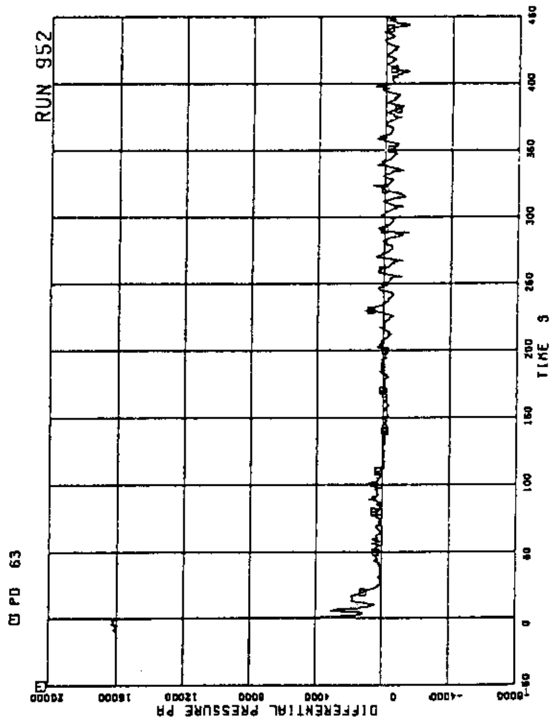

FIG.5. 32 DIFFERENTIAL PRESSURE ACROSS CHANNEL INLET ORIFICE D

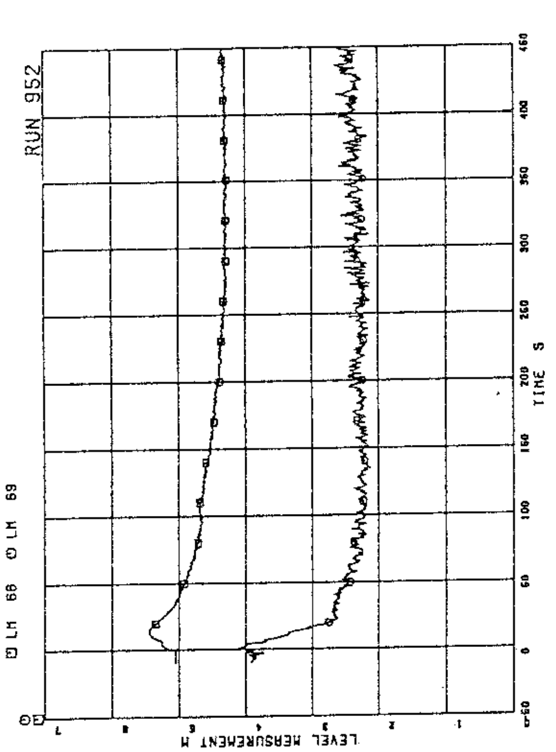

FIG.5. 35 LIQUID LEVELS IN UPPER AND LOWER DOWNCOMER

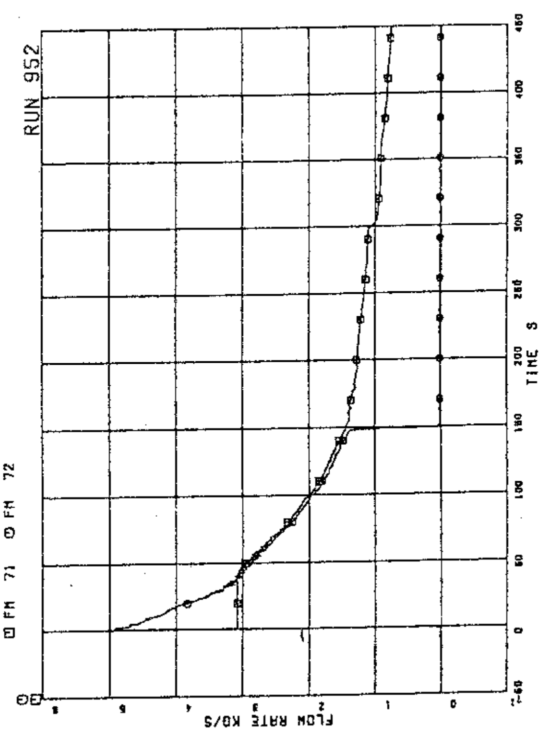

FIG.5. 36 MASS FLOW RATE IN MSL

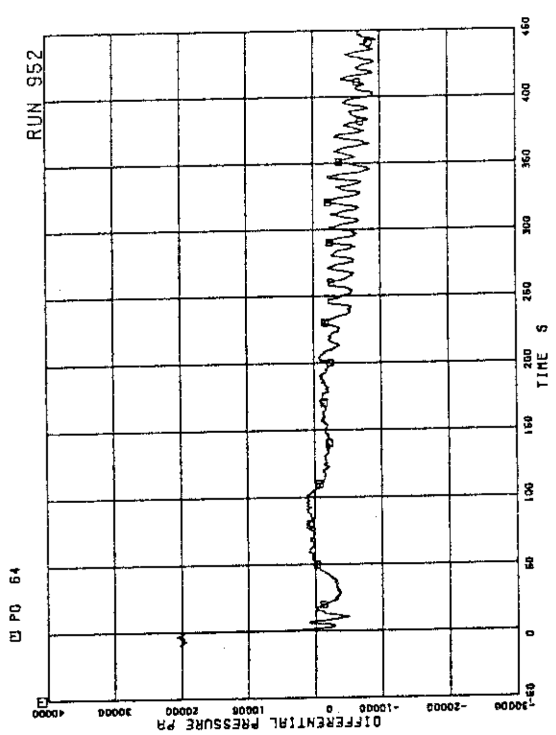

FIG.5. 33 DIFFERENTIAL PRESSURE ACROSS BYPASS HOLE

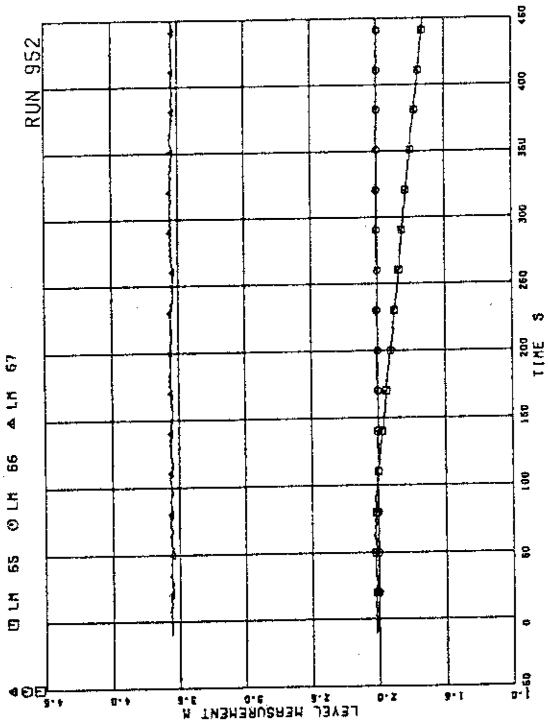

FIG.5. 34 LIQUID LEVELS IN ECCS TANKS

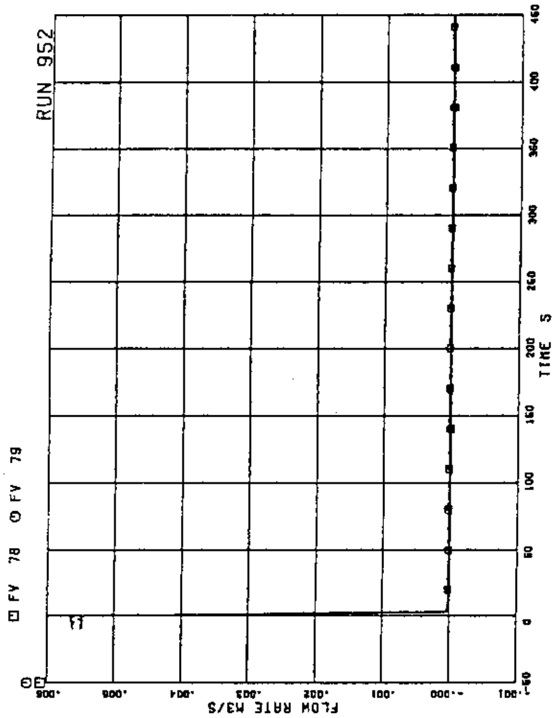

FIG.5. 39 JP-1.2 DISCHARGE FLOW RATE

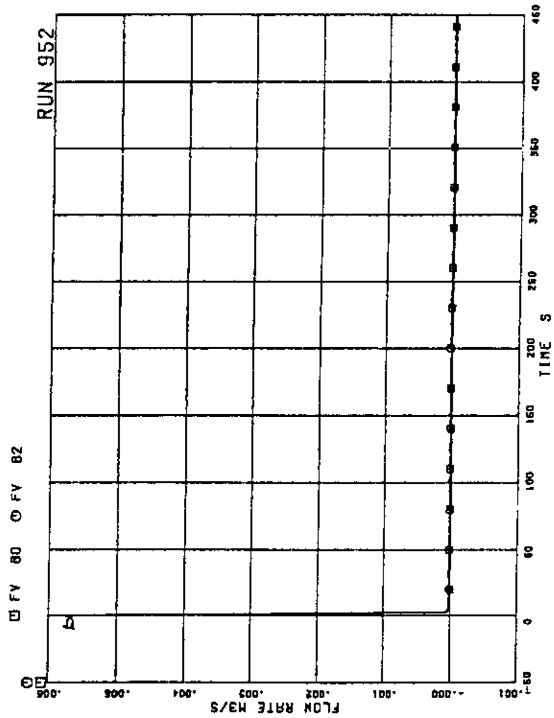

FIG.5. 40 JP-3.4 DISCHARGE FLOW RATE

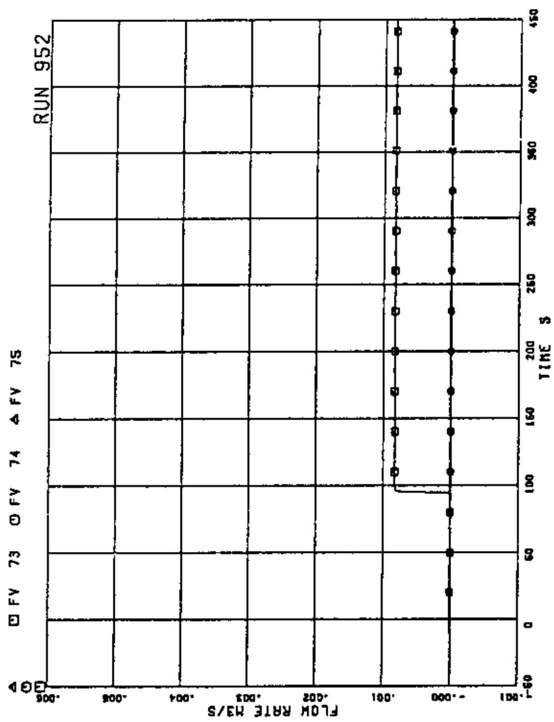

FIG.5. 37 ECC INJECTION FLOW RATE

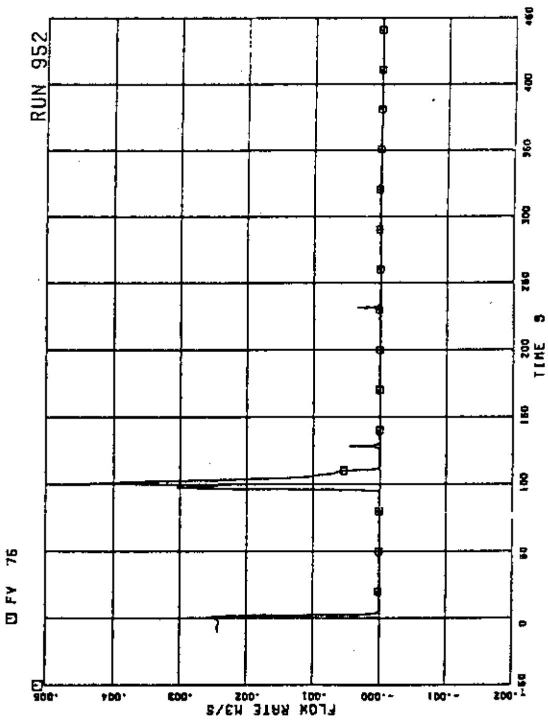

FIG.5. 38 FEEDWATER FLOW RATE

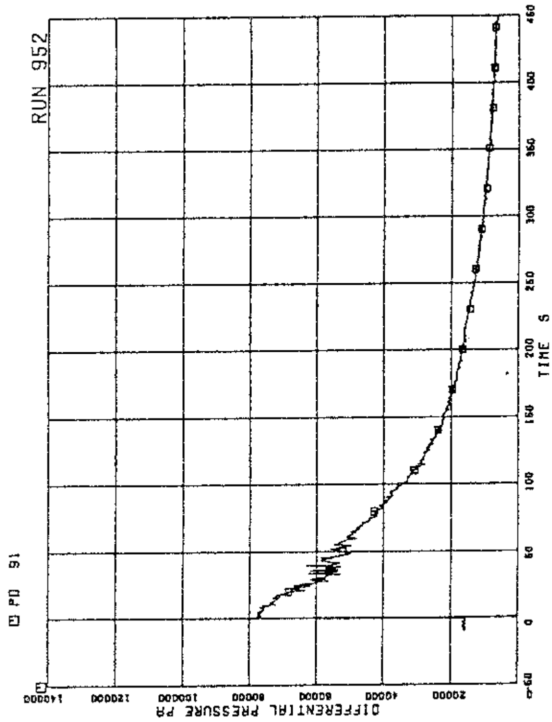

FIG.5. 43 DIFF. PRESSURE ACROSS ORIFICE F-2 IN MSL (MID)

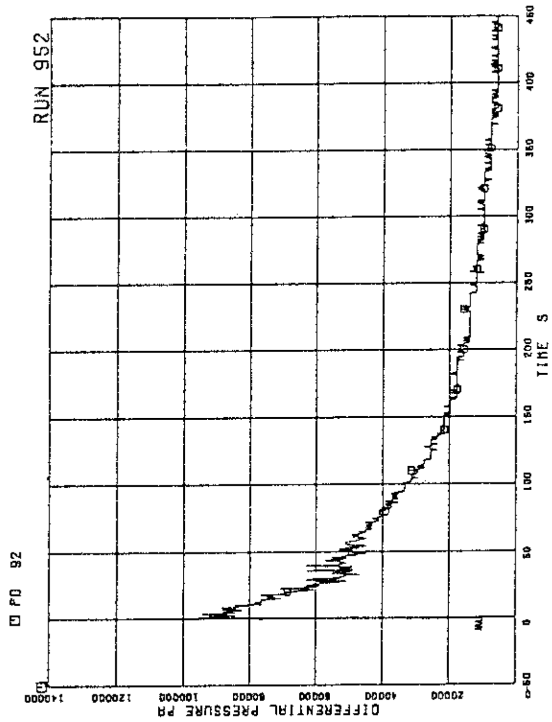

FIG.5. 44 DIFF. PRESSURE ACROSS ORIFICE F-3 IN MSL (HIGH)

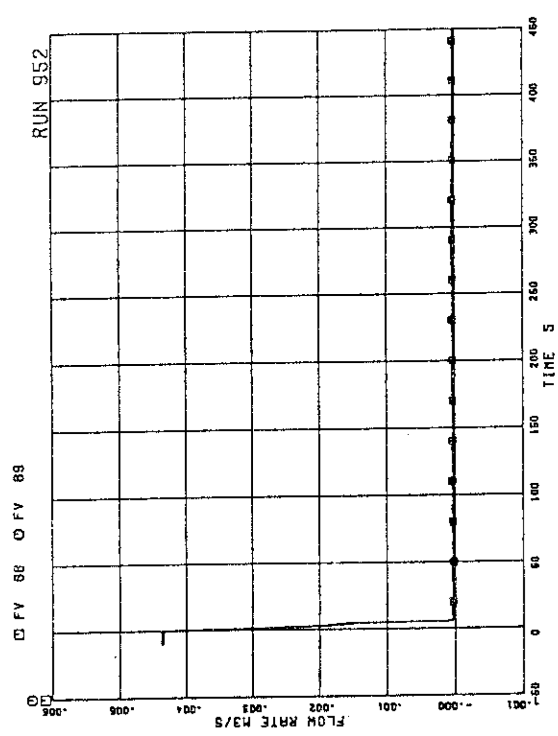

FIG.5. 41 MRP FLOW RATE

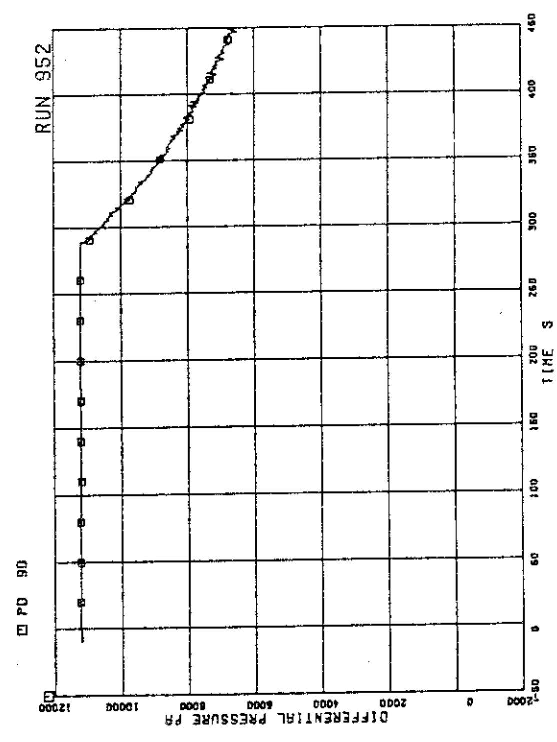

FIG.5. 42 DIFF. PRESSURE ACROSS ORIFICE F-1 IN MSL (LOW)

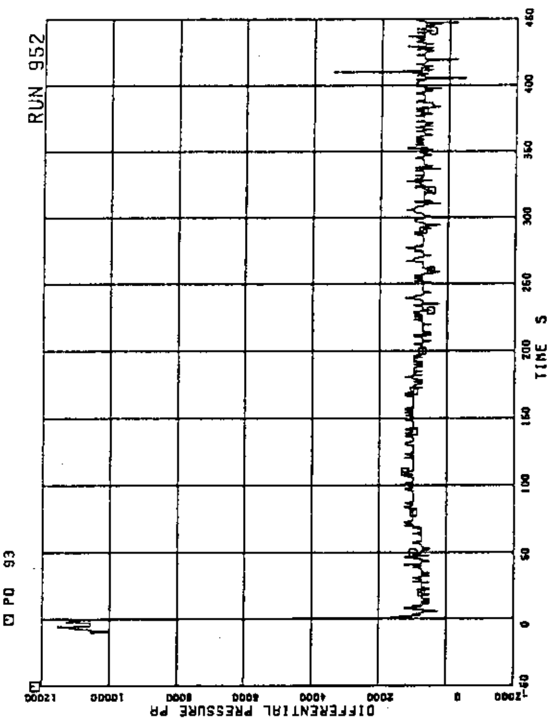

FIG.5. 45 DIFF. PRESSURE ACROSS VENTURI F-17 IN JP1

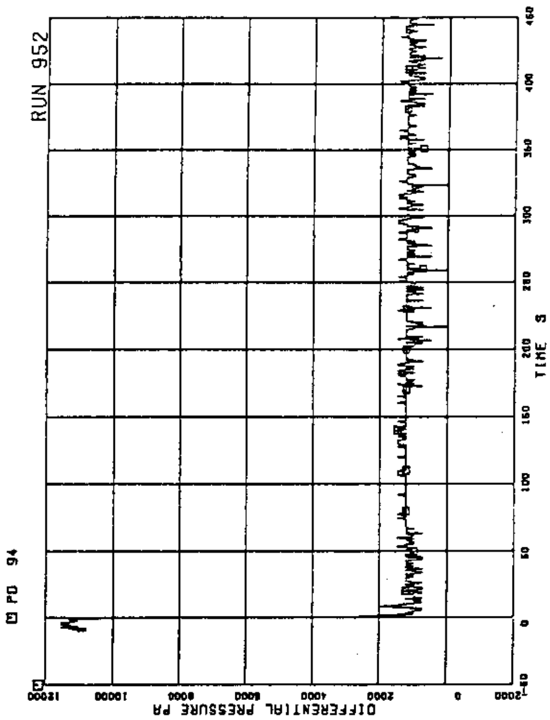

FIG.5. 46 DIFF. PRESSURE ACROSS VENTURI F-18 IN JP2

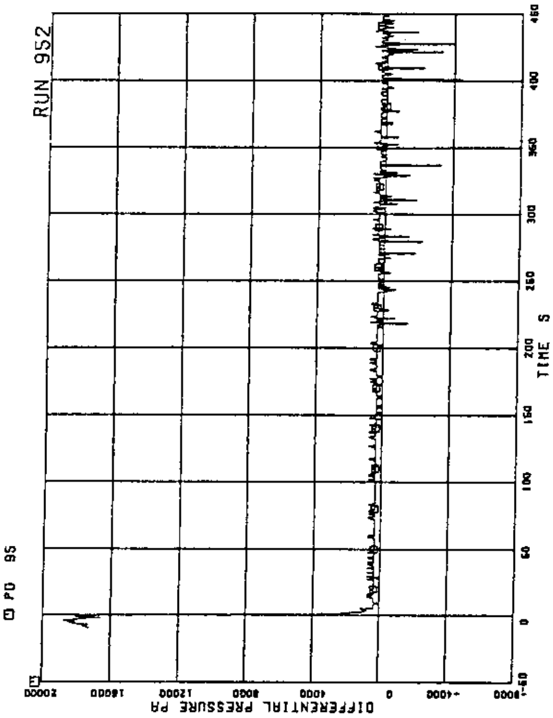

FIG.5. 47 DIFF. PRESSURE ACROSS ORIFICE F-19 IN JP3

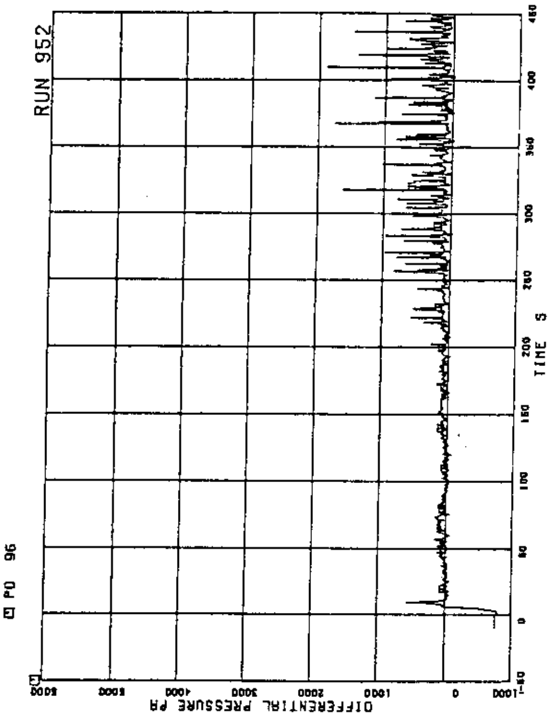

FIG.5. 48 DIFF. PRESSURE ACROSS ORIFICE F-20 IN JP4

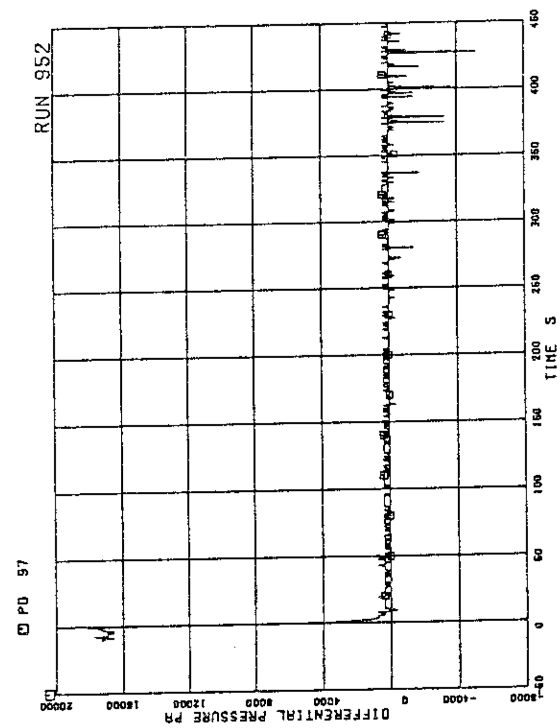

FIG.5. 49 DIFF. PRESSURE ACROSS ORIFICE
F-21 IN JP3

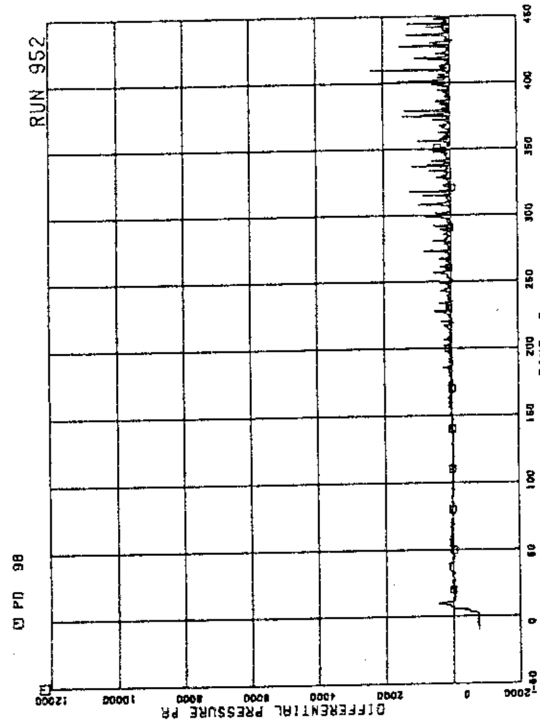

FIG.5. 50 DIFF. PRESSURE ACROSS ORIFICE
F-22 IN JP4

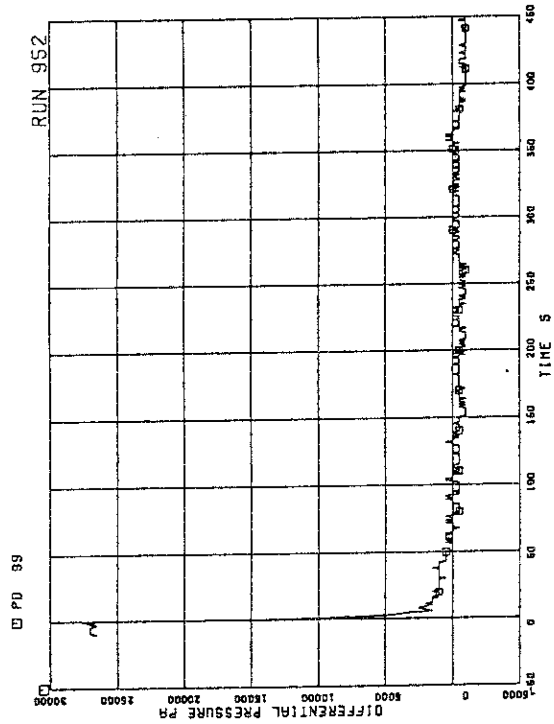

FIG.5. 51 DIFF. PRESSURE ACROSS VENTURI
F-27 IN MRP-1

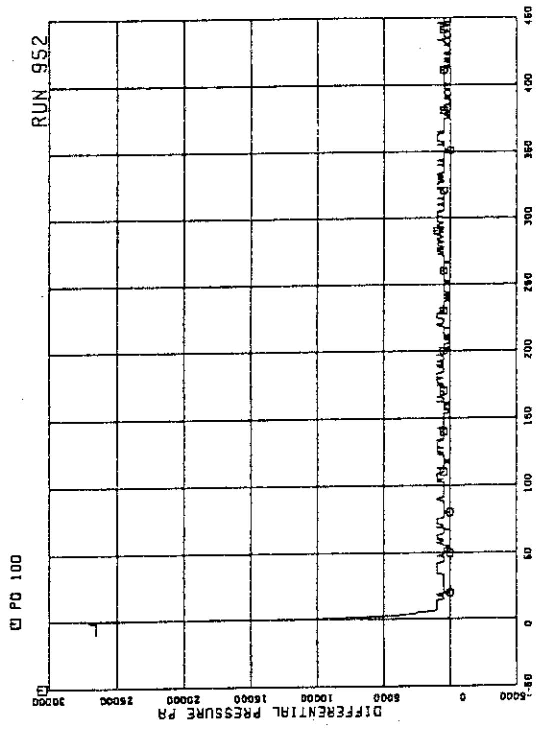

FIG.5. 52 DIFF. PRESSURE ACROSS VENTURI
F-28 IN MRP-2

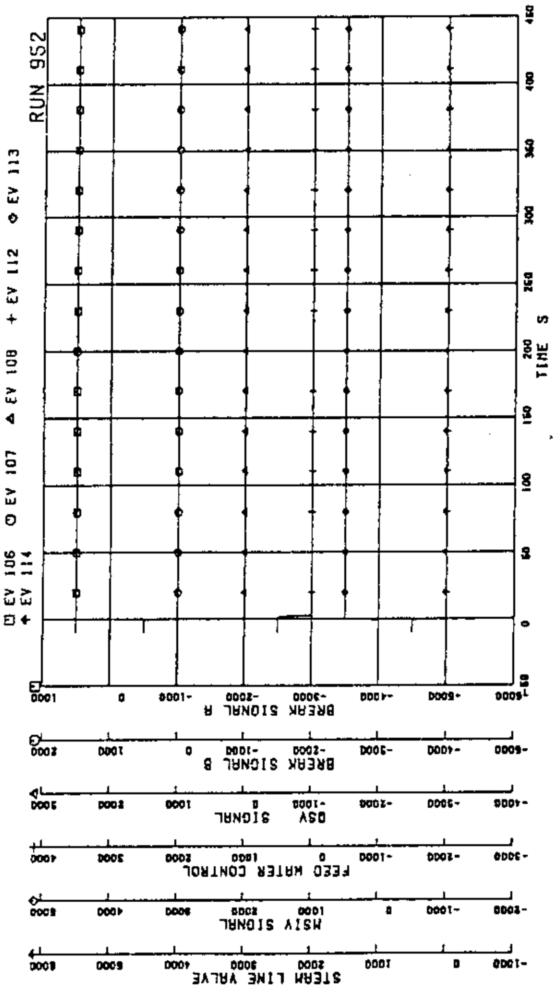

FIG.5. 55 VALVE OPERATION SIGNALS

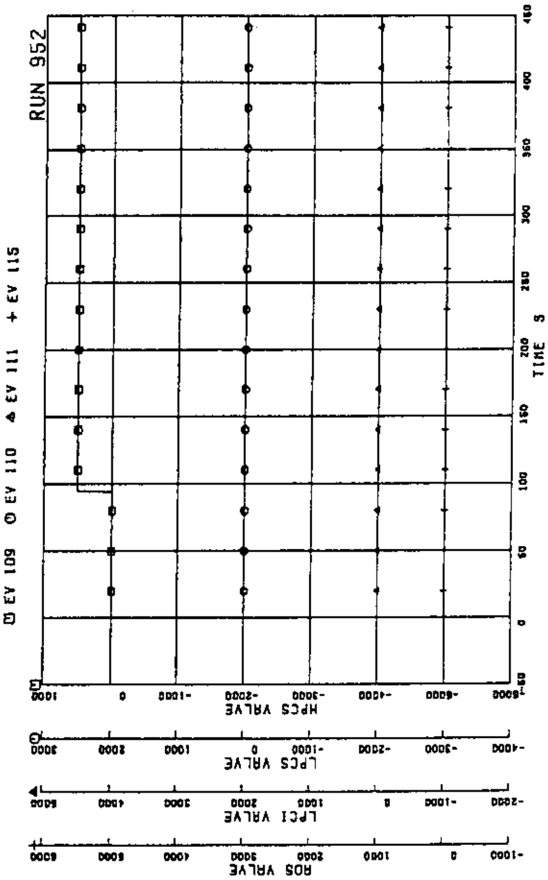

FIG.5. 56 ECCS OPERATION SIGNALS

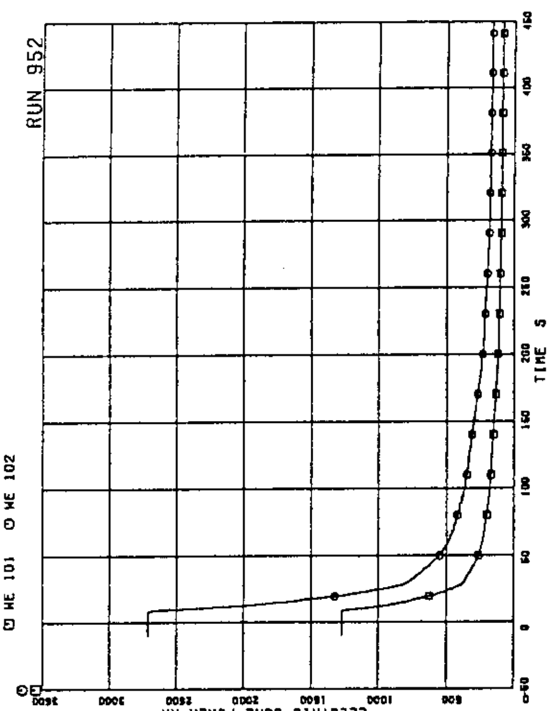

FIG.5. 53 ELECTRIC CORE POWER

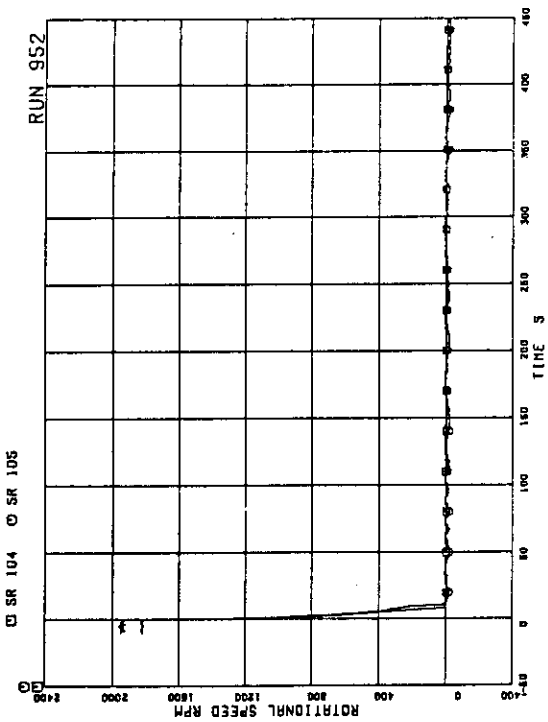

FIG.5. 54 MRP REVOLUTION

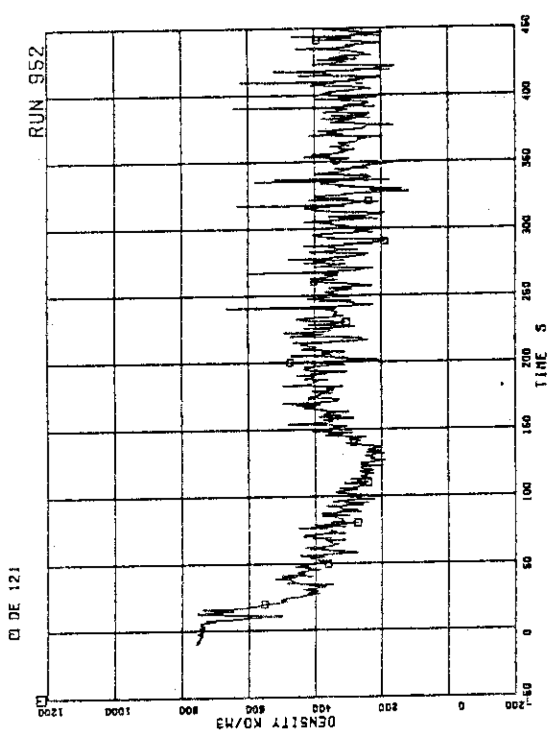

FIG.5. 59 FLUID DENSITY AT JP-1.2 OUTLET, BEAM B

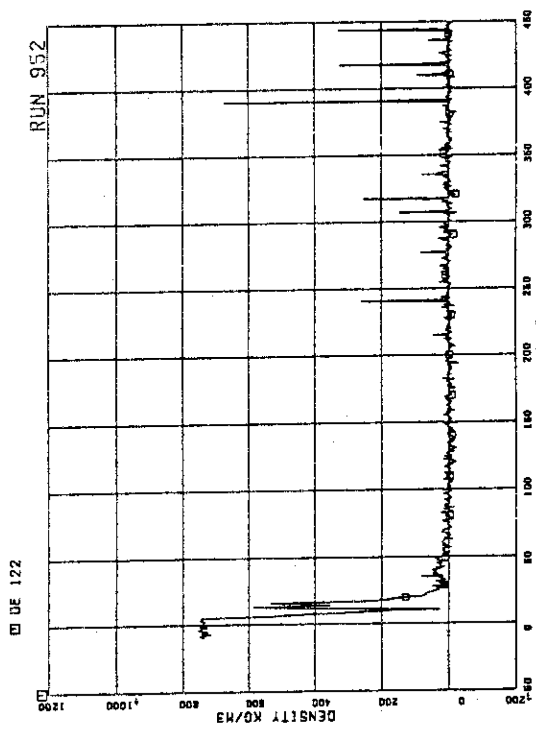

FIG.5. 60 FLUID DENSITY AT JP-1.2 OUTLET, BEAM C

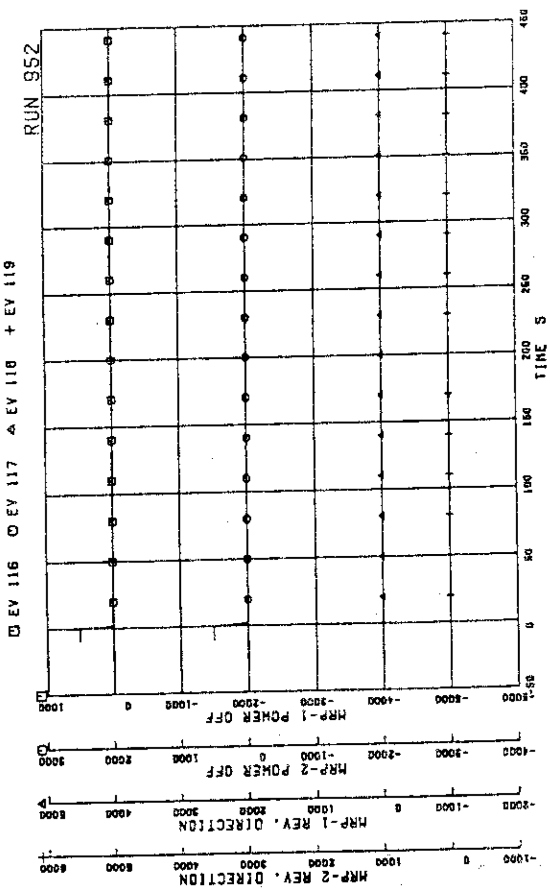

FIG.5. 57 MRP OPERATION SIGNALS

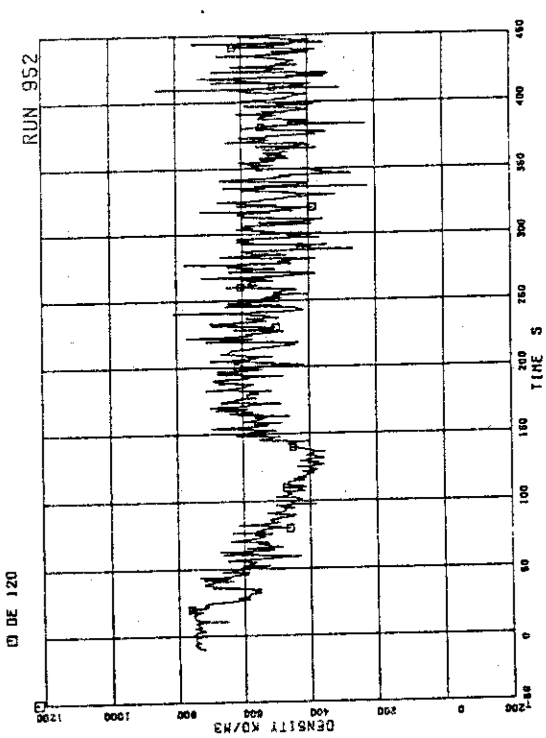

FIG.5. 58 FLUID DENSITY AT JP-1.2 OUTLET, BEAM A

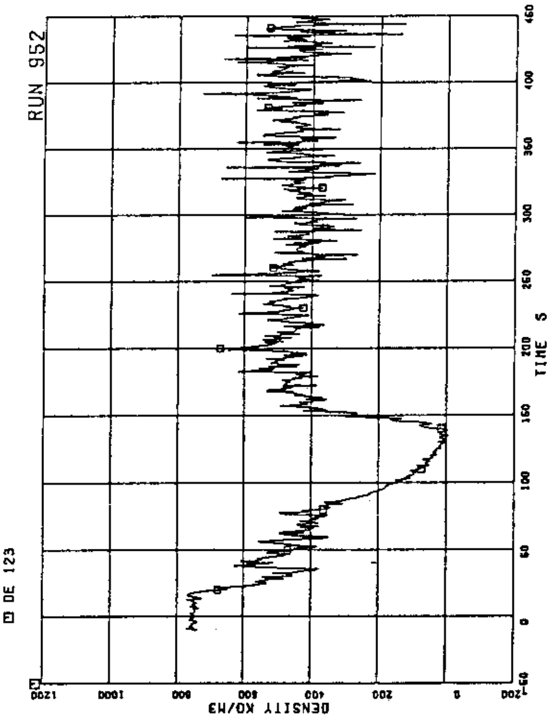

FIG.5. 61 FLUID DENSITY AT JP-3,4 OUTLET, BEAM A

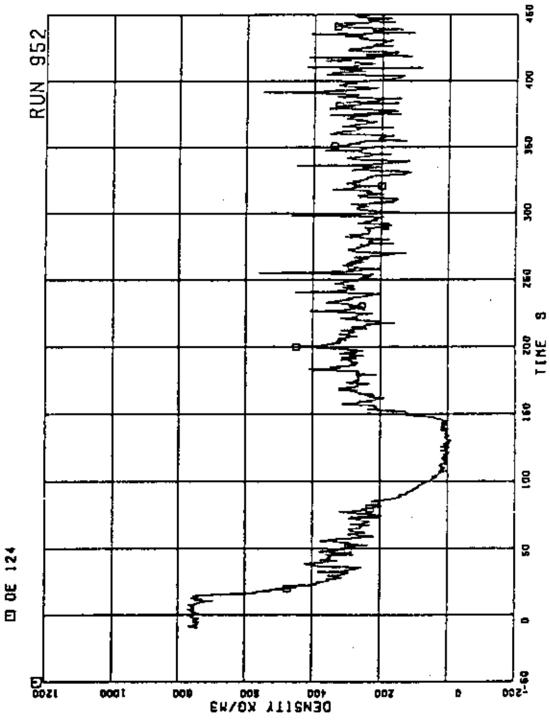

FIG.5. 62 FLUID DENSITY AT JP-3,4 OUTLET, BEAM B

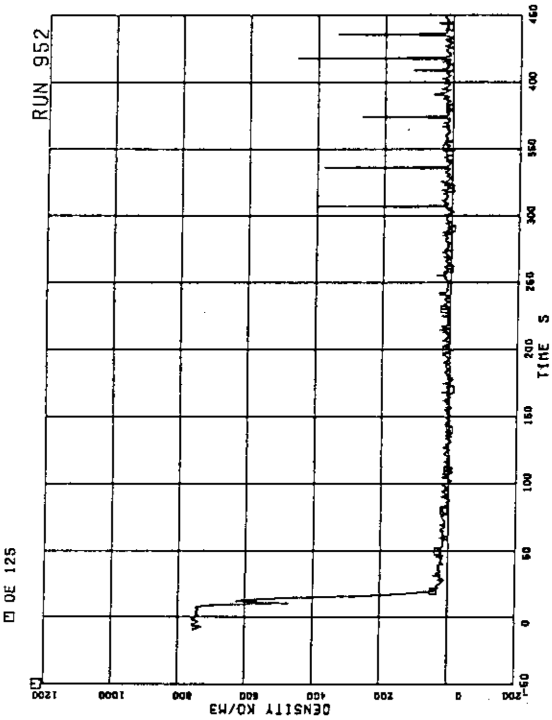

FIG.5. 63 FLUID DENSITY AT JP-3,4 OUTLET, BEAM C

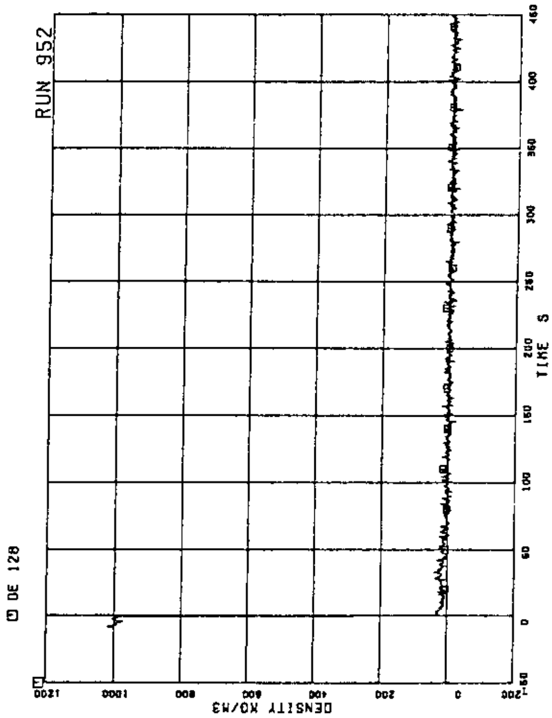

FIG.5. 64 FLUID DENSITY AT BREAK,(BEAM A)

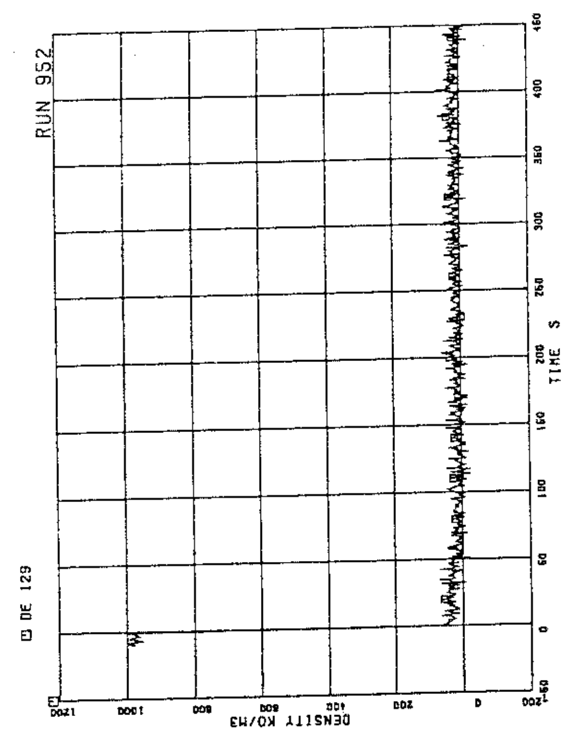

FIG.5. 65 FLUID DENSITY AT BREAK.(BEAM B)

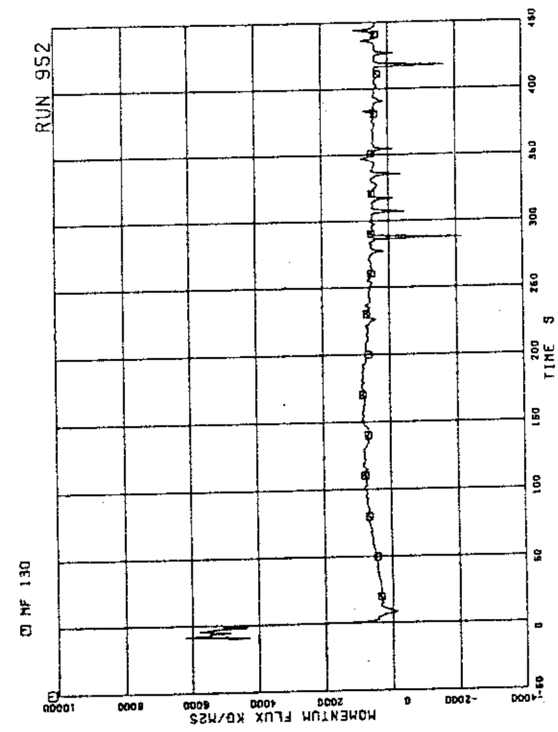

FIG.5. 66 MOMENTUM FLUX AT JP-1.2 OUTLET

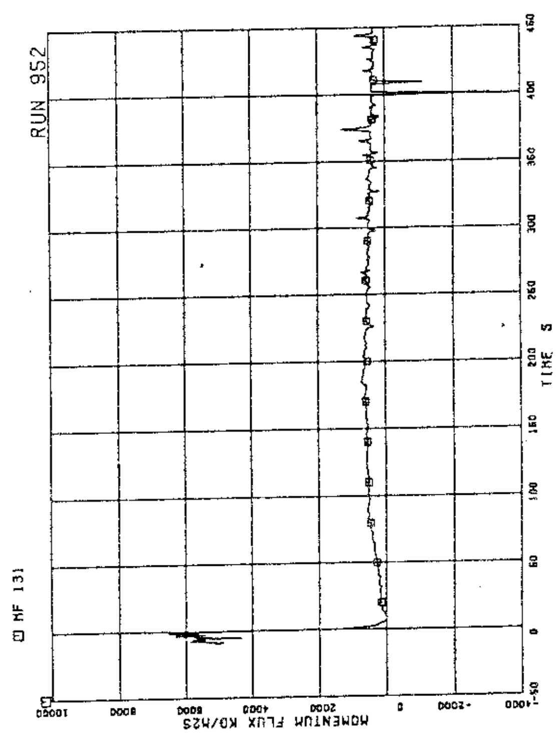

FIG.5. 67 MOMENTUM FLUX AT JP-3.4 OUTLET

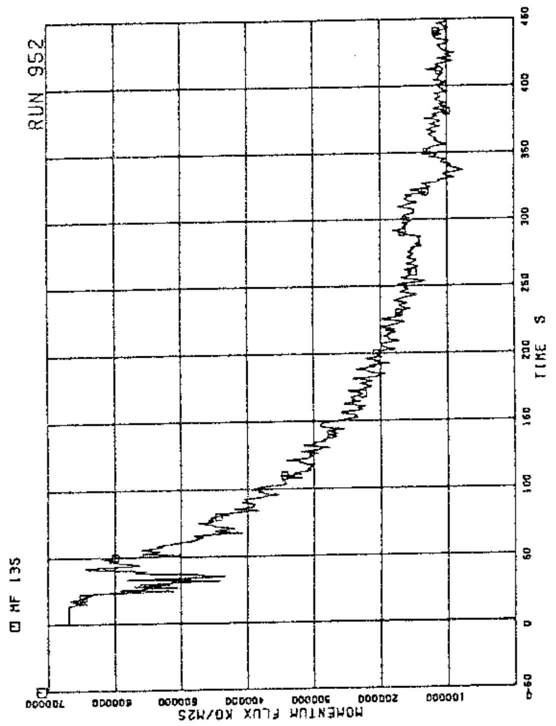

FIG.5. 68 MOMENTUM FLUX AT BREAK B SPOOL PIECE (HIGH RANGE)

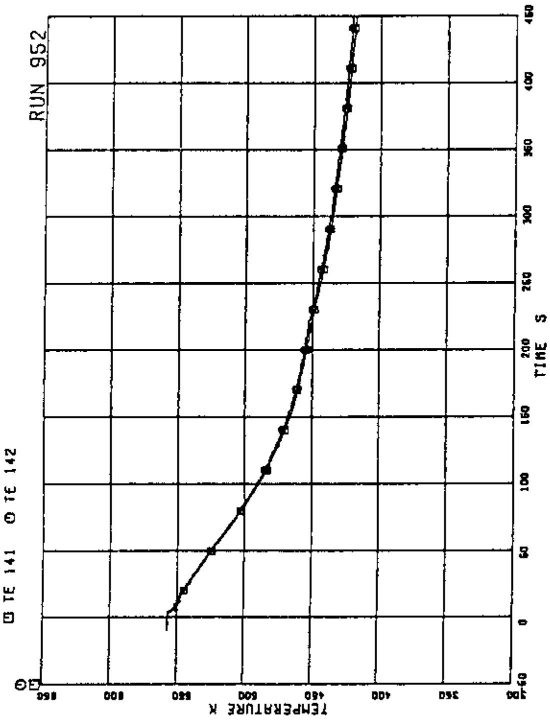

FIG.5. 71 FLUID TEMPERATURES IN DOWNCOMER

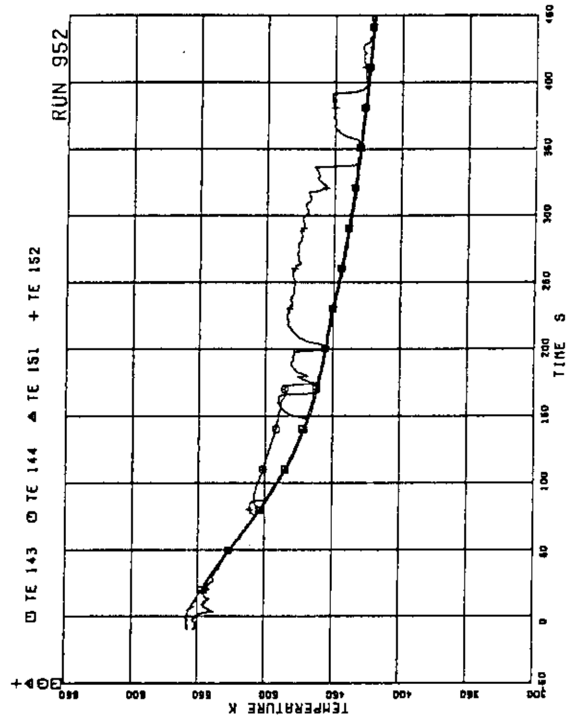

FIG.5. 72 FLUID TEMPERATURES IN RECIRCULATION LOOP A

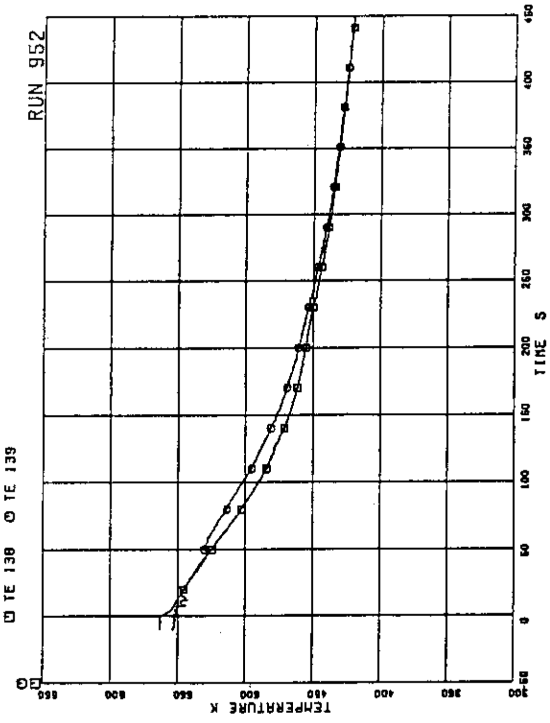

FIG.5. 69 FLUID TEMPERATURES IN LOWER PLENUM AND UPPER PLENUM

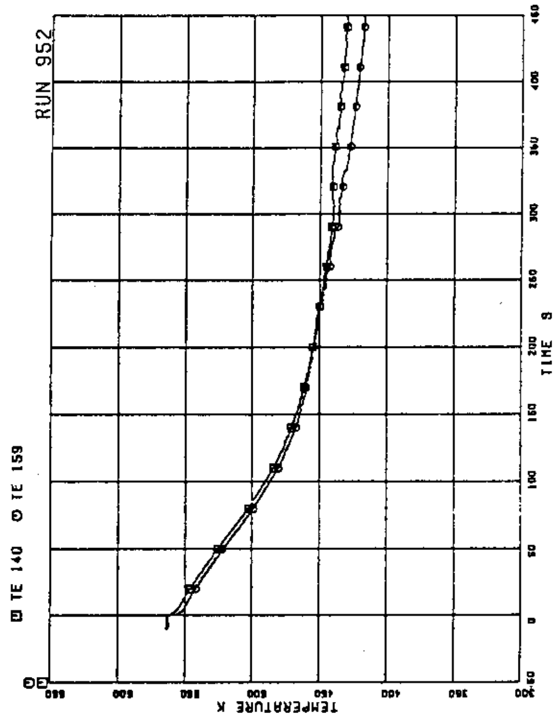

FIG.5. 70 FLUID TEMPERATURES IN STEAM DOME AND MSL

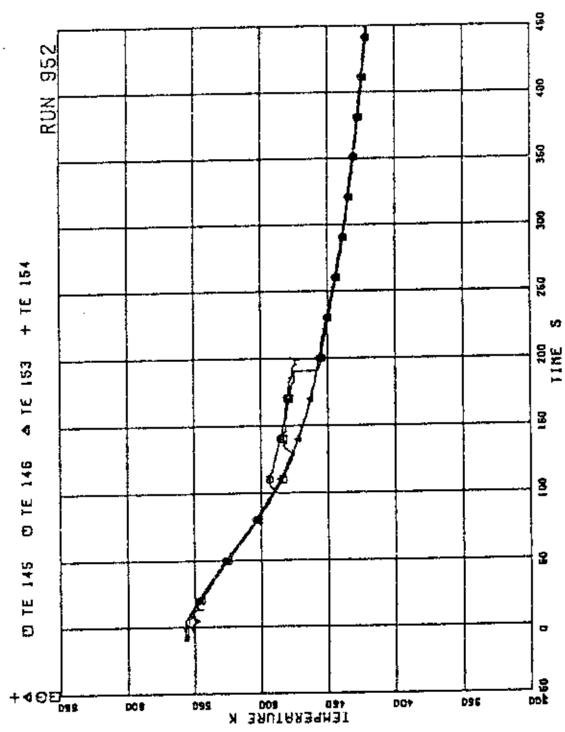

FIG.5. 73 FLUID TEMPERATURES IN RECIRCULATION LOOP B

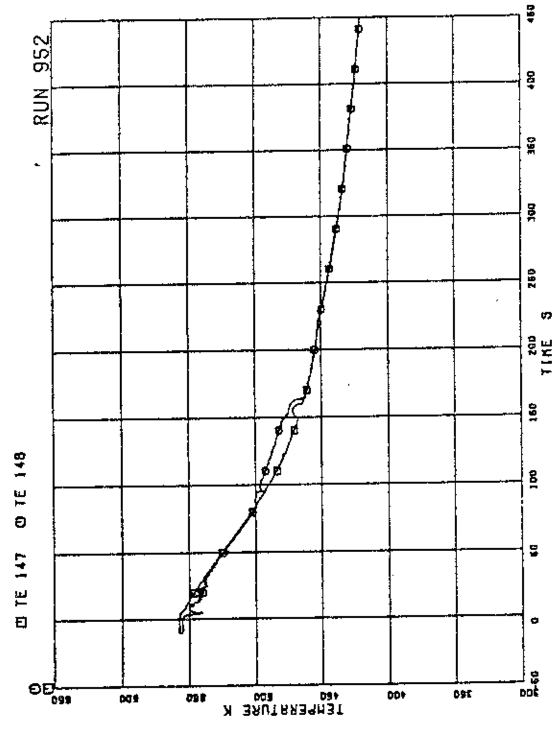

FIG.5. 74 FLUID TEMPERATURES AT JP-1.2 OUTLET

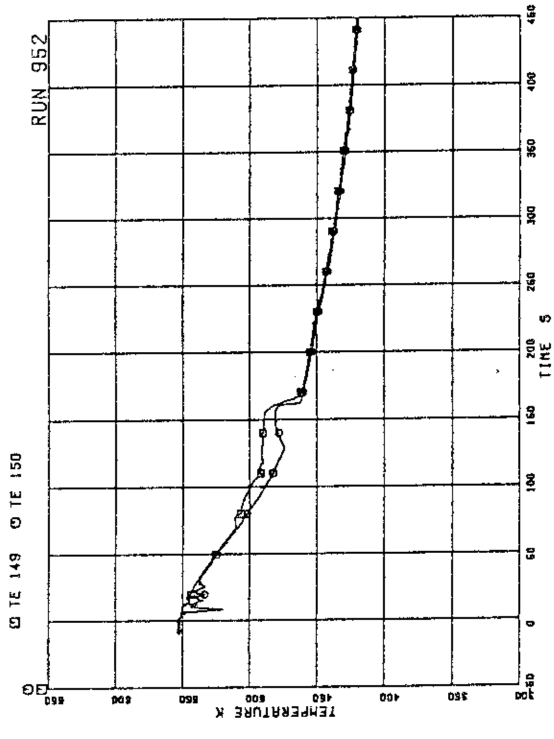

FIG.5. 75 FLUID TEMPERATURES AT JP-3.4 OUTLET

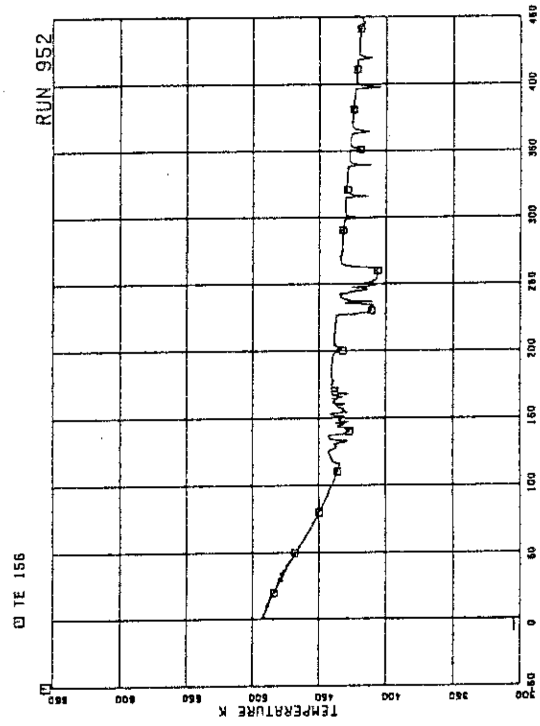

FIG.5. 76 FLUID TEMPERATURE UPSTREAM OF BREAK

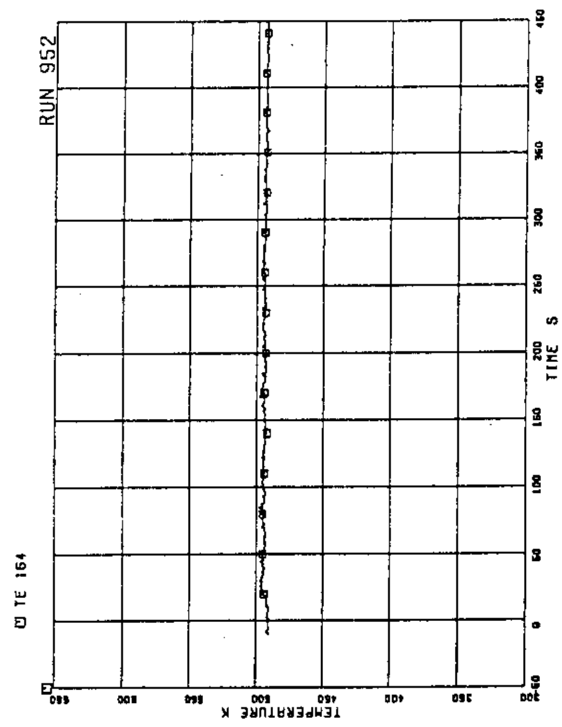

FIG.5. 77 FEEDWATER TEMPERATURE

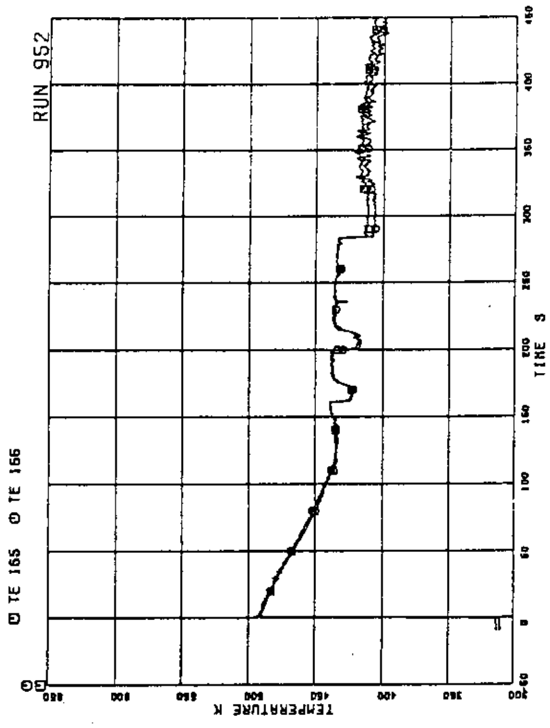

FIG.5. 78 FLUID TEMPERATURES AT BREAK ORIFICE

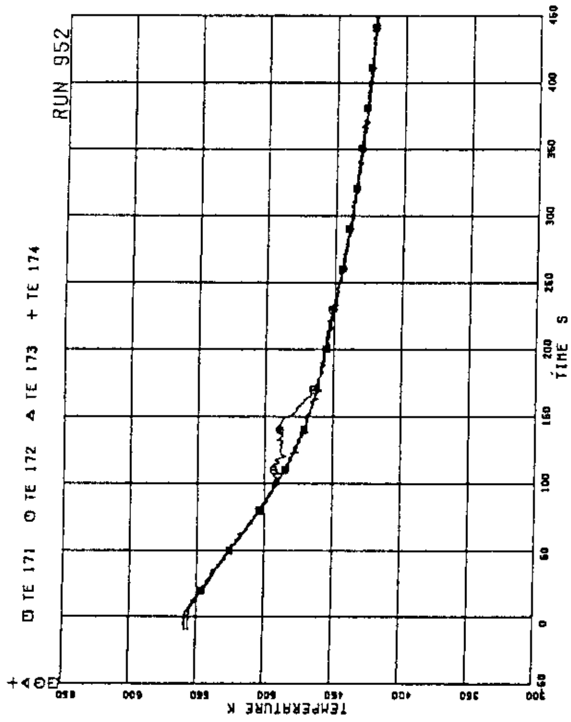

FIG.5. 79 JP DIFFUSER WALL TEMPERATURES

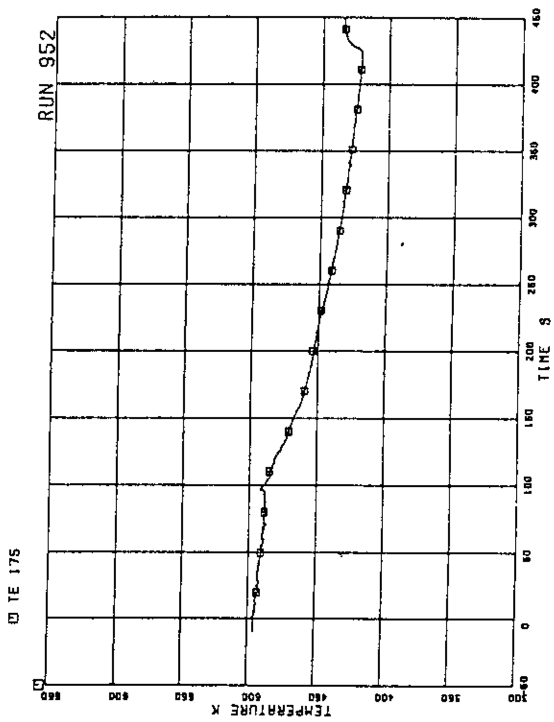

FIG.5. 80 PV FEEDWATER FLUID TEMPERATURE

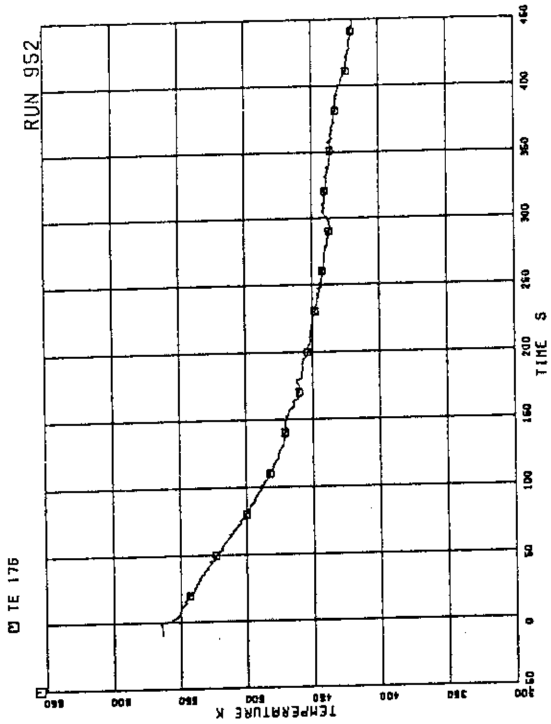

FIG.5. 81 DISCHARGED STEAM TEMPERATURE

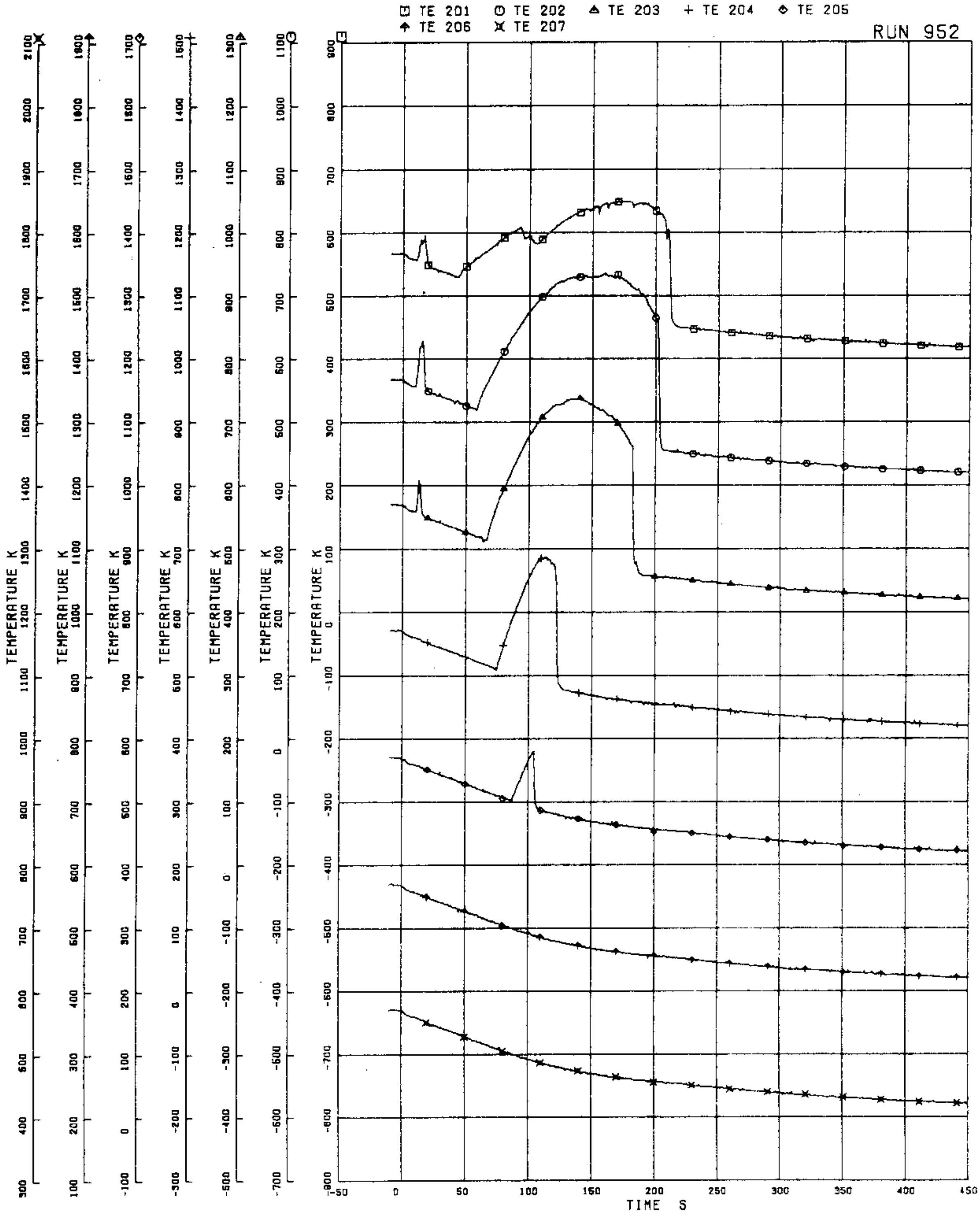

FIG.5. 82 SURFACE TEMPERATURES OF FUEL ROD A11

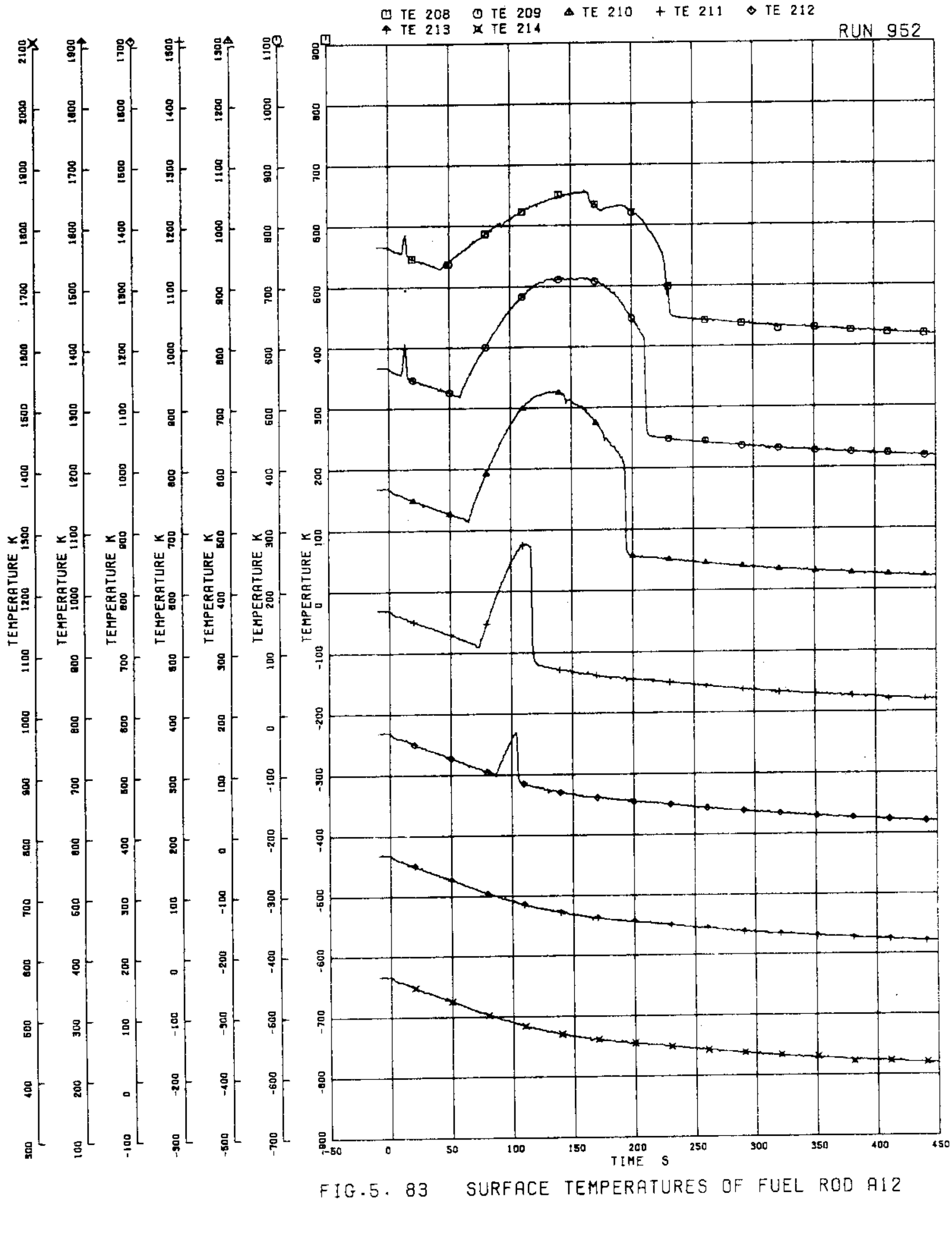

FIG.5. 83 SURFACE TEMPERATURES OF FUEL ROD A12

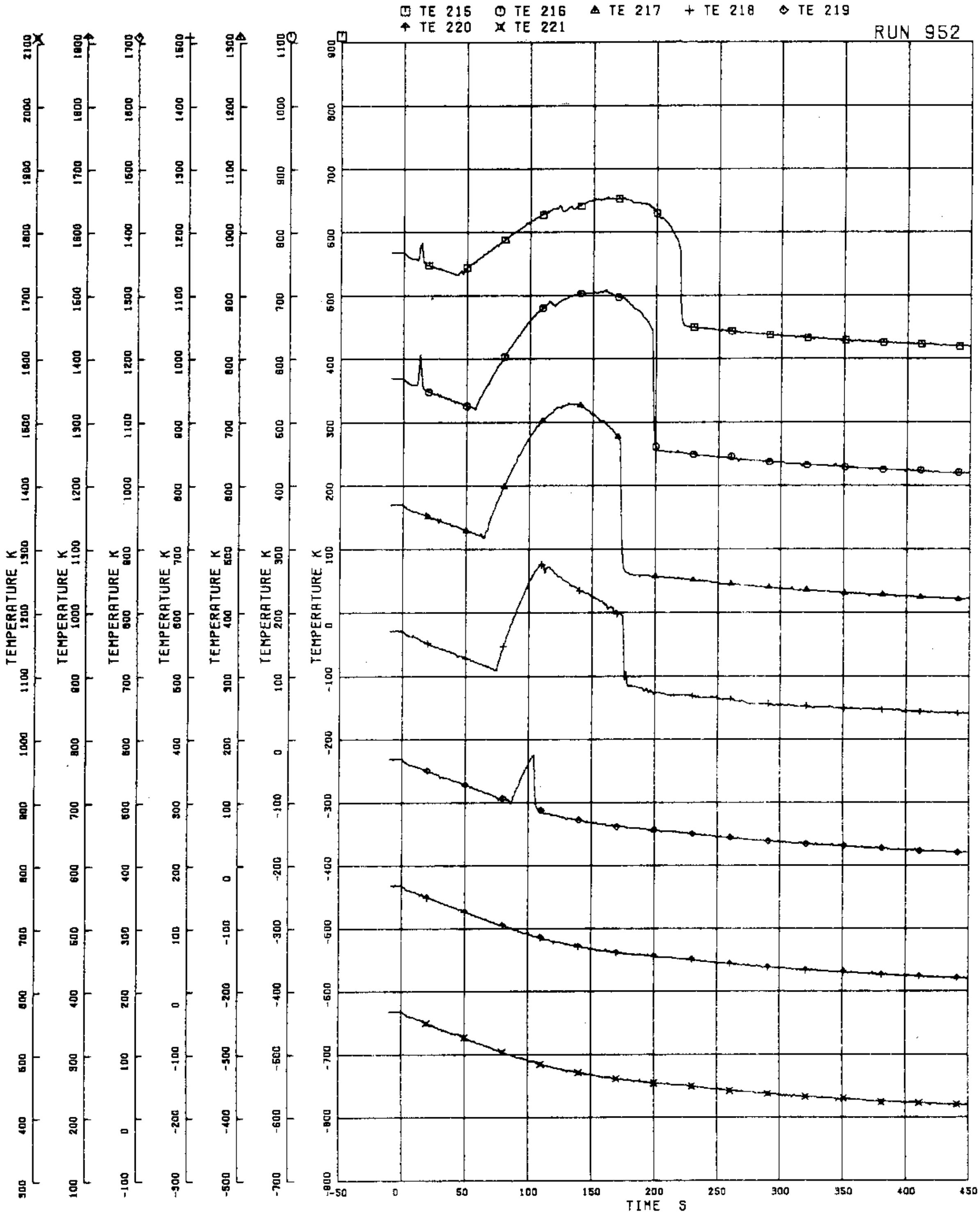

FIG.5. 84 SURFACE TEMPERATURES OF FUEL ROD A13

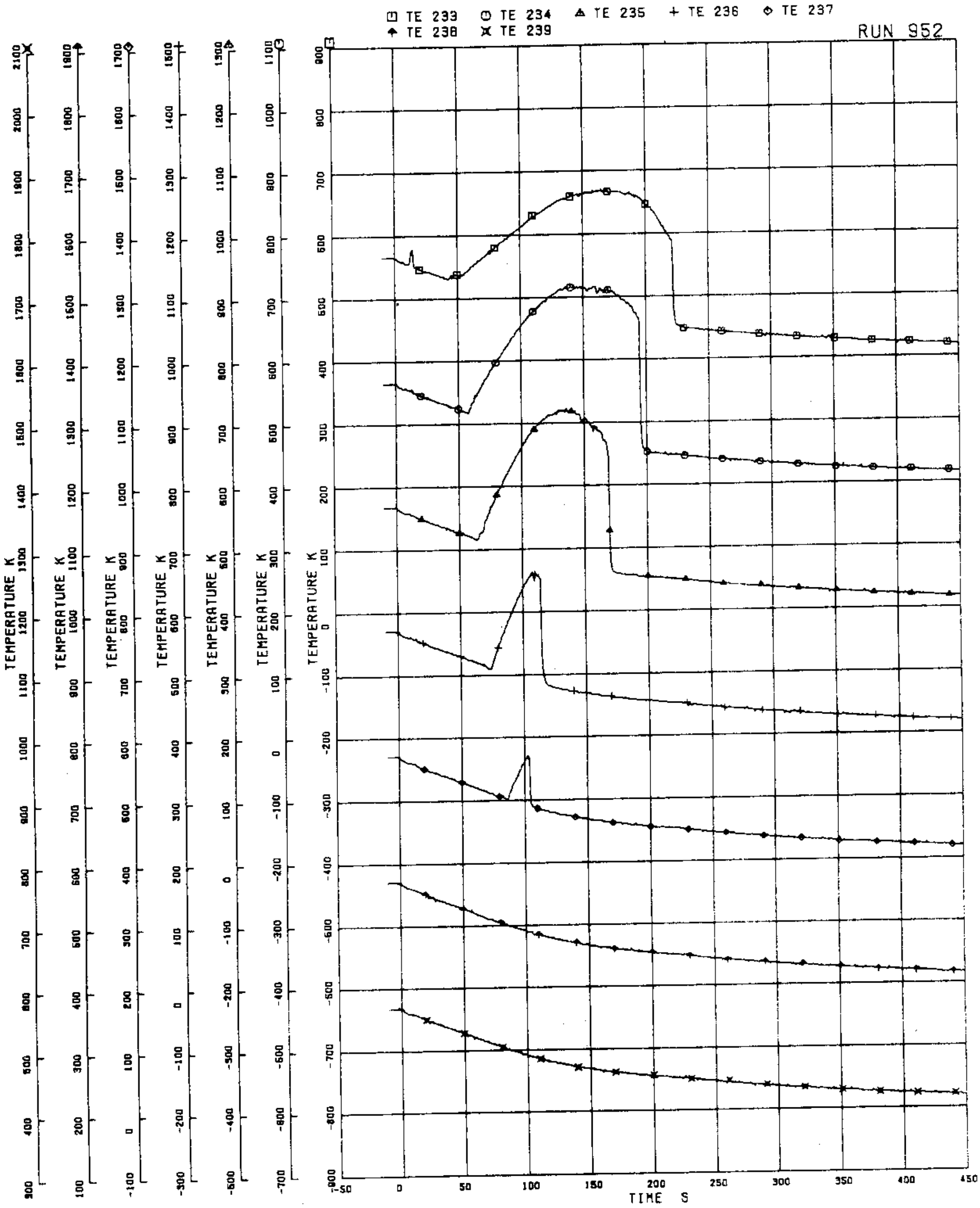

FIG.5. 85 SURFACE TEMPERATURES OF FUEL ROD A22

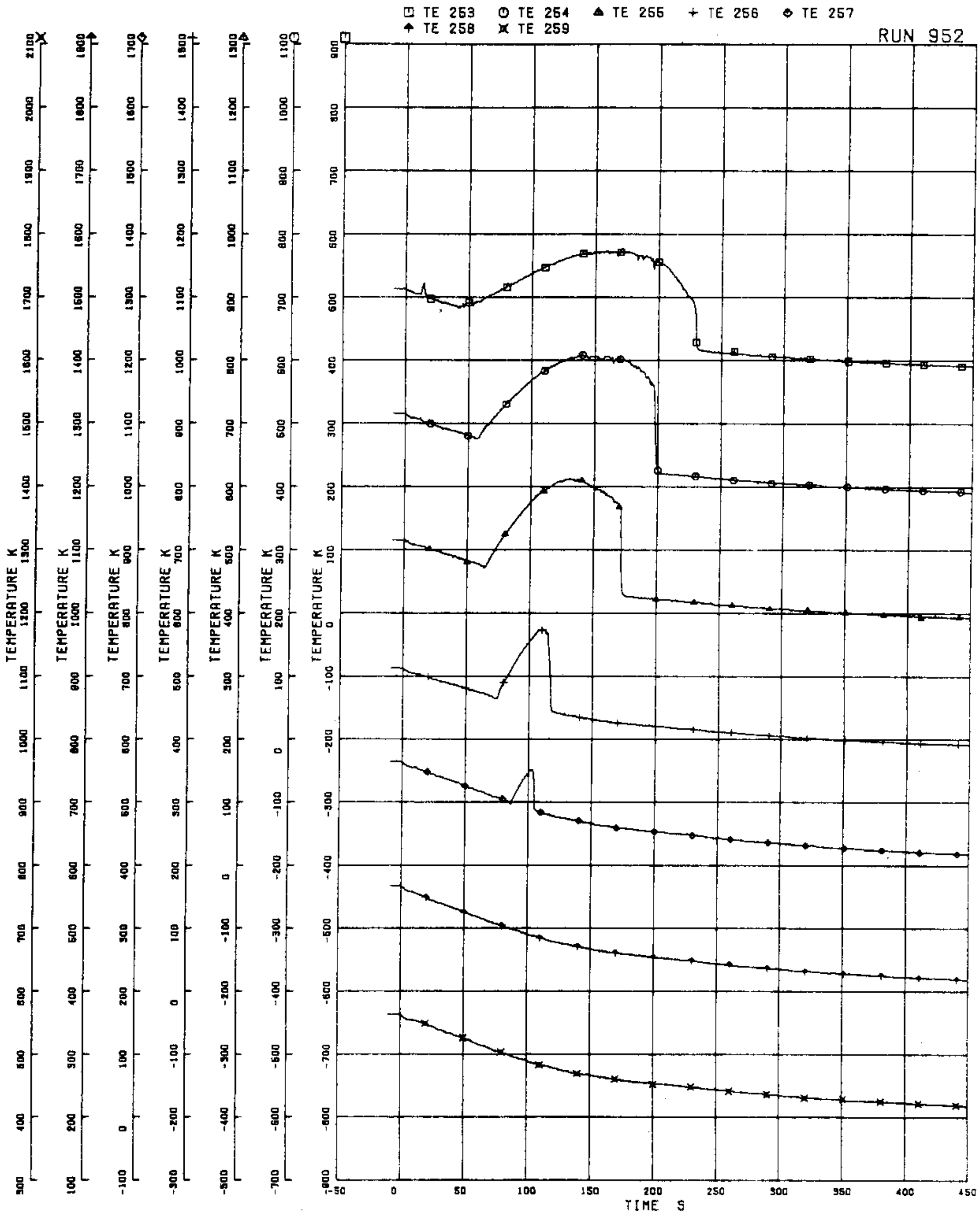

FIG.5. 86 SURFACE TEMPERATURES OF FUEL ROD A33

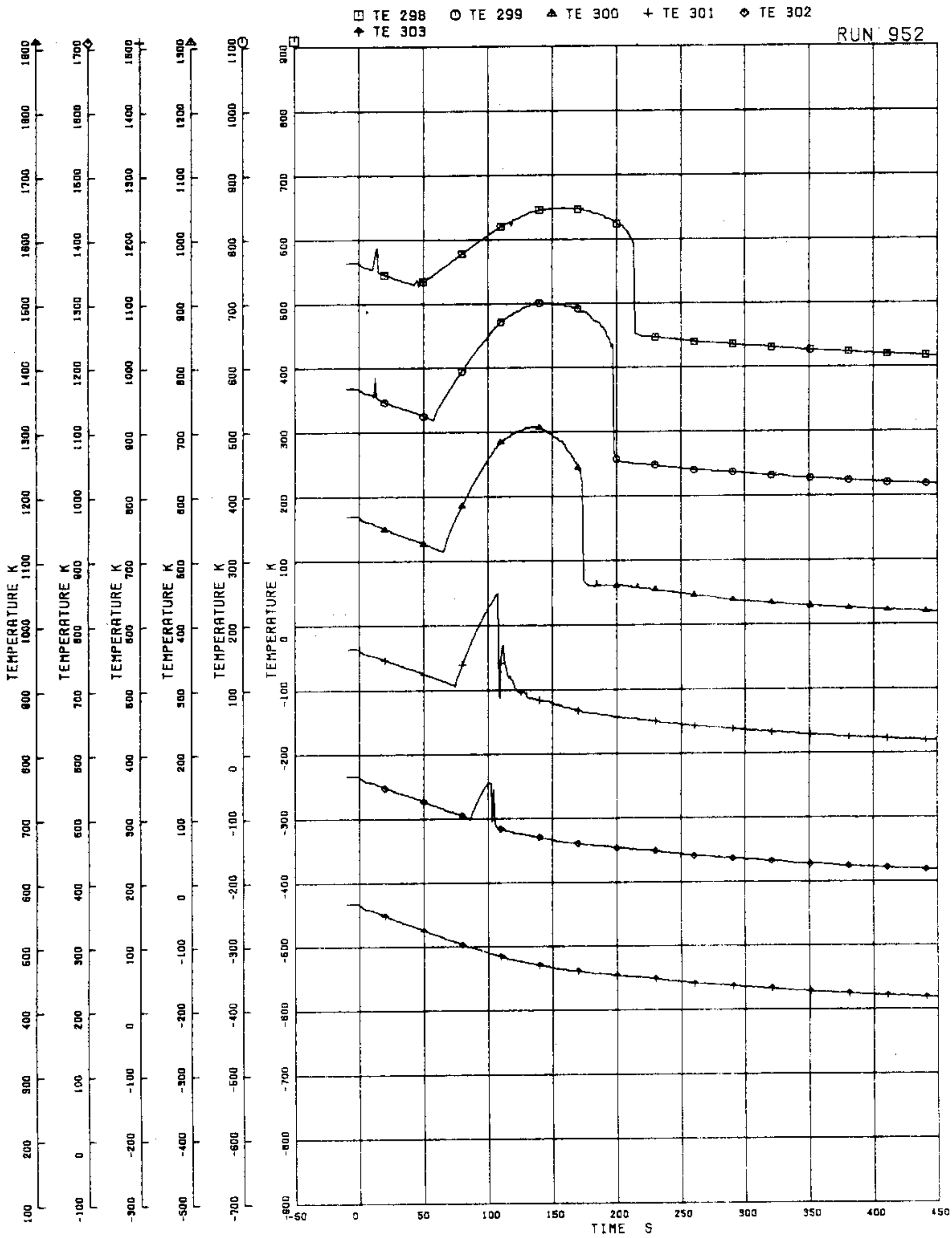

FIG.5. 87 SURFACE TEMPERATURES OF FUEL ROD A77

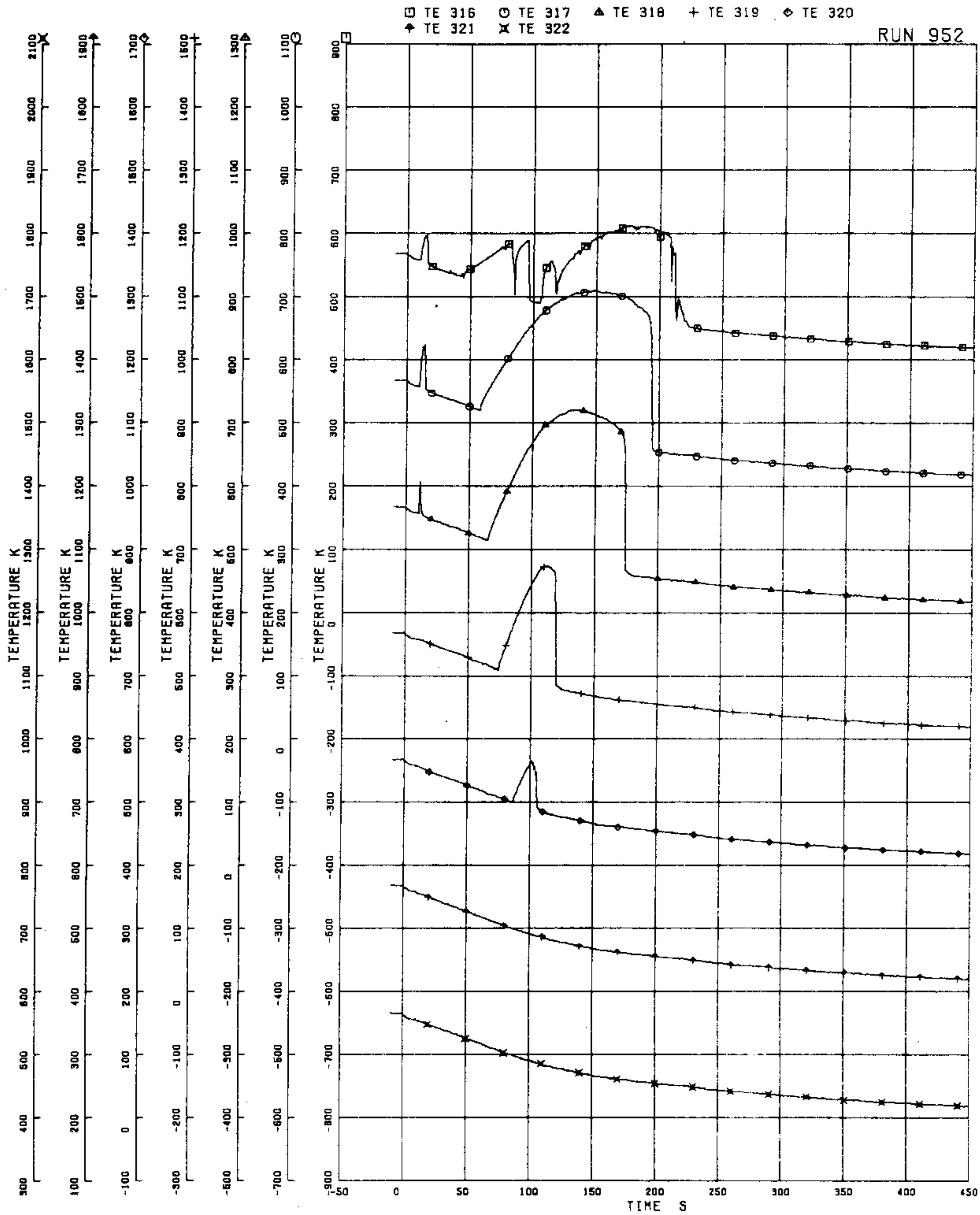

FIG.5. 88 SURFACE TEMPERATURES OF FUEL ROD A87

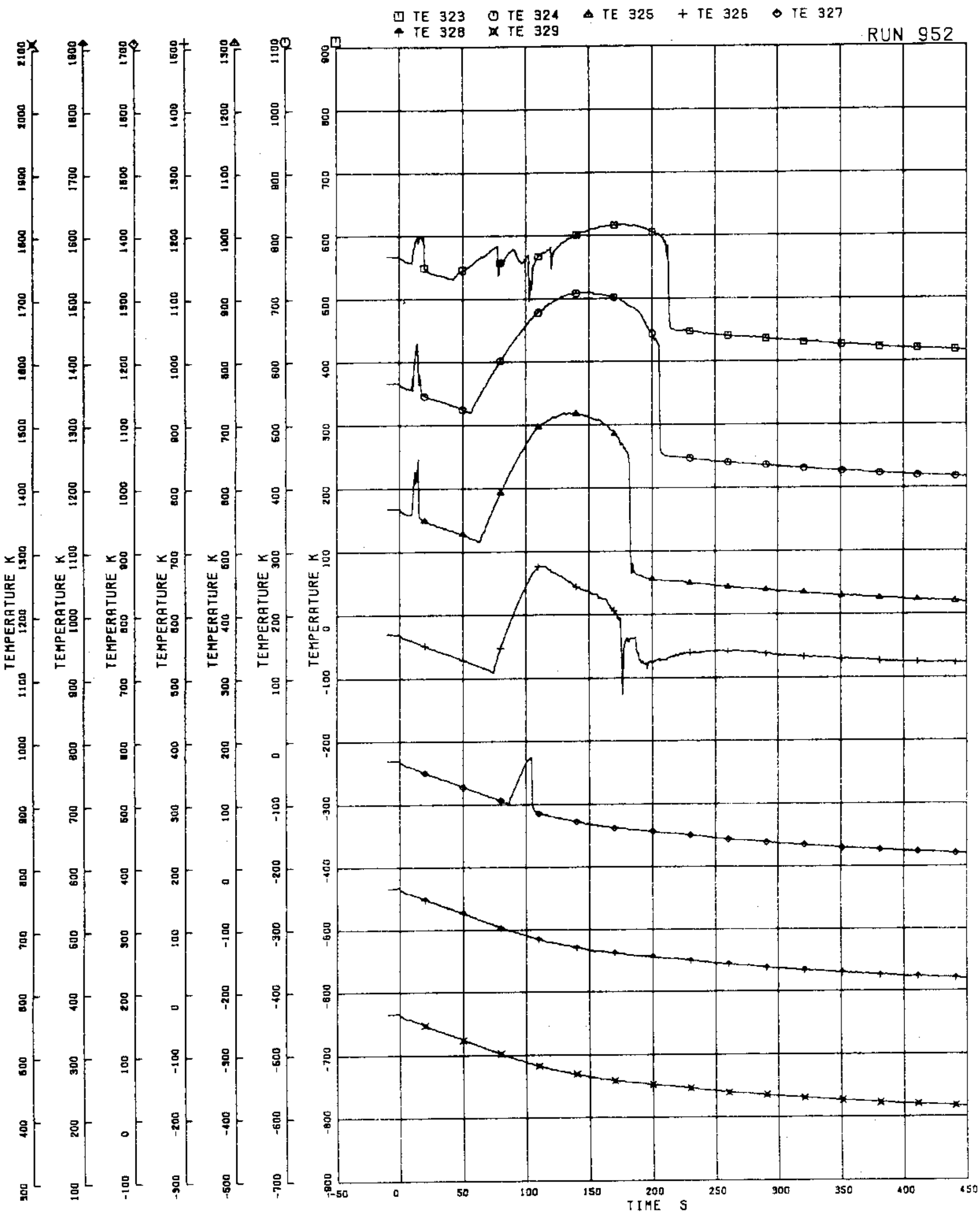

FIG.5. 89 SURFACE TEMPERATURES OF FUEL ROD A88

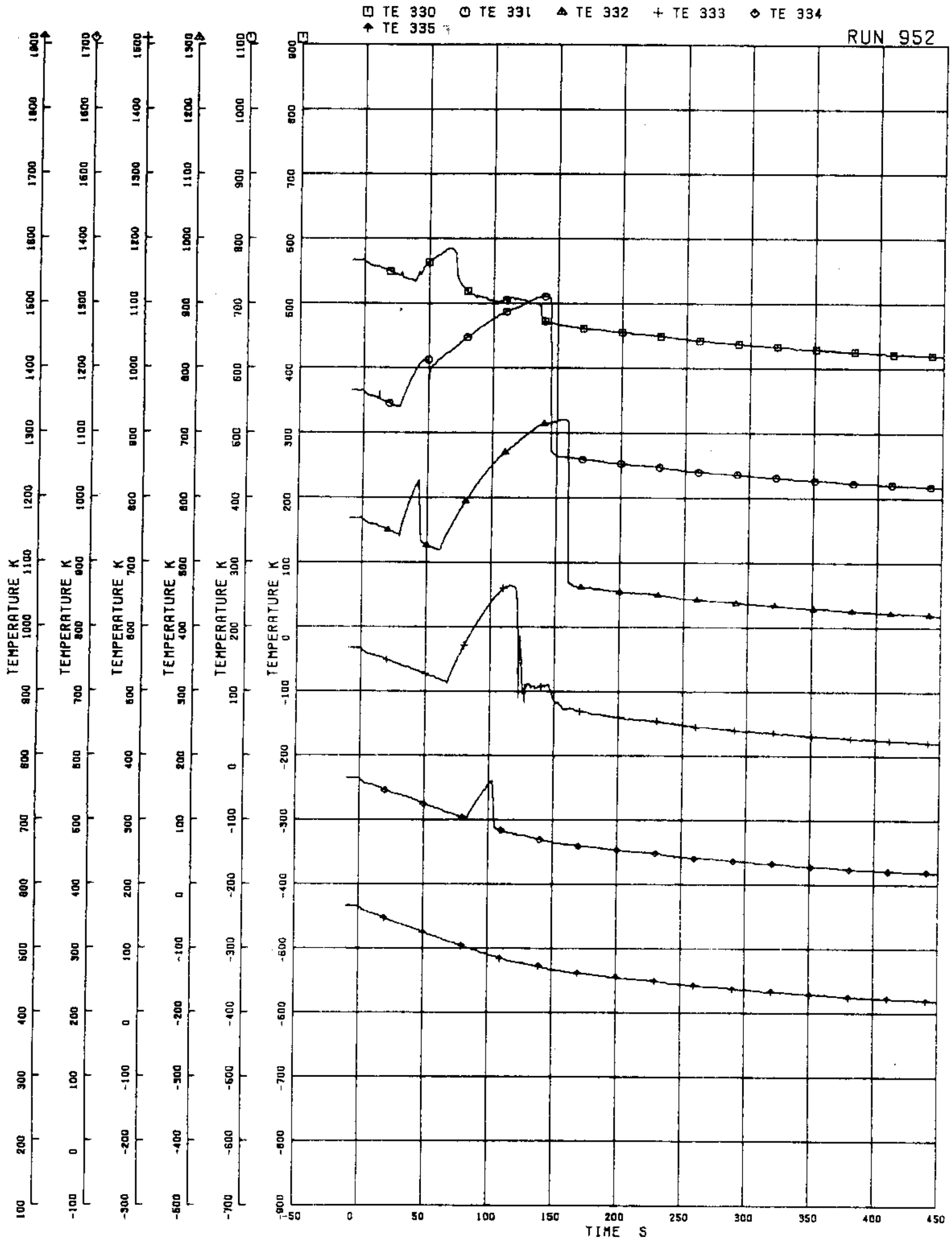

FIG.5. 90 SURFACE TEMPERATURES OF FUEL ROD B11

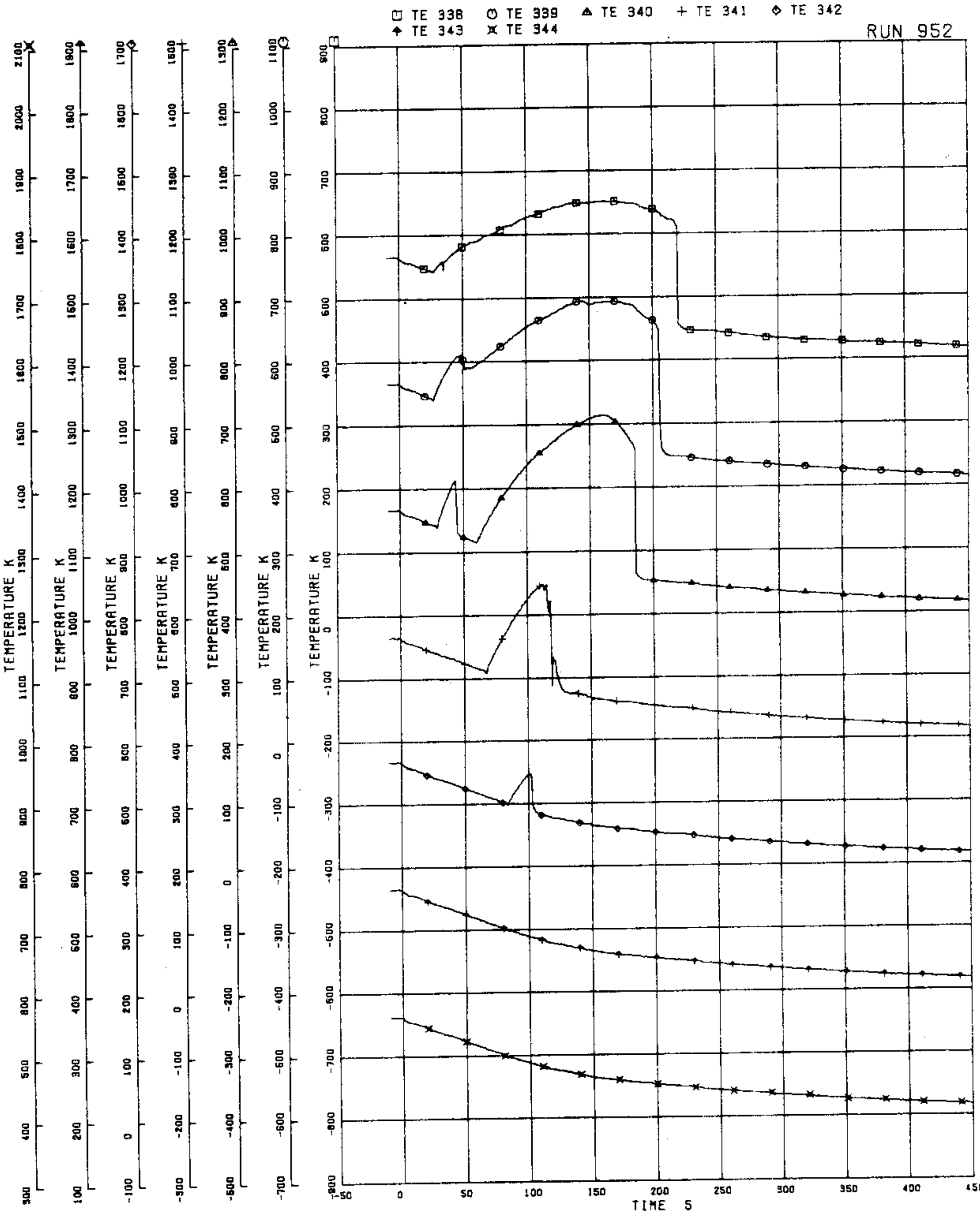

FIG.5. 91 SURFACE TEMPERATURES OF FUEL ROD B22

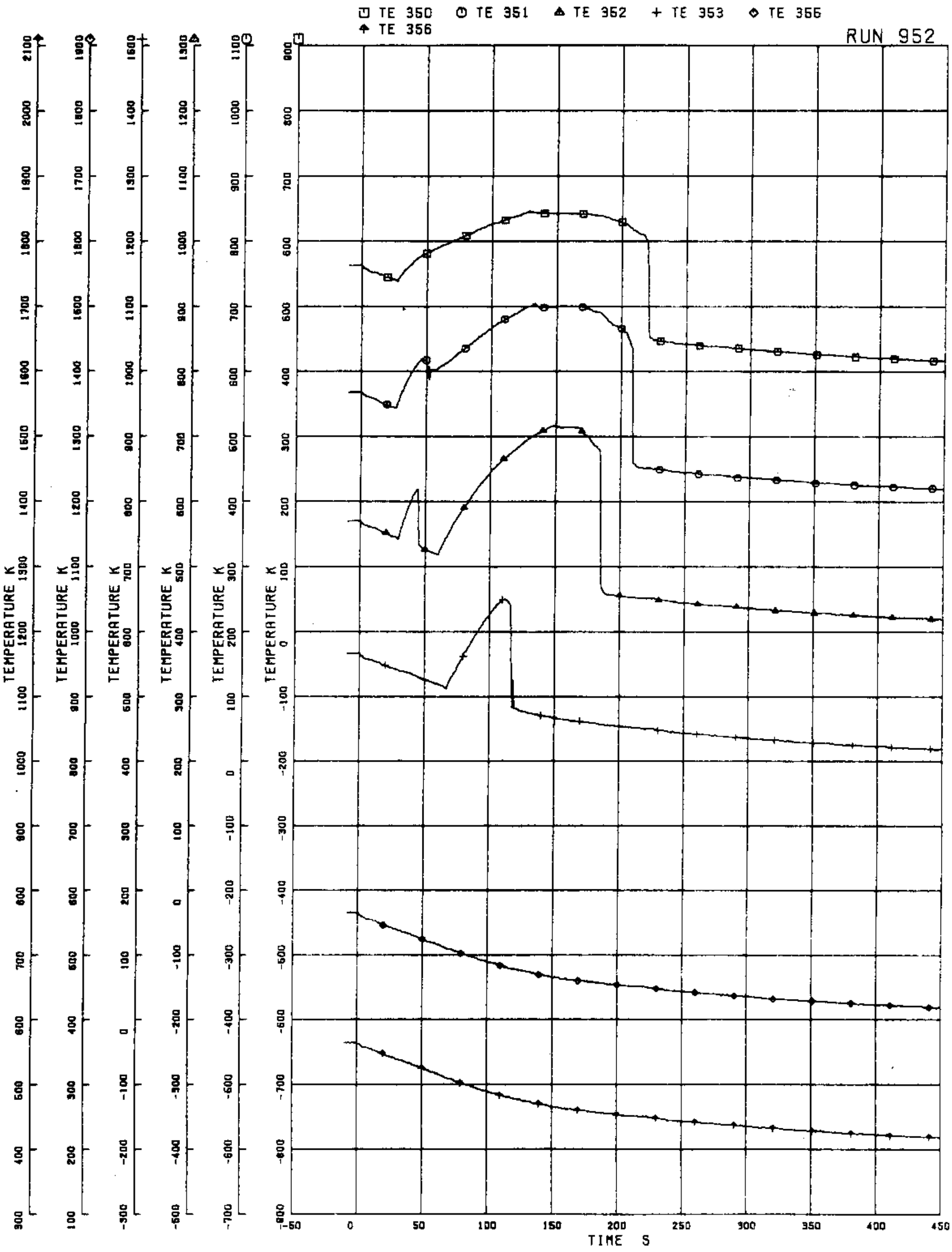

FIG.5. 92 SURFACE TEMPERATURES OF FUEL ROD B77

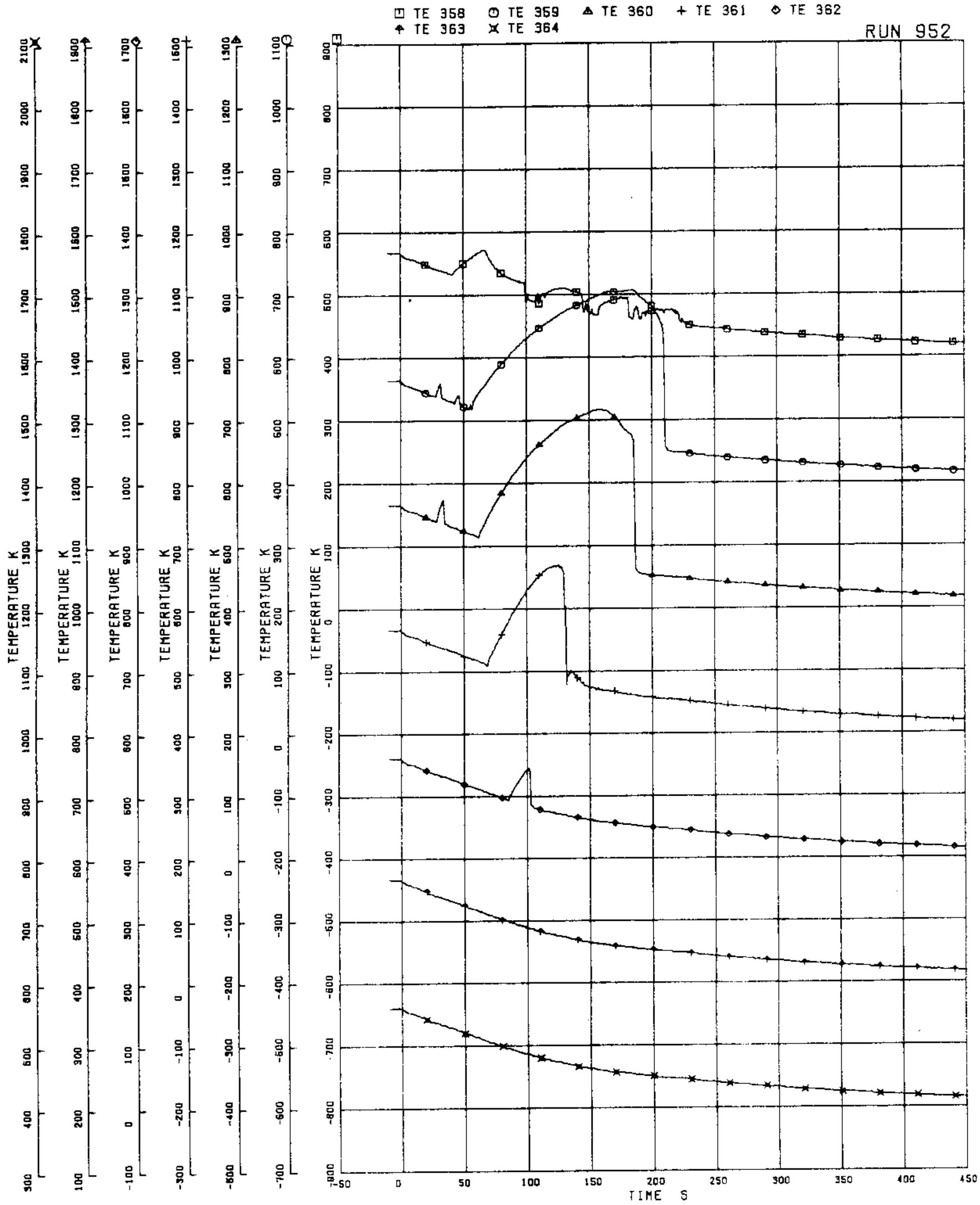

FIG.5. 93 SURFACE TEMPERATURES OF FUEL ROD C11

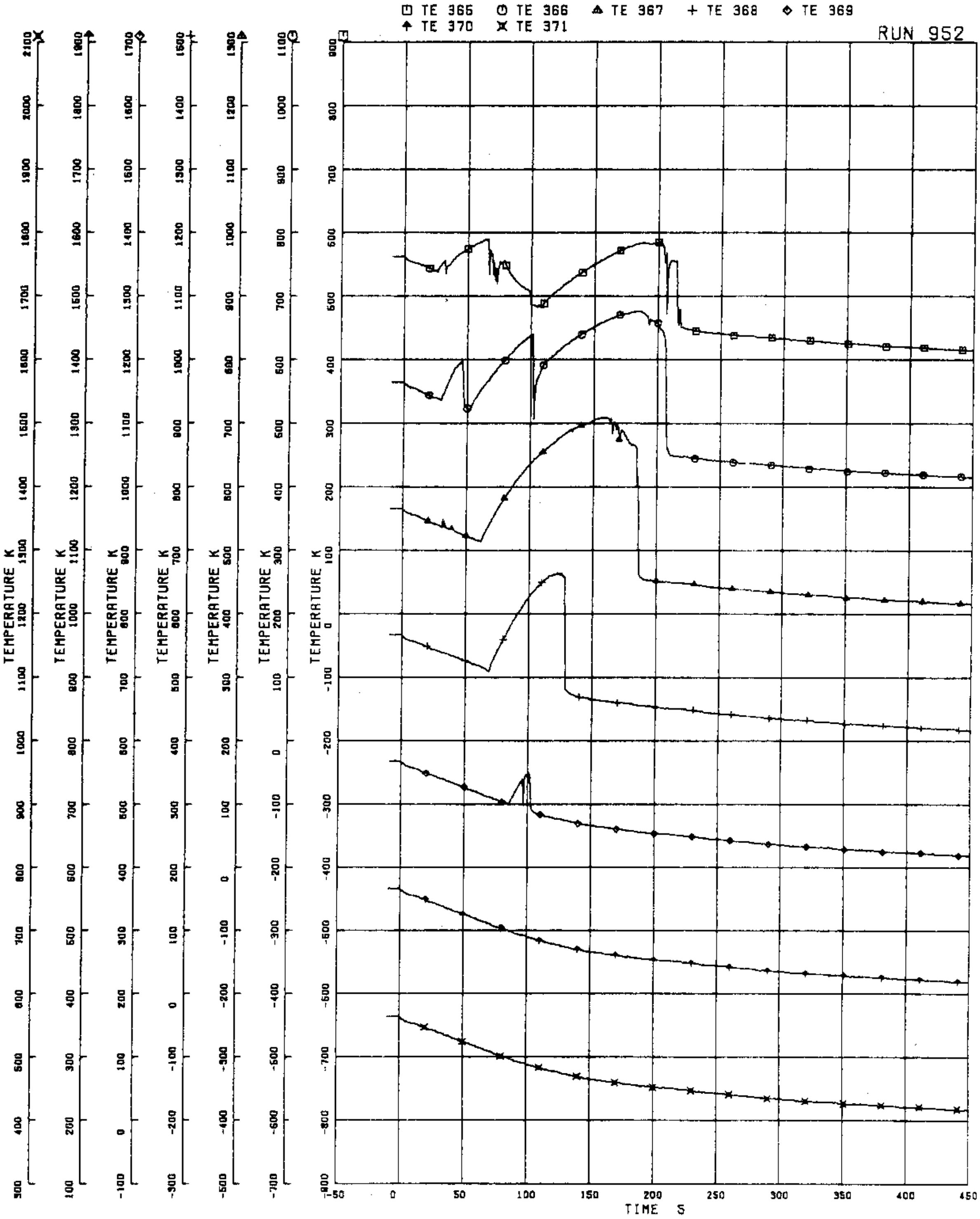

FIG.5. 94 SURFACE TEMPERATURES OF FUEL ROD C13

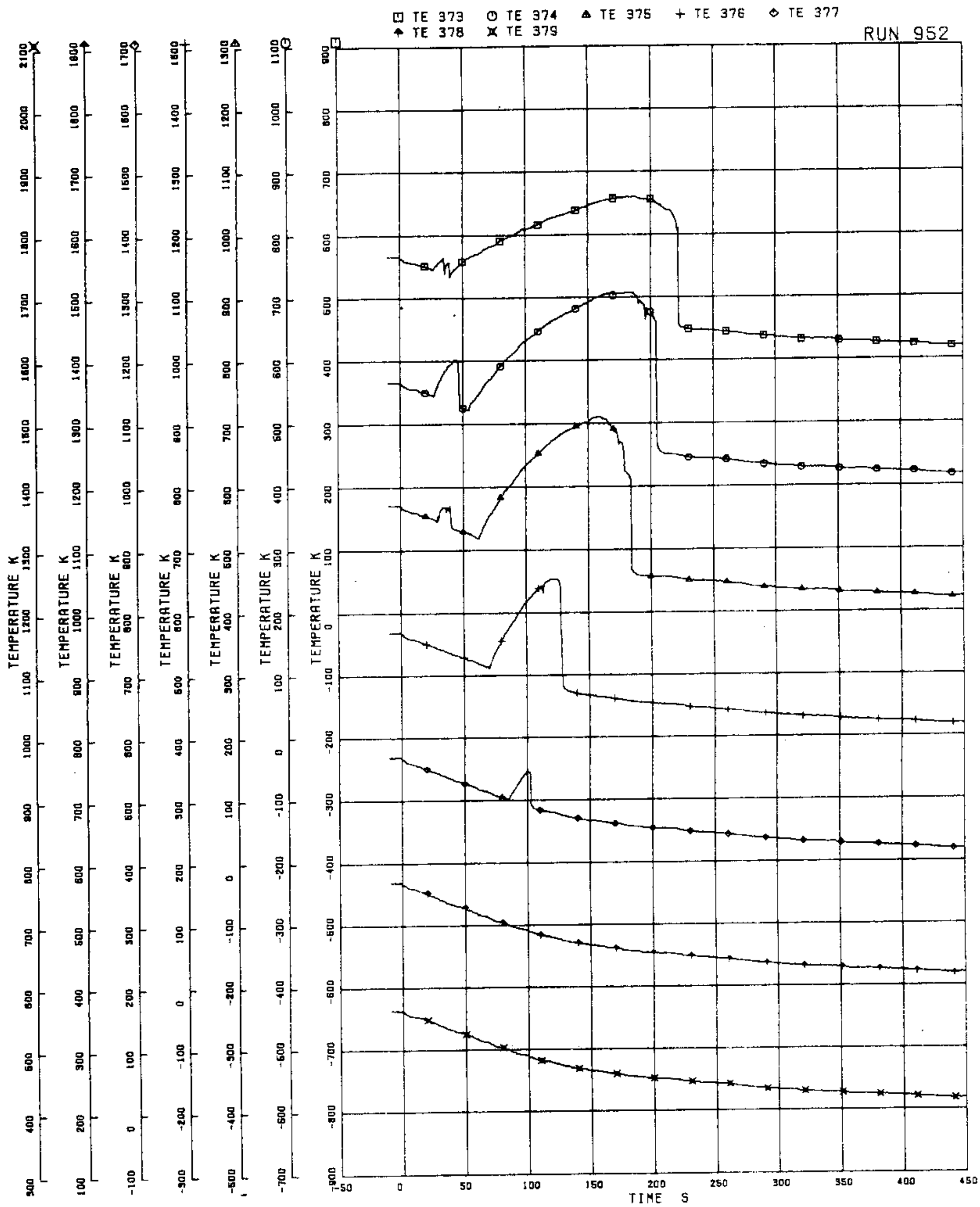

FIG.5. 95 SURFACE TEMPERATURES OF FUEL ROD C22

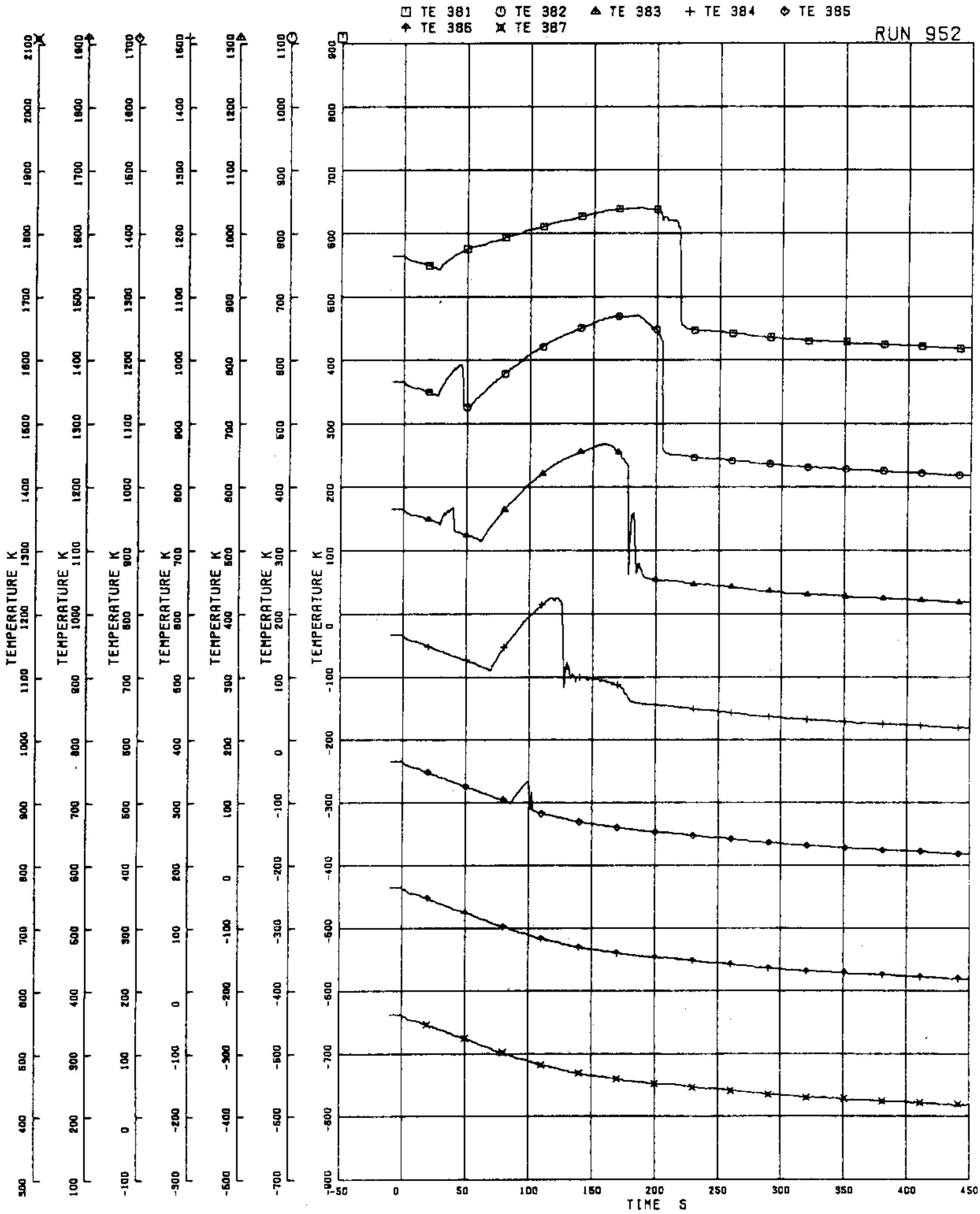

FIG.5. 96 SURFACE TEMPERATURES OF FUEL ROD C33

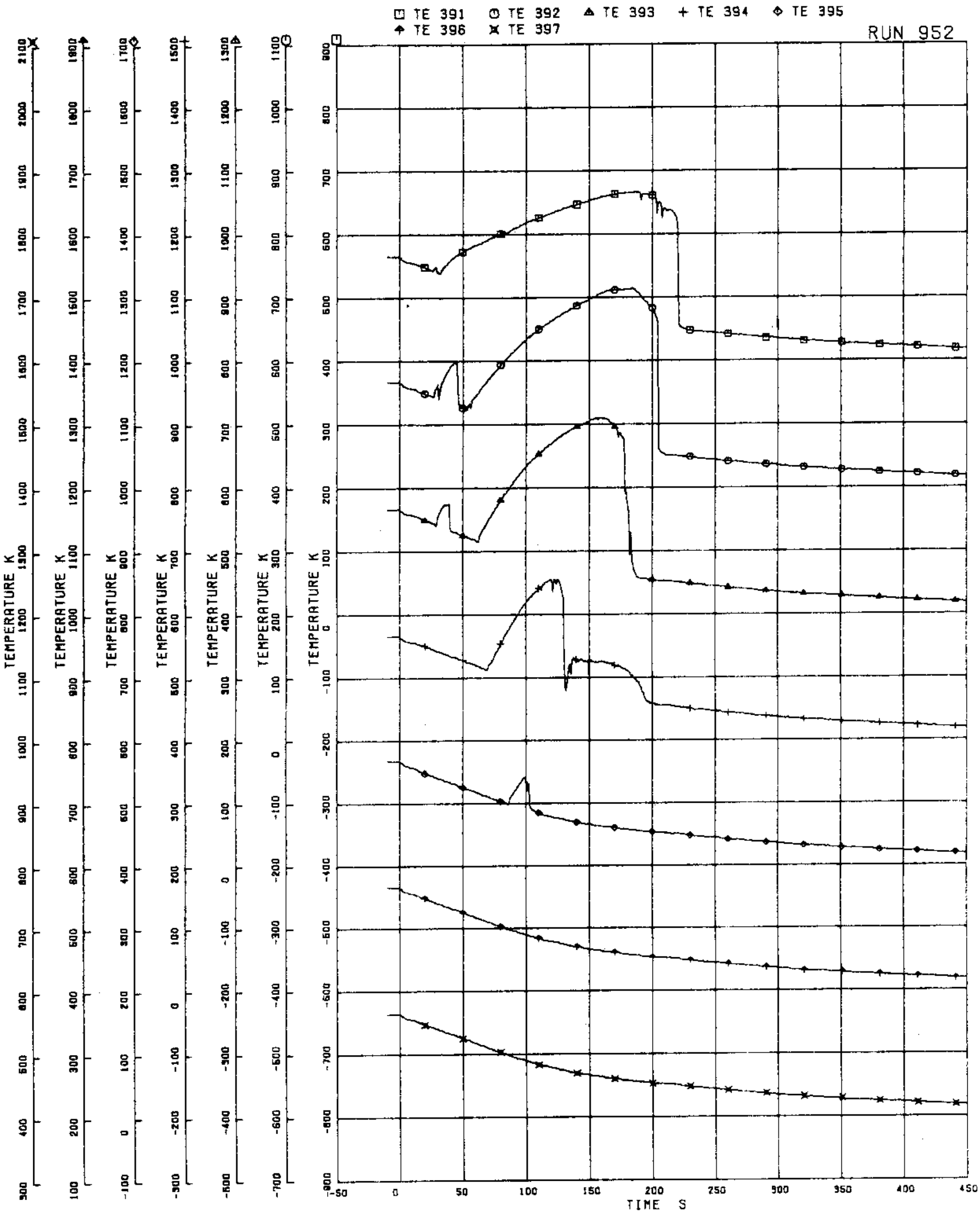

FIG.5. 97 SURFACE TEMPERATURES OF FUEL ROD C77

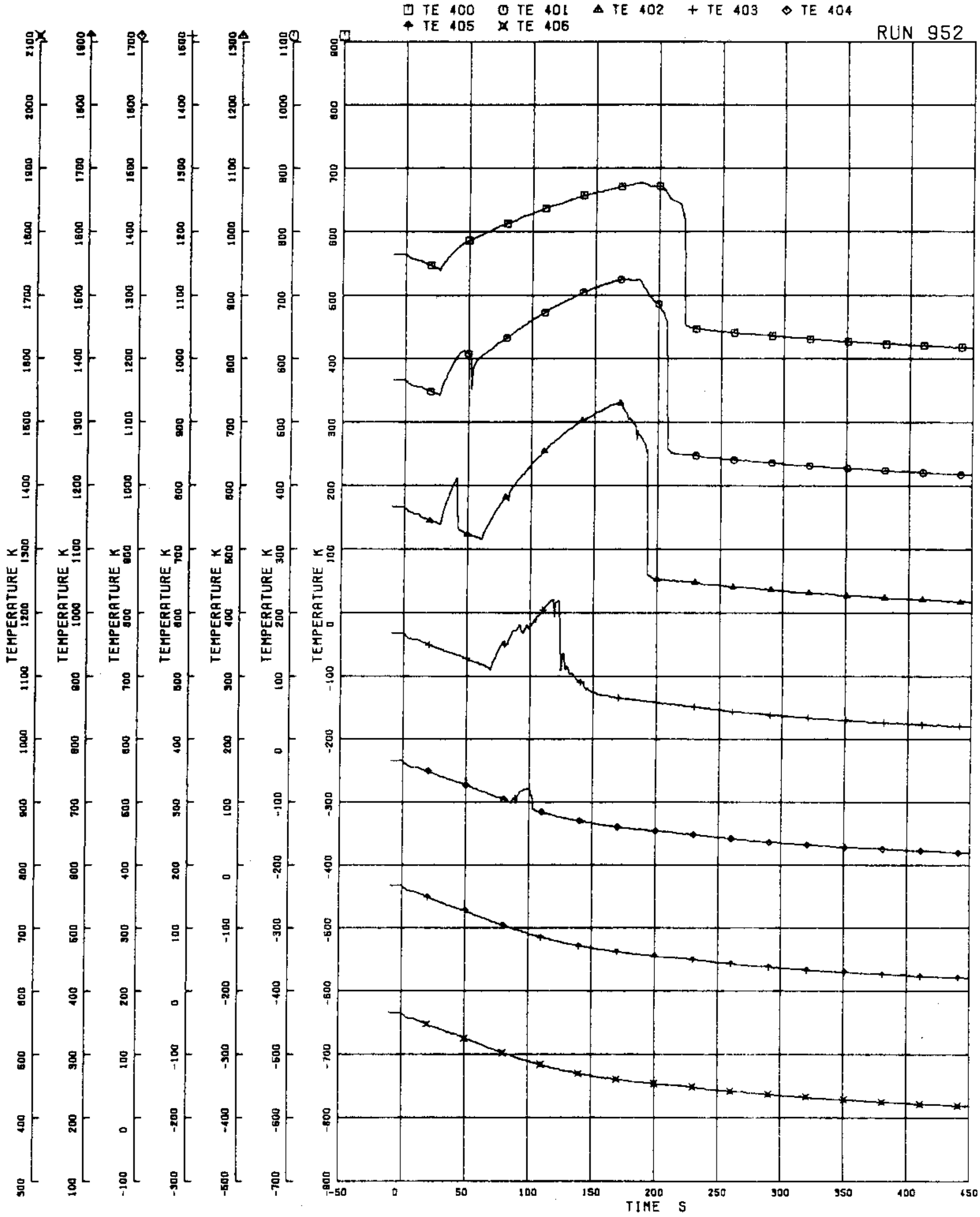

FIG.5. 98 SURFACE TEMPERATURES OF FUEL ROD D22

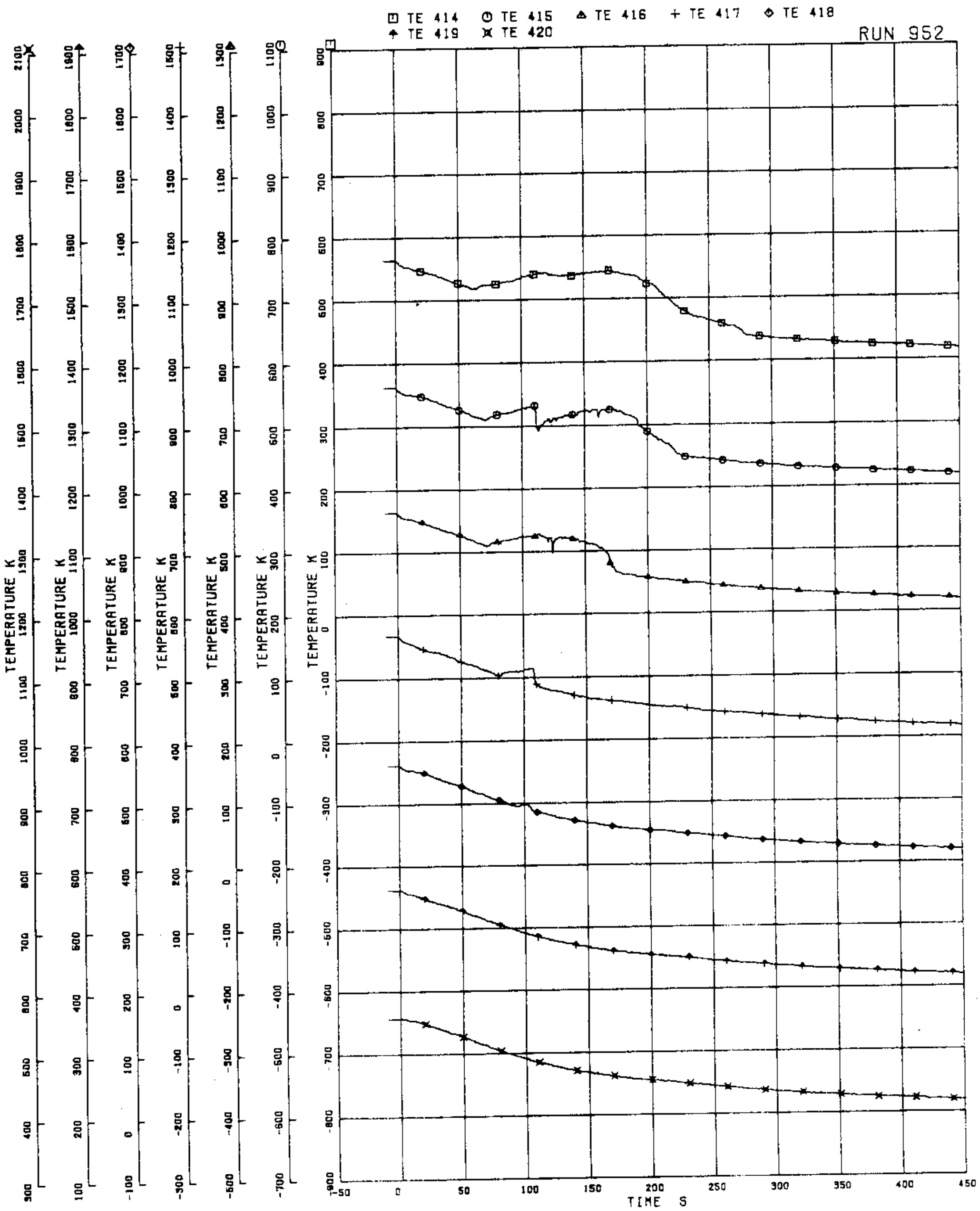

FIG.5. 99 SURFACE TEMPERATURES OF WATER ROD SIMULATOR A45

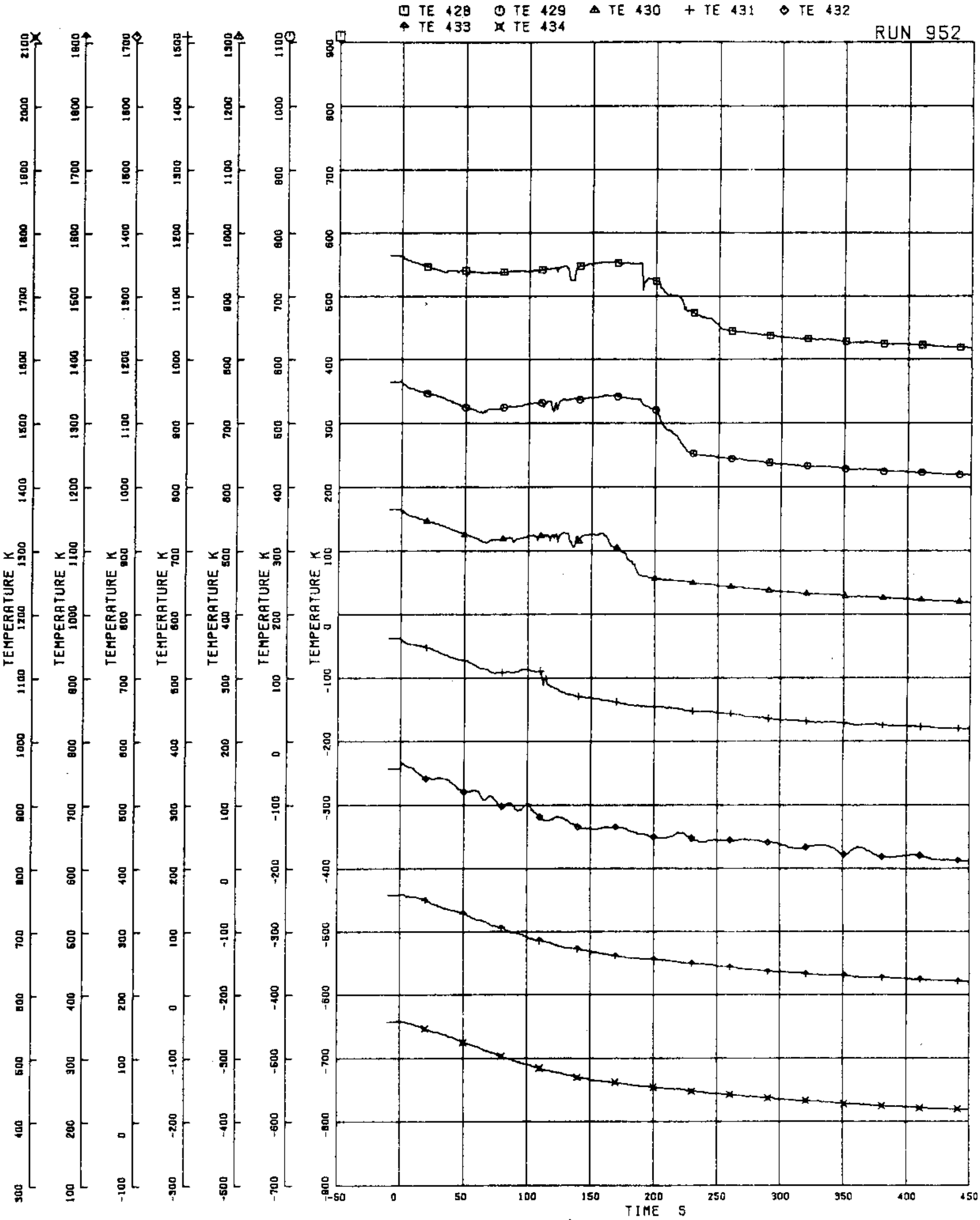

FIG.5.100 SURFACE TEMPERATURES OF WATER ROD SIMULATOR C45

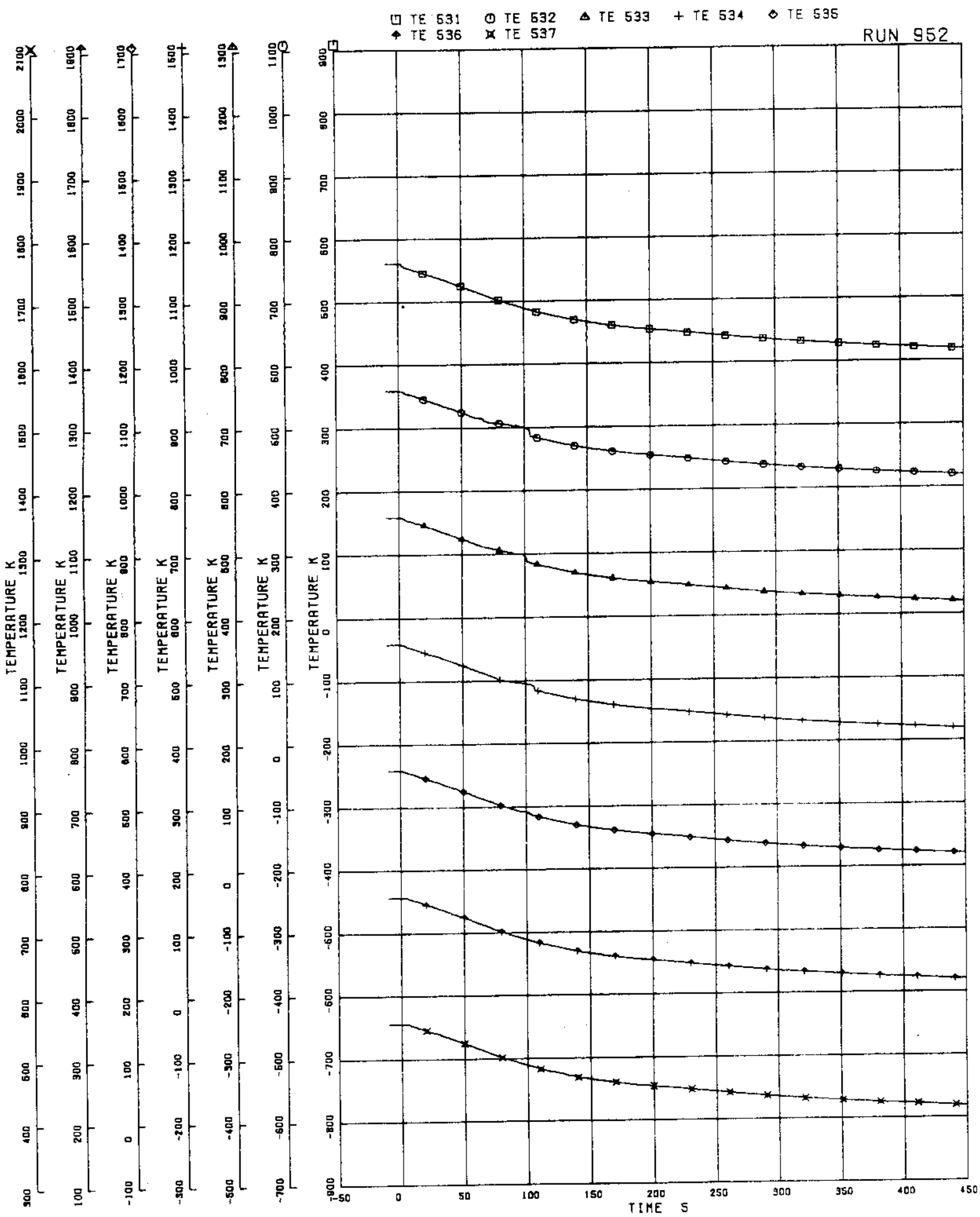

FIG.5.101 OUTER SURFACE TEMPERATURES OF CHANNEL BOX A

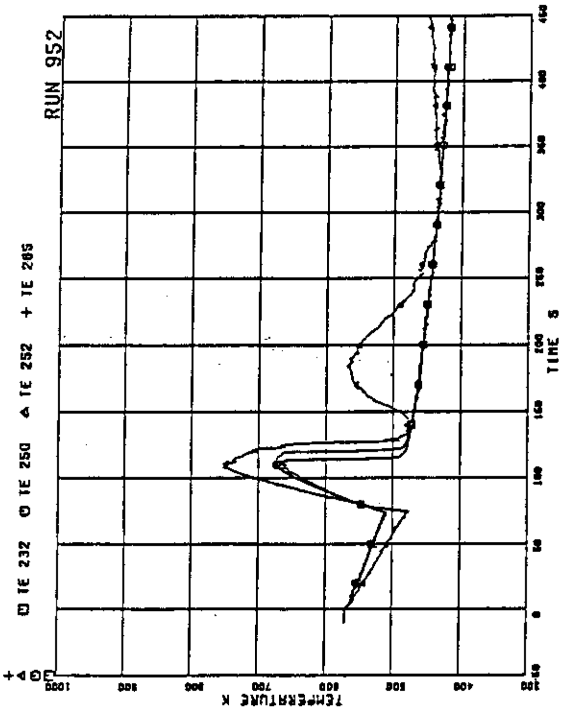

FIG.5.102 SURFACE TEMPERATURE OF FUEL RODS A17,A28,A31,A57 AT POSITION 4

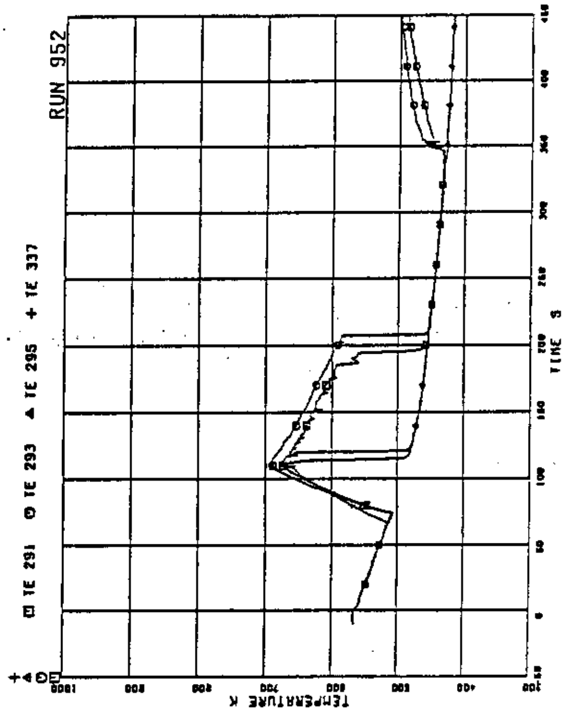

FIG.5.103 SURFACE TEMPERATURE OF FUEL RODS A68,A71,A73,B13 AT POSITION 4

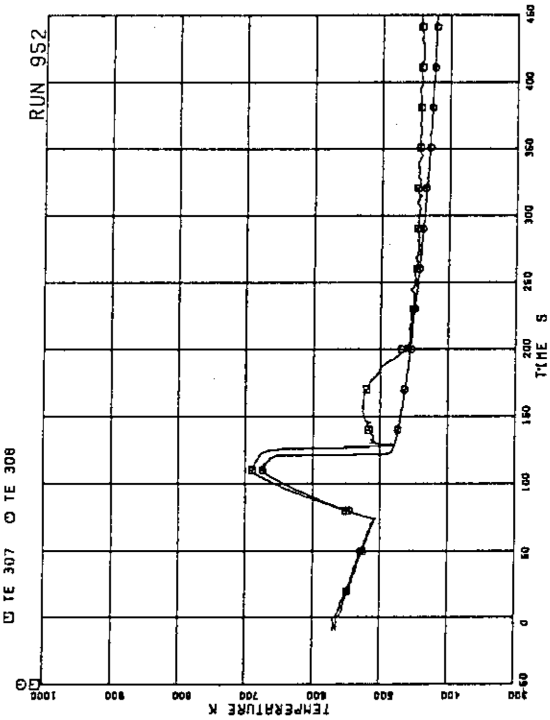

FIG.5.104 SURFACE TEMPERATURES OF FUEL ROD A84 AT POSITIONS 1 AND 4

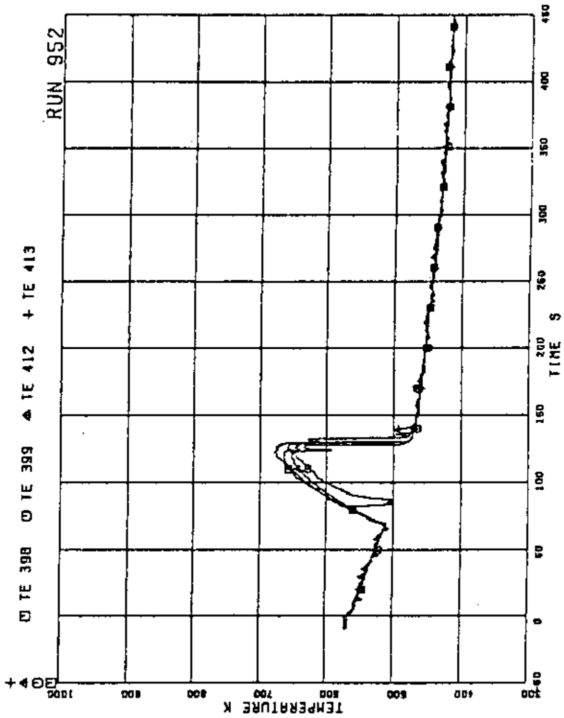

FIG.5.105 SURFACE TEMPERATURES OF FUEL RODS D11,D13,D77,D86 AT POSITION 4

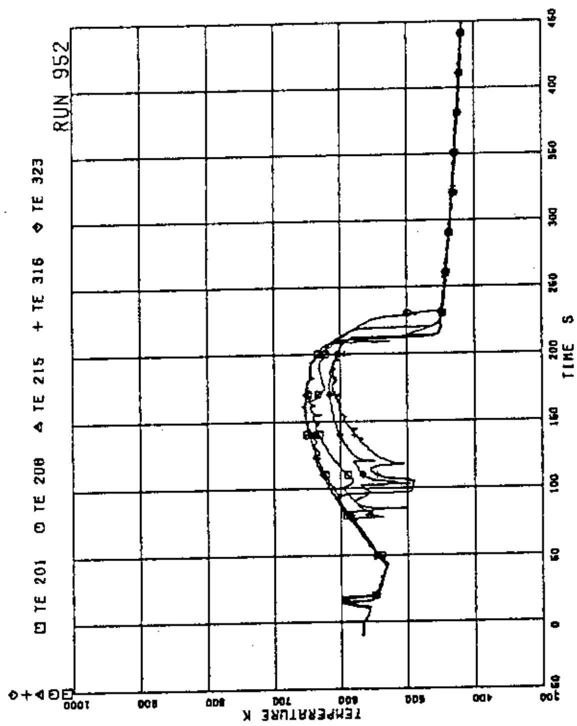

FIG.5.106 SURFACE TEMPERATURES OF FUEL RODS A11,A12,A13,A87,A88 AT POSITION 1

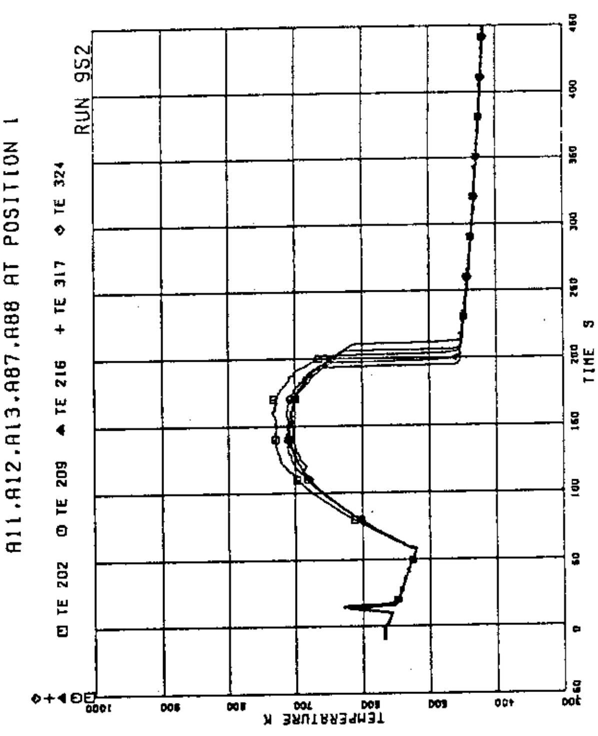

FIG.5.107 SURFACE TEMPERATURES OF FUEL RODS A11,A12,A13,A87,A88 AT POSITION 2

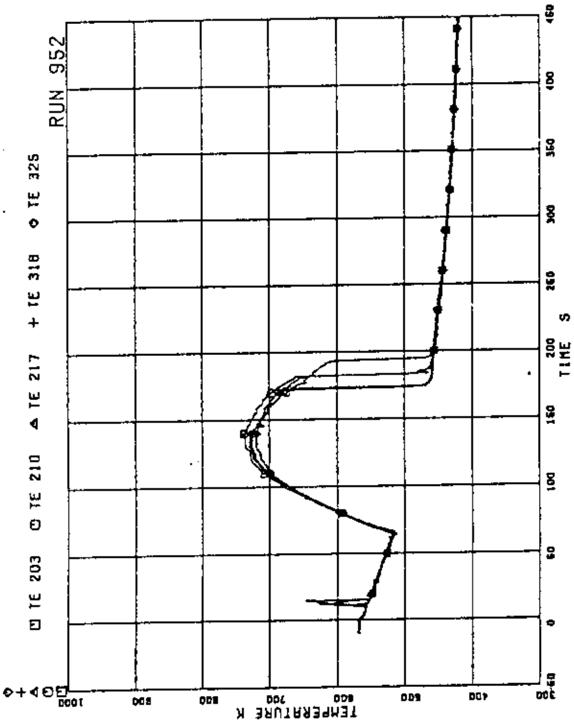

FIG.5.108 SURFACE TEMPERATURES OF FUEL RODS A11,A12,A13,A87,A88 AT POSITION 3

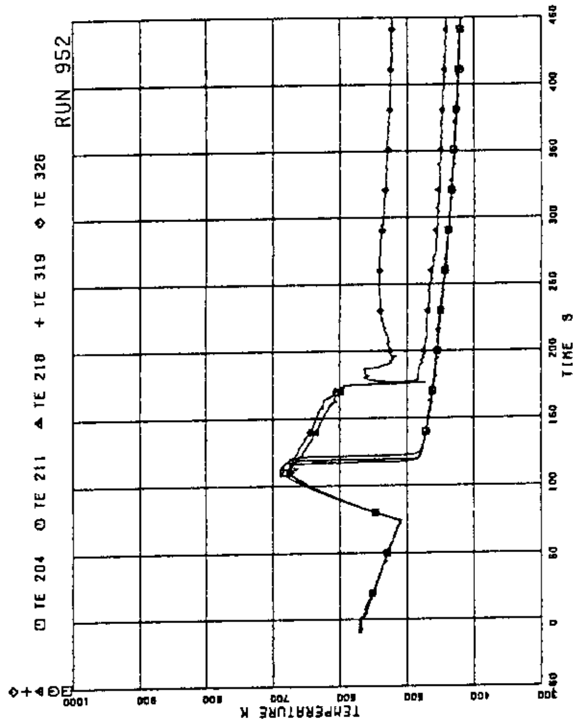

FIG.5.109 SURFACE TEMPERATURES OF FUEL RODS A11,A12,A13,A87,A88 AT POSITION 4

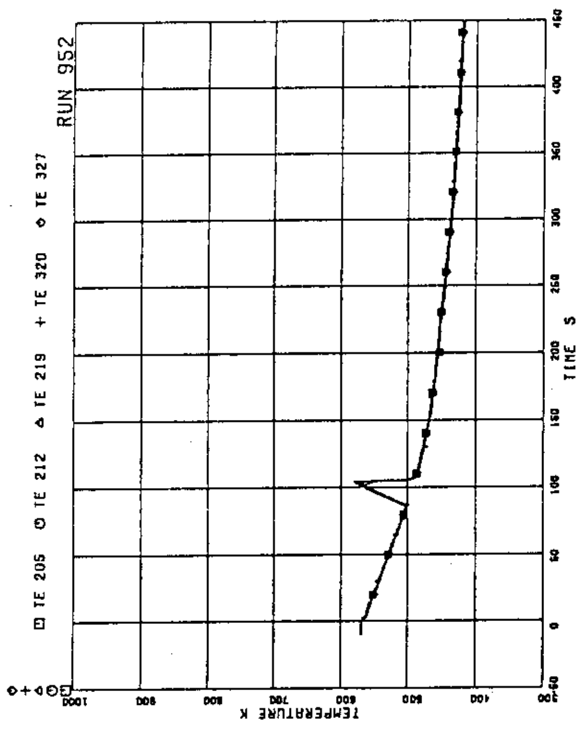

FIG.5.110 SURFACE TEMPERATURES OF FUEL RODS A11.A12.A13.A87.A88 AT POSITION 5

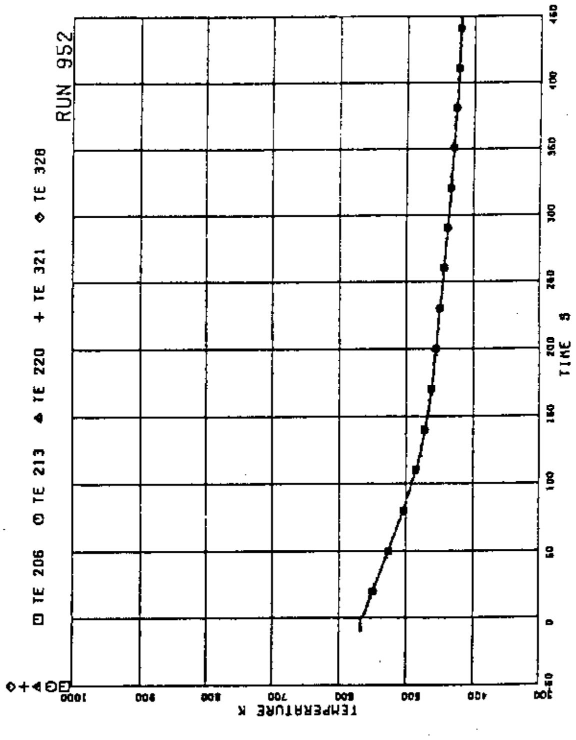

FIG.5.111 SURFACE TEMPERATURES OF FUEL RODS A11.A12.A13.A87.A88 AT POSITION 6

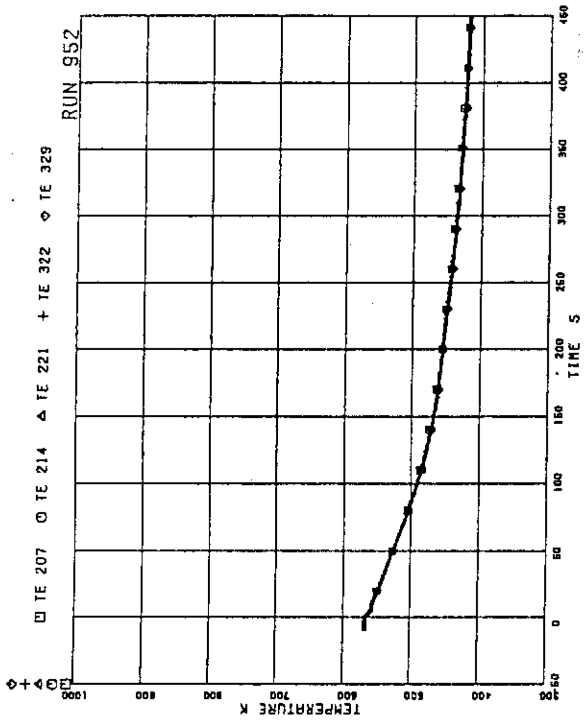

FIG.5.112 SURFACE TEMPERATURES OF FUEL RODS A11.A12.A13.A87.A88 AT POSITION 7

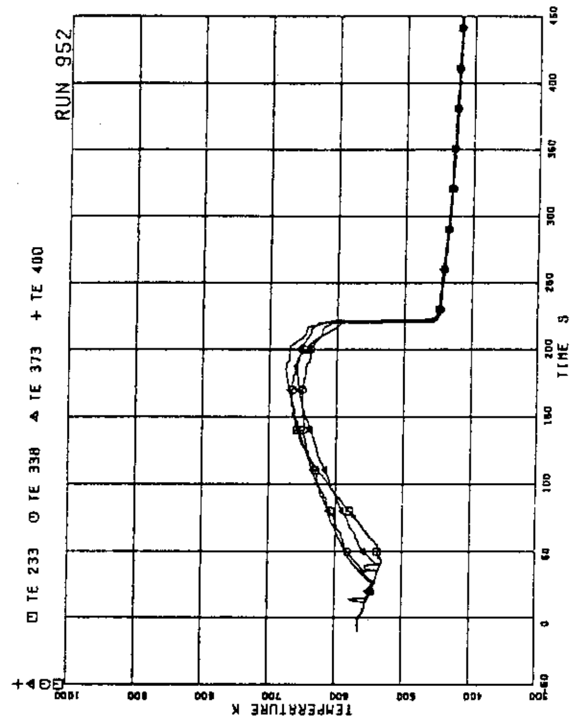

FIG.5.113 SURFACE TEMPERATURES OF FUEL RODS A22.B22.C22.D22 AT POSITION 1

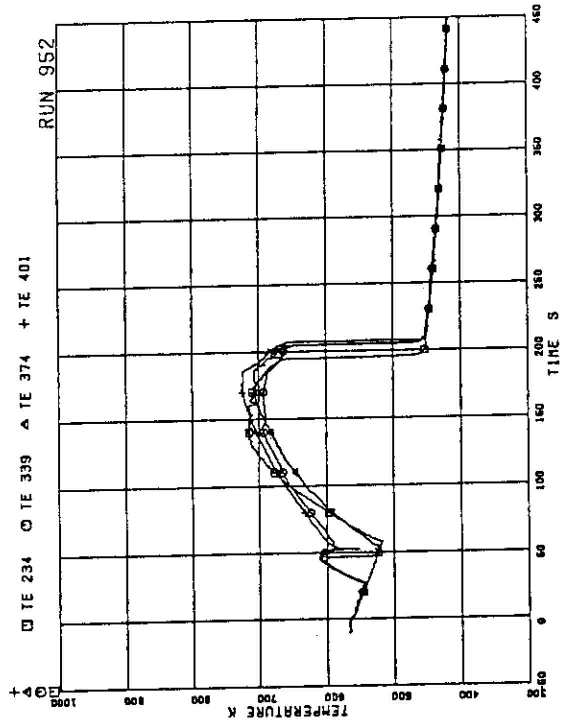

FIG.5.114 SURFACE TEMPERATURES OF FUEL RODS
A22.B22.C22.D22 AT POSITION 2

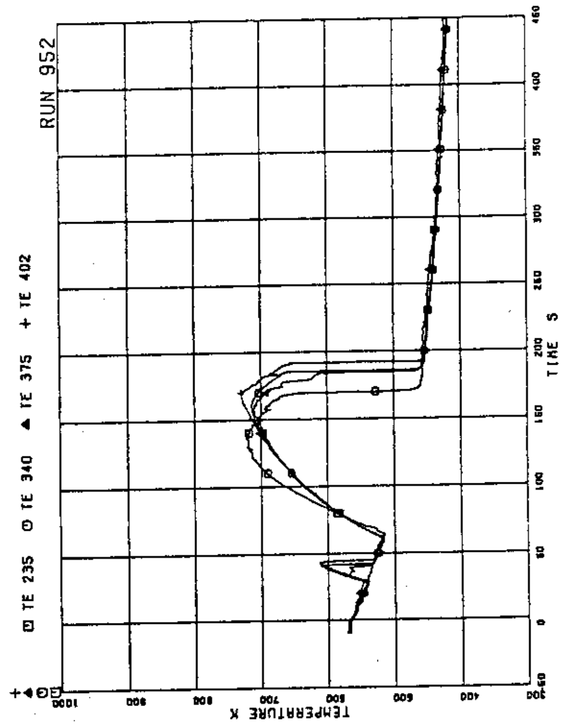

FIG.5.115 SURFACE TEMPERATURES OF FUEL RODS
A22.B22.C22.D22 AT POSITION 3

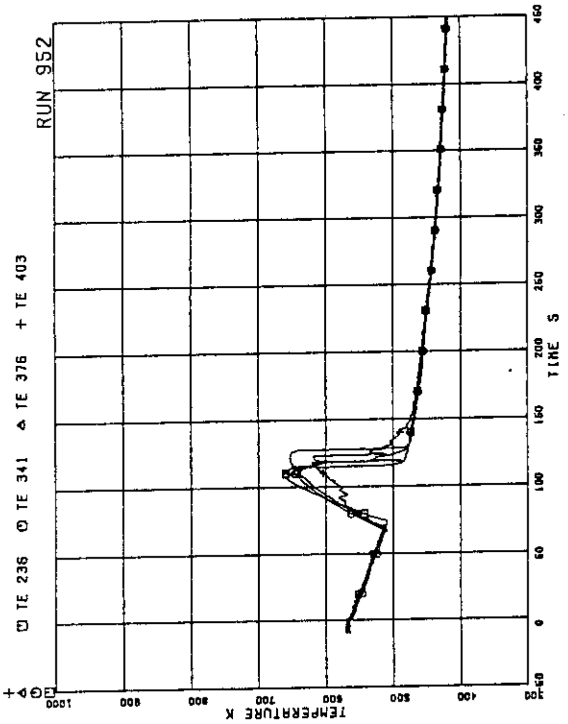

FIG.5.116 SURFACE TEMPERATURES OF FUEL RODS
A22.B22.C22.D22 AT POSITION 4

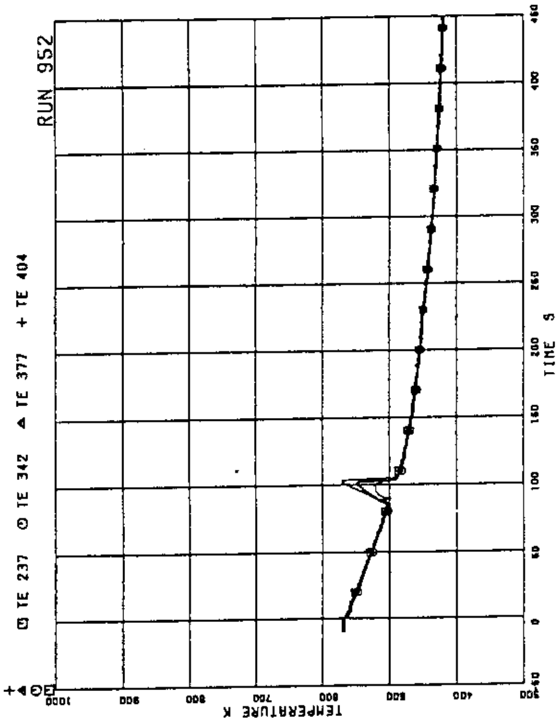

FIG.5.117 SURFACE TEMPERATURES OF FUEL RODS
A22.B22.C22.D22 AT POSITION 5

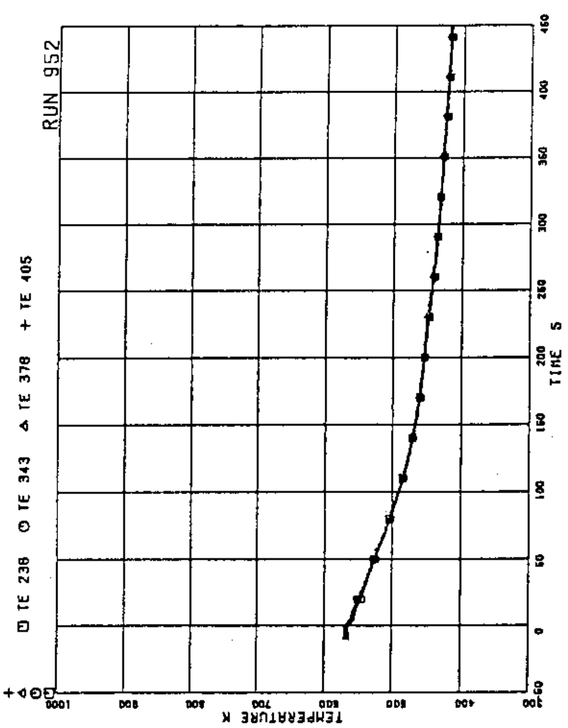

FIG.5.118 SURFACE TEMPERATURES OF FUEL RODS A22,B22,C22,D22 AT POSITION 6

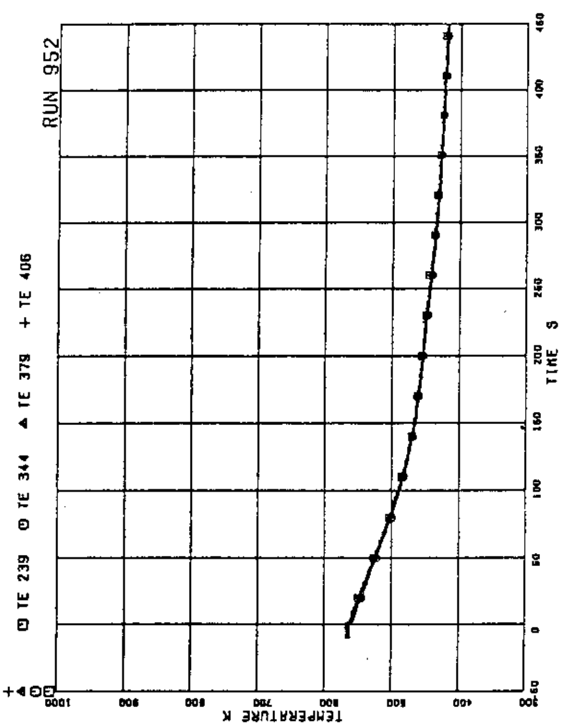

FIG.5.119 SURFACE TEMPERATURES OF FUEL RODS A22,B22,C22,D22 AT POSITION 7

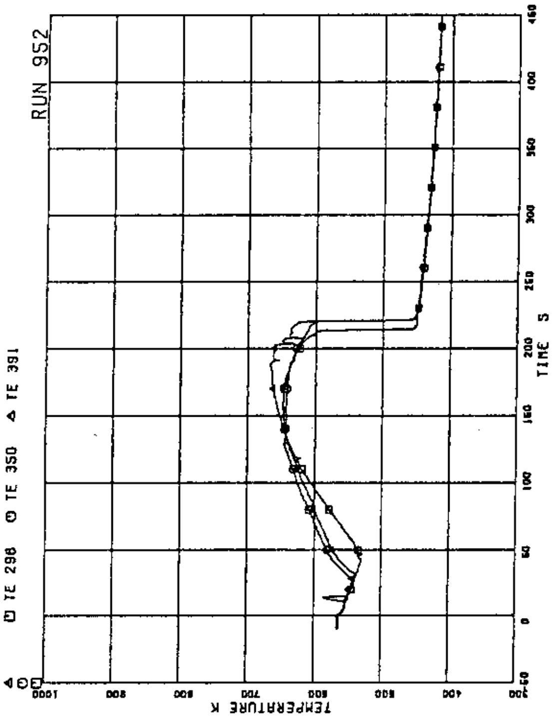

FIG.5.120 SURFACE TEMPERATURES OF FUEL RODS A77,B77,C77 AT POSITION 1

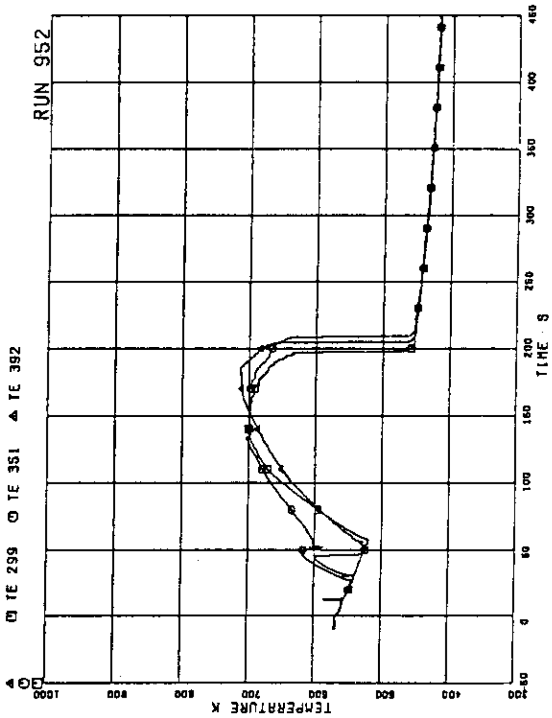

FIG.5.121 SURFACE TEMPERATURES OF FUEL RODS A77,B77,C77 AT POSITION 2

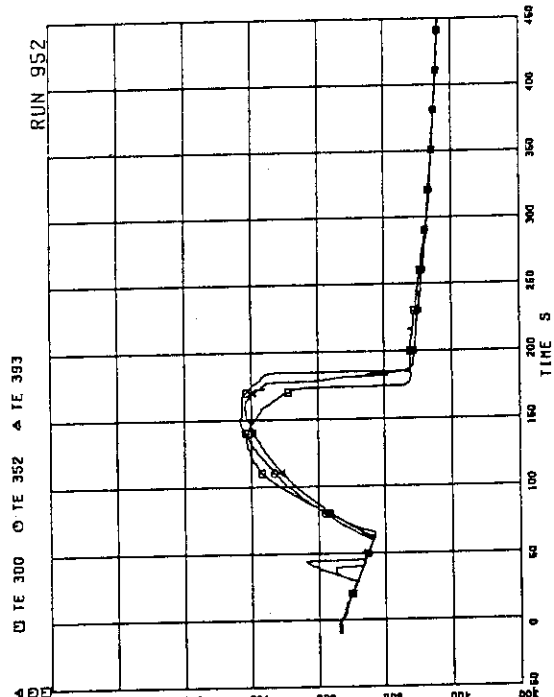

FIG.5.122 SURFACE TEMPERATURES OF FUEL RODS A77.B77.C77 AT POSITION 3

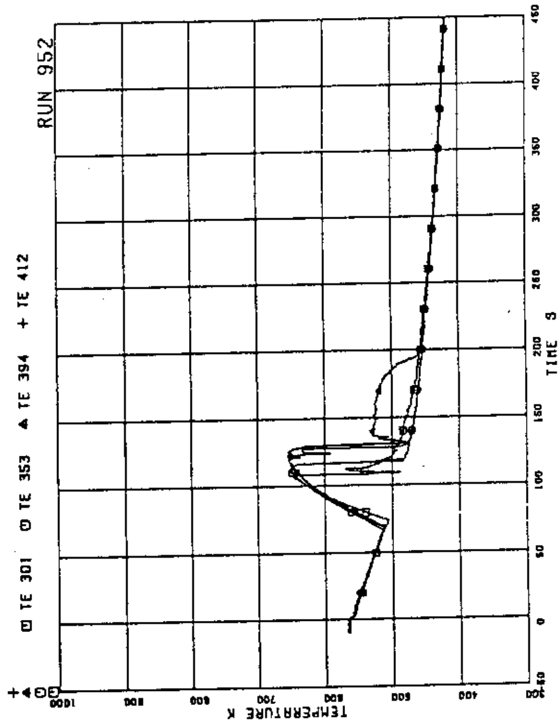

FIG.5.123 SURFACE TEMPERATURES OF FUEL RODS A77.B77.C77 AT POSITION 4

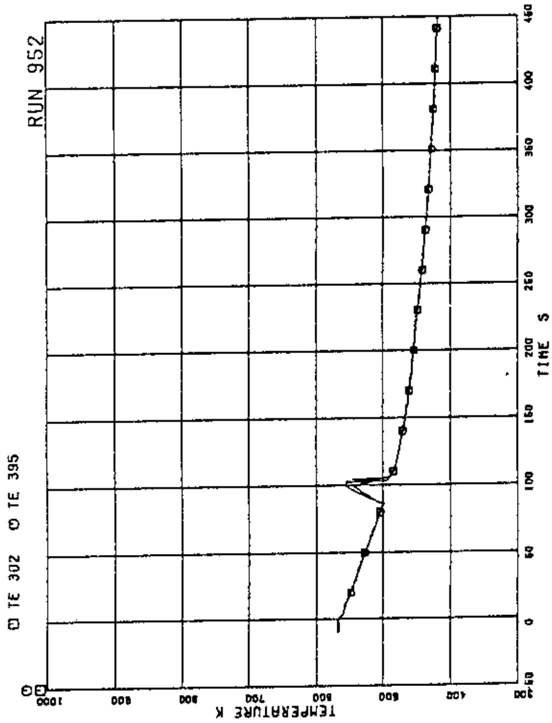

FIG.5.124 SURFACE TEMPERATURES OF FUEL RODS A77,C77 AT POSITION 5

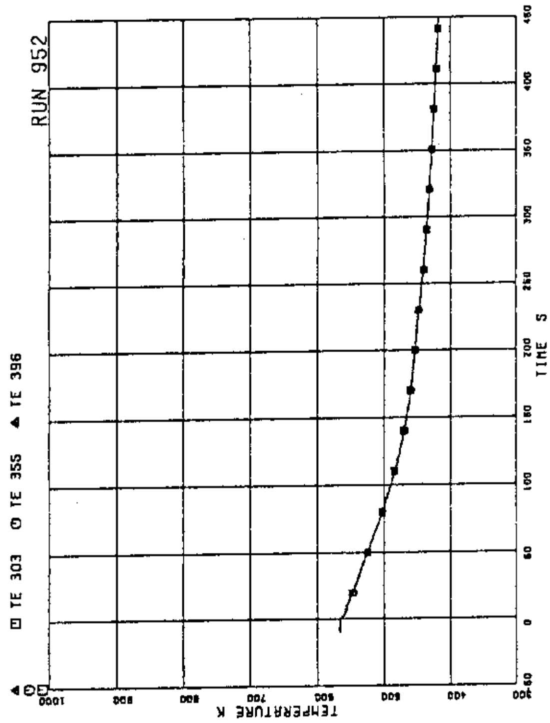

FIG.5.125 SURFACE TEMPERATURES OF FUEL RODS A77.B77.C77 AT POSITION 6

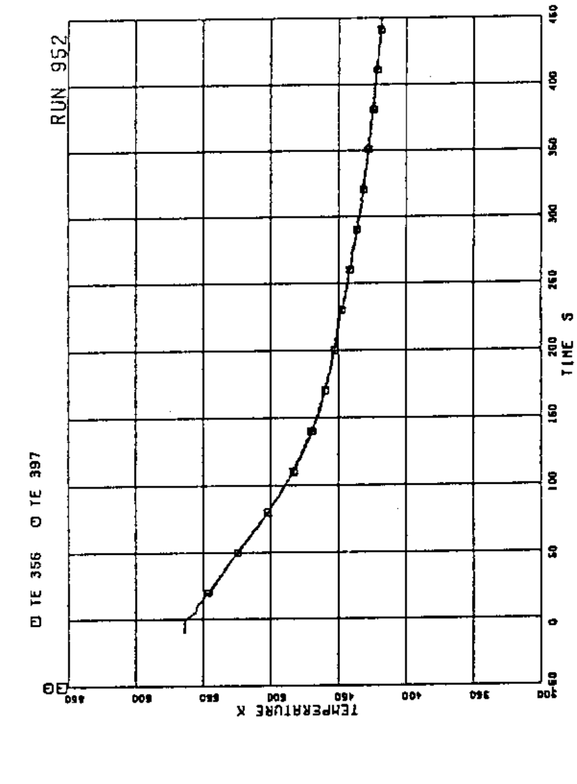

FIG.5.126 SURFACE TEMPERATURES OF FUEL RODS
B77,C77 AT POSITION 7

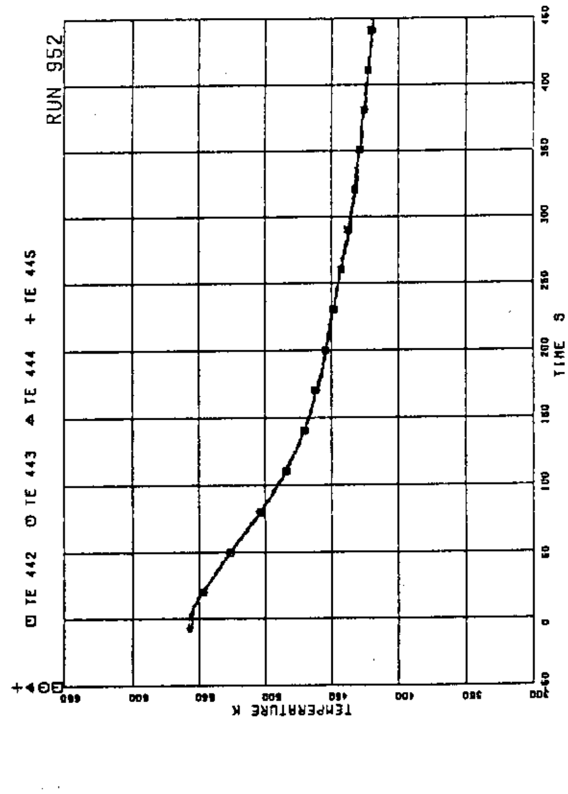

FIG.5.127 FLUID TEMPERATURES AT CHANNEL INLET

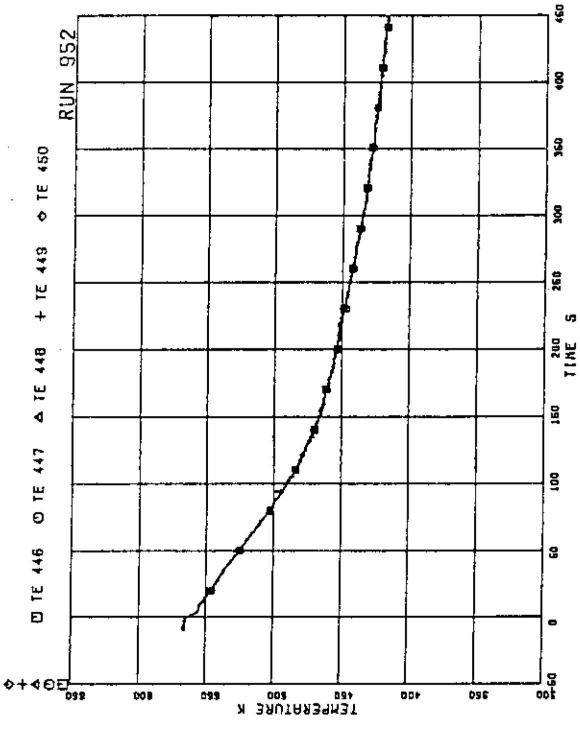

FIG.5.128 FLUID TEMPERATURES AT CHANNEL A OUTLET

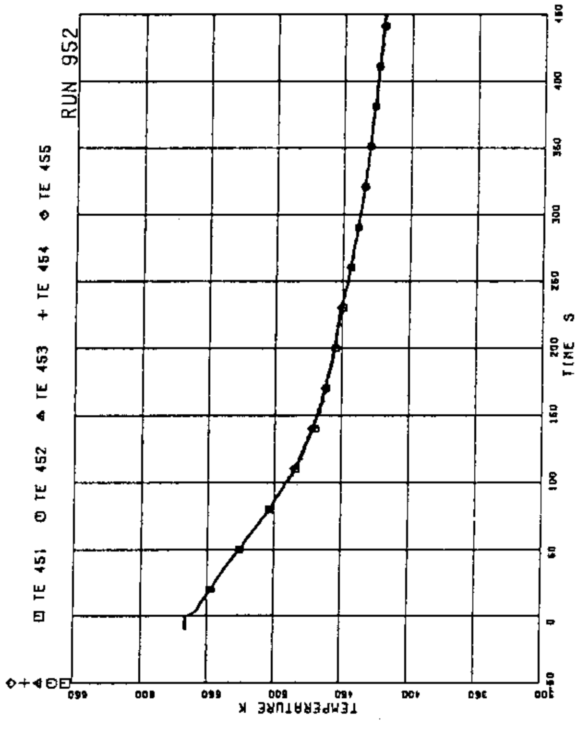

FIG.5.129 FLUID TEMPERATURES AT CHANNEL C OUTLET

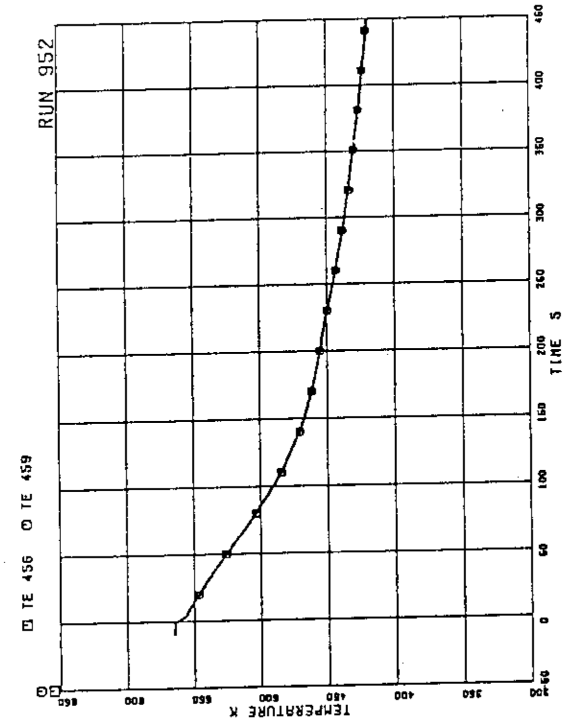

FIG.5.130 FLUID TEMPERATURES ABOVE UTP OF CHANNEL A, OPENINGS 1 AND 4

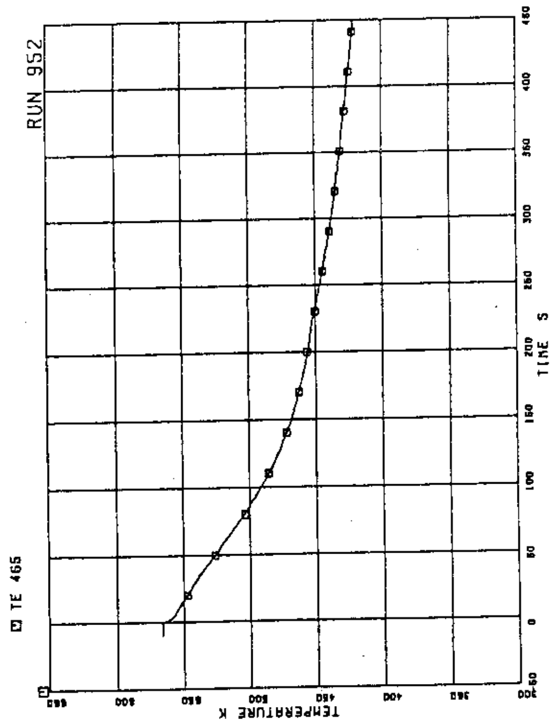

FIG.5.131 FLUID TEMPERATURE ABOVE UTP OF CHANNEL A, OPENING 10

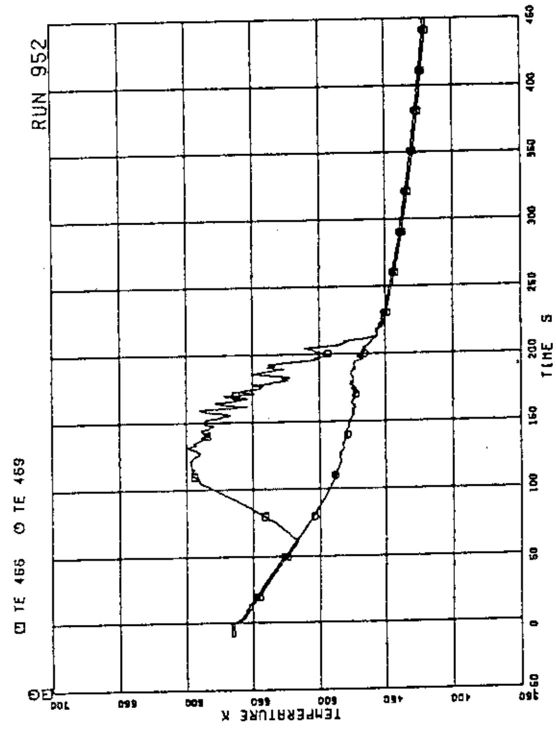

FIG.5.132 FLUID TEMPERATURES BELOW UTP OF CHANNEL A, OPENING 1 AND 4

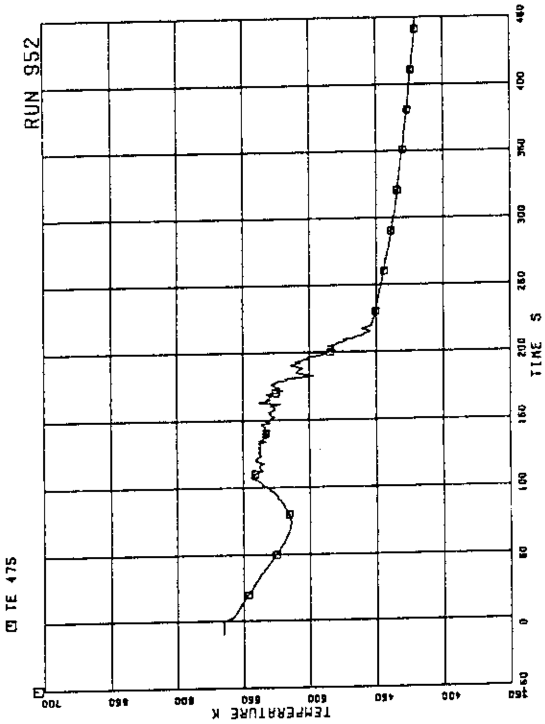

FIG.5.133 FLUID TEMPERATURES BELOW UTP OF CHANNEL A, OPENING 10

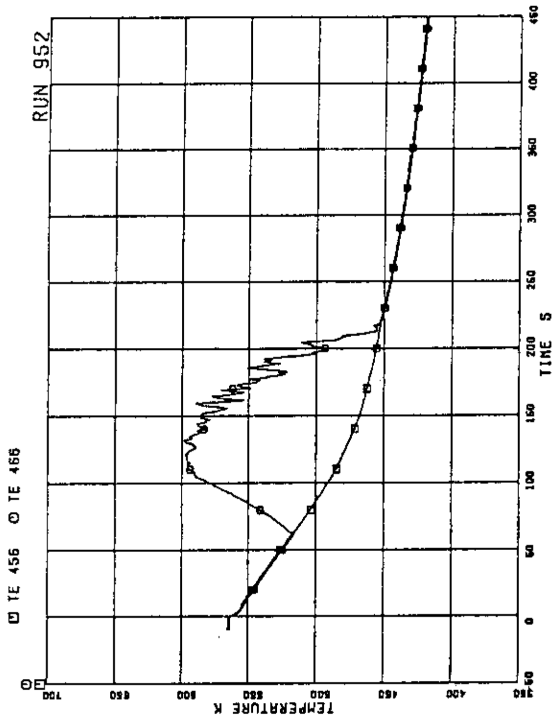

FIG.5.134 FLUID TEMPERATURES ACROSS UTP IN CHANNEL A, OPENING 1

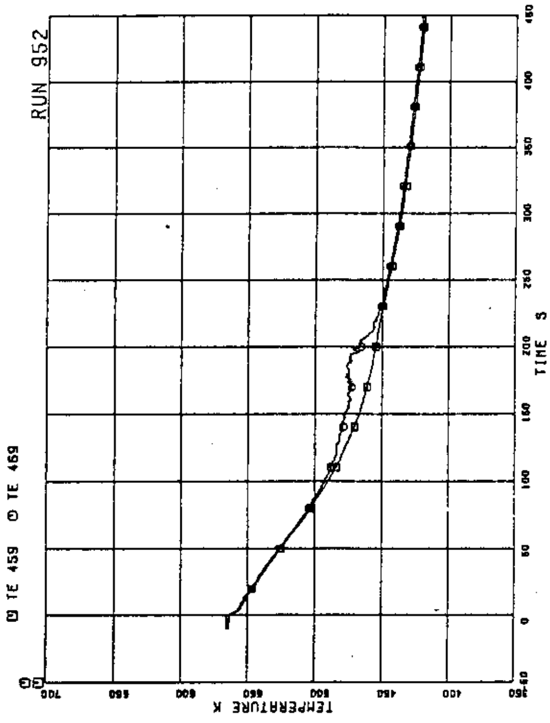

FIG.5.135 FLUID TEMPERATURES ACROSS UTP IN CHANNEL A, OPENING 4

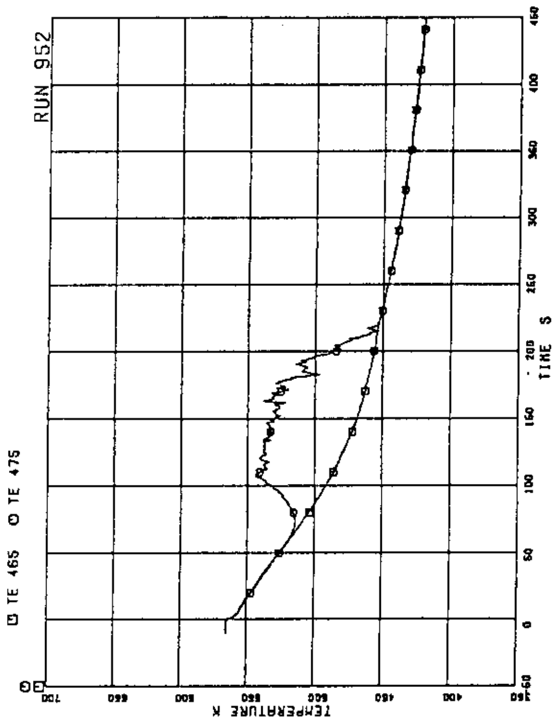

FIG.5.136 FLUID TEMPERATURES ACROSS UTP IN CHANNEL A, OPENING 10

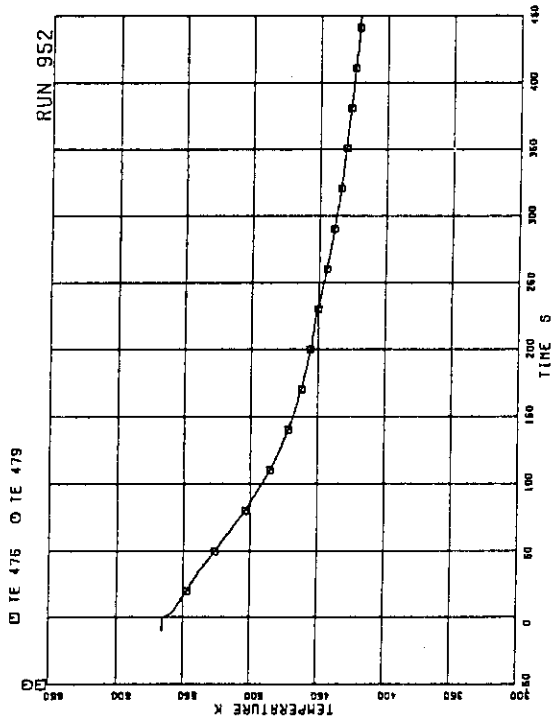

FIG.5.137 FLUID TEMPERATURES ABOVE UTP OF CHANNEL C, OPENINGS 1 AND 4

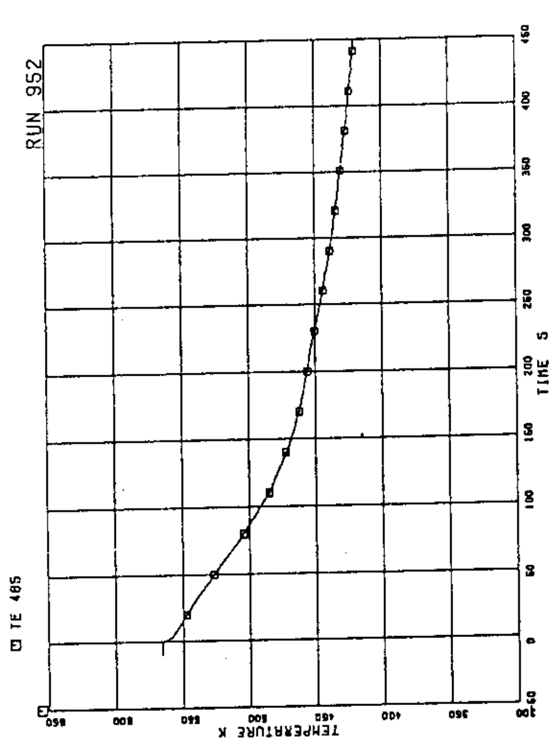

FIG.5.138 FLUID TEMPERATURES ABOVE UTP OF CHANNEL C, OPENING 10

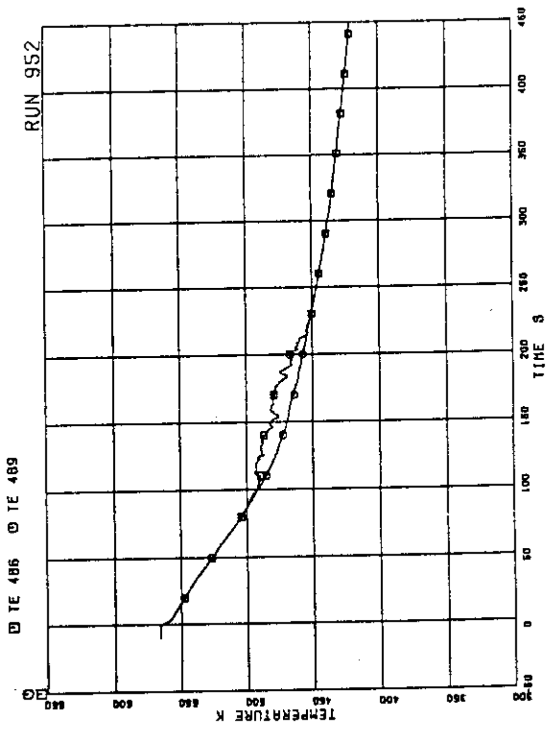

FIG.5.139 FLUID TEMPERATURES BELOW UTP OF CHANNEL C, OPENINGS 1 AND 4

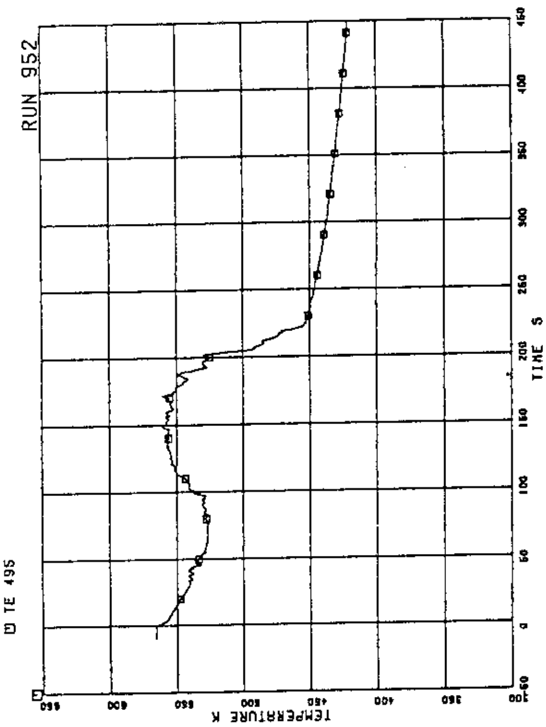

FIG.5.140 FLUID TEMPERATURES BELOW UTP OF CHANNEL C, OPENING 10

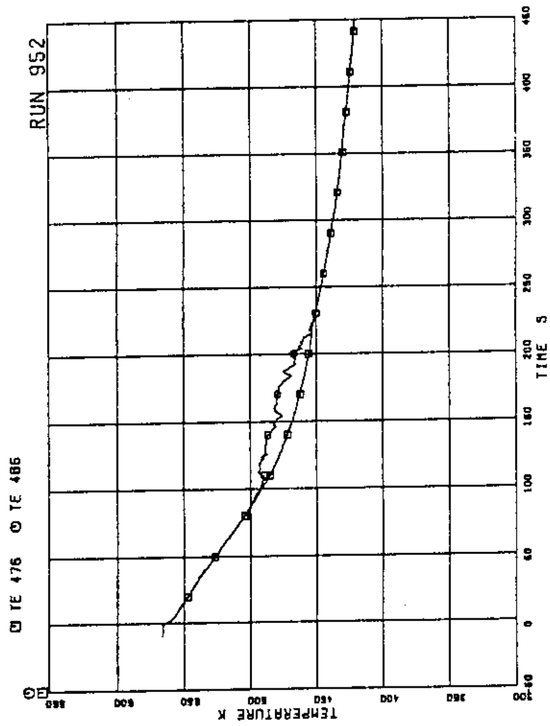

FIG.5.141 FLUID TEMPERATURES ACROSS UTP IN CHANNEL C, OPENING 1

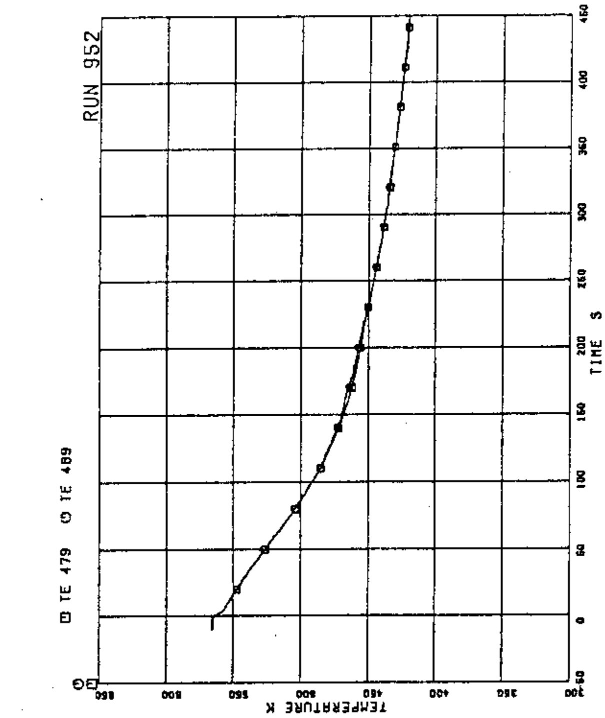

FIG.5.142 FLUID TEMPERATURES ACROSS UTP IN CHANNEL C, OPENING 4

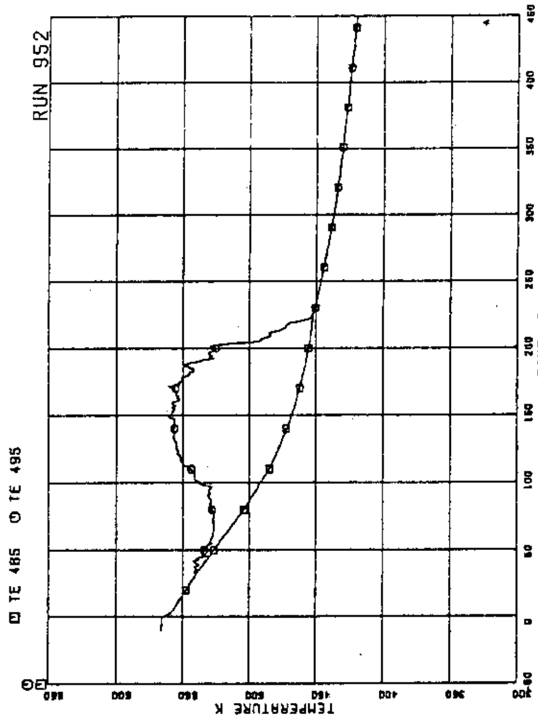

FIG.5.143 FLUID TEMPERATURES ACROSS UTP IN CHANNEL C, OPENING 10

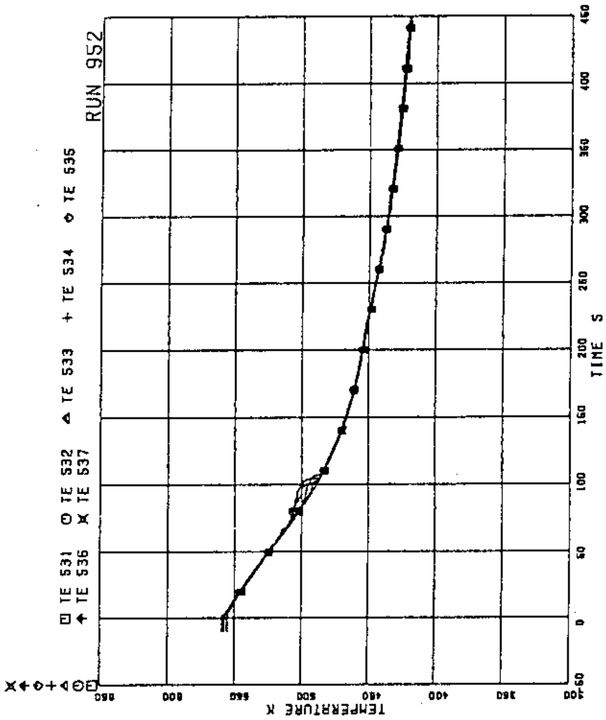

FIG.5.144 OUTER SURFACE TEMPERATURES OF CHANNEL BOX A

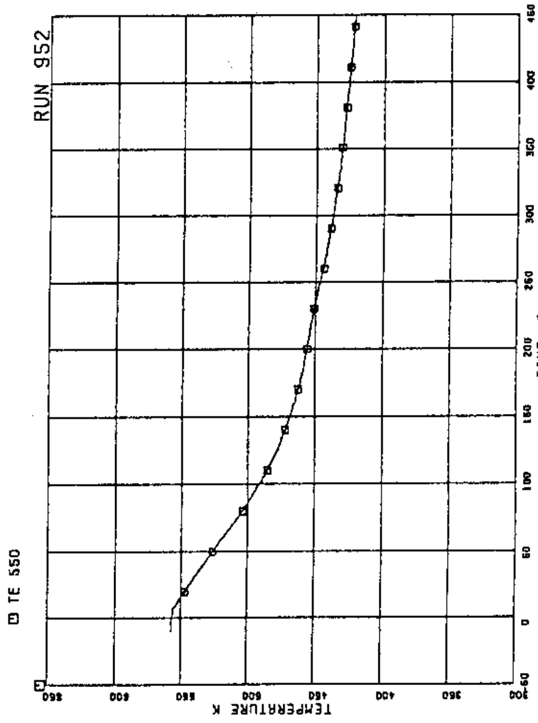

FIG.5.145 FLUID TEMPERATURE IN LOWER PLENUM, CENTER

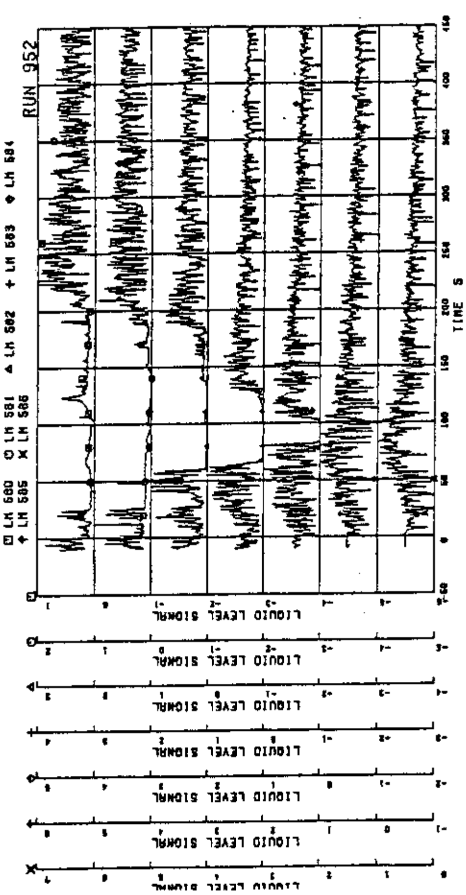

FIG.5.148 LIQUID LEVEL SIGNALS IN CHANNEL BOX C

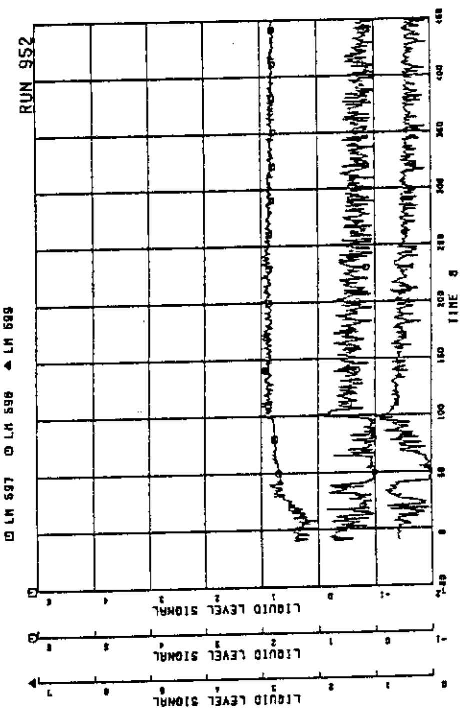

FIG.5.149 LIQUID LEVEL SIGNALS IN CHANNEL A OUTLET LOCATION A2

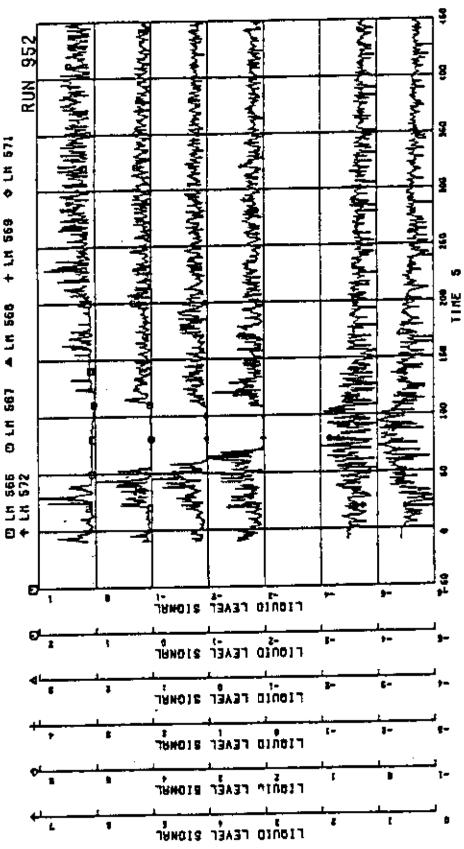

FIG.5.146 LIQUID LEVEL SIGNALS IN CHANNEL BOX A LOCATION A2

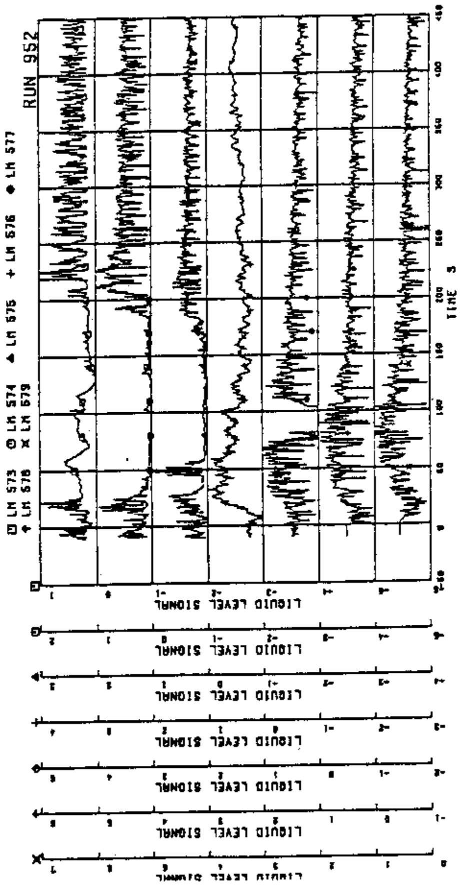

FIG.5.147 LIQUID LEVEL SIGNALS IN CHANNEL BOX B

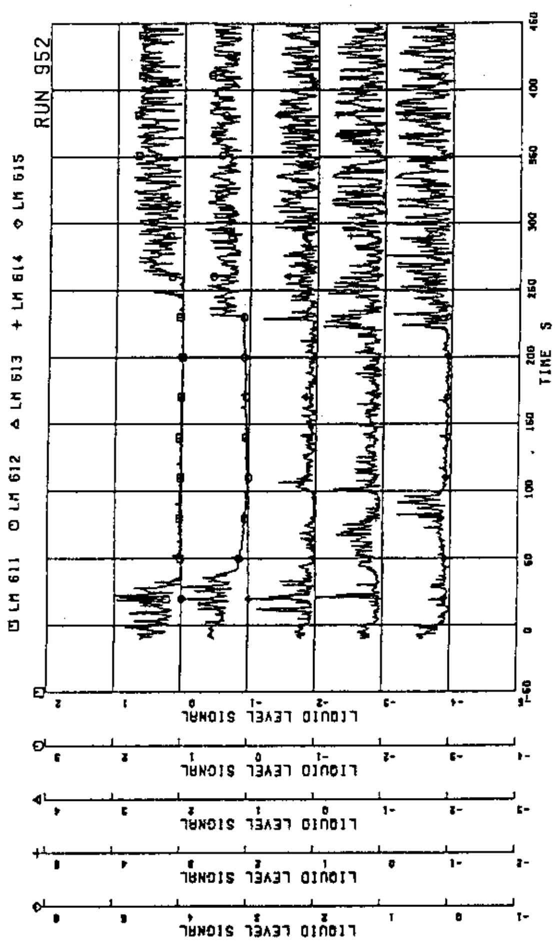

FIG.5.152 LIQUID LEVEL SIGNALS IN CHANNEL C OUTLET CENTER

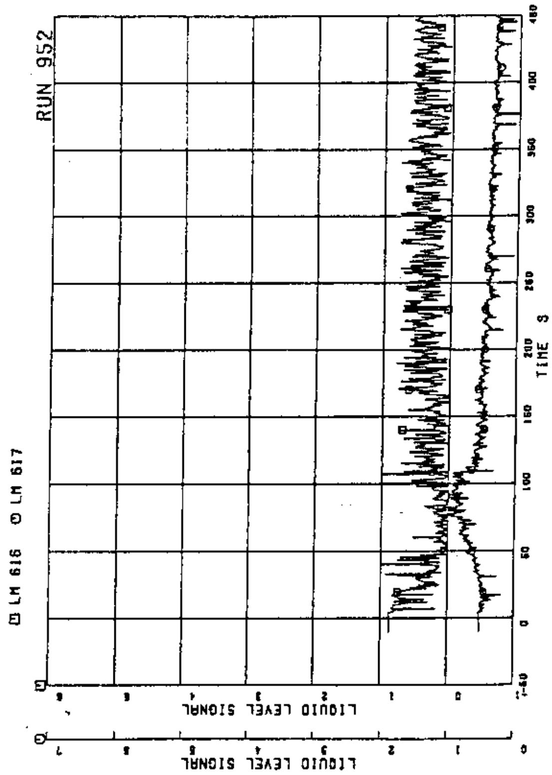

FIG.5.153 LIQUID LEVEL SIGNALS IN CHANNEL A INLET

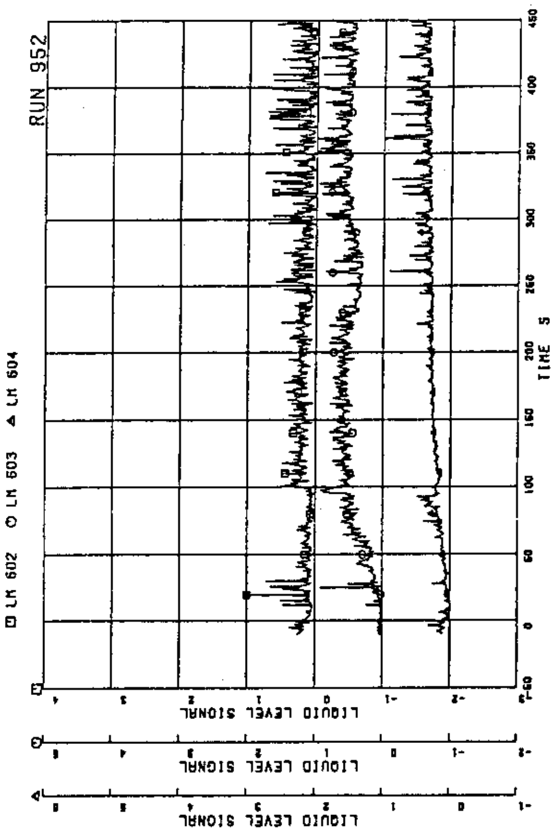

FIG.5.150 LIQUID LEVEL SIGNALS IN CHANNEL A OUTLET CENTER

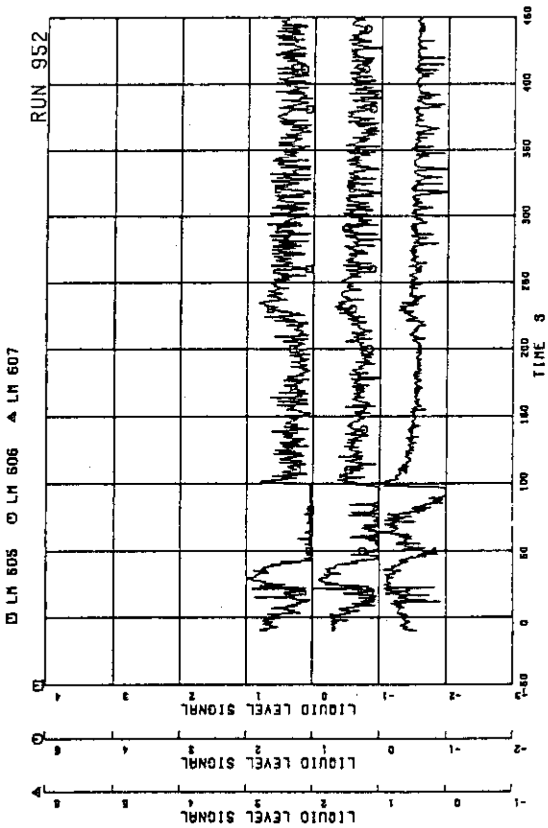

FIG.5.151 LIQUID LEVEL SIGNALS IN CHANNEL C OUTLET LOCATION C1

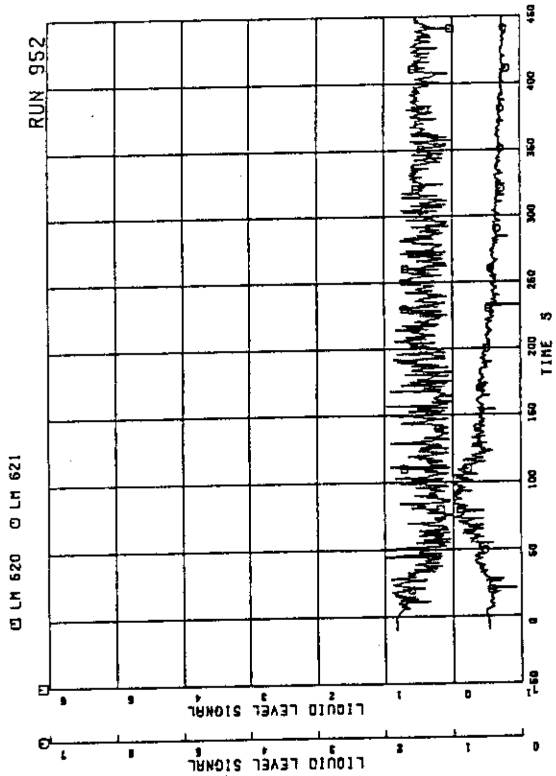

FIG.5.154 LIQUID LEVEL SIGNALS IN CHANNEL C INLET

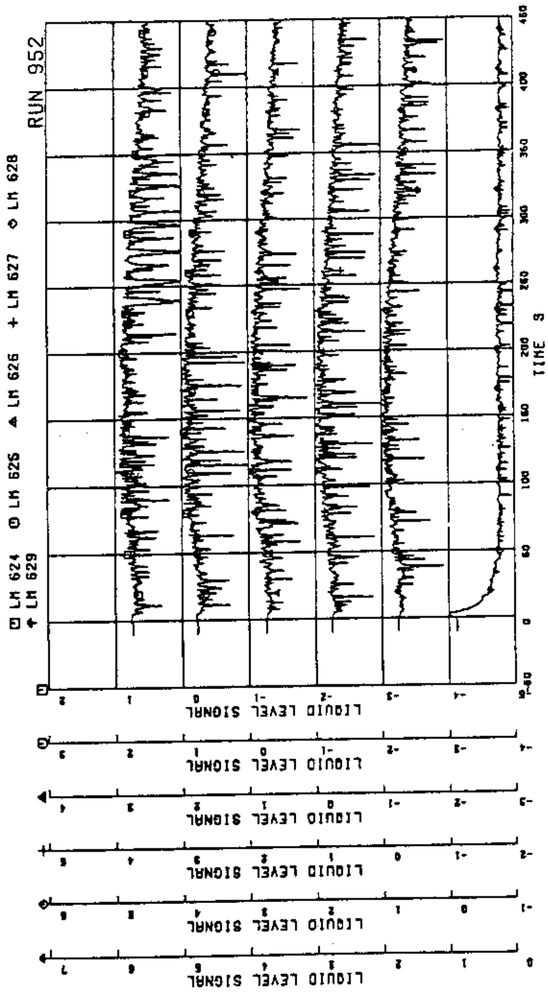

FIG.5.155 LIQUID LEVEL SIGNALS IN LOWER PLENUM NORTH

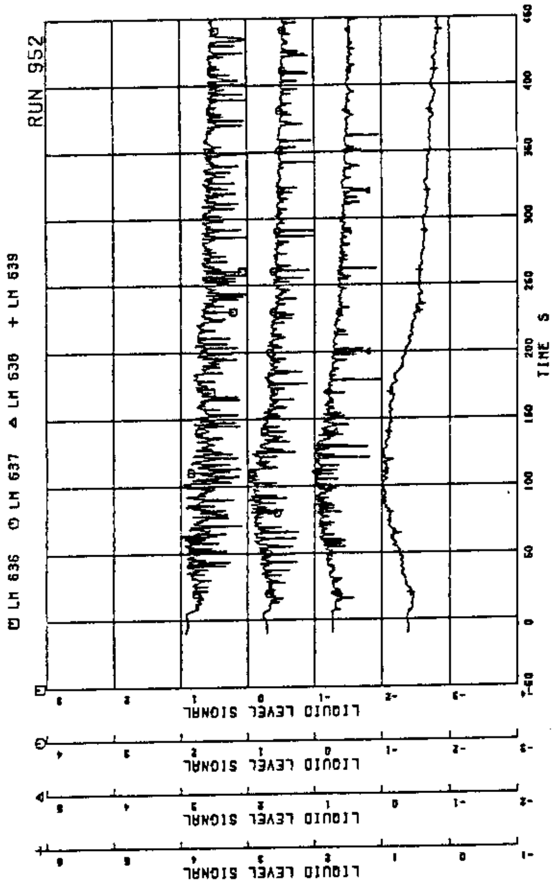

FIG.5.156 LIQUID LEVEL SIGNALS IN GUIDE TUBE NORTH

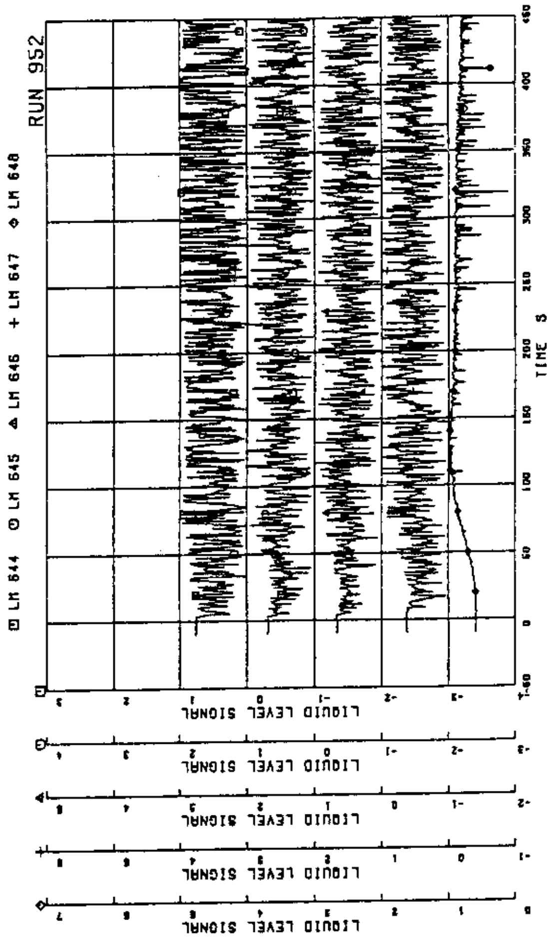

FIG.5.157 LIQUID LEVEL SIGNALS IN DOWNCOMER D SIDE

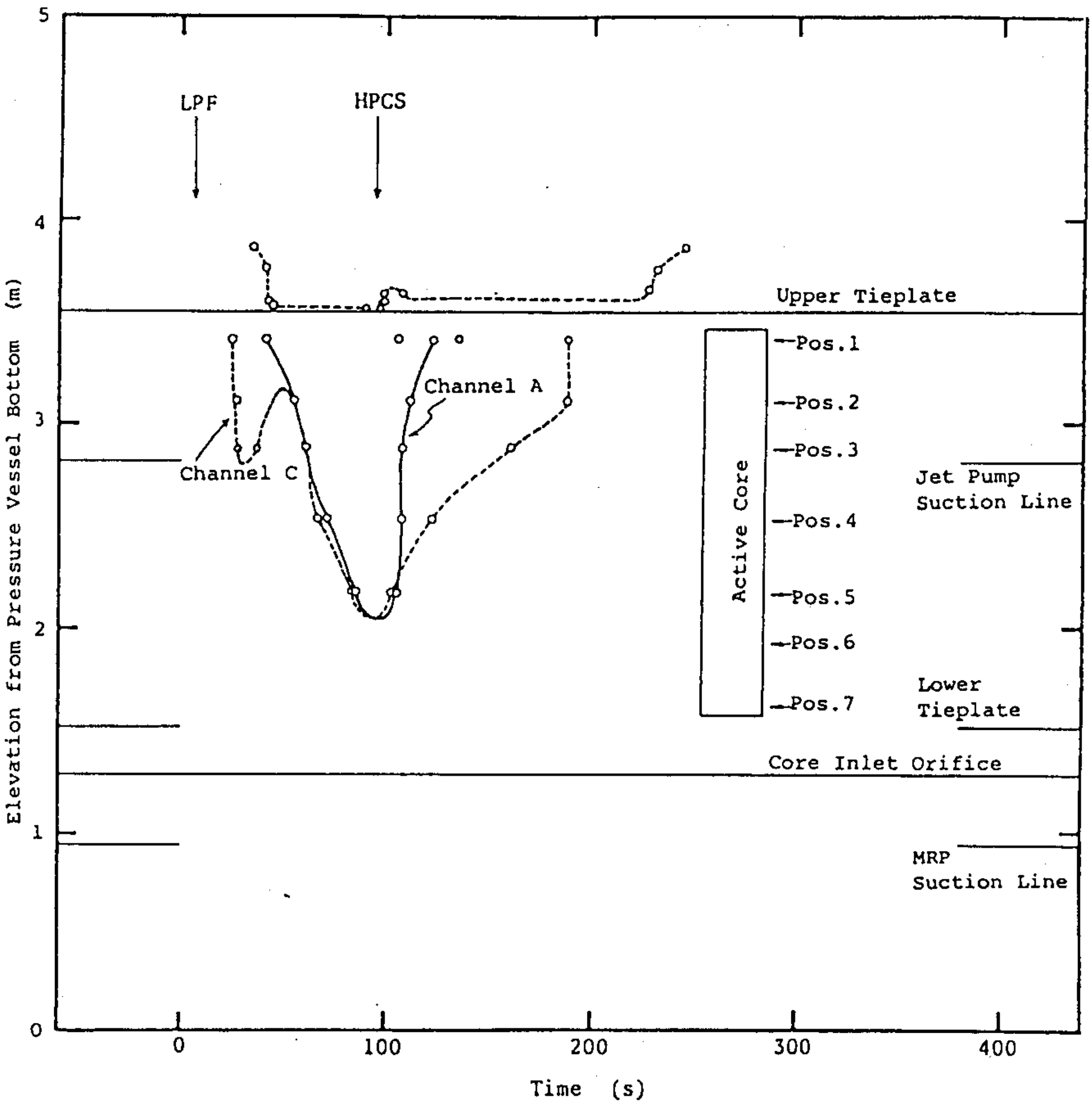

Fig.5.158 Estimated Liquid Levels in Upper Plenum and Core

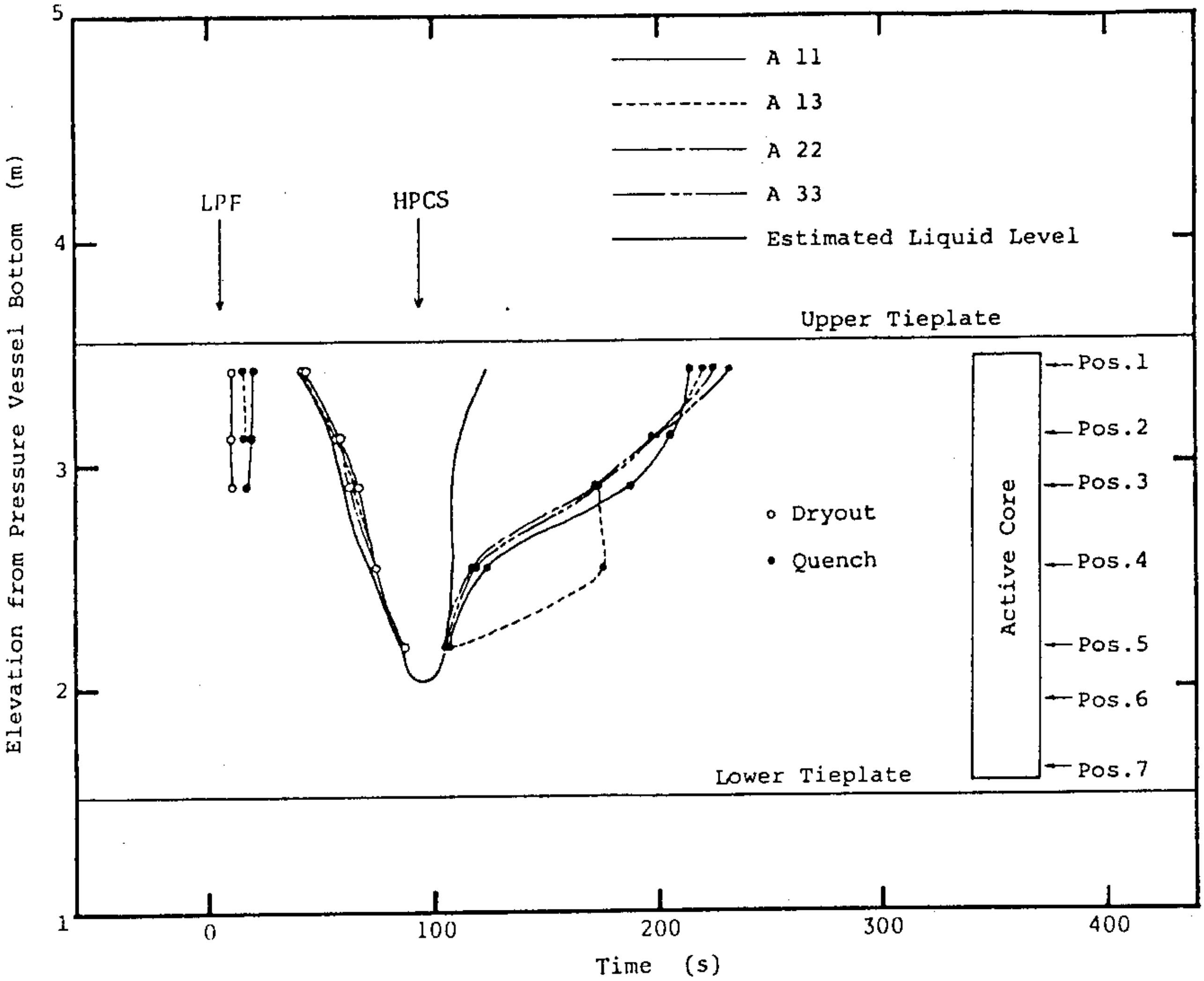

Fig. 5.159 Dryout and Quench Front Transients in Channel A

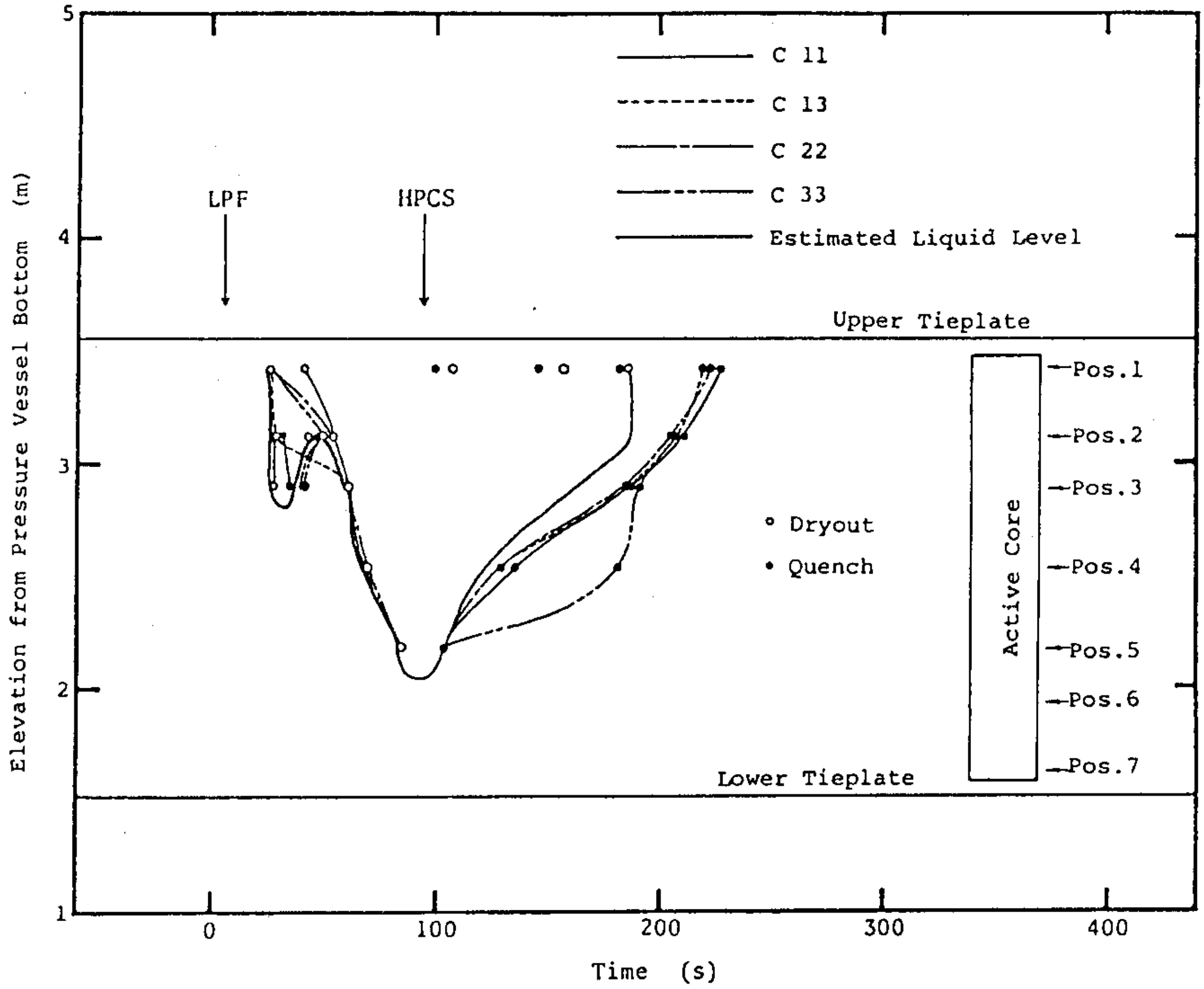

Fig. 5.160 Dryout and Quench Front Transients in Channel C

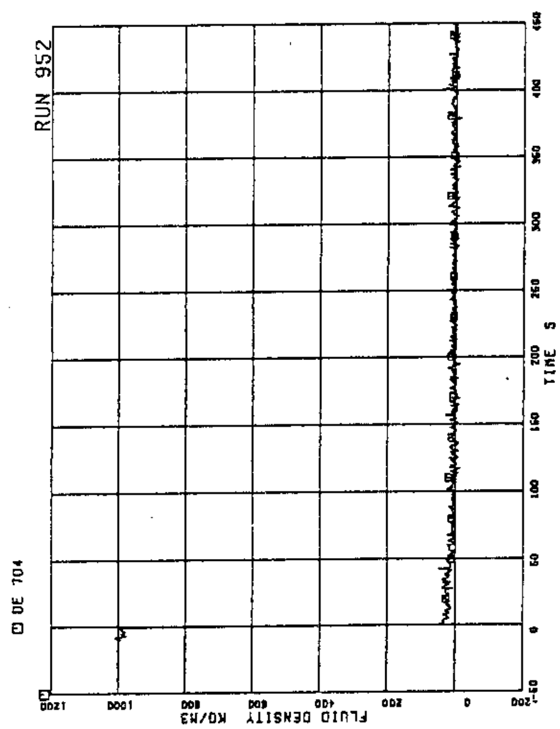

FIG.5.163 AVERAGE DENSITY AT BREAK

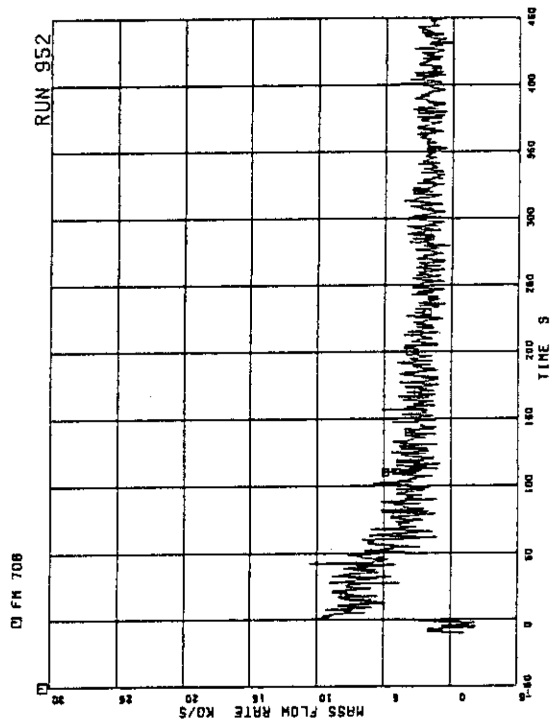

FIG.5.164 FLOW RATE AT BREAK (BASED ON HIGH RANGE DRAG DISK DATA)

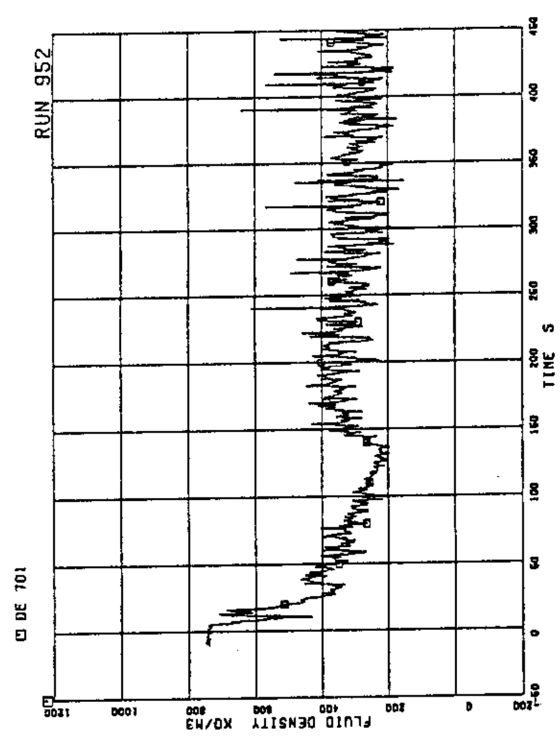

FIG.5.161 AVERAGE DENSITY AT JP-1.2 OUTLET

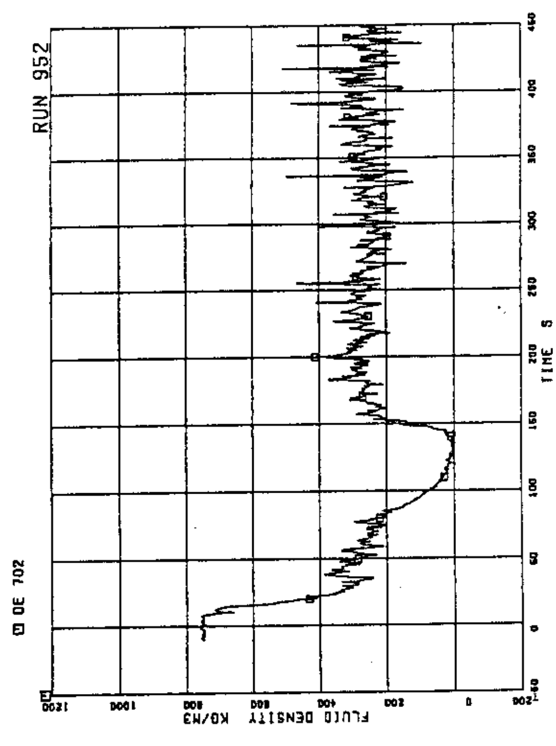

FIG.5.162 AVERAGE DENSITY AT JP-3.4 OUTLET

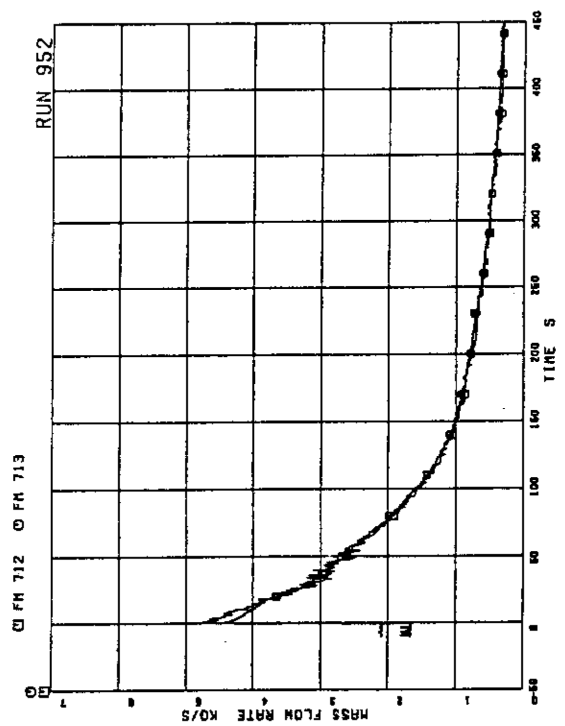

FIG.5.165 STEAM DISCHARGE FLOW RATE THROUGH MSL

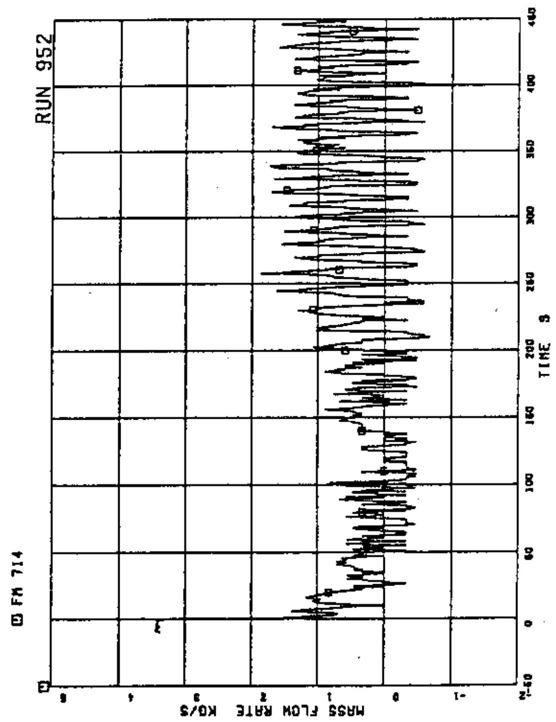

FIG.5.166 FLOW RATE AT CHANNEL A INLET

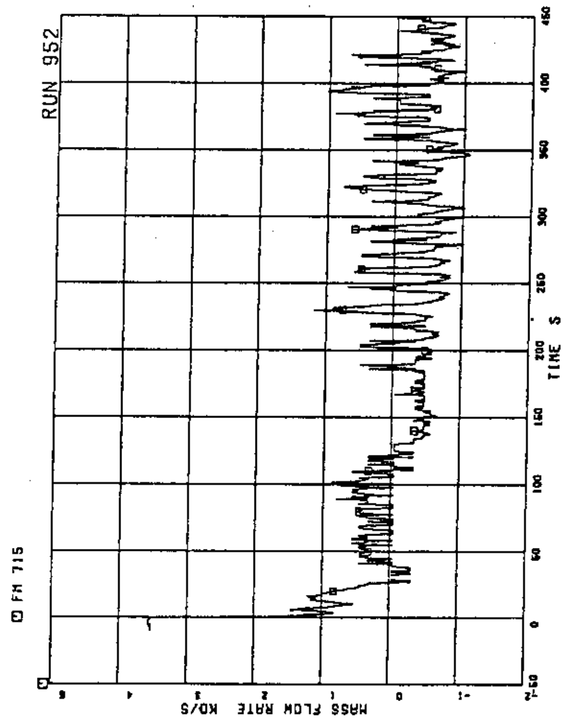

FIG.5.167 FLOW RATE AT CHANNEL B INLET

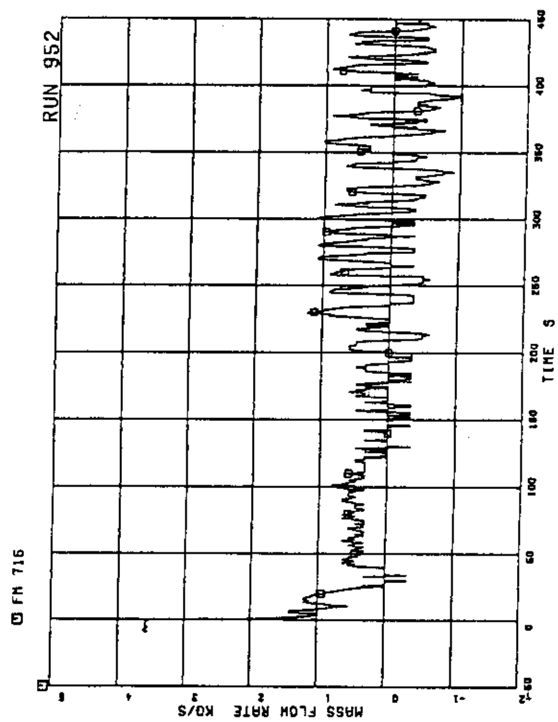

FIG.5.168 FLOW RATE AT CHANNEL C INLET

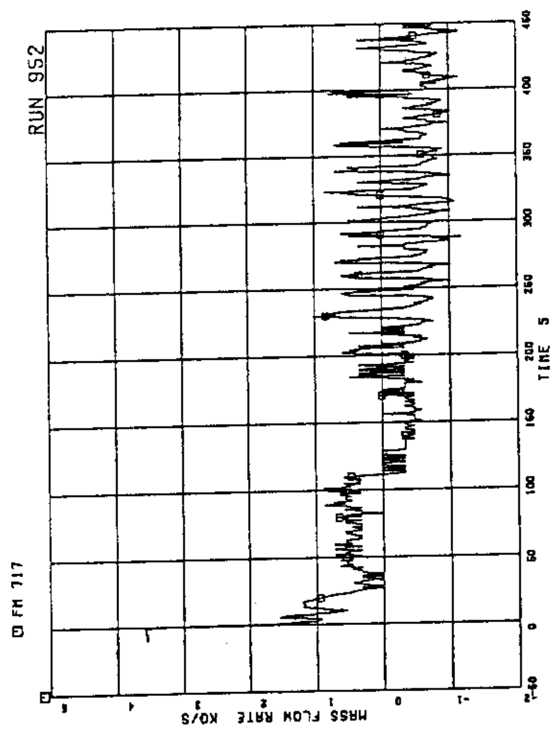

FIG.5.169 FLOW RATE AT CHANNEL D INLET

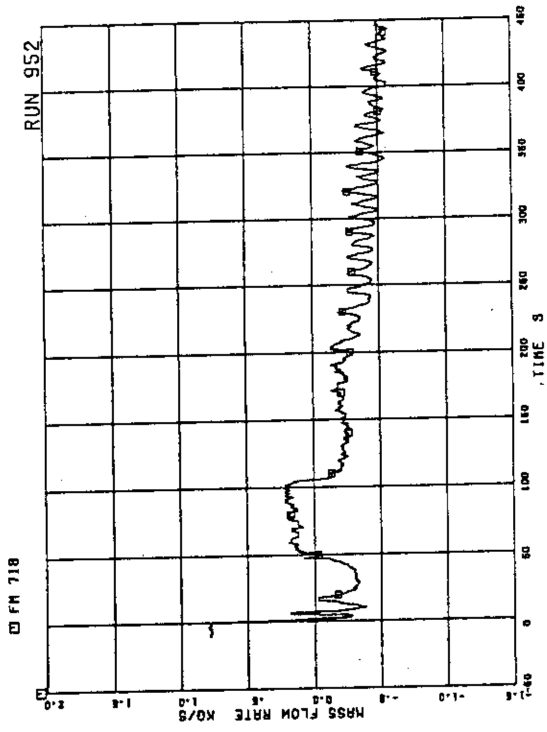

FIG.5.170 FLOW RATE AT BYPASS HOLE

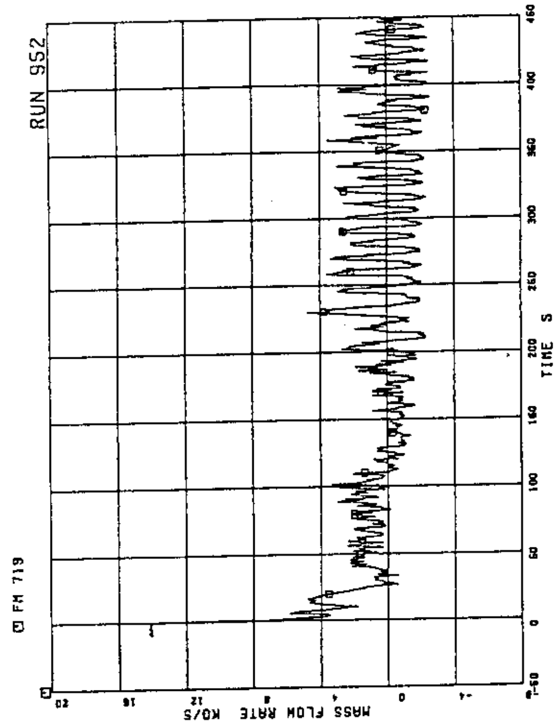

FIG.5.171 TOTAL CHANNEL INLET FLOW RATE

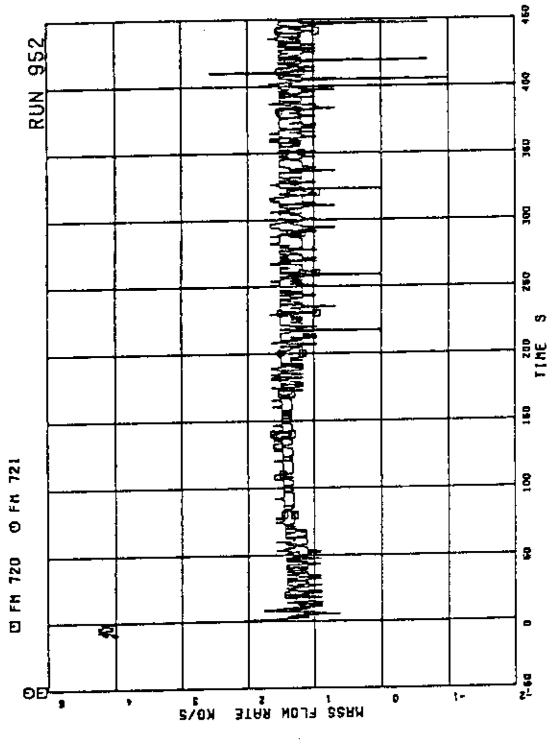

FIG.5.172 FLOW RATE AT JP-1.2 OUTLET (POS. FLOW)

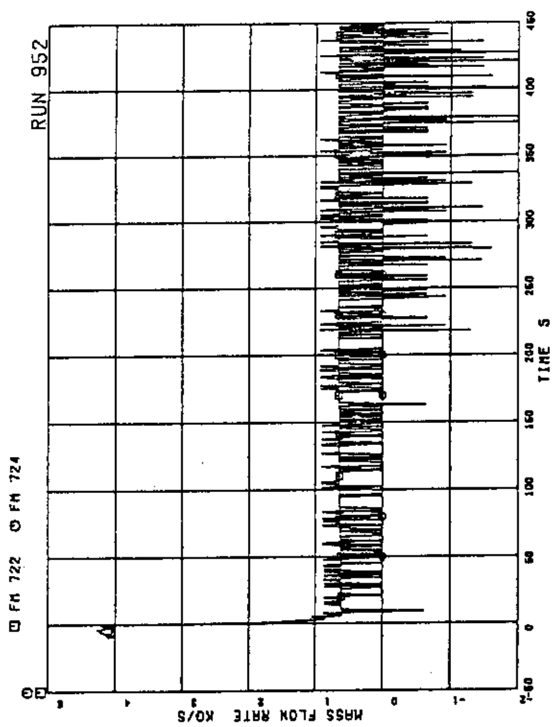

FIG.5.173 FLOW RATE AT JP-3,4 OUTLET (POS. FLOW)

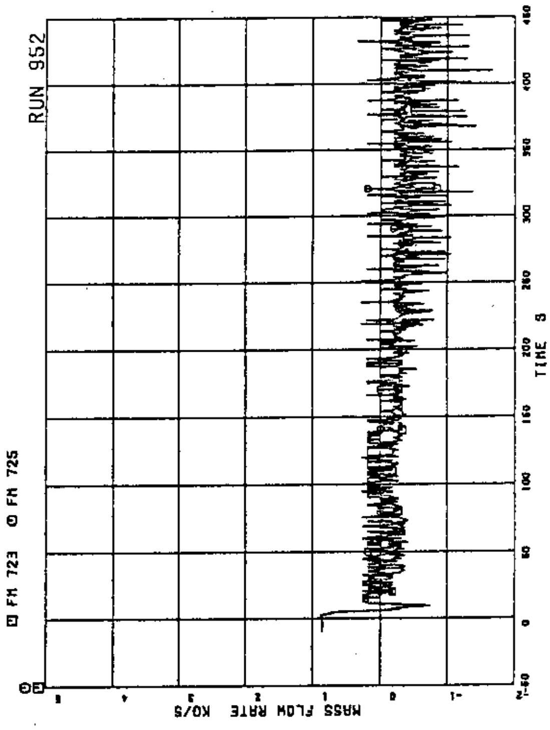

FIG.5.174 FLOW RATE AT JP-3,4 OUTLET (NEG. FLOW)

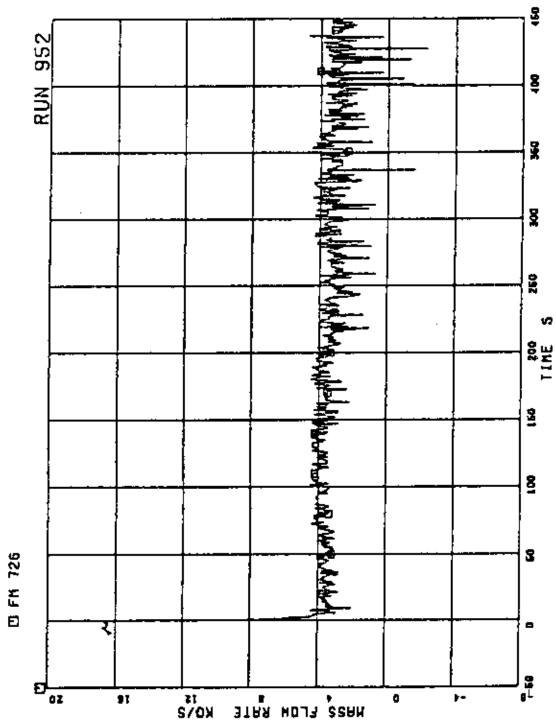

FIG.5.175 TOTAL JP OUTLET FLOW RATE (POS. FLOW)

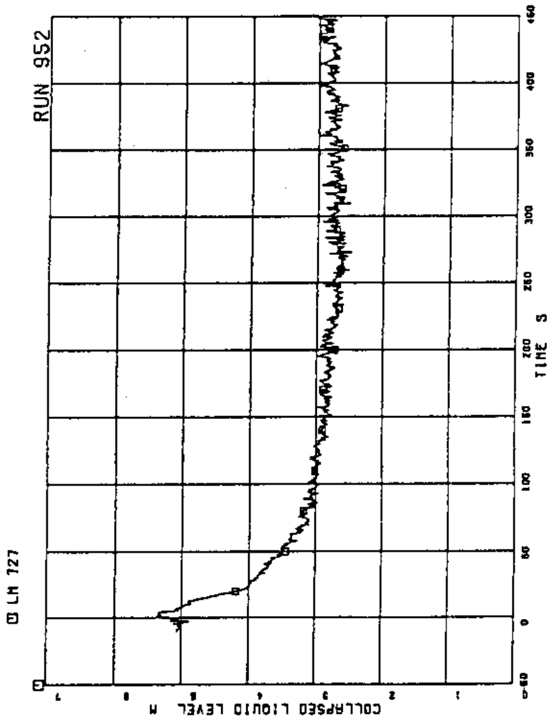

FIG.5.176 COLLAPSED LIQUID LEVEL IN DOWNCOMER

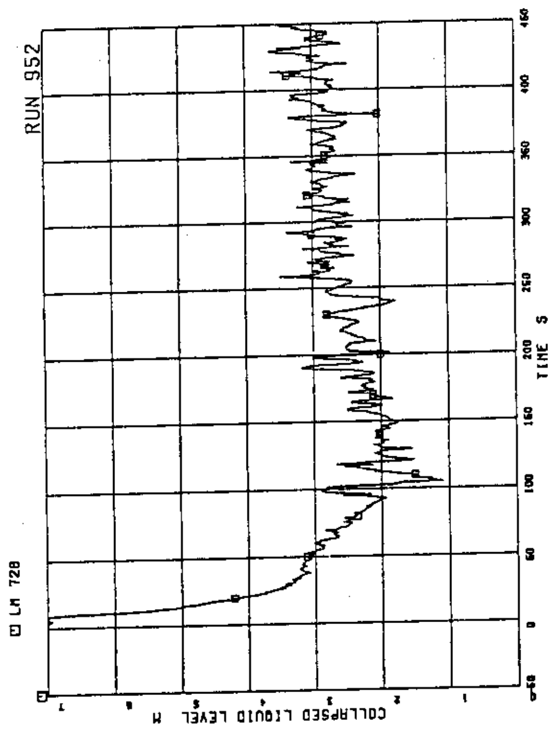

FIG.5.177 COLLAPSED LIQUID LEVEL INSIDE CORE SHROUD

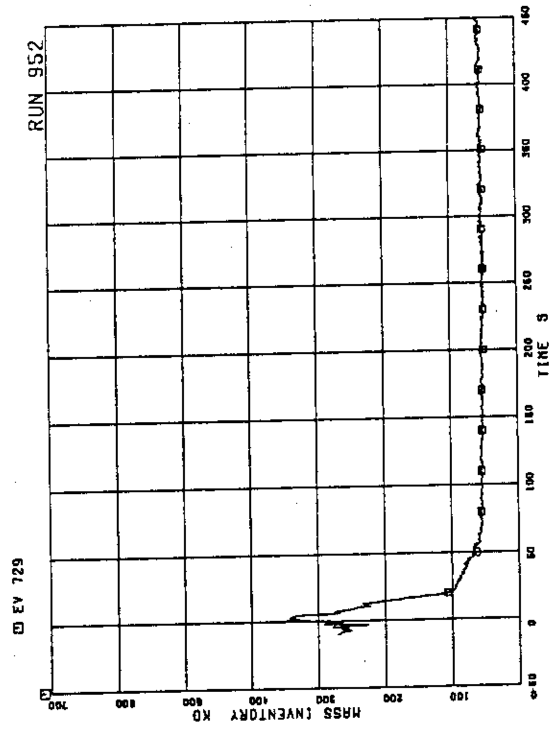

FIG.5.178 FLUID INVENTORY IN DOWNCOMER

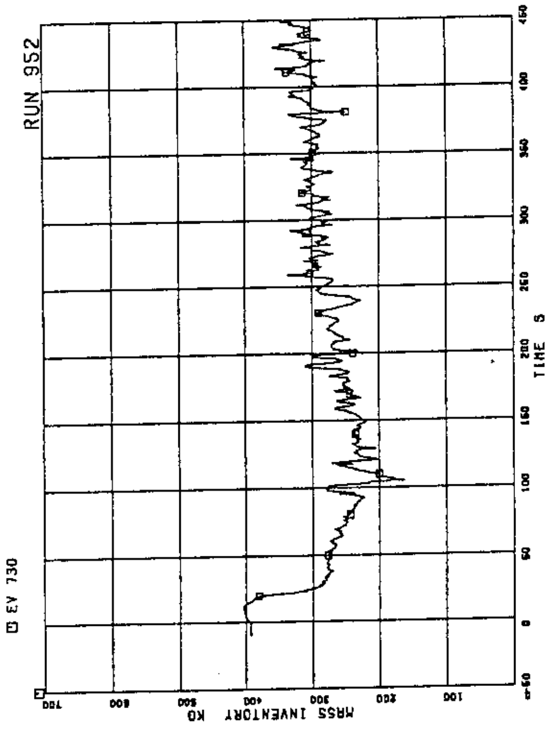

FIG.5.179 FLUID INVENTORY INSIDE CORE SHROUD

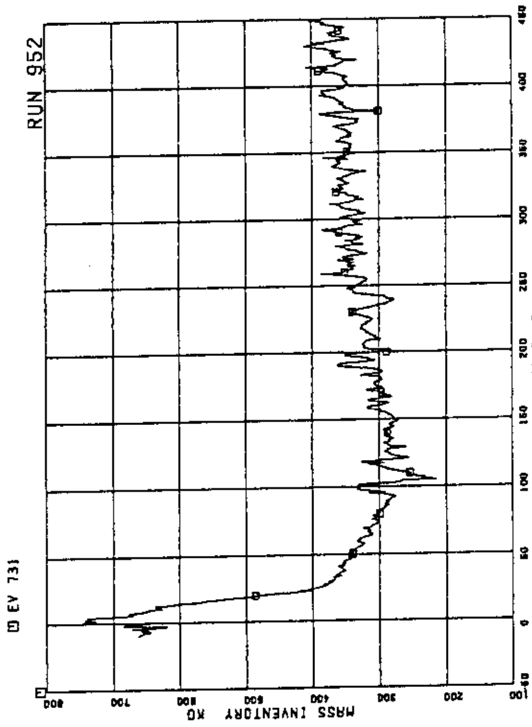

FIG.5.180 TOTAL FLUID INVENTORY IN PRESSURE VESSEL

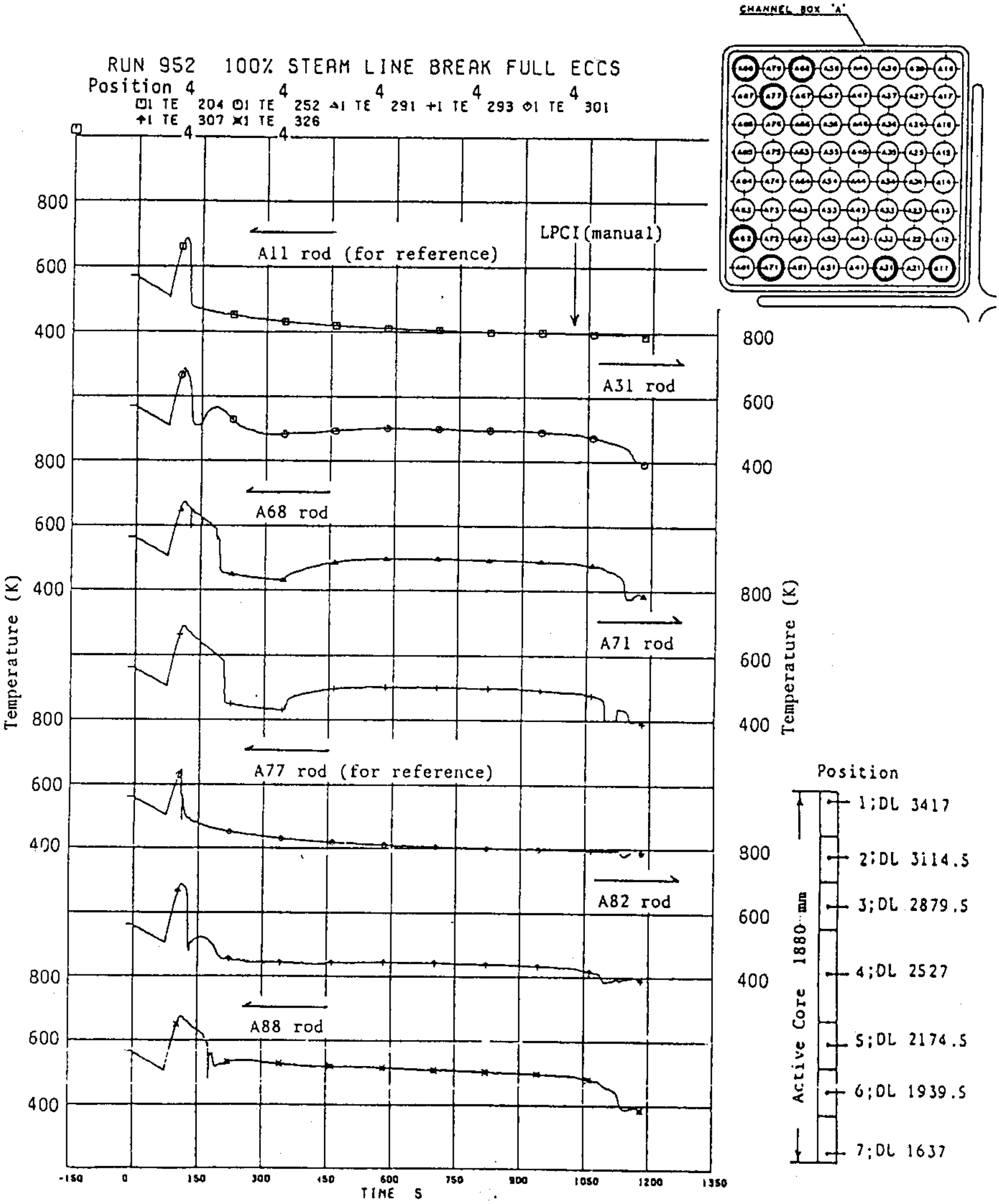

Fig. 5.181 Re-Dryout Phenomena in Channel Box A

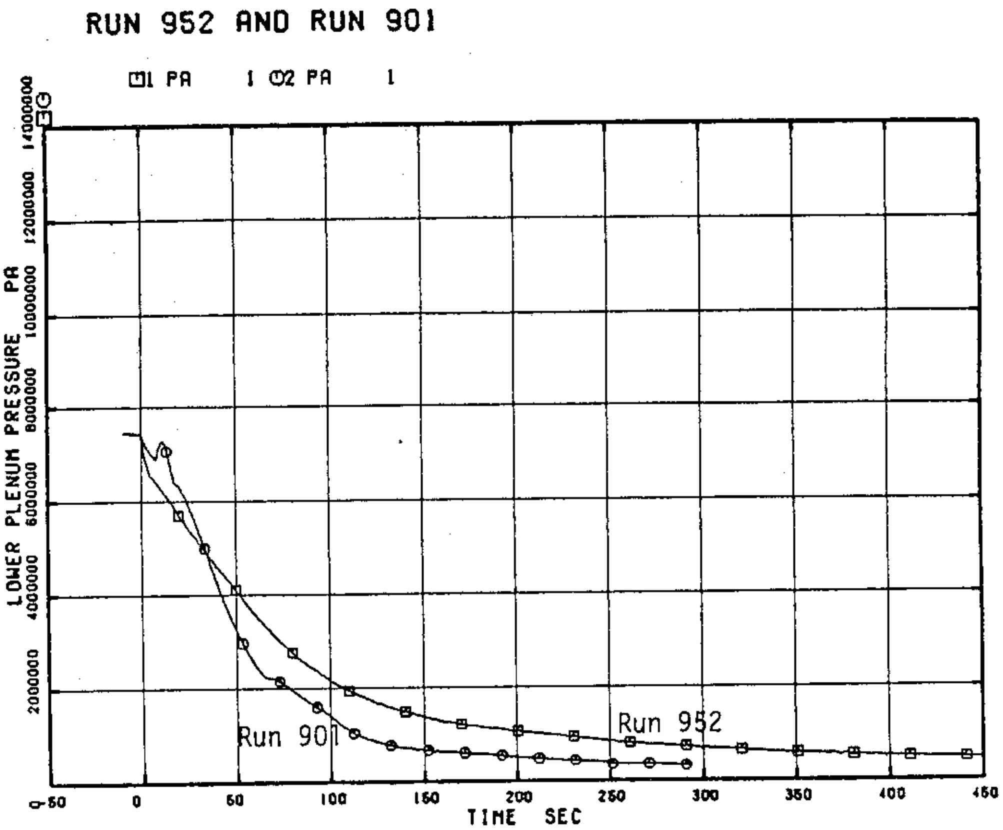

Fig. 7.1 Lower Plenum Pressure Transients in Run 952 and Run 901

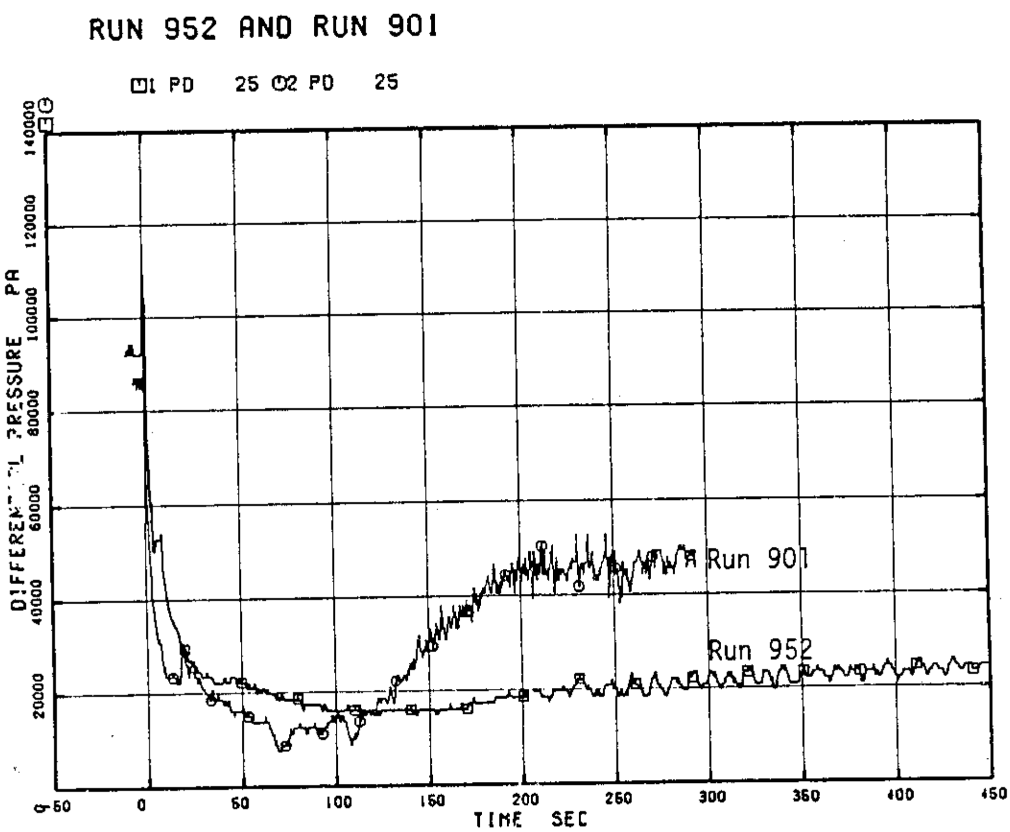

Fig. 7.2 Differential Pressure across Core

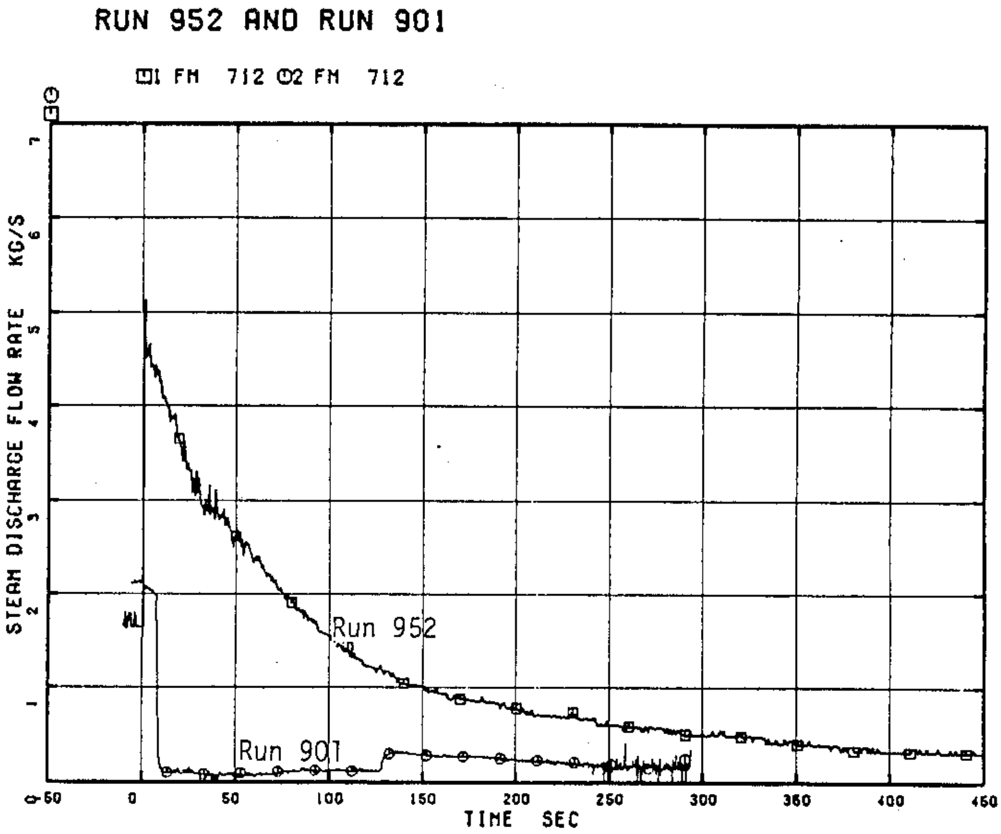

Fig. 7.3 Steam Flow Rate in Main Steam Line

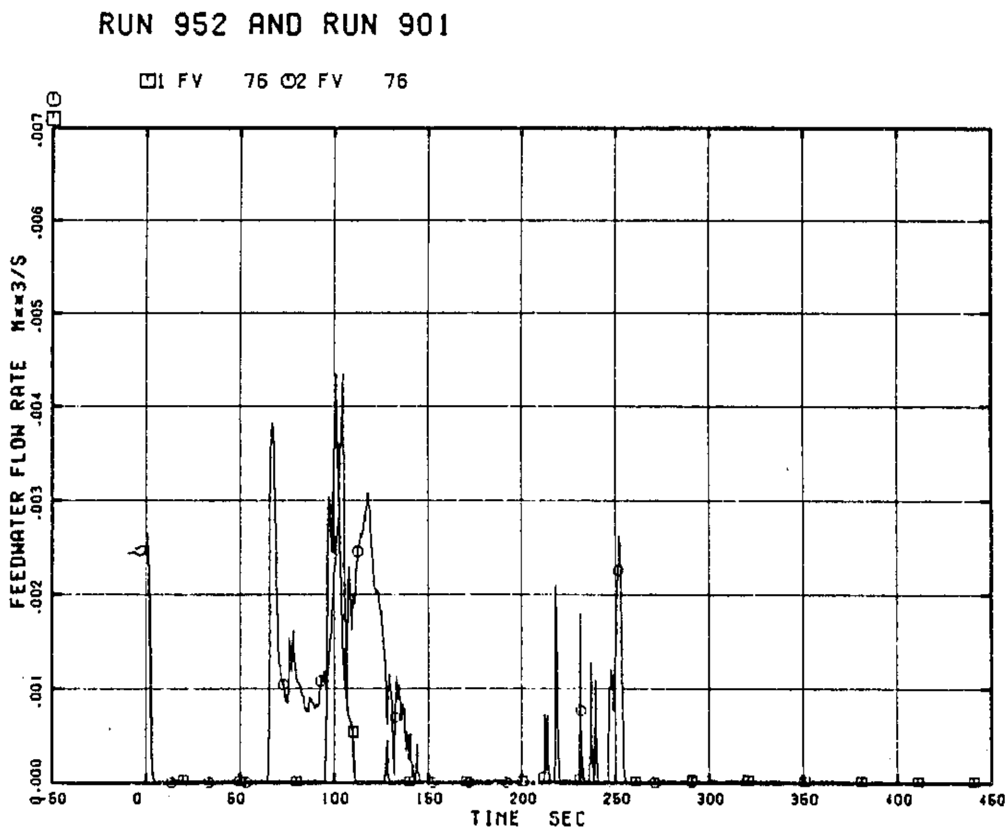

Fig. 7.4 Feedwater Flow Rate

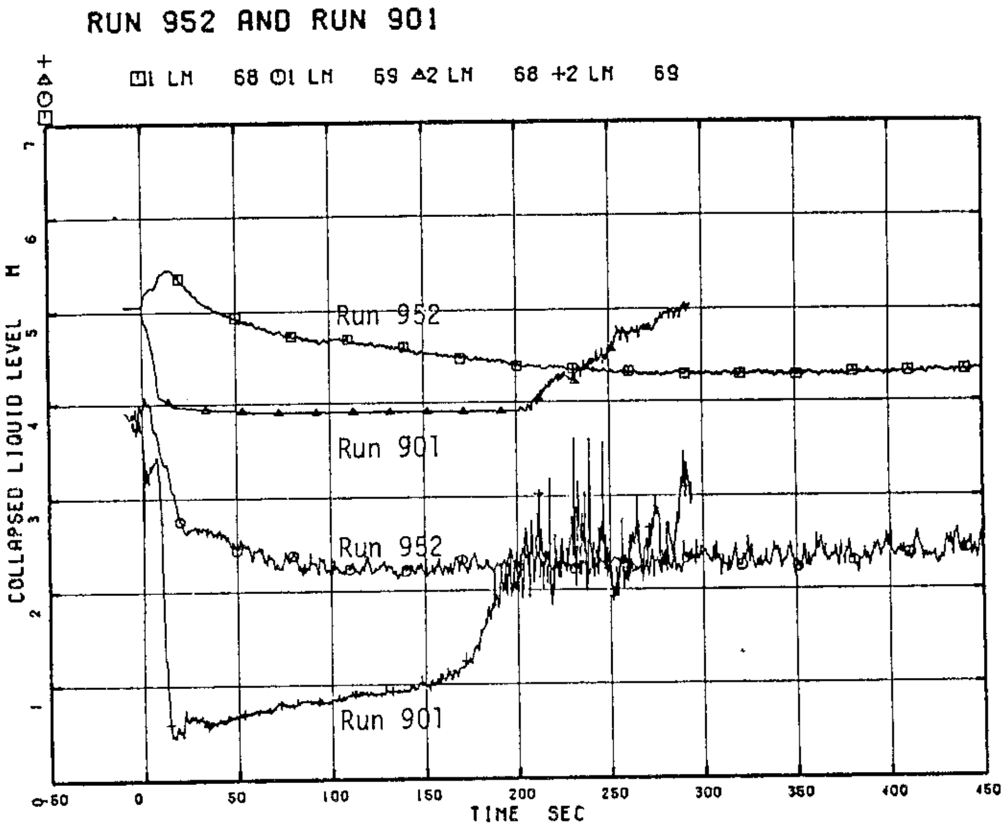

Fig. 7.5 Collapsed Water Level in Downcomer

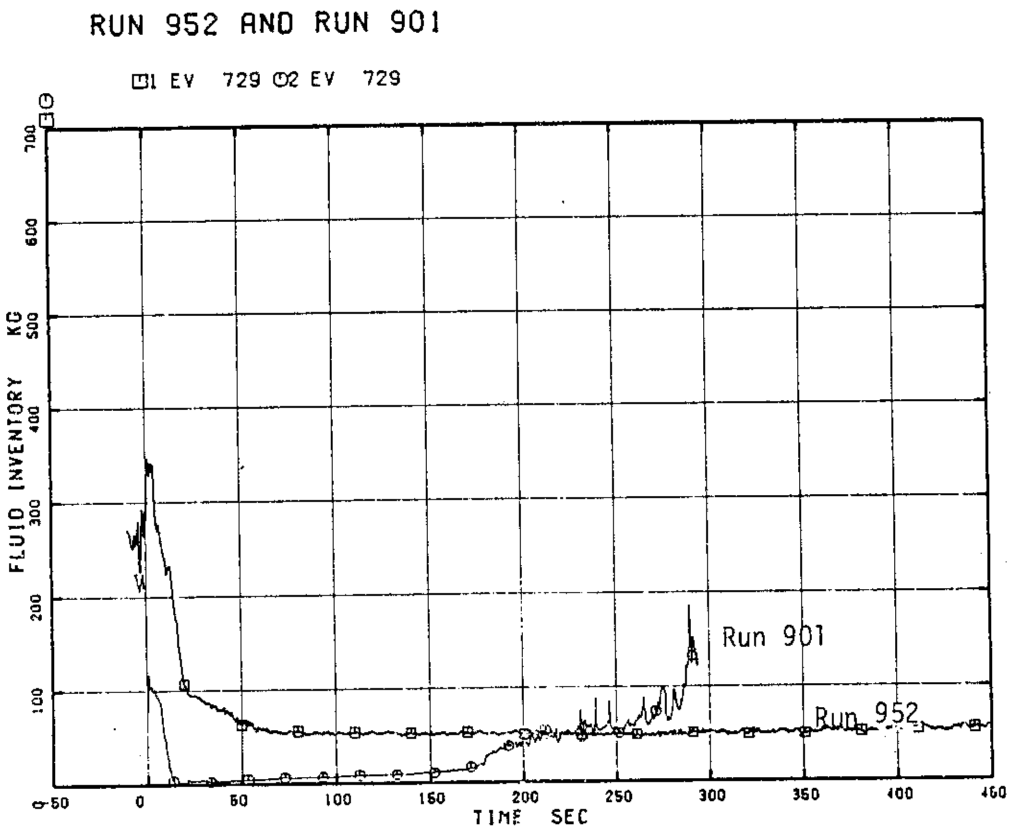

Fig. 7.6 Mass Inventory in Downcomer

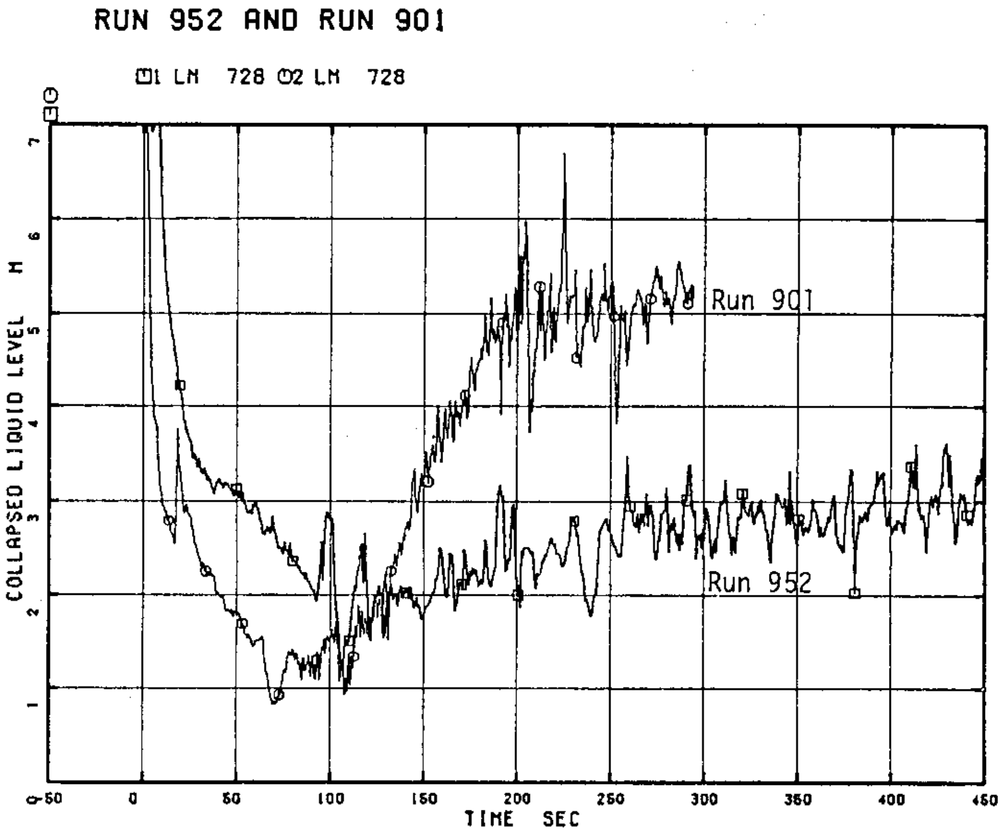

Fig. 7.7 Collapsed Water Level in Core Shroud

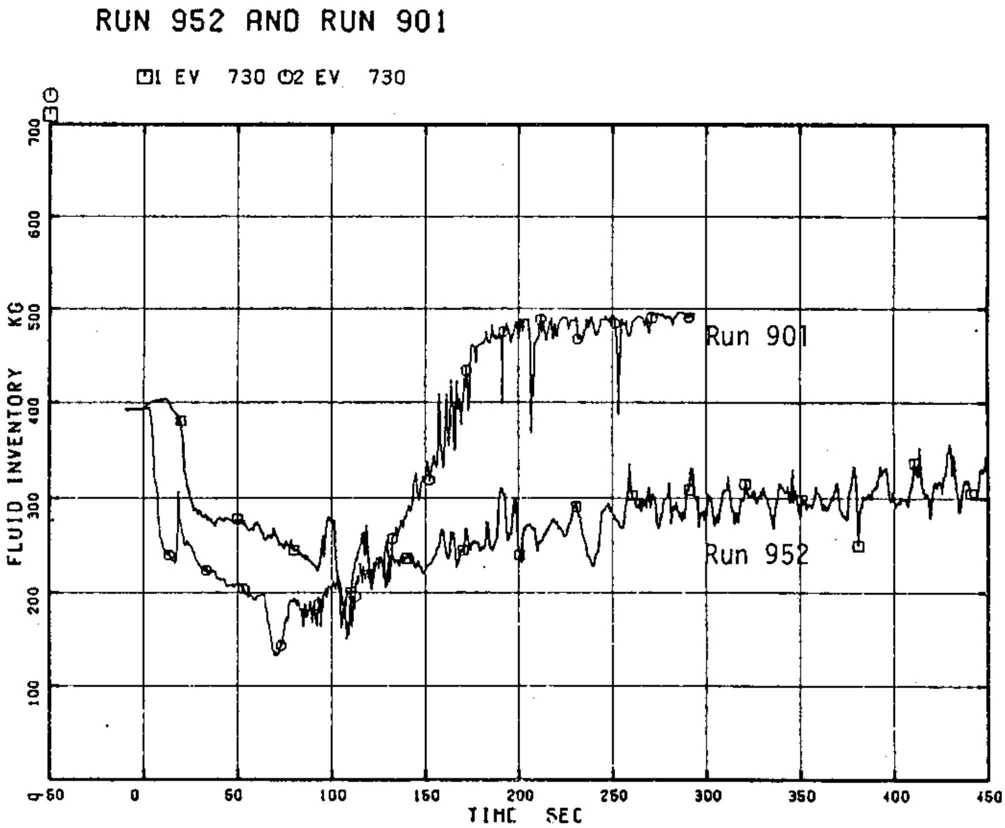

Fig. 7.8 Mass Inventory in Core Shroud

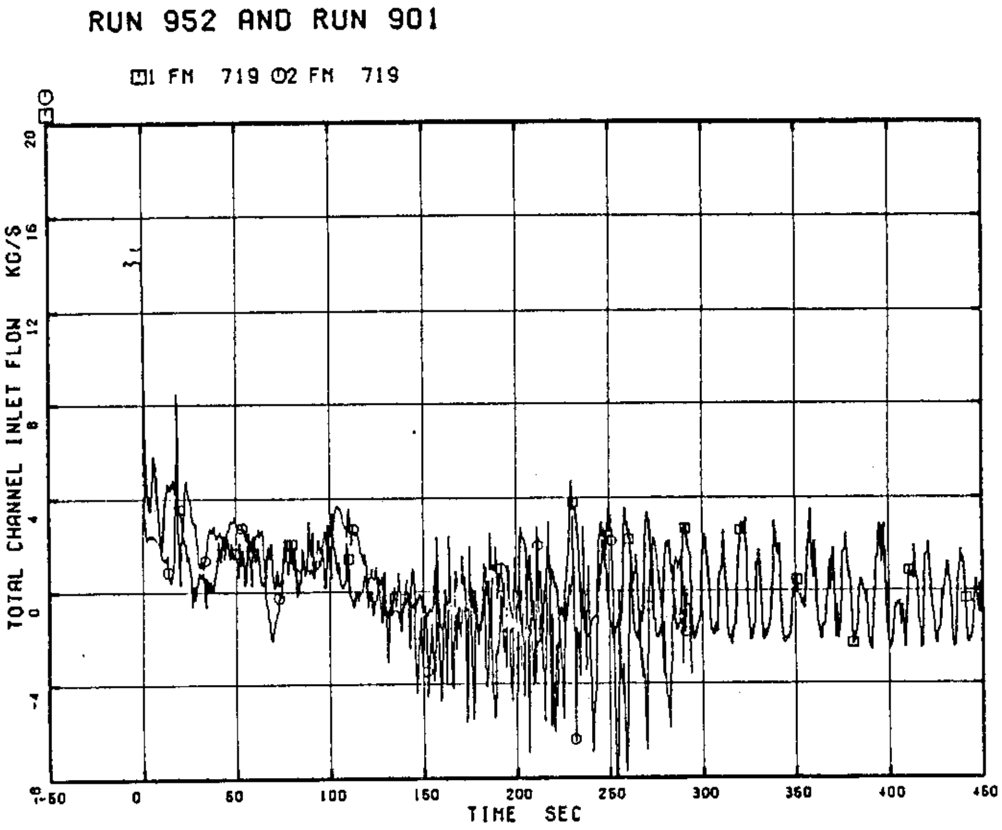

Fig. 7.9 Flow Rate inside Core Shroud

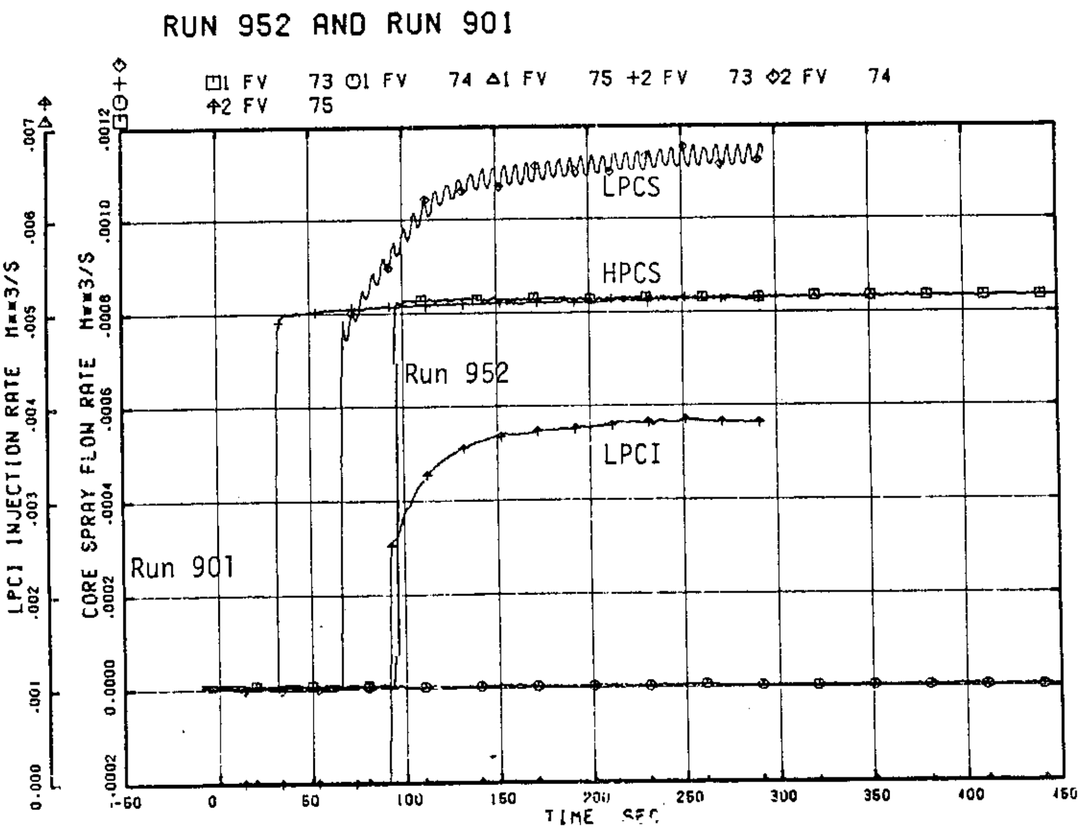

Fig. 7.10 ECCS Flow Rate

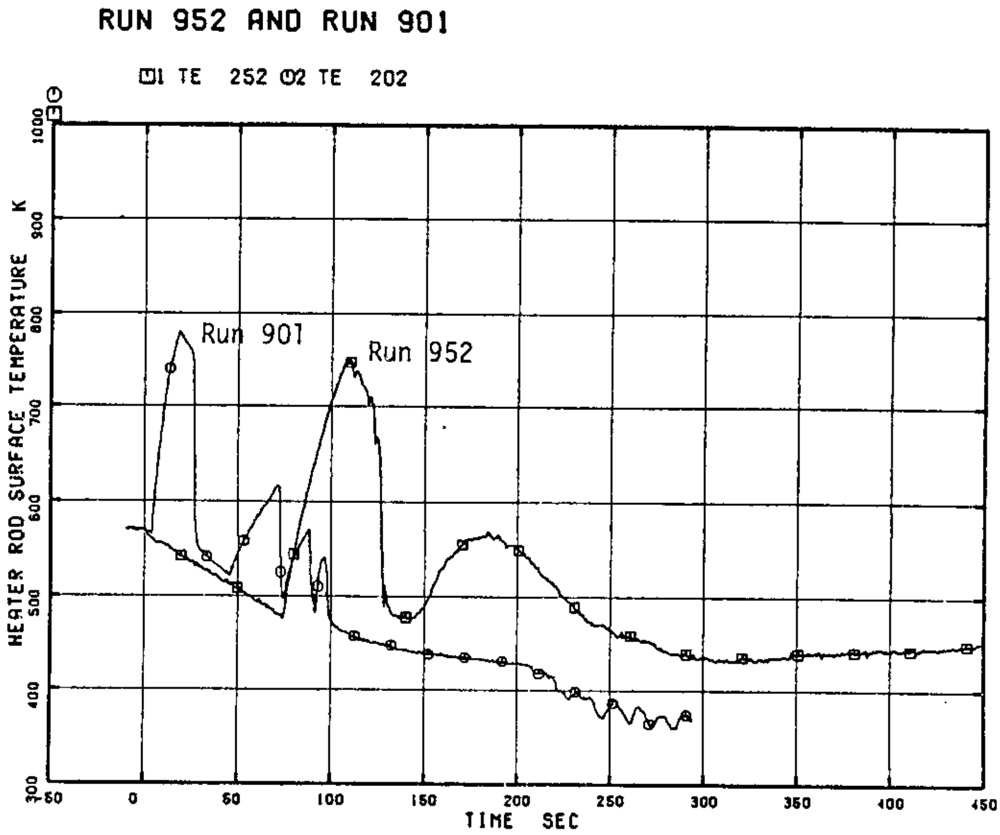

Fig. 7.11 Comparison of Peak Cladding Temperatures